SYNTHESIS, CHARACTERIZATION, AND TESTING OF ACRYLAMIDE-BASED POLYMERS

by

KEITH ADRIAN KLIMCHUK
B.Sc., University of Victoria, 1991

A THESIS SUBMITTED IN PARTIAL FULFILLMENT

OF THE REQUIREMENTS FOR THE DEGREE OF

MASTER OF SCIENCE

in the Department of Chemistry

We accept this thesis as conforming
to the required standard

[redacted]

Dr. M.B. Hocking, Supervisor (Department of Chemistry)

[redacted]

Dr. R.H. Mitchell, Departmental Member (Department of Chemistry)

[redacted]

Dr. T.M. Fyles, Departmental Member (Department of Chemistry)

[redacted]

Dr. C.D. Scarfe, Outside Member (Department of Physics and Astronomy)

[redacted]

Dr. R.J. Mikula, CANMET (Additional Member)

[redacted]

Dr. G.W. Vickers, External Examiner (Department of Mechanical Engineering)

Abstract

In relation to polyacrylamide, copolymers of acrylamide with N,N-dimethylacrylamide, methacrylamide, and N-t-butylacrylamide were prepared to study the effect of steric bulk and its degree and proximity to the polymer back-bone on synthesis to high conversions and molecular weights, polymer chain extension, solution behaviour, and flocculant ability. Cationic derivatives of copolymers containing a low proportion of the substituted acrylamide component were also prepared to study the effect of charged groups in relation to steric bulk on polymer chain extension and flocculant ability.

All copolymers were characterized by photoacoustic FTIR, ^{13}C NMR, and viscometry. Elemental analysis was used to determine the compositions of the copolymers of N,N-dimethylacrylamide and methacrylamide with acrylamide. The percentage cationicity was determined for the cationic derivatives.

For equivalent experimental conditions, only the copolymers of N,N-dimethylacrylamide with acrylamide gave similar conversions and higher molecular weights than polyacrylamide. Copolymerization of N-t-butylacrylamide with acrylamide was made possible by using a 1:1, t-butanol / distilled water solvent. However, only the copolymers containing less than 60 mol % of N-t-butylacrylamide were water soluble.

Multi-angle laser light scattering in the batch mode was used to determine polymer chain extensions in solvents adjusted to various pH levels and solvents adjusted to a constant pH but varied in electrolyte concentration. Polymer chain extensions

greater than those of polyacrylamide were measured only for the copolymers of N,N-dimethylacrylamide with acrylamide. Solution conformations of all the copolymers and polyacrylamide were resistant to variations in pH, but only the copolymers were resistant to changes in electrolyte concentration at constant pH. The solution conformations of the commercial flocculants Percol 721 (cationic polyacrylamide), Percol E-24 (anionic polyacrylamide), and Percol 351 (nonionic polyacrylamide) were all affected by changes in electrolyte concentration at constant pH.

Viscometric analysis of the cationic derivatives of the nonionic copolymers containing the lowest proportion of the substituted acrylamide component showed a greater contribution to polymer chain extension from charged groups than from steric bulk.

All the copolymers functioned as flocculants for a 1% Na-kaolinite test medium at near neutral pH and containing 1.138×10^{-4} M NaCl, but only the copolymers of N,N-dimethylacrylamide with acrylamide perfomed better than polyacrylamide as flocculants. Also, the flocculation performance of the copolymers with a low proportion of N,N-dimethylacrylamide was comparable to the performance of commercial flocculants. The flocculation performance of the cationic derivatives was poorer than the performance of their nonionic precursors.

It was concluded from the results of the polymerization, solution behaviour, and flocculation experiments that copolymers of acrylamide with N,N-dimethylacrylamide can give improved polymer chain extension and flocculation performance in the presence or absence of electrolyte, as compared to polyacrylamide. In addition,

copolymerization of N,N-dimethylacrylamide with acrylamide to give molecular weights greater than 5×10^6 g/mol and conversions greater than 70 %, as well as the conversion of the nonionic copolymer precursor to a cationic derivative containing 26 mol % cationicity, could offer useful starting points for commercial use.

Examiners:

[redacted]

Dr. M.B. Hocking, Supervisor (Department of Chemistry)

[redacted]

Dr. R.H. Mitchell, Departmental Member (Department of Chemistry)

[redacted]

Dr. T.M. Fyles, Departmental Member (Department of Chemistry)

[redacted]

Dr. C.D. Scarfe, Outside Member (Department of Physics and Astronomy)

[redacted]

Dr. R.J. Mikula, CANMET (Additional Member)

[redacted]

Dr. G.W. Vickers, External Examiner (Department of Mechanical Engineering)

Table of Contents

	Page
Abstract	i
Table of Contents	v
List of Figures	xv
List of Tables	xxii
Acknowledgements	xxvi
Dedication	xxvii
1. Introduction	1
1.1. Polyacrylamide and Polymerization Kinetics	1
1.2. Acrylamide-Based Copolymers and Derivatives	5
1.3. Copolymerization Reactivity Ratios	10
1.4. Light Scattering and the Solution Behaviour of Polyacrylamide	12
1.4.1. Polyacrylamide and its conformation in aqueous solution	15
1.4.2. Polyacrylamide and the effect of electrolyte concentration on $< r_g >$	16
1.4.3. Polyelectrolytes and the effect of electrolyte concentration on $< r_g >$	17
1.5. Flocculation	18
1.5.1. Interactions between colloid particles	18
Van der Waals interactions	19
Electrostatic interactions	20
Steric interactions	22

1.5.2. Total free energy contribution to colloid stability 23

1.5.3. Polymeric flocculants and flocculation mechanisms 25

1.5.4. Flocculation kinetics 27

Adsorption 27
Re-conformation 29
Aggregation 29
Degradation 30

1.6. Purpose of Research 30

1.7. Glossary of Acronyms 37

2. Experimental 38

2.1. Chemicals 38

2.2. Equipment 39

2.3. General Homo- and Co-Polymerization Procedures 44

2.4. Tests of Polymerization Atmosphere on the Molecular Weight of Poly(acrylamide) (PAM) 47

2.5. Homopolymerizations to Determine the Conditions which Give High Molecular Weights 49

2.5.1. Homopolymerization of N,N-dimethylacrylamide (DMAM) 2 49

2.5.2. Homopolymerization of methacrylamide (MeAM) 3 51

2.5.3. Homopolymerization of N-t-butylacrylamide (NTBAM) 4 51

(a) In methanol and methanol - water mixtures 51
(b) In t-butanol and t-butanol - water mixtures 54

2.6. Copolymerizations to Determine the Conditions which Give High Molecular Weight Copolymers 57

2.6.1. Copolymerization of DMAM with AM 57

2.6.2. Copolymerization of MeAM with AM 57

2.6.3. Copolymerization of NTBAM with AM 60

2.7. Conversion of Poly(DMAM-co-AM), Poly(MeAM-co-AM), Poly(NTBAM-co-AM), and PAM to Their Cationic Derivatives 60

2.8. Characterization of the Newly Synthesized, Acrylamide-Based Polymers 66

2.8.1. Viscometric analysis 66

(a) Stock solutions of the newly-synthesized homopolymers 68
(b) Stock solutions of the newly-synthesized copolymers 69
(c) Stock solutions of the cationic derivatives and their nonionic polymer substrates 70
(d) Stock solutions of the commercial polymers 70

2.8.2. Gel permeation chromatography (GPC) / multi-angle laser light scattering (MALLS) methods and theory 70

2.8.3. Recording photoacoustic FTIR spectra of the newly synthesized, acrylamide-based polymers 76

2.8.4. Recording ^{13}C NMR spectra of the newly synthesized, acrylamide-based polymers 77

2.8.5. Direct titration to determine the % cationicity of newly synthesized cationic derivatives and Percol 721 78

2.9. Solution Behaviour Measurements of Acrylamide-Based Polymers 79

2.9.1. Batch multi-angle laser light scattering (MALLS) sample preparation 79

2.9.2. Batch multi-angle laser light scattering (MALLS) theory and methods 82

Calibration and normalization of the Dawn DSP-F laser photometer 82
Acquisition and processing of the light scattering data 86

2.10. Measurement of the Refractive Index Increment, dn/dc, for Acrylamide-Based Polymers in Various Aqueous Solvents ... 92

2.10.1. Calculation of a calibration constant, dn/dV, to determine dn/dc 92

2.10.2. Experimental procedure 94

2.11. Flocculation 96

2.11.1 Preparation of the flocculation test medium 96

2.11.2. Measurement of the NaCl concentration in the supernatant of the settled slurry 97

Theory 97
Experimental 98

2.11.3. Flocculation test procedure for polymer addition to a 3% Na-kaolinite test medium 98

2.11.4. Investigation of the physical variables associated with the flocculation test procedure 102

2.11.5. Flocculation of 3% Na-kaolinite using the copolymers from MeAM-co-AM-2b to -4 and control PAM 103

2.11.6. Flocculation of 1% Na-kaolinite using commercial PAM and control PAM 104

2.11.7. Flocculation of 1% Na-kaolinite using 25, 50, and 100 ppm of commercial PAM and control PAM 104

2.11.8. Flocculation of 1% Na-kaolinite using the newly synthesized polymers and commercial polymers 105

3. Results 106

3.1. Evaluation of the Sample Preparation Procedure and the Molecular Weight Accuracy of the GPC / MALLS Analysis of Commercial PAM 106

3.2. Effect of Polymerization Atmosphere on the Molecular Weight of PAM 108

3.3. Evaluation of Homopolymerization Experimental Conditions . 108

3.3.1. Homopolymerization of DMAM 108

3.3.2. Homopolymerization of MeAM 110

3.3.3. Homopolymerization of NTBAM 112

(a) In methanol and methanol / distilled water mixtures 112
(b) In t-butanol and t-butanol / distilled water mixtures 114

3.4. Evaluation of Copolymerization Experimental Conditions 116

3.4.1. Copolymerization of DMAM with AM 116

3.4.2. Copolymerization of MeAM with AM 119

3.4.3. Copolymerization of NTBAM with AM 120

3.5. Characterization of the Copolymers 121

3.5.1. Viscometric analysis 121

3.5.2. Photoacoustic FTIR 123

3.5.3. ^{13}C NMR 131

^{13}C NMR data from the spectra of AM and control PAM's complementary to DMAM-co-AM-6, MeAM-co-AM-6, and NTBAM-co-AM-4 131
^{13}C NMR data from the spectra of DMAM, PDMAM from DMAM-co-AM-6, and copolymers from DMAM-co-AM-2 to -5 136
^{13}C NMR data from the spectra of MeAM, PMeAM from MeAM-co-AM-6, and copolymers from MeAM-co-AM-2b to -5 136
^{13}C NMR data from the spectra of NTBAM, PNTBAM from NTBAM-co-AM-6b, and copolymers from NTBAM-co-AM-1b to -6a 143

3.5.4. Elemental analysis 160

3.6. Copolymer Composition 160

3.6.1. Copolymers from DMAM-co-AM-2 to -5 and -7 162

3.6.2. Copolymers from MeAM-2b to -5 164

3.6.3. Copolymers from NTBAM-co-AM-1b to -3 and -6a 166

3.7. Evaluation of the Experiments to Determine the % Cationicity of the Newly Synthesized Cationic Derivatives and the Commercial Polymer, Percol 721 166

3.8. Comparison of the Intrinsic Viscosities for the Purified and Unpurified Cationic Derivatives of the Nonionic Copolymers and PAM with the Intrinsic Viscosities of their Polymer Substrates and Commercial Polymers 168

3.9. Measurement of the Refractive Index Increment, dn/dc, for Acrylamide-Based Polymers in Various Aqueous Solvents 170

3.10. Solution Behaviour Measurements of Acrylamide-Based Polymers 175

3.10.1. Copolymers from DMAM-co-AM-2 to -5 and -7 and the homopolymer (PDMAM) from DMAM-co-AM-6 176

3.10.2. Copolymers from MeAM-co-AM-2b to -5 and PAM from control-6 (complementary to MeAM-co-AM-6) 178

3.10.3. Copolymers from NTBAM-co-AM-1b (clouded layer), -1b (clear layer), and -2 (dialyzed fraction) 180

3.10.4. Commercial polymers Percol 351, Percol 721, and Percol E-24 182

3.11. Characterization of the Flocculation Test Medium 184

3.11.1. Measurement of the NaCl concentration in the supernatant of the settled slurry 184

3.11.2. Measurement of the surface area of Na-kaolinite 185

Theory 185
Measurement 186
3.11.3. Measurement of the isoelectric point of Na-kaolinite 186

Theory 186
Measurements 187

3.12. Flocculation 188

3.12.1. Effects of polymer dosage, agitation rate, and rate of polymer addition on settling rate using control PAM and 3% Na-kaolinite 188

3.12.2. Comparison of the flocculation performance of copolymers from MeAM-co-AM-2b to -4 and control PAM using 3% Na-kaolinite 192

3.12.3. Comparison of the flocculation by commercial PAM and control PAM using 1% Na-kaolinite 194

3.12.4. Evaluation of flocculation of 1% Na-kaolinite using 25, 50, and 100 ppm of control PAM 201

3.12.5. Flocculation of 1% Na-kaolinite using 25, 50, and 100 ppm dosages of newly synthesized, acrylamide-based polymers and commercial polymers 201

Copolymers from DMAM-co-AM-3 to -5 and PAM from control-6 (complementary to DMAM-co-AM-6) 206
Copolymers from MeAM-co-AM-2b to -5 and PAM from control-6 (complementary to MeAM-co-AM-6) 206
Copolymers from NTBAM-co-AM-1b (clouded layer), -1b (clear layer), -2 (dialyzed fraction), and PAM from control-6 (complementary to MeAM-co-AM-6) 211
Purified cationic derivatives of the copolymers from DMAM-co-AM-7, MeAM-co-AM-2b, NTBAM-co-AM-1b (clouded layer), and control PAM 211
Commercial polymers labelled Percol 351, Percol 721, and Percol E-24 and control PAM 215
Overall comparison of the flocculation of 1% Na-kaolinite by the newly synthesized, acrylamide-based polymers and commercial polymers 217

4. Discussion 223

4.1. Evaluation of the Sample Preparation Procedure and the Molecular Weight Accuracy of the GPC / MALLS Analysis of Commercial PAM 223

4.2. Effect of Polymerization Atmosphere on the Molecular Weight of PAM 225

4.3. Synthesis of Acrylamide-Based Polymers 227

4.3.1. Evaluation of homopolymerization conditions 229

Evaluation of the conditions for homopolymerization of DMAM 230
Evaluation of the conditions for homopolymerization of MeAM 232
Evaluation of the conditions for homopolymerization of NTBAM 235
PNTBAM-1 to -6 236
PNTBAM-7 to -14 237

4.3.2. Evaluation of Copolymerization Conditions 239

Copolymerization of DMAM with AM 239
Copolymerization of MeAM with AM 239
Copolymerization of NTBAM with AM 240

4.4. Verification of Copolymerizations by PAS-FTIR and ^{13}C NMR .. 242

4.4.1. Copolymers of DMAM with AM 242

4.4.2. Copolymers of MeAM with AM 243

4.4.3. Copolymers of NTBAM with AM 245

4.5. Evaluation of the Copolymer Compositions 246

4.5.1. Use of ^{13}C NMR 246

4.5.2. Use of Elemental Analysis 248

4.6. Homopolymer and Copolymer Conversion to Cationic Derivatives 250

4.6.1. Experimental conditions 250

4.6.2. Evaluation of experimental conditions for cationic derivatization 252

4.7. Evaluation of the Measurements of the Refractive Index Increments, dn/dc 255

4.8. Solution Behaviour of Acrylamide-Based Polymers 258

4.8.1. Evaluation of MALLS for the study of the solution behaviour of acrylamide-based polymers 258

4.8.2. Evaluation of the solution behaviour of the acrylamide-based polymers as given by values for M_w, $< r_g >$, and A_2 259

4.8.3. Effect of solution pH on polymer chain extension 260

4.8.4. Effect of electrolyte concentration on polymer chain extension 261

4.8.5. Trends in M_w, $< r_g >$, and A_2 from MALLS and in [η] from viscometry 263

Commercial polymers 264
Copolymers of DMAM with AM 267
Copolymers of MeAM with AM 269
Copolymers of NTBAM with AM 271

4.9. Flocculation 272

4.9.1. Development of a flocculation test procedure 272

Selection and modification of the flocculation test medium .. 272
Suitability of the test medium for bridging flocculation 275
Equipment for flocculation tests 277
Evaluation of the chemical and physical variables associated with the flocculation test procedure using a 3% Na-kaolinite test medium 279
Effect of polymer concentration on flocculation efficiency .. 279
Effect of agitation rate on flocculation efficiency 280
Effect of addition rate on flocculation efficiency 281
Sensitivity of the flocculation test procedure to polymer chain extension 281
For copolymers from MeAM-co-AM-2b to -4 and PAM .. 281
For commercial PAM from Polysciences and control PAM 282

Suitability of the evaluation techniques for the flocculation test procedure 284
Settling rate 284
Supernatant turbidity 286
Sediment volume 286
Capillary suction time 287
Evaluation of the physical variables associated with the flocculation test procedure using 1% Na-kaolinite 288

4.9.1. Evaluation of the flocculation performance of newly synthesized, acrylamide-based polymers 289

Average settling rate of nonionic, newly synthesized polymers 290
Supernatant turbidity of nonionic, acrylamide-based polymers 291

4.9.3. Comparison of the flocculation performance of the newly synthesized, acrylamide-based polymers and their cationic derivatives 292

4.9.4. Comparison of the flocculation performance of the newly synthesized acrylamide-based polymers and commercial polymers 293

5. Conclusions 295

5.1. Synthesis 295

5.2. Solution Behaviour 298

5.3. Flocculation Test-Work 299

6. References 303

List of Figures

		Page
Fig. 1	Reaction scheme for conversion of nonionic polyacrylamides to cationic derivatives using the Hofmann degradation reaction as the first stage	8
Fig. 2	Reaction scheme for cationic conversion of nonionic polyacrylamides using the Mannich reaction followed by quaternization	9
Fig. 3	Diagram of the electric double layer surrounding a colloid particle suspended in solution	21
Fig. 4	Diagram of total free energy versus particle separation for colloid particles suspended in solution	24
Fig. 5	Diagram of colloid particle aggregation by polymer bridging	26
Fig. 6	Diagram of colloid particle aggregation by charge neutralization involving the electrostatic patch mechanism	26
Fig. 7	Diagram of the four distinct processes which contribute to flocculation; adsorption, reconformation, aggregation, and degradation	28
Fig. 8	Schematic diagram of the standard mix tank used for flocculation tests	43
Fig. 9	Equipment assembly for polymerization test-work	45
Fig. 10	Debye plot for PAM from PAM-1	74
Fig. 11	Plot of normalized voltage versus detector number for PDMAM from DMAM-co-AM-6 at pH 4.0 with no added electrolyte	87
Fig. 12	Zimm plot for PDMAM from DMAM-co-AM-6 at pH 4.0 with no added electrolyte	89
Fig. 13	Refractive indexes, n, versus the auxiliary detector voltages (volts) for NaCl standards	93

Fig. 14 Plot of equivalent conductance (S cm^2) of NaCl standards versus $([NaCl])^{0.5}$ for NaCl solution standards 99

Fig. 15 PAS-FTIR spectra of the copolymers from DMAM-co-AM-2 to -5, PDMAM from DMAM-co-AM-6, and PAM from control-6 ... 127

Fig. 16 PAS-FTIR spectra of the copolymers from MeAM-co-AM-2b to -5, PMeAM from MeAM-co-AM-6, and PAM from control-6 128

Fig. 17 PAS-FTIR spectra of the copolymers from NTBAM-co-AM-1b and -2, PNTBAM from NTBAM-co-AM-6b, and PAM from control-4 129

Fig. 18 PAS-FTIR spectra of the copolymers from NTBAM-co-AM-3 and -6a, PNTBAM from NTBAM-co-AM-6b, and PAM from control-4 130

Fig. 19 ^{13}C NMR spectrum of acrylamide (AM) 132

Fig. 20 ^{13}C NMR spectrum of PAM from control-6 (complementary to DMAM-co-AM-6) 133

Fig. 21 ^{13}C NMR spectrum of PAM from control-6 (complementary to MeAM-co-AM-6) 134

Fig. 22 ^{13}C NMR spectrum of PAM from control-4 (complementary to NTBAM-co-AM-4) 135

Fig. 23 ^{13}C NMR spectrum of N,N-dimethylacrylamide (DMAM) 137

Fig. 24 ^{13}C NMR spectrum of PDMAM from DMAM-co-AM-6 138

Fig. 25 ^{13}C NMR spectrum of the copolymer from DMAM-co-AM-2 .. 139

Fig. 26 ^{13}C NMR spectrum of the copolymer from DMAM-co-AM-3 .. 140

Fig. 27 ^{13}C NMR spectrum of the copolymer from DMAM-co-AM-4 .. 141

Fig. 28 ^{13}C NMR spectrum of the copolymer from DMAM-co-AM-5 .. 142

Fig. 29 ^{13}C NMR spectrum of methacrylamide (MeAM) 144

Fig. 30 ^{13}C NMR spectrum of PMeAM from MeAM-co-AM-6 145

Fig. 31 ^{13}C NMR spectrum of the copolymer from MeAM-co-AM-2b . 146

Fig. 32 ^{13}C NMR spectrum of the copolymer from MeAM-co-AM-3 .. 147

Fig. 33 ^{13}C NMR spectrum of the copolymer from MeAM-co-AM-4 .. 148

Fig. 34 ^{13}C NMR spectrum of the copolymer from MeAM-co-AM-5 .. 149

Fig. 35 ^{13}C NMR spectrum of N-t-butylacrylamide (NTBAM) 151

Fig. 36 ^{13}C NMR spectrum of PNTBAM from NTBAM-co-AM-6b ... 152

Fig. 37 ^{13}C NMR spectrum of the copolymer from NTBAM-co-AM-1b (clouded layer) 153

Fig. 38 ^{13}C NMR spectrum of the copolymer from NTBAM-co-AM-1b (clear layer) 154

Fig. 39 ^{13}C NMR spectrum of the copolymer from NTBAM-co-AM-2 (dialyzed fraction) 155

Fig. 40 ^{13}C NMR spectrum of the copolymer from NTBAM-co-AM-2 (non-dialyzed fraction) 156

Fig. 41 ^{13}C NMR spectrum of the copolymer from NTBAM-co-AM-3 (gelatinous material) 157

Fig. 42 ^{13}C NMR spectrum of the copolymer from NTBAM-co-AM-3 (tan coloured solution) 158

Fig. 43 ^{13}C NMR spectrum of the copolymer from NTBAM-co-AM-6a 159

Fig. 44 Average settling rate versus polymer dosage for flocculation of 3% Na-kaolinite using control PAM. Conditions were: 1000 rpm agitation and the addition of 10 mL of PAM (10^{-4} - 10^{-3} g/mL) over 60 seconds 189

Fig. 45 Average settling rate versus agitation rate for flocculation of 3% Na-kaolinite using control PAM. Conditions were: 700 ppm polymer dosage, 60 sec. agitation duration, and the addition of 10 mL of polymer solution (10^{-4} - 10^{-3} g/mL) over 60 seconds .. 190

Fig. 46 Average settling rate versus the rate of polymer addition for flocculation of 3% Na-kaolinite using control PAM. Conditions were : 1000 rpm agitation and a polymer dosage of 700 ppm .. 191

Fig. 47 Initial average settling rate versus polymer dosage for flocculation of 3% Na-kaolinite using PAM (5E+05 MW, Polysciences) or control PAM (5E+06 to 10E+06 MW). Conditions were : 1000 rpm agitation and addition of 10 mL of polymer solution (10^{-4} to 10^{-3} g/mL) over 60 seconds 195

Fig. 48 Average settling rate to compaction versus polymer dosage for flocculation of 3% Na-kaolinite using PAM (5E+05 MW, Polysciences) or the control PAM 5E+06 - 10E+06 MW). Conditions were : 1000 rpm agitation and addition of 10 mL of polymer solution (10^{-4} to 10^{-3} g/mL) over 60 seconds 196

Fig. 49 Average settling rate versus polymer dosage for flocculation of 3% Na-kaolinite using PAM (5E+05 MW, Polysciences) or control PAM (5E+06 - 10E+06 MW). Conditions were : 1000 rpm agitation and addition of 10 mL of polymer solution (10^{-4} to 10^{-3} g/mL) over 60 seconds. 197

Fig. 50 Sediment volume versus polymer dosage for flocculation of 3% Na-kaolinite using control PAM (5E+06 - 10E+06 MW) or PAM (5E+05 MW, Polysciences). Conditions were : 1000 rpm agitation and addition of 10 mL of polymer solution over 60 seconds. ... 198

Fig. 51 Supernatant turbidity versus polymer dosage for flocculation of 3% Na-kaolinite using control PAM (5E+06 - 10E+06 MW) or PAM (5E+05 MW, Polysciences). Conditions were : 1000 rpm agitation and addition of 10 mL of polymer solution over 60 seconds. ... 199

Fig. 52 Average capillary suction time versus polymer dosage for flocculation of 3% Na-kaolinite using control (PAM, 5E+06 - 10E+06 MW) or PAM (5E+05 MW, Polysciences). Conditions were : 1000 rpm agitation and addition of 10 mL of polymer solution over 60 seconds. 200

Fig. 53 Average settling rate versus polymer dosage for flocculation of 1% Na-kaolinite using control PAM. Conditions were : polymer dosages of 25, 50, and 100 ppm, agitation rates of 750, 1000, 1250 rpm, and a polymer solution addition rate of 10 mL per 60 seconds. 202

Fig. 54 30 minute supernatant turbidity versus polymer dosage for flocculation of 1% Na-kaolinite using control PAM. Conditions were : polymer dosages of 25, 50, and 100 ppm, agitation rates of 750, 1000, and 1250 rpm, and a polymer solution addition rate of 10 mL per 60 seconds. 203

Fig. 55 Average settling rate versus polymer dosage for flocculation of 1% Na-kaolinite using control PAM. Conditions were : polymer dosages of 25, 50, and 100 ppm, an agitation rate of 1000 rpm, and polymer solution addition rates of 10 mL over 30 seconds, 60 seconds, and 90 seconds. 204

Fig. 56 30 minute supernatant turbidity versus polymer dosage for flocculation of 1% Na-kaolinite using control PAM. Conditions were : polymer dosages of 25, 50, and 100 ppm, an agitation rate of 1000 rpm, and polymer solution addition rates of 10 mL over 30, 60, and 90 seconds. 205

Fig. 57 Average settling rate versus polymer dosage for flocculation of 1% Na-kaolinite using 25, 50, and 100 ppm dosages of the copolymers from DMAM-co-AM-3 to -5 and PAM from control-6. Conditions were : 1000 rpm agitation and addition of 10 mL of polymer solution over 60 seconds. 207

Fig. 58 30 minute supernatant turbidity versus polymer dosage for flocculation of 1% Na-kaolinite using 25, 50, and 100 ppm polymer dosages of the copolymers from DMAM-co-AM-3 to -5 and PAM from control-6. Conditions were : 1000 rpm agitation and addition of 10 mL of polymer solution over 60 seconds. 208

Fig. 59 Average settling rate versus polymer dosage for flocculation of 1% Na-kaolinite using 25, 50, and 100 ppm dosages of the copolymers from MeAM-co-AM-2b to -5 and PAM from control-6. Conditions were 1000 rpm agitation and addition of 10 mL of polymer solution over 60 seconds 209

Fig. 60 30 minute supernatant turbidity versus polymer dosage for flocculation of 1% Na-kaolinite using 25, 50, and 100 ppm dosages of the copolymers from MeAM-co-AM-2b to -5 and PAM from control-6. Conditions were : 1000 rpm agitation and addition of 10 mL of polymer solution over 60 seconds 210

Fig. 61 Average settling rate versus polymer dosage for flocculation of 1% Na-kaolinite using 25, 50, and 100 ppm dosages of the copolymers from NTBAM-co-AM-1b (clouded layer), -1b (clear layer) and -2 (dialyzed fraction) and control PAM. Conditions were : 1000 rpm agitation and addition of 10 mL of polymer solution over 60 seconds. 212

Fig. 62 30 minute supernatant turbidity versus polymer dosage for flocculation of 1% Na-kaolinite using 25, 50, and 100 ppm dosages of the copolymers from NTBAM-co-AM-1b (clouded layer), -1b (clear layer), and -2 (dialyzed fraction) and control PAM. Conditions were : 1000 rpm agitation and addition of 10 mL of polymer solution over 60 seconds. 213

Fig. 63 Average settling rate versus polymer dosage for flocculation of 1% Na-kaolinite using the purified cationic derivatives from DMAM-co-AM-7, MeAM-co-AM-2b, NTBAM-co-AM-1b (clouded layer) and control PAM and their nonionic polymer substrates. Conditions were : 1000 rpm agitation and addition of 10 mL of polymer solution over 60 seconds. 214

Fig. 64 Average settling rate versus polymer dosage for flocculation of 1% Na-kaolinite using 25, 50, and 100 ppm dosages of Percol 351, Percol 721, and Percol E-24 and the control PAM. Conditions were : 1000 rpm agitation and addition of 10 mL of polymer solution over 60 seconds. 218

Fig. 65 30 minute supernatant turbiditiy versus polymer dosage for flocculation of 1% Na-kaolinite using 25, 50, and 100 ppm dosages of Percol 351, Percol 721, and Percol E-24 and control PAM. Conditions were : 1000 rpm agitation and addition of 10 mL of polymer solution over 60 seconds. 219

Fig. 66 Average settling rate versus polymer dosage for flocculation of 1% Na-kaolinite using Percol 351, Percol 721, and Percol E-24, the nonionic copolymers from DMAM-co-AM-3, MeAM-co-AM-2b, and NTBAM-co-AM-1b (clouded layer), and control PAM. Conditions were : 1000 rpm agitation and addition of 10 mL of polymer solution over 60 seconds. 220

Fig. 67 30 minute supernatant turbidity versus polymer dosage for flocculation of 1% Na-kaolinite using Percol 351, Percol 721, and Percol E-24, the copolymers from DMAM-co-AM-3, MeAM-co -AM-2b, and NTBAM-co-AM-1b (clouded layer), and control PAM. Conditions were : 1000 rpm agitation and addition of 10 mL of polymer solution over 60 seconds. 221

Fig. 68 Reaction scheme for methylene crosslinking of the cationic derivatives of nonionic polyacrylamides 254

Fig. 69 Atom arrangement in the unit cell of a 1:1 layer mineral 273

Fig. 70 Variations in edge face charge characteristics with solution pH for the edge face of kaolinite 273

List of Tables

		Page
Table 1	Homopolymerizations of acrylamide (AM) at 60.0 ± 0.2°C for 2 hours under atmospheres of oxygen, filtered air, and nitrogen	48
Table 2	Homopolymerization of N,N-dimethylacrylamide (DMAM) and acrylamide (AM) under equivalent conditions	50
Table 3	Homopolymerization of methacrylamide (MeAM) and acrylamide (AM) under equivalent conditions at 60.0 ± 0.2°C	52
Table 4	Solubility of N-t-butylacrylamide (NTBAM) in 30 mL of water / methanol mixtures at (55 ± 2)°C	53
Table 5	Homopolymerization of N-t-butylacrylamide (NTBAM) and acrylamide (AM) under equivalent conditions in methanol, and methanol / distilled water mixtures	55
Table 6	Homopolymerization of N-t-butylacrylamide (NTBAM) and acrylamide (AM) under equivalent conditions in 98% t-butanol, and t-butanol / distilled water mixtures	56
Table 7	Copolymerizations of N,N-dimethylacrylamide (DMAM) with acrylamide (AM) and control homopolymerizations of AM at (50.0 ± 0.2)°C	58
Table 8	Copolymerization of methacrylamide (MeAM) with acrylamide (AM) and control homopolymerizations of AM under equivalent conditions	59
Table 9	Copolymerization of N-t-butylacrylamide (NTBAM) with acrylamide (AM) and the control homopolymerizations of AM under equivalent conditions at (50.0 ± 0.2)°C	61
Table 10	Conversion of poly(DMAM-co-AM), poly(MeAM-co-AM), poly(NTBAM-co-AM), and PAM to weakly cationic derivatives using the Mannich reaction for 18 hours at (25 ± 2)°C	64

Table 11 Quaternization of the weakly cationic derivatives of poly(DMAM-co-AM), poly(MeAM-co-AM), poly(NTBAM-co-AM), and PAM for 4 hours at (30 ± 2)°C 65

Table 12 Molecular weights determined by GPC / MALLS for filtered and unfiltered, duplicate stock solutions of Polysciences PAM ... 107

Table 13 Molecular weight and intrinsic viscosity for PDMAM and PAM produced under identical experimental conditions. 109

Table 14 Molecular weight and intrinsic viscosity for PDMAM and PAM produced under identical experimental conditions 111

Table 15 The molecular weight and intrinsic viscosity for PMeAM and PAM pairs produced under identical experimental conditions 113

Table 16 Molecular weight and intrinsic viscosity for PNTBAM and PAM pairs produced by homopolymerization under identical experimental conditions 115

Table 17 Molecular weights and intrinsic viscosities for PNTBAM and PAM pairs produced by homopolymerization under identical experimental conditions 117

Table 18 Intrinsic viscosities for the copolymers from DMAM-co-AM-2 to -5, PDMAM from DMAM-co-AM-6, and PAM from control-6 122

Table 19 Intrinsic viscosities for the copolymers from MeAM-co-AM-2b to -5, PMeAM from MeAM-co-AM-6, and PAM from control-6 124

Table 20 Intrinsic viscosities for the copolymers from NTBAM-co-AM-1a, -1b, -2, -3, and -6a, PNTBAM from NTBAM-co-AM-6b, and PAM from control-4 125

Table 21 Elemental analysis of the copolymers from DMAM-co-AM-2 to -5 and -7, the copolymers from MeAM-co-AM-2b to -5, PMeAM from MeAM-co-AM-6, PAM from control-6, and commercial PAM 161

Table 22 Comparison of the copolymer compositions obtained for DMAM -co-AM-2, -3, -4, -5, and -7 from the copolymer equation, ^{13}C NMR integration, and elemental analyis 163

Table 23 Comparison of the copolymer compositions obtained for MeAM -co-AM-2b to -6 from the copolymer equation, ^{13}C NMR integration, and elemental analyis 165

Table 24 Copolymer compositions obtained for NTBAM-co-AM copolymers from ^{13}C NMR integration 167

Table 25 Comparison of the intrinsic viscosities of nonionic copolymers, control PAM, and commercial polymers with the intrinsic viscosities of the purified and unpurified cationic derivatives of the nonionic copolymers and PAM 169

Table 26 Refractive index increments, dn/dc, for the copolymers from DMAM-co-AM -2 to -5 and -7 and the homopolymer (PDMAM) from DMAM-co-AM-6 171

Table 27 Refractive index increments, dn/dc, for the copolymers from MeAM-co-AM-2b to -5 and control PAM 172

Table 28 Refractive index increments, dn/dc, for the copolymers from NTBAM-co-AM-1b (clouded layer), -1b (clear layer), and -2 (dialyzed fraction) 173

Table 29 Refractive index increments, dn/dc, for Percol 351, Percol 721, and Percol E-24 174

Table 30 M_W, $< r_g >$, and A_2 for the copolymers from DMAM-co-AM-2 to -5 and PDMAM from DMAM-co-AM-6 177

Table 31 M_W, $< r_g >$, and A_2 for the copolymers from MeAM-co-AM-2b to -5 and control PAM 179

Table 32 M_W, $< r_g >$, and A_2 for the copolymers from NTBAM-co-AM-1b (clouded layer), -1b (clear layer), and -2 (dialyzed fraction) .. 181

Table 33 M_W, $< r_g >$, and A_2 for the commercial polymers Percol 351, Percol 721, and Percol E-24 183

Table 34 Initial, average to compaction, and average settling rates, as well as sediment volumes, 30 minute supernatant turbidities, and capillary suction times for flocculation of 3% Na-kaolinite using copolymers from MeAM-co-AM-2b to -4 and control PAM .. 193

Table 35 30 minute supernatant turbidities for flocculation of 1% Na-kaolinite using the nonionic copolymers or their purified cationic derivatives originating from DMAM-co-AM-7, MeAM-co-AM-2b, and NTBAM-co-AM-1b (clouded layer) and control PAM and its cationic derivative 216

Table 36 Estimated X_n values for the copolymers from DMAM-co-AM-2 to -5 and -7 265

Table 37 Estimated X_n values for the copolymers from MeAM-co-AM-2b to -5 and control PAM 265

Table 38 Estimated X_n values for the copolymers from NTBAM-co-AM-1b (clouded layer), -1b (clear layer), and -2 (dialyzed fraction) .. 266

Table 39 Estimated X_n values for the commercial polymers, Percol 351, Percol 721, and Percol E-24 266

Acknowledgements

I would like to thank my supervisors Dr. Martin Hocking of the University of Victoria and Dr. Steven Lowen of CANMET's Western Research Centre for their guidance with this project. I would also like to thank Dr. John Donini, Dr. Randy Mikula, Dr. Slobodan Petrovic, and others at CANMET's Western Research Centre for their assistance. I am grateful to Dr. Steven Lowen, Dr. Kirk Michaelian, Dr. Martin Hocking, and Dr. Rick Reeve for their efforts to arrange a M.Sc. Co-op programme. Finally, I would like to thank Natural Resources Canada, the Government of British Columbia, Dr. Hocking, and the University of Victoria for their financial support.

Dedicated to the enormous sacrifice of my wife and children and the ever present support of my parents.

1. Introduction

1.1. Polyacrylamide and Polymerization Kinetics

Water soluble polymers are found in a very broad range of industrial applications. An important class of these are acrylamide-based polymers which are widely used as flocculants, rheology control agents, and adhesives.[1-3] More specifically, acrylamide-based polymers are employed in oil field operations as viscosity control agents for enhanced oil recovery and to a lesser degree in engineering fluids used for lubrication, for effluent reclaiming, and for opening oil passage channels in oil bearing rock.[1,4-6] Paper manufacture[1,7-9], mining[1,10,11], and water treatment[1,12] processes also benefit from the use of acrylamide-based polymers to flocculate solids in aqueous suspensions.

The basis for acrylamide-based polymers and their derivatives is polyacrylamide. Polyacrylamide is made by the free radical polymerization of acrylamide which includes bulk, solution, suspension, emulsion, inverse emulsion, and precipitation techniques[1,13-15]. Of these, solution polymerization of acrylamide in water avoids the high viscosities and difficulty with temperature and agitation control of bulk polymerization, and the purification difficulties and costs of surfactants and solvents for suspension, emulsion, inverse emulsion, and precipitation polymerization. The free radical mechanism includes initiation, propagation, chain transfer, and termination steps as shown by the following kinetic scheme.

Initiation

$$I \xrightarrow{k_D} 2\,R\cdot$$

$$R\cdot + M \xrightarrow{k_I} R{-}M\cdot$$

Chain Transfer

$$M_N\cdot + TrH \xrightarrow{k_{Tr}} M_NH + Tr\cdot$$

$$Tr\cdot + M \longrightarrow Tr{-}M\cdot$$

Eq. 1

Propagation

$$M_1\cdot + M \xrightarrow{k_P} M_2\cdot$$

$$M_2\cdot + M \longrightarrow M_3\cdot$$

$$M_N\cdot + M \longrightarrow M_{N+1}\cdot$$

Termination

$$M_N\cdot + M_N\cdot \xrightarrow{k_T} M_N{-}M_N$$

$$M_N\cdot + M_N\cdot \longrightarrow M_N + M_N$$

where

I	is the initiator.
k_D	is the rate constant for initiator decomposition.
k_I	is the rate constant for initiation.
k_P	is the rate constant for propagation.
k_{Tr}	is the rate constant for chain transfer.
Tr	is the chain transfer agent.
Tr·	is the chain transfer radical.
k_T	is the rate constant for termination.

Depending on the polymerization technique, initiation can use various ways of generating free radicals including peroxides, persulfates, redox couples, azo compounds, ultrasonic energy, uv light, ionized gas plasmas, or ionizing radiation.[1,14,15] In many cases the rate of decomposition of the initiator molecule is rate controlling for free radical polymerization. Typically, persulfates and peroxides are used for initiation of acrylamide polymerizations in aqueous solutions, and peroxides and azo compounds are used in organic solvents or organic / aqueous mixtures.[15]

Two mechanisms exist for termination (Eq. 1). It can occur by coupling whereby two propagating radicals combine to give dead polymer. Or it can occur by disproportionation whereby a propagating radical abstracts a hydrogen atom beta to the radical centre of another propagating radical to give one saturated and one unsaturated polymer molecule. It is believed that termination by disproportionation is the likely mechanism for polyacrylamide propagating radicals.[15]

Chain transfer agents may be used to limit polymer molecular weight. As shown by the kinetic equations for chain transfer (Eq. 1), a typical mechanism for chain transfer is the abstraction of a hydrogen atom from the chain transfer reagent by the propagating radical. Although polymerization may or may not continue by way of the chain transfer radical, propagation and, hence, molecular weight increase is halted for the propagating radical. Isopropanol is a commonly used chain transfer agent to limit the molecular weight of polyacrylamide.[1,15,16]

Polymer molecular weight may also be limited by other chain transfer mechanisms such as chain transfer to initiator, to monomer, to solvent, or to another polymer chain. The resulting polymer molecular weight can be affected significantly by these other chain transfer mechanisms depending on the identity and relative concentrations of the polymerization reagents as well as the polymerization conditions. For solution polymerization of acrylamide in distilled water, chain transfer to monomer is reported to be the dominant process limiting polymer molecular weight.[17]

As a result of the free radical mechanism, polymer molecular weight is related to the number average degree of polymerization, X_n, by the following equation.[14]

$$M_n = M_o \times X_n \qquad \text{Eq. 2}$$

where M_n is the number average molecular weight.

M_o is the molecular weight of a single monomer unit, assuming a homopolymer.

X_n is the average number of monomer units in the polymer.

If terms for chain transfer are excluded a relationship can be derived for X_n in terms of the polymerization reagents and associated rate constants by assuming termination by disproportionation and thermal homolysis of the initiator.[14]

$$X_n = \frac{k_p^2[M]^2}{2k_t R_p} = \frac{k_p[M]}{2[fk_d k_t]^{0.5}[I]^{0.5}} \qquad \text{Eq. 3}$$

where

$$R_p = k_p[M]\frac{(fk_d[I])^{0.5}}{(k_t)^{0.5}} \qquad \text{Eq. 4}$$

and k_p is the propagation rate constant.

R_p is the rate of polymerization.

$[M]$ is the concentration of monomer.

f is the collision efficiency factor for initiation.

k_d is the initiator decomposition rate constant.

k_t is the termination rate constant.

$[I]$ is the concentration of initiator.

To maximize X_n and, therefore, polymer molecular weight, it is necessary to minimize the concentration of chain transfer agent, $[Tr]$, and maximize $k_p/(k_t)^{0.5}$ and $[M]/[I]^{0.5}$. Since $k_p/(k_t)^{0.5}$ is an intrinsic function of the monomer itself, only $[M]$, $[I]$, and $[Tr]$ can be modified experimentally to affect polymer molecular weight.[13] In addition to the chemical variables, physical variables, such as the polymerization temperature and the duration, affect X_n. Whereas increasing the polymerization duration increases the conversion of monomer to polymer, increasing the polymerization temperature decreases X_n.[1,13,15]

Since R_p and X_n are inversely related, many of the experimental modifications necessary to maximize X_n adversely affect R_p. For this reason, a compromise is needed to achieve adequate values of X_n and, therefore, molecular weights, reasonable values of R_p, and adequate conversions of monomer to polymer.

1.2. Acrylamide-Based Copolymers and Derivatives

Acrylamide-based copolymers can be prepared by either copolymerization of acrylamide with another vinyl-type monomer or by the chemical modification of polyacrylamide. Substituted acrylamides containing mono- or di-substitution of the amide nitrogen atom of acrylamide and / or substitution of the α-carbon atom of the vinyl component of acrylamide can be copolymerized with acrylamide to give nonionic copolymers. Methacrylamide, N,N-dimethylacrylamide, and N-phenylacrylamide are only a few of the substituted acrylamides which have been copolymerized successfully

with acrylamide.[15,18-20]

Anionic acrylamide copolymers usually contain either carboxylate or sulfonate functional groups. The copolymers may be prepared by copolymerization of acrylamide with another vinyl-type monomer containing either a carboxylate or sulfonate functional group, or by chemical modification of polyacrylamide to introduce carboxylate or sulfonate functional groups. Sulfomethylation of polyacrylamide may be used to introduce sulfonate functional groups[21] (Eq. 5) and alkaline hydrolysis of polyacrylamide may be used to introduce carboxylate functional groups[22] (Eq. 6).

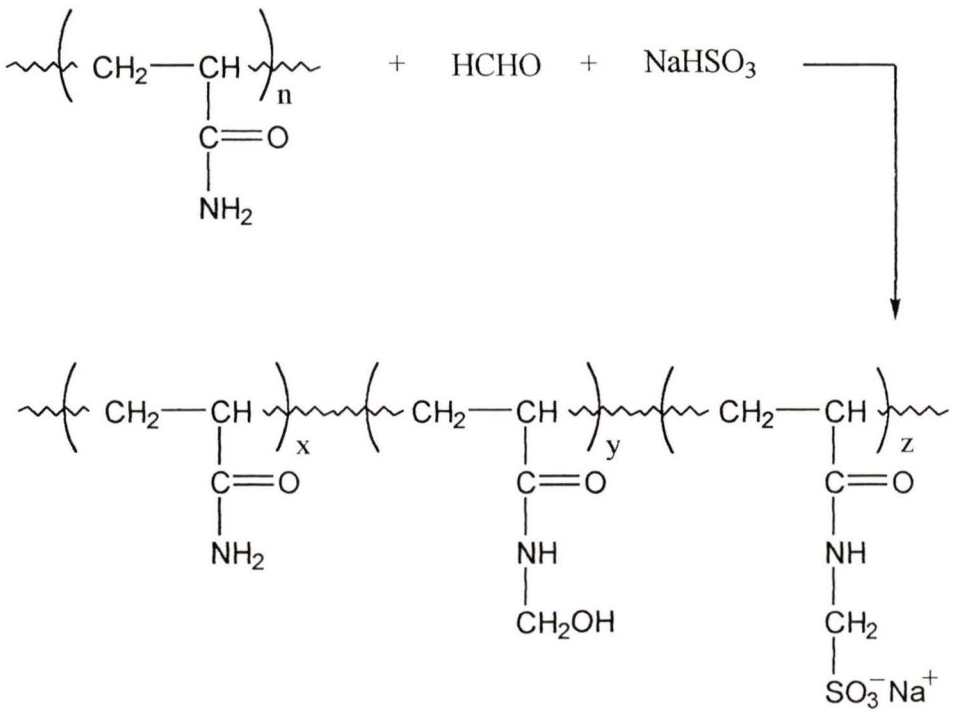

Eq. 5

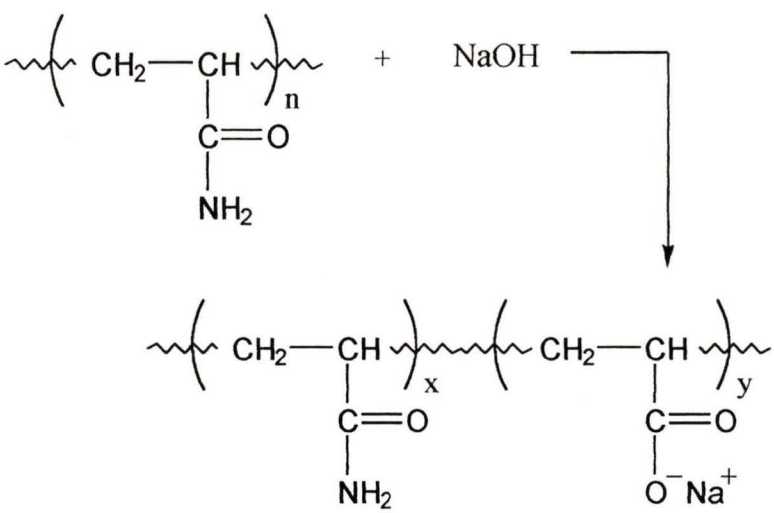

Eq. 6

Anionic polyacrylamides having high molecular weights and low charge densities have found application as flocculants and viscosity control agents. However, anionic polyacrylamides having low molecular weights and high charge densities have found commercial application as dispersants.[23-25]

Cationic acrylamide copolymers usually contain quaternized amine functional groups. Copolymerization of acrylamide with another vinyl-type monomer containing a quaternized amine functional group or modification of polyacrylamide to introduce quaternized amine functional groups are two methods used to prepare cationic acrylamide copolymers. Both the Hoffmann degradation reaction (Fig. 1) followed by methylation,[21,26,27] or the Mannich reaction followed by methylation (Fig. 2),[1,21,28-31] have been used to introduce quaternized amine functional groups into polyacrylamide. Since the particles of most solid suspensions are negatively charged, cationic polyacrylamides have found commercial application mainly as flocculants.[23]

Hofmann degradation reaction

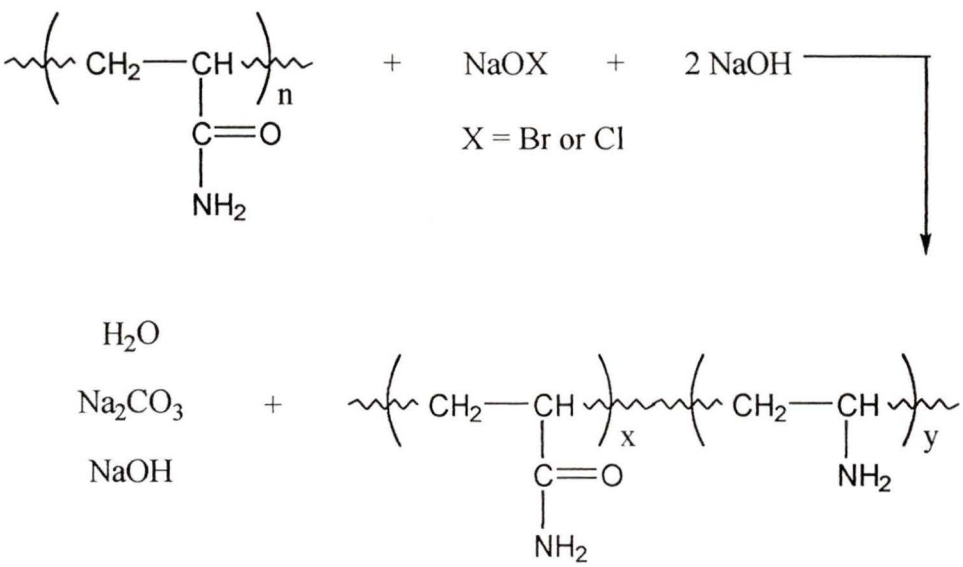

Hofmann degradation product

Fig. 1 Reaction scheme for conversion of nonionic polyacrylamides to cationic derivatives using the Hofmann degradation reaction as the first stage.

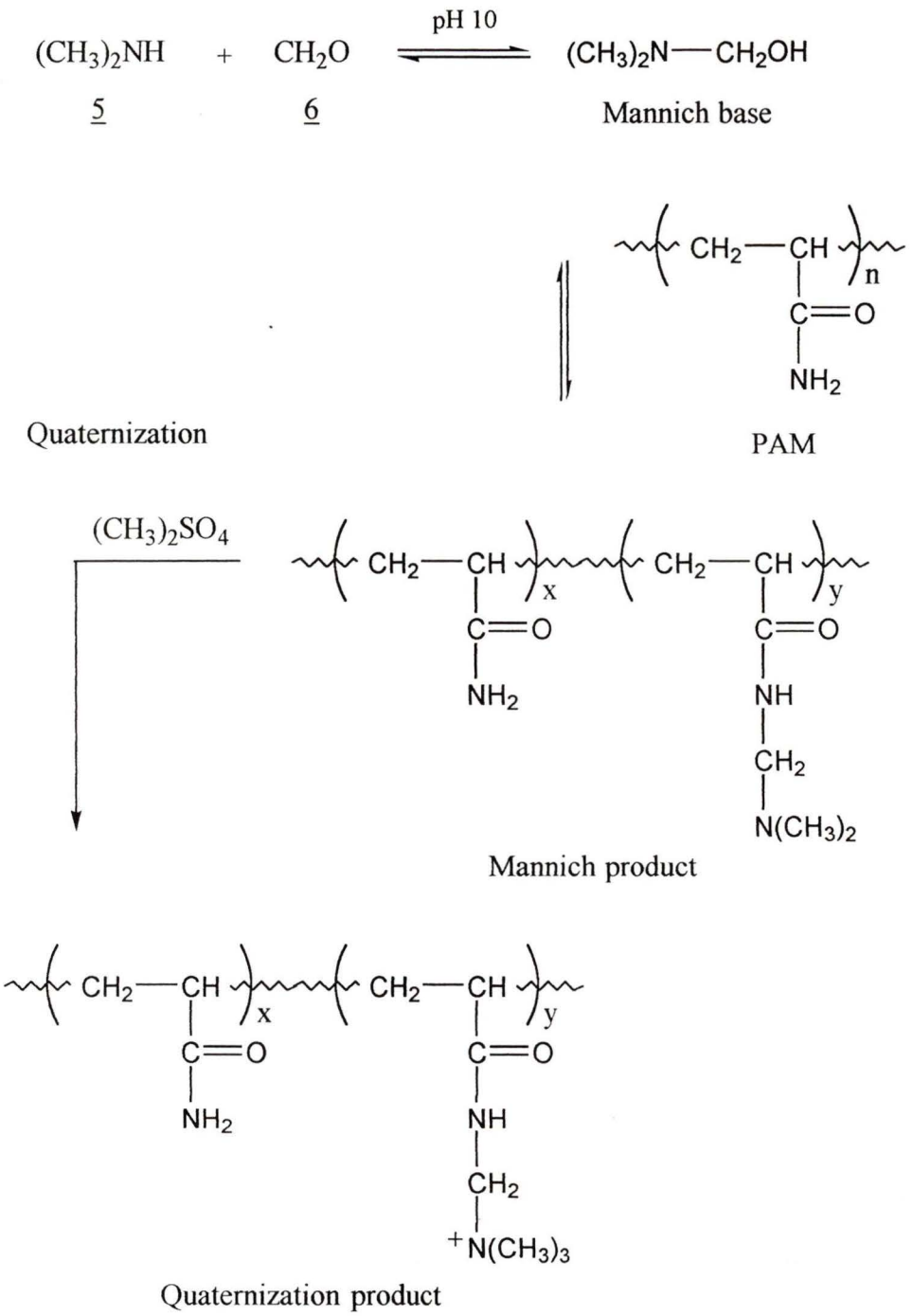

Fig. 2 Reaction scheme for cationic conversion of nonionic polyacrylamides using the Mannich reaction followed by quaternization.

1.3. Copolymerization Reactivity Ratios

By assuming that the polymer chain reactivity depends on only the monomer unit at the propagating end of the polymer chain, the propagation equations derived for homopolymerization of acrylamide (Eq. 1) can be expanded to include copolymerization of acrylamide with another vinyl-type monomer.[32]

$$
\begin{aligned}
M_1\cdot + M_1 &\xrightarrow{k_{11}} M_1\cdot \\
M_1\cdot + M_2 &\xrightarrow{k_{12}} M_2\cdot \\
M_2\cdot + M_1 &\xrightarrow{k_{21}} M_1\cdot \\
M_2\cdot + M_2 &\xrightarrow{k_{22}} M_2\cdot
\end{aligned}
\qquad \text{Eq. 7}
$$

where k_{11} is the rate constant for a propagating chain ending in $M_1\cdot$ and adding M_1.

k_{12} is the rate constant for a propagating chain ending in $M_1\cdot$ and adding M_2.

k_{21} is the rate constant for a propagating chain ending in $M_2\cdot$ and adding M_1.

k_{22} is the rate constant for a propagating chain ending in $M_2\cdot$ and adding M_2.

The mole ratio of monomer components incorporated into the copolymer can be obtained from a newly derived form of the copolymerization equation (Eq. 8).[33] Originally this equation was derived for terpolymer systems but then shown that it could be extended by inspection to these two component systems as well as for tetra- and higher monomer component systems.

$$d[M_1] : d[M_2] = \frac{[M_1]\left\{[M_1] + \frac{[M_2]}{r_{12}}\right\}\left\{1 + \frac{r_{12}}{r_{21}}\right\}}{[M_2]\left\{\frac{[M_1]}{r_{21}} + [M_2]\right\}\left\{\frac{r_{21}}{r_{12}} + 1\right\}} \quad \text{Eq. 8}$$

where $d[M_1] : d[M_2]$ is the molar ratio of the two monomer components in the copolmer.

r_{12} is the reactivity ratio defined by the ratio of the rate constant for a propagating chain ending with $M_1^{\cdot}$ and adding M_1 to the rate constant for a propagating chain ending with $M_1^{\cdot}$ and adding M_2.

r_{21} is the reactivity ratio defined by the ratio of the rate constant for a propagating chain ending with $M_2^{\cdot}$ and adding M_2 to the rate constant for a propagating chain ending with $M_2^{\cdot}$ and adding M_1.

or

$$r_{12} = \frac{k_{11}}{k_{12}} \qquad r_{21} = \frac{k_{22}}{k_{21}} \quad \text{Eq. 9}$$

For reactivity ratios greater than unity the propagating radical, $M_1^{\cdot}$, preferentially adds M_1 instead of M_2 and for reactivity ratios less than unity the propagating radical, $M_1^{\cdot}$, preferentially adds M_2 instead of M_1.

1.4. Light Scattering and the Solution Behaviour of Polyacrylamide

A key feature of interest of a macromolecule in solution is its molecular size. Various methods are available to probe this such as viscometry, gel permeation chromatography, osmometry, and light scattering. Use of viscometry or gel permeation chromatography requires prior calibration to standards which are structurally similar to those intended for analysis and osmometry requires a membrane suitable for the particular macromolecule.[34] Although the reliability of light scattering data may be affected by the macromolecule size, the size information derived from light scattering data is generally considered absolute.[35] In addition, graphical procedures are available to treat the light scattering data and extract values for the weight average molecular weight, the root mean squared radius, and the second virial coefficient which otherwise would require three separate experiments.

The interaction of light with matter can be interpreted by quantum physics as it pertains to spectrophotometry, or by a classical approach as it pertains to light scattering.[35-39] Even though the scientific origins of spectrophotometry and light scattering differ, they are directly related with respect to experimentation. Light incident upon a sample may absorb if the energy of the light matches the energy spacing of quantum states, or may be transmitted if the energy of the light does not match the energy spacing of quantum states. In addition, the incident light may interact with the electrons in molecules of the sample, which is then redistributed in all directions as scattered light. Since the intensity of scattered light is much less than the intensity of absorbed light, the portion of the spectrum which is generally free from absorption peaks is used for light

scattering studies.

A light wave may be thought of as a rapidly oscillating electric field having a frequency of approximately 10^{15} Hz.[34] Interaction of the light wave with a solute particle induces oscillation of the polarizable electrons of the solute particle at the same frequency as the incident light wave. Polarizable electrons are present in a random orientation in the absence of an applied electric field which is ordered in the presence of an applied electric field.[34,36,39] An oscillating electric field is radiated in all directions from each solute particle. Even though the different refractive index of the scattering solution as compared to vacuum of the incident light alters the wavelength and velocity of the light upon entering the solution, scattered light having the same wavelength and velocity as the incident light is collected from the scattering cell (Rayleigh scattering). The intensity of the scattered light is given by the square of the amplitude of the associated electric field and, in general, the scattered intensity depends on $1/(\lambda)^4$, the scattering angle θ, and the polarizability of the molecules.

For solute particles having diameters much less than the wavelength of incident light (Rayleigh scattering) the polarizable electrons all oscillate together in phase, and radiate waves which are in phase. As such, a direct relationship is obtained between the scattered wave amplitude and the number of polarizable electrons times the incident wave amplitude. Since the number of polarizable electrons is proportional to the average molecular weight of the solute particles, a proportionality constant based on the optical properties of the analyte solution can be formed to relate the scattered intensity to the average molecular weight of the solute particles.[40]

$$I_s = f(n_p, n_s)\ (M_W)^2\ I_0 \qquad \text{Eq. 10}$$

where I_s is the scattered intensity.

$f(n_p, n_s)$ is a function of particle refractive index, n_p, and solvent refractive index, n_s, which serves as the proportionality constant to relate the scattered intensity to the average molecular weight.

M_w is the weight average molecular weight.

I_0 is the intensity of the incident light.

For solute particles having diameters which approach the wavelength of the incident radiation, Eq. 10 is altered to account for scattering from different positions within the same particle and the destructive interference by the scattered rays. A form factor which is related to the distance between scattering centers in a molecule is used to modify the Rayleigh theory to extend its application to solute particles having diameters comparable to the wavelength of the incident radiation.

The method of Zimm, or the method of Debye can be used to obtain the size of the solute molecules as recorded by the root mean squared radius of gyration, $< r_g >$, by graphical procedures which involve plotting the scattered intensity versus the angular dependence or the reciprocal scattered intensity versus the angular dependence, respectively.[35,37,38] By extrapolating the plots to zero concentration and zero angle, the weight average molecular weight, M_w, is obtained. M_w is defined by the following equation.[41]

$$M_W = \frac{\sum c_x M_x}{\sum c_x} = \frac{\sum c_x M_x}{c} = \frac{\sum N_x M_x^2}{\sum N_x M_x} \qquad \text{Eq. 11}$$

where c_x is the weight concentration of molecules.

M_x is the individual weight of the molecules.

c is the total weight concentration of all polymer molecules.

N_x is the number of moles of molecules.

Extrapolating the Debye or Zimm plot to zero concentration gives $< r_g >$ whereas extrapolating to zero angle gives the solute / solvent interaction parameter, A_2.

1.4.1. Polyacrylamide and its conformation in aqueous solution

Dissolution of a nonionic macromolecule in an aqueous solvent constitutes reorganization of water molecules to accommodate the macromolecule. The structure of the aqueous solvent consists of individual tetrahedra which are linked by hydrogen bonding to give some short range order to the liquid. Incorporation of a nonionic macromolecule into the aqueous solvent is interpreted by the free energy required to create a cavity in the solvent and the interaction energy between the macromolecule with water molecules.[42,43] With respect to polyacrylamide, incorporation into an aqueous solvent involves a positive free energy contribution from the increased ordering of water tetrahedra around the apolar, polymer backbone. In contrast, a negative free energy contribution results from the disruption of any interamide hydrogen bonds by competitive hydrogen bonding by water molecules. For a polar macromolecule like polyacrylamide

the net free energy contribution is negative which causes dissolution of polyacrylamide in the aqueous solvent. In addition, the competitive hydrogen bonding by water molecules with interamide hydrogen bonds interfers with any ordered structure of polyacrylamide to yield the solution conformation as a random coil.[42]

1.4.2. Polyacrylamide and the effect of electrolyte concentration on $< r_g >$

Similar to dissolution in an aqueous solvent, solubilization of a nonionic macromolecule in an aqueous salt solution involves reorganization of the solvent structure to accommodate the macromolecule. However, the association of water tetrahedra around ions may add greater order to the structure of the aqueous salt solution than an aqueous solvent without added electrolyte.[44] Many physical measurements have been used to try to quantify salting-in and salting-out of macromolecules such as dielectric constant, internal pressure, Langmuir-type isotherms, surface tension, cloud point, and heats of dilution.[45] With respect to polyacrylamide in an aqueous electrolyte solution, it was reported that solubility changes were governed by the repulsion of ions by the hydrophobic groups of the macromolecule. Although variations in ionic radius and the charge of ions can show varied behaviour with respect to the stabilization and destabilization of the macromolecule conformation,[42,44] some studies report an increase in $< r_g >$ for an increase in concentration of added electrolyte.[45-47] One of several explanations offered for this was the increased "goodness" of the solvent with increased concentration of added electrolyte as attributed to the higher dielectric constants of aqueous solvents with increased concentration of added electrolyte. However, studies

which contradict this trend in $< r_g >$ establish that there is no reliable theory that successfully predicts the effect of electrolyte concentration on polymer chain extension.[48]

1.4.3. Polyelectrolytes and the effect of electrolyte concentration on $< r_g >$

Unlike dissolution of a nonionic macromolecule in an aqueous salt solution, dissolving a polyelectrolyte in an aqueous salt solution involves association of salt ions with the charged groups of the polyelectrolyte. The association of salt ions with the polyelectrolyte and release of water molecules from solvated ions to the bulk of solution imparts an entropy increase to the water molecules and thermodynamic favorability to dissolving a polyelectrolyte in an aqueous salt solution.[42]

The solution behaviour of a polyelectrolyte in an aqueous salt solution depends on solution pH, the valency and concentration of the salt solution, and the charge density and charge type of the polyelectrolyte.[2] However, the mobility of counterions to the charged groups of the polyelectrolyte controls the polyelectrolyte chain extension. Greater polyelectrolyte chain extension is observed in dilute salt solutions rather than in more concentrated salt solutions. This is attributed to increased diffusion of the mobile counterions from within the polyelectrolyte domain to outside the polyelectrolyte in dilute salt solutions, and suppressed diffusion of the counterions from within the polyelectrolyte in more concentrated salt solutions. Since the solution conformation of the polyelectrolyte is influenced by the repulsive interactions between neighboring charged groups of the polyelectrolyte, the concentration of counterions in the vicinity of the charged groups of the polyelectrolyte affects the magnitude of the electrostatic force

between charged groups. As the concentration of counterions increases, the relative permittivity of the area between charged groups increases which reduces the electrostatic force between the charged groups.[34]

1.5. Flocculation

For raw and waste-water clarification, sludge dewatering, mineral processing, papermaking, and other industrial processes, efficient solid / liquid separation is necessary to allow rapid separation or drainage of the liquid phase from a suspended solids phase, to minimize the solids remaining in the liquid phase, and to maximize the solids content in the suspended solid phase.[49]

1.5.1. Interactions between colloid particles

Small suspended particles or colloids impede the solid / liquid separation of many industrial water streams.[1,49] This type of colloid is classified as lyophobic due to a distinct solid and liquid phase. In general, colloid particles have diameters ranging from 0.1 μm to 1.0 μm, although various colloid dispersions are known to contain particles outside this range.[50-53]

Inorganic coagulants based upon the hydrolyzable salts of aluminum and iron, and polymeric flocculants of the acrylamide type are used to increase the efficiency of solid / liquid separations. Coagulation refers to the agglomeration of suspended particles by the addition of inorganic flocculants and flocculation refers to the agglomeration of suspended particles by the addition of polymeric flocculants.[49,52,54] Even though synthetic polymeric flocculants are more expensive, they produce flocs which are larger, stronger,

and formed more rapidly to give much smaller settled sludge volumes than can be obtained with inorganic coagulants.[49]

Contributions to free energy originate from three basic types of interactions between particles: Van der Waals, electrostatic, and steric. The total free energy is the summation of contributions from these interactions and represents the free energy component of the free energy versus particle separation graphs.[51,55]

Van der Waals interactions

In general, Van der Waals interactions are defined by the following equation.[51,55]

$$V_{vdW} = -A_{12}\, f(h) \qquad \text{Eq. 12}$$

where V_{vdW} is the free energy contribution from Van der Waals interactions.

A_{12} is the material constant or Hamaker constant which is characteristic of the particles 1 and 2 but independent of particle geometry.

$f(h)$ is a function depending on the particle distance and shape but independent of the nature of particles 1 and 2.

In deriving the Hamaker constant the attraction energy between similar particles and different particles as well as the effect on a solution medium by attractive forces bringing two particles together are included. Two identical particles always give a positive Hamaker constant and, therefore, a negative V_{vdW}, which indicates attraction. Two different particles may give a negative Hamaker constant and, therefore, a positive V_{vdW}, which indicates repulsion. Due to a more rapid decay of Van der Waals forces at larger particle separations than can be accounted for by the relations for $f(h)$, a correction

factor is applied to Eq. 12. As expected, strong Van der Waals attractive forces predominate at short particle separations and weak forces are experienced at large particle separations.[56]

Electrostatic interactions

Due to the preferential adsorption of certain ionic species, dissociation of surface groups, and isomorphic substitution, the colloid particles typically bear a charge in solution and in many cases this charge is negative.[51,55,58] The interaction between colloid particles as a consequence of the charge type and surface potential of the particles is classified as electrostatic. Interpretation of the electrostatic forces between particles is governed by DLVO theory - named after Derjaguin, Landau, Verwey, and Overbeek.[50,51,58] In principle the colloid particle is surrounded by an electric double layer which yields electroneutrality to the surface charge (Fig. 3). Included in the electric double layer is a monolayer of counterions termed the Stern layer which is generally slightly less than the amount required to achieve complete neutralization of the surface charge of the colloid particle. The balance of the neutralization of the surface charge occurs in a diffuse outer layer termed the Gouy-Chapman layer. Based on the principles of electrostatics, colloid particles with like charges repel and, even though the electric double layers are electroneutral, DLVO theory predicts repulsion between the double layers of colloid particles. This is because the interaction of double layers and subsequent mixing of counterions is entropically unfavorable such that work must be done to bring the particles closer together. Although there are various equations in the

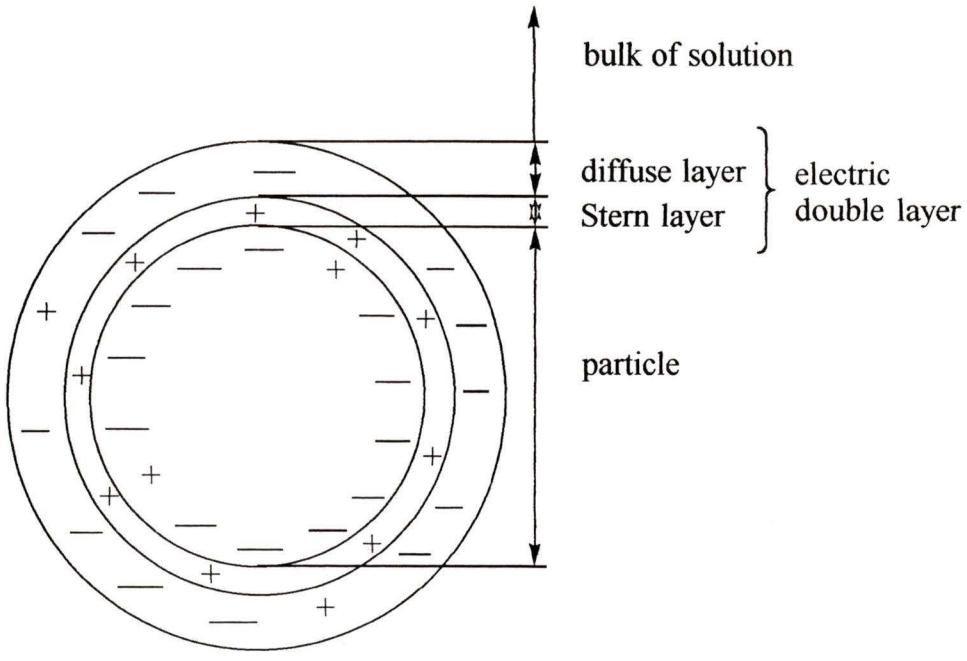

Fig. 3 Diagram of the electric double layer surrounding a colloid particle suspended in solution

literature for the contribution of electrostatic interactions to free energy, the dominant factor in the equations which is used to influence the electrostatic interactions of colloid particles is the double layer thickness or reciprocal Debye length, κ^{-1}.[50,51,61]

$$\kappa^{-1} = \left(\frac{\varepsilon \varepsilon_0 RT}{\sum_i z_i^2 c_i F^2} \right)^{0.5} \qquad \text{Eq. 13}$$

where z is the valency of the electrolyte.

c is the electrolyte concentration.

F is the Faraday constant.

ε is the relative dielectric constant of the medium.

ε_0 is the permittivity of free space.

RT is the thermal energy.

As shown by Eq. 13, the double layer thickness is influenced by the valency and concentration of added electrolyte, upon interaction of the ions with the colloid particles.

Steric interactions

The addition of polymer to a colloidal dispersion can either stabilize the dispersion or destabilize the dispersion and, therefore, cause the aggregation of colloid particles. Whereas stabilization contributes to a positive free energy and, therefore, repulsion, destabilization contributes to a negative free energy and, therefore, attraction.

Stabilization or protection occurs generally for high concentrations of polymer and / or the dispersion medium having a high affinity for the polymer. As such, the colloid

particles are covered by a polymer sheath and the affinity of the dispersion medium for the polymer yields repulsion to the approach of covered particles.[51,59,60,61]

Destabilization of a colloidal dispersion and, therefore, aggregation of the colloid particles can be achieved through polymer addition by increasing the susceptibility of the colloid particles to added electrolyte (sensitization), or by flocculating the system.[51,54,60,61] Sensitization or incipient flocculation is likely for polymers with a higher affinity for polymer chain association than the dispersion medium or the colloid particles. As such, the colloid particles are forced together by excluding them from the polymer domain of the solution and, therefore, exposed to higher local concentrations of added electrolyte. Polymeric flocculation involves the interaction of the polymer chains with the colloid particles to either bridge the barrier between colloid particles or reduce the repulsion between particles by virtue of charged polymers.

1.5.2. Total free energy contribution to colloid stability

Fig. 4 is a typical representation for the plot of total free energy, G, versus particle separation, h, for colloid particles suspended in an aqueous solution.[50,51,61] The primary minimum at small particle separations is attributed to short range Van der Waals attractive forces. At sufficient depth the primary minimum represents irreversible coagulation. The steep rise in free energy for very small particle separations is attributed to strong repulsion as a result of orbital overlap. G_{max} represents electrostatic repulsion between the double layers of colloid particles. If G_{max} is much greater than the thermal energy (kT) then coagulation is very slow. Increasing the electrolyte concentration or

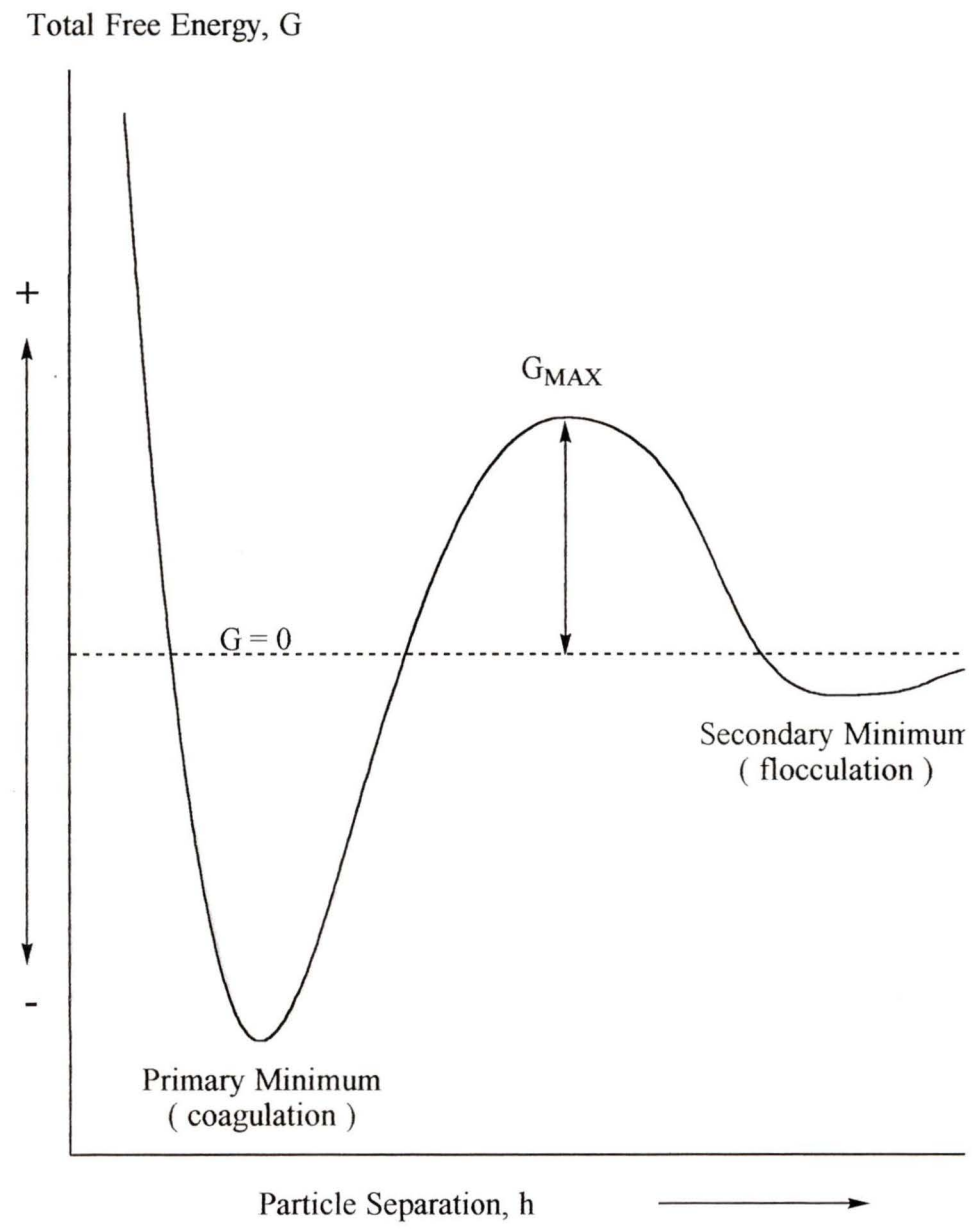

Fig. 4 Diagram of total free energy versus particle separation for colloid particles suspended in solution

electrolyte valency of the added electrolyte reduces the double layer thickness and, therefore, reduces G_{max} and promotes coagulation. Charged polymers have a similar effect on G_{max} as added electrolyte.

The secondary minimum at larger particle separations is attributed to flocculation whereby the polymers bridge the barrier between colloid particles. Generally, the secondary minimum is shallow because flocs are susceptible to shearing forces from agitation. Although not shown by Fig. 4, stabilization of the colloidal dispersion by polymer addition would cause the plot to be shifted a distance representative of the thickness of the polymer sheath covering the colloid particles and their associated repulsion.

1.5.3. Polymeric flocculants and flocculation mechanisms

Polymeric flocculants are classified by charge type, charge density, and molecular weight. Whereas anionic and cationic polymers are categorized as polyelectrolytes, nonionic polymers may be regarded as non-electrolytes. Low, medium, high, and ultrahigh molecular weights correspond to 10^4 - 10^5 g/mol, 10^5 - 10^6 g/mol, 10^6 - 5×10^6 g/mol, and above 5×10^6 g/mol, respectively.[49] Charge density refers to the mol % of charged groups in the polyelectrolytes and extends from very low values of 5 - 10 mol % to 100 mol %.

Both nonionic polymers and polyelectrolytes having low charge densities and each having either high or ultrahigh molecular weights function as flocculants by a bridging mechanism (Fig. 5).[49,54,61] Polymer bridging involves adsorption of small segments of the

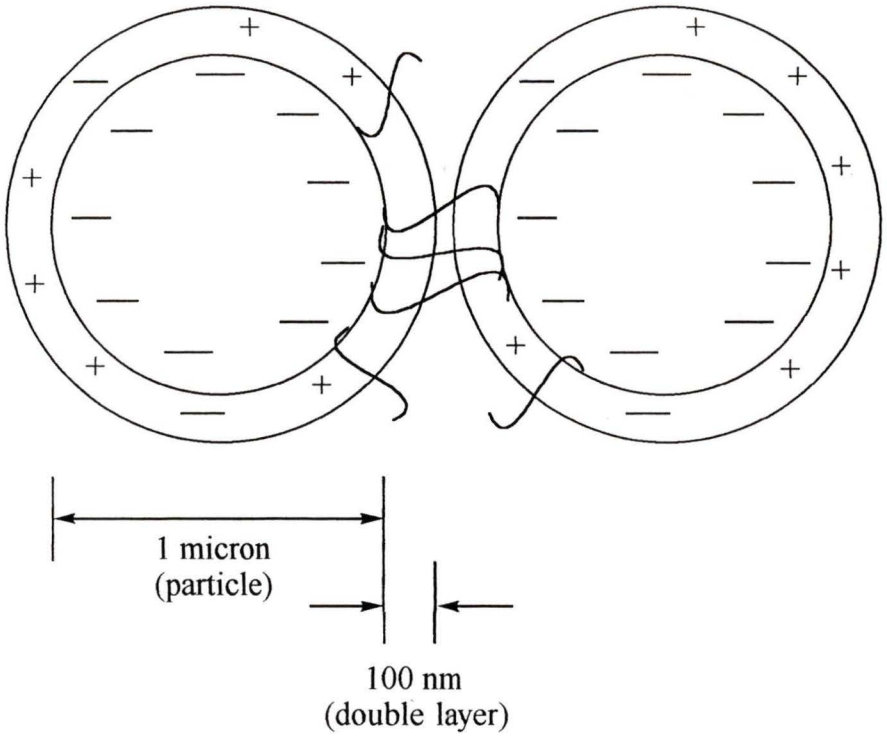

Fig. 5 Diagram of colloid particle aggregation by polymer bridging

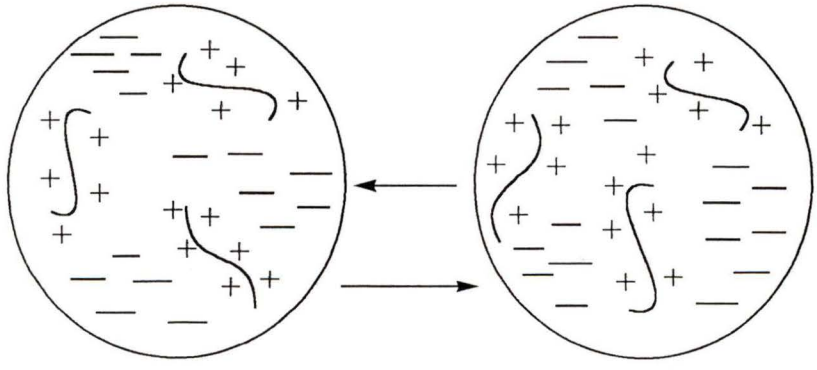

Fig. 6 Diagram of colloid particle aggregation by charge neutralization involving the electrostatic patch mechanism

polymer chains on colloid particles so as to leave loops or trains dangling in solution. If the loops or trains are sufficient in extension to overcome the barrier imposed by electrostatic interactions, and therefore, κ^{-1}, and the polymer chains do not have a high affinity for the dispersion medium, then polymer bridging is favourable.[49,51]

Polyelectrolytes having low or medium molecular weights, moderate charge densities, and charge types opposite to that of the colloid particles function as flocculants by charge neutralization and, therefore, the electrostatic patch mechanism (Fig. 6).[49,54,61,62] Charge neutralization involves the adsorption of the polyelectrolyte in a flat conformation on the oppositely charged surface of the colloid particles. By neutralizing the surface charge of the colloid particles the double layer thickness is reduced which reduces G_{max} and allows closer approach of the colloid particles. Coagulation of the colloid particles occurs by an electrostatic patch mechanism whereby alternating positively and negatively charged patches on each particle interact electrostatically.

1.5.4. Flocculation kinetics

Although there are many models for flocculation kinetics in the literature, the lack of agreement between the various models illustrates the complexity of the flocculation process.[49,54,55,63,64] In spite of this lack of agreement, it is generally accepted that flocculation develops from four distinct processes; adsorption, re-conformation, aggregation, and degradation as shown in Fig. 7.[54]

Adsorption

Depending on the system, adsorption of nonionic polymers may occur by

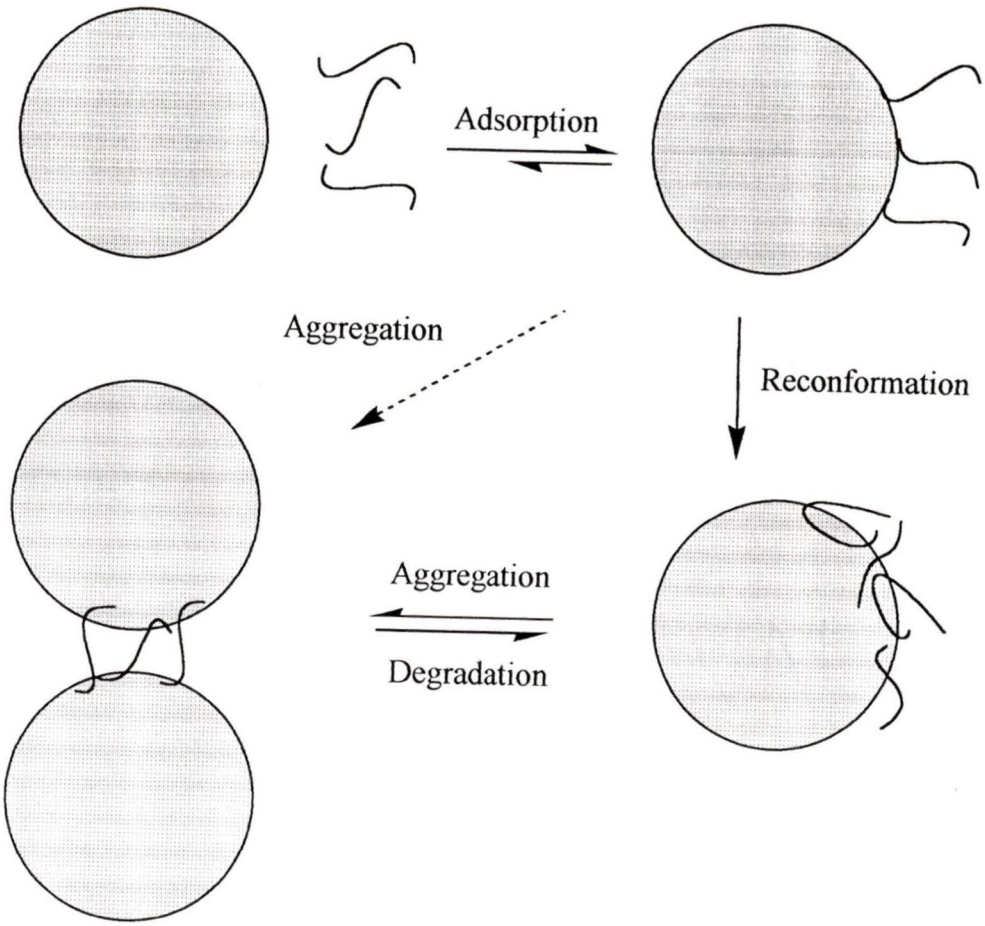

Fig. 7 Diagram of the four distinct processes which contribute to flocculation; adsorption, reconformation, aggregation, and degradation

hydrophobic association, hydrogen bonding, or dipole / crystal interactions. In general, adsorption of nonionic polymers is rapid and irreversible.[49,60]

Polyelectrolytes containing charged groups which are opposite in charge to the surface charge of the colloid particles adsorb by electrostatic interaction, and therefore, charge neutralization. When polyelectrolytes contain charged groups of the same sign as the colloid surface charge, colloid particles can absorb by complexation with inorganic ions. Adsorption to achieve charge neutralization is reversible.[60]

Re-conformation

Flocculation which involves agitation (orthokinetic flocculation) increases the rate of collisions relative to polymer adsorption and / or colloid particle aggregation processes. The probability for re-conformation of the polymer chains to adopt an equilibrium conformation is affected by the collision rate as well as the concentration of the colloidal dispersion.[49,54,60] On the one hand rapid agitation and concentrated colloidal dispersions reduce the probability for polymer chain re-conformation, whereas mild agitation and dilute colloidal dispersions increase the probability for polymer chain re-conformation. Since polyelectrolytes have the ability to function as flocculants by bridging or the electrostatic patch mechanism, conditions which oppose re-conformation as well as polymer chains which lack the flexibility necessary for re-conformation favour bridging flocculation.

Aggregation

Aggregation of colloidal particles is related to the collision rate of particles which

have adsorbed polymer and, therefore is affected by agitation. Since several polymer bridges are necessary to form flocs capable of withstanding the shearing forces of agitation, the concentration of the colloidal dispersion and the agitation rate may affect the floc strength and size by favouring either particle / particle collisions or polymer / particle collisions.[49,54] Particle / particle collisions limit floc size and strength since some collisions result in the collapse of polymer bridges, whereas polymer / particle collisions give improved polymer adsorption which improves floc size and strength.

Degradation

Aggregation of colloid particles to form flocs is controlled by an opposing reaction (degradation) which breaks flocs.[54,60] Since polymer bridges are more susceptible to the shearing forces of agitation than the electrostatic interactions of the electrostatic patch mechanism, degradation has a greater effect on the floc size when it forms via the bridging mechanism. In addition, the efficiency of bridging flocculation to solid / liquid separation is hampered by the irreversible adsorption of polymer in bridging flocculation. The efficiency of the electrostatic patch mechanism is affected to a lesser degree by degradation owing to reversible adsorption.

1.6. Purpose of the Research

The purpose of this research was to investigate the effect of steric bulk on polymer chain extension as it might be affected by the degree of steric hindrance and the proximity of the bulky group to the polymer backbone. To do this, the steric bulk was limited to the alkyl groups of substituted acrylamides which included N,N-

dimethylacrylamide 2, methacrylamide 3, and N-t-butylacrylamide 4 . Each substituted acrylamide was copolymerized with acrylamide 1 at various proportions using conditions to maximize the percentage conversion of monomer to polymer and the copolymer molecular weight (Eq. 14, 15, 16).

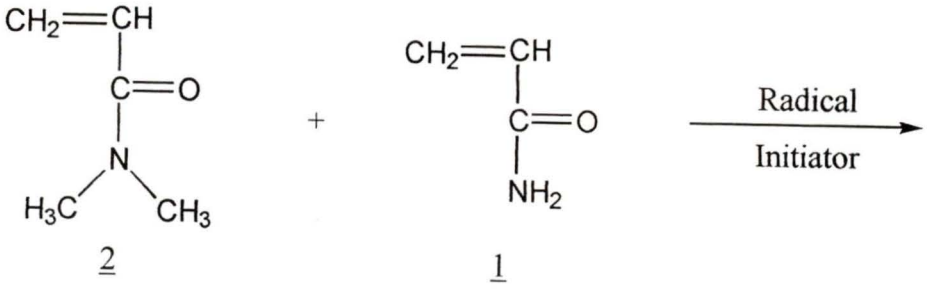

Eq. 14

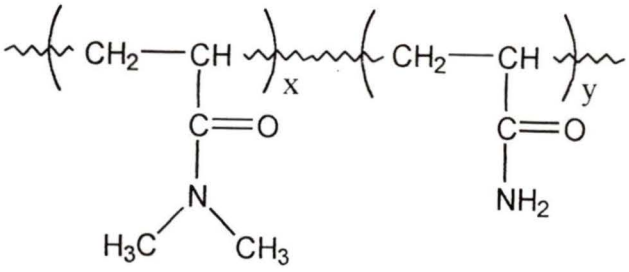

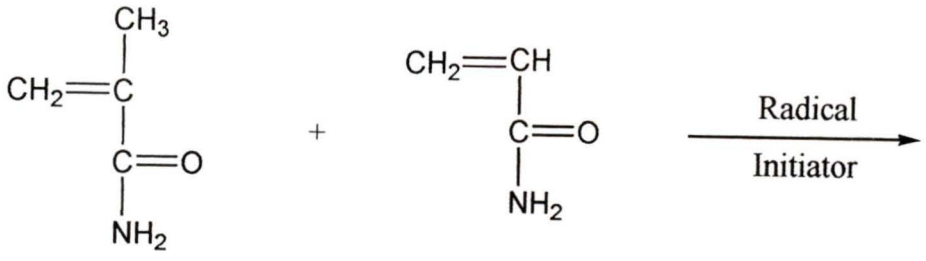

3 1

Eq. 15

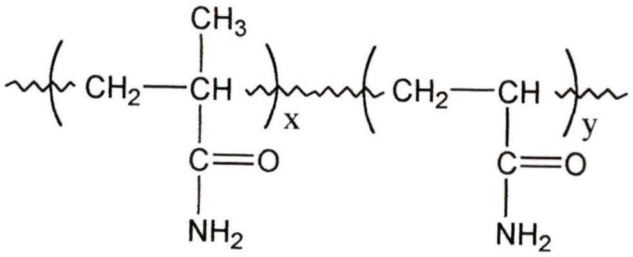

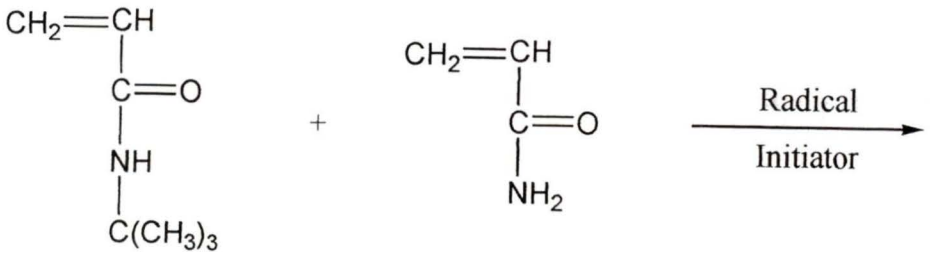

4 1

Eq. 16

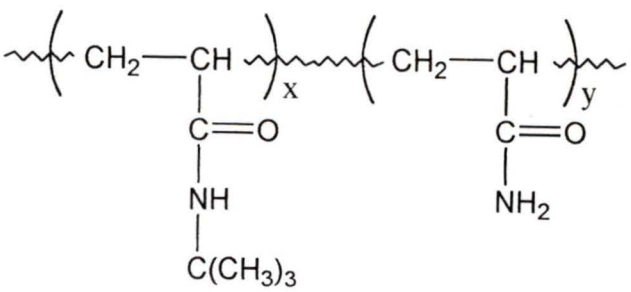

High percentage conversions of monomer to polymer and high copolymer molecular weights were wanted, both for their commercial value, and to compare the

copolymerization aptitude of the comonomers to the homopolymerization of acrylamide, itself. Also, the high copolymer molecular weights were wanted to gauge the flocculant ability of the new copolymers against polyacrylamide, itself, as well as commercial flocculants. High copolymer molecular weights were needed for this purpose because the nonionic acrylamide-based polymers are known to function as flocculants by a bridging mechanism which is favoured by high polymer chain extension and, therefore, high polymer molecular weights.[49,54]

Since the kinetics for homopolymerization of acrylamide favoured rapid rates to achieve high molecular weights,[13] it was reasoned that substituted acrylamides exhibiting steric bulk would not sacrifice much reactivity in comparison to acrylamide. In addition, it was felt that the structural similarity of the substituted acrylamides to acrylamide would facilitate copolymerization of each substituted acrylamide with acrylamide. N,N-dimethylacrylamide, methacrylamide, and N-t-butylacrylamide were selected as comonomers for copolymerization with acrylamide based on their range in the degree of steric hindrance and its proximity to the polymer backbone. In addition, each of the substituted acrylamides was reported to be soluble in water which was conducive to the conditions necessary for homopolymerization of acrylamide to high molecular weight.[1,14,15,66] Also, reactivity ratios were published for the copolymerization of N,N-dimethylacrylamide and methacrylamide with acrylamide.[1,18] In both cases the substituted acrylamide comonomer was slightly favoured for incorporation into the copolymer.

It was intended for this research to use multi-angle laser light scattering (MALLS)

in the batch mode to determine the polymer chain extensions recorded as the root mean squared radius of gyration, $< r_g >$, for the newly synthesized polymers. From these measurements it was thought that the effect of steric bulk on $< r_g >$ could be gauged within each copolymer series and against $< r_g >$ for polyacrylamide, assuming insignificant differences in the number average degree of polymerization, X_n, within each copolymer series and in relation to polyacrylamide. Also, it was intended to gauge the impact of steric bulk size and proximity to the polymer backbone by comparing the $< r_g >$ values from the three copolymer types, assuming insignificant differences in X_n among the three copolymer types.

Reports that the solution conformation of polyacrylamide was resistant to solvent pH but susceptible to added electrolyte,[1,46,47] the procedure of using polyacrylamide as controls, and reports that the polymer chain extensions of anionic and cationic polyacrylamides were greater than that of nonionic polyacrylamide[65] except in high electrolyte containing waste-water streams helped to direct research towards the solution behaviour of the polymers. It was planned to investigate the resistance of the newly synthesized acrylamide-based copolymers and commercial polymers which included cationic and anionic polyacrylamide to solvents containing added electrolyte and solvents at various pH levels. Electrolyte concentrations and solvent pH levels were selected to cover a broad range to explore potential commercial applications under these conditions.[1,2]

As research progressed, it became apparent that important information could be obtained about the impact of steric bulk to increasing polymer chain extension by

functionalizing a particular copolymer of each copolymer series and polyacrylamide, itself, to include charged groups for a constant kinetic chain length. Patents involving the Mannich reaction followed by methylation to introduce cationic groups into polyacrylamide as quaternized amines for a constant kinetic chain length[1,28-31] directed research toward preparing the cationic derivatives of the newly synthesized, acrylamide-based copolymers. It was planned to compare the polymer chain extensions of the cationic derivatives of the three copolymer types and the cationic derivative of polyacrylamide with the polymer chain extensions of their nonionic precursors, knowing constant values of X_n between the derivatives and the precursors.

Originally, flocculation test-work was intended to compare the flocculant ability of the newly synthesized, acrylamide-based polymers to commercial flocculants by using ASTM or ISO/CD flocculation test procedures.[67,68] However, the successful measurement of the polymer chain extensions by MALLS in the batch mode redirected research towards the development of a flocculation test procedure which was sensitive to polymer structure and polymer chain extension in order to be able to link the solution behaviour of the polymers to flocculation performance. This focussed experiments on the effects of the chemical and physical variables of flocculation as they related to flocculation kinetics and the bridging mechanism. Again, like the polymerizations and the study of the solution behaviour of the acrylamide-based polymers, the flocculation performance of the newly synthesized polyacrylamide was to be used as a baseline for comparing the performance of the newly synthesized, acrylamide-based polymers and commercial polymeric flocculants of the Percol trade-name.

It was determined that flocculation parameters such as average settling rates, 30 minute supernatant turbidities, sediment volumes, and capillary suction times would be measured. These results would then be related to polymer chain extension and polymer structure for the newly synthesized polymers and commercial polymers. In this way it was hoped that the effects of molecular size and charge, low and high concentrations of electrolyte, and low and high pH's could be correlated to the flocculation performance of well defined, consistent solid suspensions.

1.7. Glossary of Acronyms

AM	- acrylamide
DMAM	- N,N-dimethylacrylamide
MeAM	- methacrylamide
NTBAM	- N-t-butylacrylamide
PAM-1 to -5	- homopolymerization experiments of AM
PDMAM-1 to -3	- homopolymerization experiments of DMAM
PMeAM-1 to -5	- homopolymerization experiments of MeAM
PNTBAM-1 to -14	- homopolymerization experiments of NTBAM
control	- homopolymerization of AM
PAM	- polyacrylamide
PDMAM	- poly (N,N-dimethylacrylamide)
PMeAM	- poly (methacrylamide)
PNTBAM	- poly (N-t-butylacrylamide)
DMAM-co-AM-2 to -7	- copolymerization experiments of DMAM with AM
MeAM-co-AM-2b to -6	- copolymerization experiments of MeAM with AM
NTBAM-co-AM-1a to -6b	- copolymerization experiments of NTBAM with AM
poly (DMAM-co-AM)	- poly (N,N-dimethylacrylamide-co-acrylamide)
poly (MeAM-co-AM)	- poly (methacrylamide-co-acrylamide)
poly (NTBAM-co-AM)	- poly (N-t-butylacrylamide-co-acrylamide)

2. Experimental

2.1. Chemicals

Acrylamide (m.p. found: 82-84°C (uncorr.), catalogue: 84.2-84.8°C), N-t-butylacrylamide (97%) (m.p. found: 126-127°C (uncorr.), m.p. catalogue: 128-129°C), and methacrylamide (99%) (m.p. found: 108-110°C (uncorr.), m.p. catalogue: 109-111°C) were from Aldrich, and were used without further purification. Aldrich N,N-dimethylacrylamide (99%) contained 500 ppm methylhydroquinone (MEHQ) which was removed using an Aldrich inhibitor removal column before use. All monomers were stored at approximately 0°C in the dark. Potassium persulfate (A.C.S. reagent grade, 99+%), dimethylamine (40 wt. % solution in water), dimethylsulfate (99+%), poly(vinylsulfate potassium salt), hexadimethrine bromide, and toluidine blue O were from Aldrich, methanol (99.8%) and t-butanol (98%) were from BDH, formaldehyde (37 wt. %, A.C.S. reagent grade), formic acid (88%), glacial acetic acid, sodium hydroxide, hydrochloric acid, and sodium chloride were Fischer reagent grade materials, and all were used without further purification. Azobisisobutyronitrile (AIBN) was from Fluka and was recrystallized twice from methanol before use.

Acrylamide was homopolymerized under UHP nitrogen (< 5 ppm O_2, Linde), research grade oxygen (99.999%, Air Gas), and filtered air (compressed air passed through a water trap). Copolymerization of acrylamide with N,N-dimethylacrylamide, acrylamide with N-t-butylacrylamide, and acrylamide with methacrylamide were done under UHP nitrogen (< 5 ppm O_2, Linde). Except where specified otherwise, distilled

water was used throughout as the polymerization medium and for dialysis.

Percol 351 (nonionic polyacrylamide, 20 million mol. wt., batch BOP2293B, July '93), Percol E-24 (10% hydrolyzed polyacrylamide, 15 million mol. wt., batch BEX2322A, July '93), and Percol 721 (ca. 10% cationic polyacrylamide, 20 million mol. wt., batch 74630 Jan '91) were obtained from Allied Colloids (Canada) Limited.

Polyacrylamide (nonionic, 500,000 mol. wt., lot no. 430449), polyacrylamide (nonionic, 1 million mol. wt., lot no. 95-6), and polyacrylamide (nonionic, 5,550,000 mol. wt., lot no. 433680) were obtained from Polysciences Incorporated.

Kaolinite used for the flocculation experiments was Reed Creek Sample Number RC-32, Lot Number T187 obtained from the Tiele Kaolin Company. Heteroionic Kaolinite was converted to its sodium form (Na-Kaolinite) before use by the procedure described by Van Olphen.[69]

2.2. Equipment

Melting points were measured using a Gallenkamp, Al block melting point apparatus, and are uncorrected. Glassware used for the homopolymerizations and copolymerizations was soaked in hot nitric acid (70 - 71%), washed with soap and water, rinsed with distilled water, soaked in distilled water, and finally oven dried at 120°C.

Dialysis of polymer solutions was performed using Spectra/Por membrane tubing (3500 molecular weight cut-off (MWCO), Spectrum).

Freeze-dried polymer was forced through a 100 mesh screen within a sample grinding instrument (Sample Processing Instrument, CANLAB).

The Accumet Model 50 pH / ion / conductivity meter equipped with a temperature probe, Fisher brand combination electrode, and Fisher brand conductivity electrode was used for all solution pH adjustments and measurements as well as measurement of the specific conductance of the supernatant of homoionic Na-kaolinite.

A Bruker 113v FTIR spectrometer fitted with a Princeton Applied Research Corporation Model 6003 photoacoustic cell and Model 6005 preamplifier was used to record photoacoustic-FTIR (PAS-FTIR) spectra of the copolymers and homopolymers at a resolution of 8 cm^{-1} with a mirror velocity of 0.059 cm/s. The carrier gas above the solid copolymer samples was nitrogen.

The Bruker AMX 360 NMR Spectrometer was used to record 90.55 MHz ^{13}C NMR spectra for acrylamide-based homopolymers and copolymers. The operating details for the spectrometer included a spectral width of 20,000 Hz, quadrature detection, a 30,000 Hz filter width, and 16 bit digitizer resolution. Spectra were run using inverse gated decoupling, a pulse width of 12.0 μs (90 degrees), a dead time delay of 30 μs, and a recycle delay of 5 s, unless stated otherwise. Trichloromethane (δ 74.4) was used as an external chemical shift reference for the ^{13}C NMR spectra.

A Bruker MSL 200 MHz NMR Spectrometer was used to record 50.3 MHz ^{13}C NMR spectra for some of the acrylamide-based homopolymers and copolymers. The operating details for the spectrometer included a spectral width of 25,000 Hz, quadrature detection, a 30,000 Hz filter width, and 12 bit digitizer resolution. Spectra were run using broad band decoupling. Deuterated methanol (δ 49.3 ppm) was used as an external chemical shift reference for the ^{13}C NMR spectra.

For elemental analysis, 20 - 30 mg of the freeze-dried polymer samples were further dried for 5 - 12 hours at ca. 60°C and < 1mm Hg pressure in a vacuum oven (National Appliance Co.). Microanalyses were performed by Canadian Microanalytical Service Ltd..

Multi-angle laser light scattering (MALLS) measurements were done using an assembly which included the Wyatt Technology Dawn DSP (Model F) laser photometer. For "batch" measurements the Wyatt Technology Dawn DSP-F laser photometer was connected to a Dell 486/33 computer which was installed with Wyatt Technology software (Dawn 2.06 with Aurora Module). For "continuous" measurements gel permeation chromatography equipment was connected to the light scattering assembly which was modified to include the Dawn DSP flow cell. In addition, Wyatt Technology software (Astra 4.00 for Windows) was installed in the Dell 486/33 computer. Included in the gel permeation chromatography equipment were the Waters In-Line Degasser, Waters Pulse Dampener, Waters 501 HPLC Pump, Waters 717 Plus Autosampler, Waters Differential Refractometer R401, and Shodex OH pak columns KB-804, -805, and -806 (polyhydroxymethylmethacrylate packing, 0.02% sodium azide in-column solvent, 4°C to 60°C useable temperature, 30 kg/cm^2 max. pressure, and 1.5 mL/min max. flow rate). The Shodex OH pak columns had the following specifications; KB-804 column with an exclusion limit of 2×10^5 to 4×10^5 mol. wt., KB-805 column with an exclusion limit of 2×10^6 to 4×10^6 mol. wt., and KB-806 column with an exclusion limit of 1×10^7 to 2×10^7 mol. wt.. Before MALLS or viscosity measurements, the polymer solutions were filtered through 0.45 μm disposable, syringe filters (MSI Cameo-II 25 mm filters: nylon

hydrophilic and PTFE membranes, polypropylene housing) and into 20 mL scintillation vials (borosilicate glass) using syringe pumps (Harvard Apparatus, syringe infusion pump 22).

Viscosity measurements were made with calibrated Ubbelohde dilution viscometers of sizes 1, 1B, 1C, and 2 using filtered polymer solutions.

Polymer samples were freeze dried by use of a Virtis, Model 10-010BA freeze drier and Na-Kaolinite and polymer samples were freeze dried by use of a Labconco Model 75200 freeze drier.

The adsorption isotherm for nitrogen gas on Na-kaolinite was measured at the Alberta Research Council laboratory in Devon, Alberta, using the Digisorb 2600 instrument. This was converted to the surface area of homoionic Na-kaolinite by the method developed by Brunauer, Emmett, and Teller.[70] In addition to size analysis, Dr. Laurier Schramm of the Petroleum Recovery Institute located in Calgary, Alberta, measured the isoelectronic point of the homoionic Na-kaolinite using the Microelectrophoresis Apparatus Mark II fitted with a rotating prism and a video viewing system.

Flocculation experiments were done with 400 mL glass beakers (7.6 cm diameters) fitted with four Plexiglass baffles each 1/10 the beaker diameter and mounted vertically against the beaker wall (Fig. 8).[71,125] A six bladed turbine impeller made from Plexiglass and having a diameter 1/3 the diameter of the beaker (2.53 cm) was fit to a stainless steel shaft driven by an overhead stirrer (Gallenkamp with digital rpm readout). A Sage syringe pump (Single-Channel Model 341B) was used to add the polymer solution to the

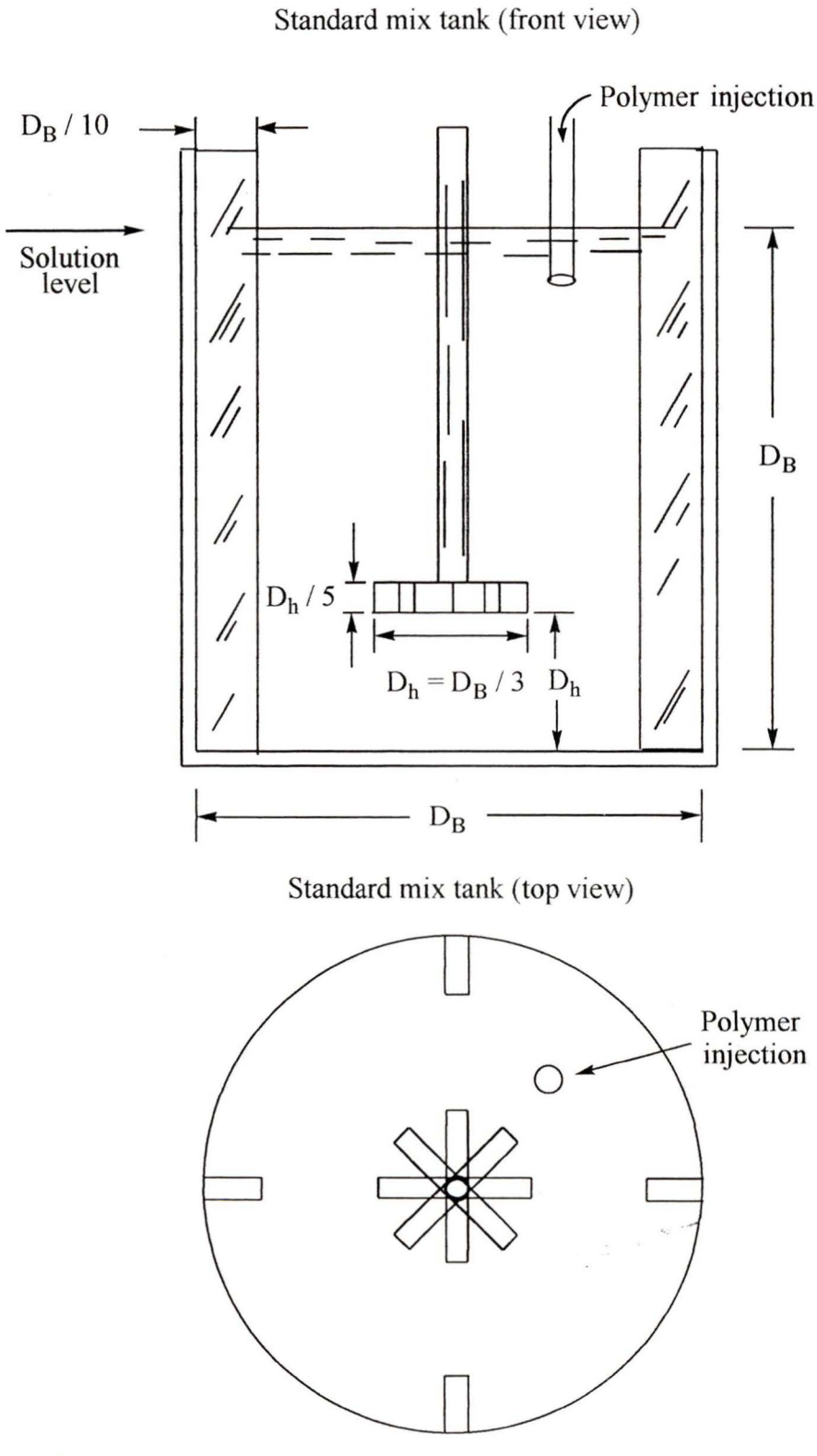

Fig. 8 Schematic diagram of the standard mix tank used for flocculation tests

400 mL beaker at a controlled rate.

Supernatant turbidities were measured with a Hack Model 2100A turbidimeter that had an operating range of 0 to 2000 nephelometric turbidity units (NTU).

Capillary suction times were measured with the Triton - W.R.C. Multipurpose Filtration Unit, Model TW166 according to the procedure of Baskerville and Gale.[72]

2.3. General Homo - and Co - Polymerization Procedures

Homopolymerization of acrylamide (AM) and substituted acrylamides and copolymerization of AM with substituted acrylamides were done with a consistent experimental arrangement (Fig. 9). The monomer(s) were weighed into a 3 vertical necked, round-bottomed flask equipped with a Liebig condenser at the central neck and a thermometer (-20°C to 110°C range) at a lateral neck. To the remaining lateral neck of the round-bottomed flask was attached a Pyrex three way connector with 105° angle, 1 inner joint, and 2 outer joints. A swivel tube which contained the polymerization initiator was connected to the 105° angle joint and the vertical joint of the three way connector was capped with a rubber septum. All ground glass joints were sealed with Nalgene ultrathin PTFE sleeves and secured with PTFE coated vacuum clamps. Except where stated otherwise, polymerizations were conducted under nitrogen (UHP, < 5 ppm O_2, Linde). A gas dispersion tube (coarse fritted glass) discharging below the surface of the solution and magnetic stirring were used to sparge the polymerization medium with the appropriate gas. Temperature was controlled by immersion of the polymerization flask in a water bath which was regulated to ± 0.1°C by a Haake immersion circulator

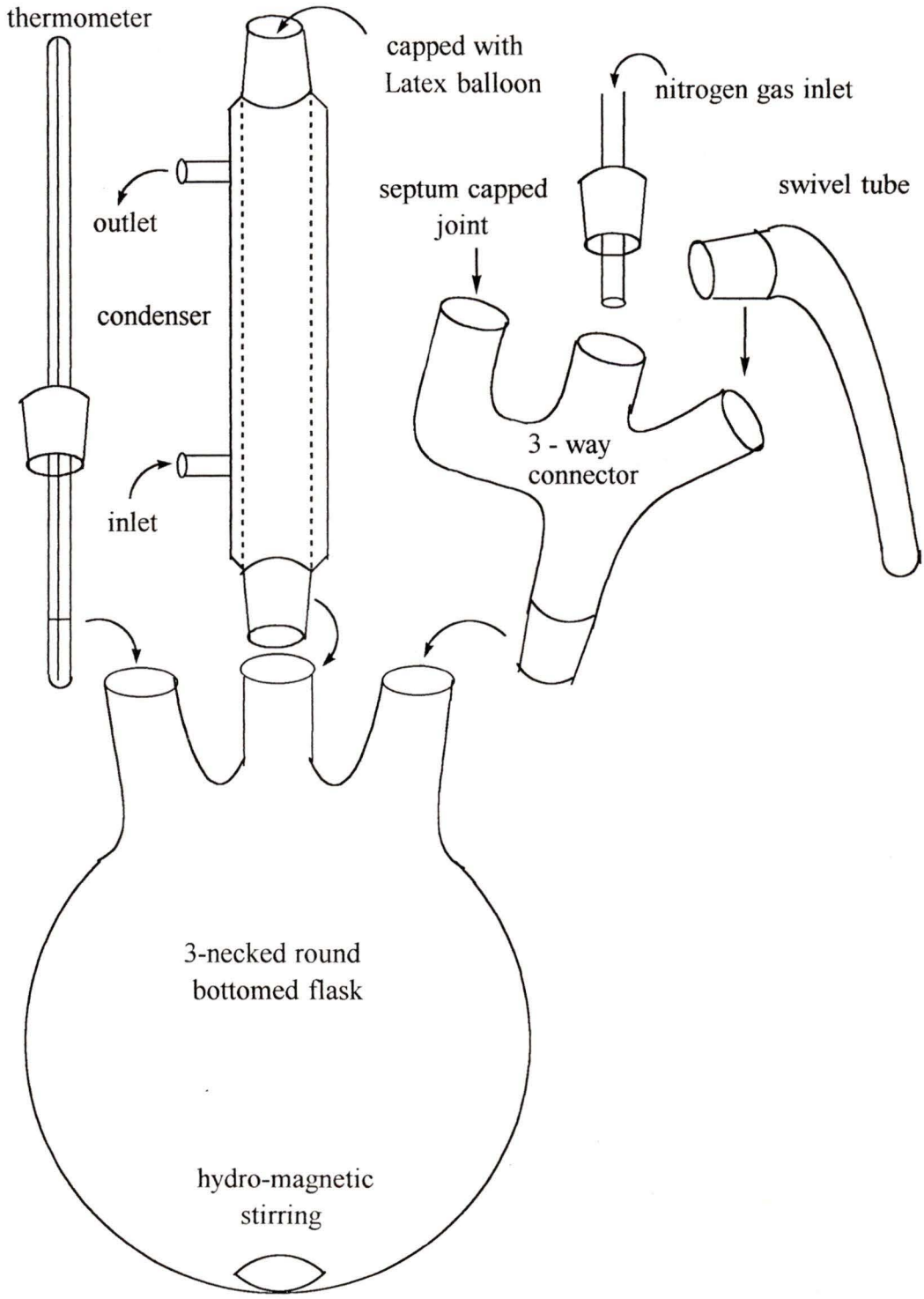

Fig. 9 Equipment assembly for polymerization test-work

(model D1) and stirring with an egg shaped stir bar rotated by a hydromagnetic stirrer (GFS Chemicals). The polymerization vessel was purged via Tygon tubing and an 18 ga. needle which pierced the septum capped joint of the Pyrex three way connector. The apparatus was sealed under the appropriate atmosphere by securing the open end of the Liebig condenser with a latex balloon which was filled and evacuated repeatedly with the appropriate gas prior to securing the open end of the Liebig condenser. The polymerization starting time was recorded at the instant the initiator was added to the monomer solution by rotating the swivel tube by approximately 180 degrees.

Except where stated otherwise, the procedure for deoxygenating the polymerization solution involved a 2 hour sparge of the polymerization medium with nitrogen in a flask which was kept separate from the polymerization flask. While the polymerization medium was sparged, the monomer(s) were sealed in the polymerization flask under a nitrogen atmosphere. Following the nitrogen sparge of the polymerization medium, the appropriate volume of the deoxygenated medium was added to the polymerization flask containing the monomer(s). The polymerization flask was purged with nitrogen for a minimum of 45 minutes as the contents stirred and warmed to the desired polymerization temperature. The initiator solution was purged with nitrogen for the same duration as the polymerization solution.

Upon completion of the polymerization, the solution was cooled to room temperature. Except for those experiments which involved N-t-butylacrylamide, the polymer solution was split into two fractions of approximately equal volumes. Each fraction was freeze-dried for 2 to 3 days but only one fraction was dialyzed against

distilled water prior to freeze-drying. This involved enclosing the polymer solution with Spectra/Por 3 dialysis tubing (3500 MW cut-off) and weighted immersion in distilled water at near 0°C. The dialysate was replaced 3 to 4 times per day and was analysed intermittently by UV spectroscopy (acrylamide, $\lambda_{max} = 200$ nm).[73] The dialysis was judged to be complete when the absorbance at λ_{max} diminished to near the baseline.

Except where stated otherwise, the polymer solutions from experiments which involved N-t-butylacrylamide were divided into two fractions of equal volume. One fraction was fully precipitated by adding distilled water dropwise until no further evidence of precipitation was observed. The other fraction was precipitated partially by adding one half the volume of distilled water to the polymer solution as was added for full precipitation. The precipitated fractions were rinsed with approximately 20 mL of distilled water and then freeze-dried for 2 to 3 days.

Without exception, the freeze-dried material from each polymer solution was forced through the product screen of a sample grinding instrument. The powdered solids were collected in glass vials.

2.4. Tests of the effects of Polymerization Atmosphere on the Molecular Weight of PAM

Solution polymerizations of AM under filtered air, nitrogen, and oxygen were done to determine the effect of polymerization atmosphere on the weight average molecular weight of PAM (experimental details, Table 1). Solution polymerizations of AM under atmospheres of filtered air (PAM-1) and oxygen (PAM-2) included differences to the general procedure under nitrogen. For these, AM and water were added to the

Table 1 **Homopolymerizations of acrylamide (AM) at 60.0 ± 0.2°C for 2 hours under atmospheres of oxygen, filtered air, and nitrogen** [a]

Experiment	Mass AM (g)	mmoles AM	Volume Water (mL)	Mass $K_2S_2O_8$ (g)	Polymerization atmosphere	Purge time	Yield[b] (%)
PAM-1	54.050	760.43	430	0.11	filtered air	30 min.	72
PAM-2	55.034	774.27	430	0.12	oxygen	30 min.	82
PAM-3	54.108	761.24	430	0.10	nitrogen	14 hrs.	94
PAM-4	54.283	763.70	430	0.10	nitrogen	6 hrs.	ca. 100

a. At natural pH, about 5.5 to 7.0 and using 8 g of 2-propanol as a chain transfer agent.
b. % yields were calculated for the polymer fractions dialyzed at 3500 MWCO.

polymerization flask and the contents sparged with filtered air for 30 minutes at room temperature, and then for an additional 30 minutes with the appropriate gas (oxygen or filtered air). This was continued for approximately 30 minutes as the contents warmed to the desired starting temperature. To start the polymerization, 8 g of isopropyl alcohol were added by injection through the septum capped joint of the Pyrex three way connector and 2 mL of a 0.05 g/mL solution of potassium persulfate in distilled water were added by rotation of the swivel tube. Both the isopropyl alcohol reagent and the potassium persulfate solution had been purged with the appropriate gas for the same duration as the polymerization solution.

Solution polymerizations of AM under a nitrogen atmosphere (PAM-3 and PAM-4) were slightly different. In the first experiment the polymerization components were sparged with nitrogen for 14 hours (overnight) following the 30 minute sparge with filtered air (PAM-3). In the second experiment the AM and distilled water were kept separate during the 30 minute sparge with filtered air and 6 hour sparge with nitrogen (PAM-4). Following this, the distilled water was added to the AM in the polymerization flask. The ensuing polymerization and subsequent polymer solution treatment followed the general procedure, as described previously.

2.5. Homopolymerizations to Determine the Conditions which Give High Molecular Weights

2.5.1. Homopolymerization of N,N-dimethylacrylamide (DMAM) 2

The homopolymers of DMAM from experiments PDMAM-1 to -3 and the control homopolymers of AM were prepared by the general procedure using the experimental

Table 2 Homopolymerization of N,N-dimethylacrylamide (DMAM) and acrylamide (AM) under equivalent conditions

Experiment	Mass DMAM (g)	Mass AM (g)	Monomer (mmoles)	Volume H_2O (mL)	Mass $K_2S_2O_8$ (g)	Polym. temp. (± 0.2°C)	Polym. duration (hours)	Yield [a] (%)
PDMAM-1	19.83		200.0	200	0.055	60.0	3.58	ca. 100 [b]
control-1		14.26	200.6					ca. 100
PDMAM-2	20.19		203.7	200	0.054	31.0	7	n/m [c]
control-2		14.26	200.6					n/m
PDMAM-3	19.99		201.7	200	0.054	50.0	3.5	94
control-3		14.21	199.9					ca. 100

a. % yields were calculated for the polymer fractions dialyzed against distilled water at 3500 MWCO.
b. The homopolymer from PDMAM-1 did not freeze-dry to a powdered solid but remained gelatinous.
c. n/m denotes not measured.

conditions given in Table 2. The monomer concentration was 1.0 M in deoxygenated water and the initiator (potassium persulfate) was added as a 2 mL aliquot to give a mole ratio of potassium persulfate to monomer of 1:1000.

2.5.2. Homopolymerization of methacrylamide (MeAM) 3

The homopolymers of MeAM from experiments PMeAM-1 to -5 and the control homopolymers of AM were prepared as aqueous solutions using the general procedure and the experimental conditions given in Table 3. A 1.0 M monomer concentration in deoxygenated water was used consistently. Mole ratios of the initiator (potassium persulfate) to monomer of 1:1000, 1:750, and 1:500 were used to investigate the effect of an increasing initiator concentration on the molecular weights of poly(methacrylamide), PMeAM, and PAM.

2.5.3. Homopolymerization of N-t-butylacrylamide (NTBAM) 4

(a) In methanol and methanol - water mixtures

The solubility of NTBAM in 99.8% methanol was determined for the quantities of reagents necessary to prepare a 1.0 M polymerization solution (Table 4). Homopolymers of NTBAM from experiments PNTBAM-1 to -6 and the control homopolymers of AM were prepared under equivalent experimental conditions which varied with respect to the percentage of methanol in the polymerization medium, polymerization temperature, and the initiator identity (Table 5). Either 2,2' -azobisisobutyronitrile (AIBN) or potassium persulfate were used as initiators after testing their solubilities in the mixed solvents and temperatures to be used for polymerization. Each was added in 2 mL of solvent, the

Table 3 Homopolymerization of methacrylamide (MeAM) and acrylamide (AM) under equivalent conditions at 60.0 ± 0.2°C

Experiment	Mass MeAM (g)	Mass AM (g)	mmoles monomer	Volume H_2O (mL)	Mass $K_2S_2O_8$ (g)	Mole ratio $K_2S_2O_8$ to monomer	Polym. duration (hours)	Yield[a] (%)
PMeAM-1	22.06		259.2	250	0.067	1 / 1000	3.58	88
control-1		18.08	254.4					n/m[b]
PMeAM-2	17.51		205.7	200	0.072	1 / 750	3.5	92
control-2		14.54	204.6					ca. 100
PMeAM-3	10.65		125.1	125	0.034	1 / 1000	5	83
control-3		8.91	125.4					ca. 100
PMeAM-4	10.64		125.0	125	0.034	1 / 1000	13.25	96
control-4		9.32	131.1					ca. 100
PMeAM-5	17.08		200.7	200	0.11	1 / 500	3.5	92
control-5		14.31	201.3					96

a. % yields were measured for polymer fractions dialyzed against distilled water (3500
b. n/m denotes not measured.

Table 4 Solubility of N-t-butylacrylamide (NTBAM) in 30 mL of water / methanol mixtures at (55 ± 2)°C

Aqueous solvent (% methanol v/v)	Dissolved NTBAM (g)	Dissolving time (minutes)	Concentration NTBAM (moles / litre)
10	0.46	16	0.12
20	0.65	9	0.17
30	0.96	7	0.25
40	1.91	5	0.50
50	2.17	5	1.08

potassium persulfate in water and AIBN in methanol.

The experimental procedure for treatment of PAM which resulted from polymerization in 99.8% methanol differed from the general procedure described previously. PAM was recovered as a precipitate with vacuum filtration and then freeze-dried for 2 to 3 days.

(b) In t-butanol and t-butanol - water mixtures

Homopolymerizations of NTBAM (PNTBAM-7 to -14) and the control homopolymerizations of AM were done under 98% t-butanol and 98% t-butanol / distilled water mixtures and otherwise identical experimental conditions (Table 6). Either AIBN in methanol, or potassium persulfate in distilled water were used as initiators as before, to deliver a mole ratio of the initiator to monomer of 1:1000 for all except PNTBAM-7 and -9 which used a mole ratio of AIBN to NTBAM of 1:423.

PNTBAM which resulted from polymerization in 98% t-butanol was recovered by using the general procedure described previously. The other recoveries departed from this. PAM was recovered from 98% t-butanol by vacuum filtration. PAM and PNTBAM were removed from 1:1 t-butanol / distilled water solutions by scraping the glass walls of the polymerization flasks with a rubber spatula. All homopolymers were freeze-dried for 2 to 3 days.

Table 5 Homopolymerization of N-t-butylacrylamide (NTBAM) and acrylamide (AM) under equivalent conditions in methanol, and methanol / distilled water mixtures

Experiment	Mass NTBAM (g)	Mass AM (g)	Monomer mmoles	Polym. medium %MeOH [a]	Volume medium (mL)	Mass initiator (g)	Polym. temp. (±0.2°C)	Polym. time (hours)	Yield (%)
PNTBAM-1	31.75		249.6	99.8	250	0.067 $K_2S_2O_8$	31.0	7	n/m
control-1		17.73	249.4						n/m
PNTBAM-2	32.00		251.6	99.8	250	0.067 $K_2S_2O_8$	55.0	3.5	n/m
control-2		17.84	250.1						60
PNTBAM-3	26.00		204.4	50	200	0.041 AIBN	55.0	3.5	69 [b]
control-3		14.15	199.1						79
PNTBAM-4	7.17		56.4	10	500	0.018 $K_2S_2O_8$	60.0	3.5	68 [b]
control-4		4.21	59.2						37
PNTBAM-5	19.11		150.3	99.8	150	0.024 AIBN	55.0	3.5	n/m
control-5		11.11	156.3						n/m
PNTBAM-6	12.83		100.9	99.8	100	0.046 AIBN	60.0	8.33	81 [b]
control-6		7.09	99.8						98

a. By volume.
b. Mole ratio of initiator to monomer 1:1000 for all except PNTBAM-6 which is 1:358.
c. % yield is based on the fraction of the polymer solution which was fully precipitated with H_2O.

$$\%\ yield = \frac{mass\ of\ polymer\ pptd.}{mass\ of\ monomer} \times 100$$

Table 6 Homopolymerization of N-t-butylacrylamide (NTBAM) and acrylamide (AM) under equivalent conditions in 98% t-butanol, and t-butanol / distilled water mixtures

Experiment	Mass NTBAM (g)	Mass AM (g)	Monomer (mmoles)	Polym.[a] medium %t-BuOH	Volume medium (mL)	Mass initiator (g)	Polym. temp. (± 0.2°C)	Polym. time (hours)	Yield [b] (%)
PNTBAM-7	12.86		101.1	98	150	0.038 AIBN	70.0	8	n/m [c]
control-7		7.14	100.5						88
PNTBAM-8	19.30		151.8	50	150	0.042 $K_2S_2O_8$	60.0	7.5	n/m
control-8		11.00	154.8						81
PNTBAM-9	19.28		151.6	50	150	0.038 AIBN	70.0	8	n/m
control-9		10.81	152.1						88
PNTBAM-10	8.96		70.5	10	700	0.019 $K_2S_2O_8$	60.0	8.5	n/m
control-10		5.31	74.7						22
PNTBAM-11	25.42		199.9	50	200	0.055 $K_2S_2O_8$	60.0	8	98
control-11		14.26	200.6						78
PNTBAM-12	25.42		199.9	50	200	0.054 $K_2S_2O_8$	50.0	3.5	46
control-12		14.61	205.6						80
PNTBAM-13	21.20		166.7	50	200	0.046 $K_2S_2O_8$	50.0	3.5	29
control-13		11.80	166.0						43
PNTBAM-14	20.01		157.3	50	200	0.044 $K_2S_2O_8$	45.0	16	87
control-14		11.19	157.4						68

a. By volume.
b. % yields were calculated for polymer fractions which precipitated from the polymerization medium (see Table 5).
c. n/m denotes not measured.

2.6. Copolymerization to Determine the Conditions Which Give High Molecular Weight Copolymers

2.6.1. Copolymerization of DMAM with AM

Copolymerization of DMAM with AM and the control homopolymerization of AM were done in water using the experimental conditions given in Table 7. Experiments DMAM-co-AM-1 to -7 included feed compositions of 20, 20, 40, 60, 80, 100, and 10 mol % of DMAM, respectively. Except for DMAM-co-AM-7, a control homopolymerization of AM accompanied each copolymerization under the same experimental conditions.

Only control-6 which involved homopolymerization of AM under equivalent experimental conditions as DMAM-co-AM-6 was worked-up by the general procedure. The other controls were freeze-dried for 2 to 3 days without prior dialysis.

2.6.2. Copolymerization of MeAM with AM

Copolymerization of MeAM with AM and the control homopolymerization of AM were done in water under identical experimental conditions as given in Table 8. Experiments MeAM-co-AM-1, -2a, -2b, and -3 to -6 included 20, 20, 20, 40, 60, 80, and 100 mol % of MeAM in the polymerization feedstock, respectively. Except for MeAM-co-AM-2a and -2b, each copolymerization was accompanied by a control homopolymerization of AM under the same experimental conditions. Potassium persulfate was used as the initiator throughout.

Control-6 was worked-up by the general procedure. All the other controls and the polymer solution from MeAM-co-AM-6 which included 100 mol % MeAM in the polymerization feedstock were freeze-dried for 2 to 3 days without prior dialysis.

Table 7 Copolymerizations of N,N-dimethylacrylamide (DMAM) with acrylamide (AM) and control homopolymerizations of AM at (50.0 ± 0.2)°C

Experiment	DMAM mmoles	AM mmoles	Volume H_2O (mL)	Total [monomer(s)] (mmoles / mL)	Mass $K_2S_2O_8$ (g)	Polym. duration (hours)	Yield [a] (%)
DMAM-co-AM-1	29.9	120.2	150	1.00	0.041	9.0	ca. 100
control-1		150.4		1.00			n/m [b]
DMAM-co-AM-2	25.1	100.5	500	0.25	0.034	18.5	78
control-2		125.1		0.25			n/m
DMAM-co-AM-3	50.0	75.0	500	0.25	0.029	16.0	n/m
control-3		124.9	250	0.50	0.035		n/m
DMAM-co-AM-4	149.7	102.3	500	0.50	0.068	16.5	93
control-4		125.4	250	0.50	0.034		n/m
DMAM-co-AM-5	201.2	50.4	500	0.50	0.067	18.0	ca. 100
control-5		124.9	250	0.50	0.034		n/m
DMAM-co-AM-6	124.6		500	0.25	0.034	16.0	71
control-6		125.8	250	0.50	0.034		n/m
DMAM-co-AM-7	12.6	125.4	500	0.28	0.034	18.0	n/m

a. Added in 2 mL of distilled water. Initiator to monomer mole ratio 1:1000 throughout.
b. % yield is calculated for the fraction of polymer dialyzed (3500 MWCO).
c. n/m denotes not measured. The control homopolymers (PAM) were not dialyzed.

Table 8 Copolymerization of methacrylamide (MeAM) with acrylamide (AM) and control homopolymerizations of AM under equivalent conditions

Experiment	MeAM mmoles	AM mmoles	Volume H_2O (mL)	Total [monomer(s)] (mmoles / mL)	Mass [a] $K_2S_2O_8$ (g)	Polym. temp. (± 0.2°C)	Polym. duration (hours)	Yield [b] (%)
MeAM-co-AM-1	50.4	204.1	500	0.51	0.068	60.0	16.0	ca. 100
control-1		130.3	250	0.52	0.034			n/m [c]
MeAM-co-AM-2a	75.0	301.6	500	0.75	0.10	50.0	16.0	92
MeAM-co-AM-2b	100.5	401.4		1.00	0.14			92
MeAM-co-AM-3	100.0	150.0	250	1.00	0.068	50.0	16.0	87
control-3		252.1		1.01				n/m
MeAM-co-AM-4	150.4	100.0	250	1.00	0.068	50.0	17.0	61
control-4		252.5		1.01				n/m
MeAM-co-AM-5	200.1	50.7	250	1.00	0.068	50.0	16.0	71
control-5		251.4		1.01				n/m
MeAM-co-AM-6	250.8		250	1.00	0.068	50.0	16.0	88
control-6		252.5		1.01				67

a. Added in 2 mL of distilled water. Initiator to monomer mole ratio 1:1000 throughout.
b. % yield is calculated for the polymer fraction dialyzed (3500 MWCO).
c. n/m denotes not measured. The PAM fractions were not dialyzed.

2.6.3. Copolymerization of NTBAM with AM

Copolymerization of NTBAM with AM and the control homopolymerization of AM were done in a 1:1, 98% t-butanol / water medium under the experimental conditions given in Table 9. Experiments NTBAM-co-AM-1a, -1b, -2, -3, -4, -5a, -5b, -6a, and -6b included 20, 20, 40, 60, 80, 100, 100, 80, and 100 mol % of NTBAM in the polymerization feedstock, respectively. Only experiments NTBAM-co-AM-2, -3, and -4 were accompanied by control homopolymerizations of AM. Potassium persulfate was used as the initiator throughout, to give a mole ratio of initiator to monomer of 1:1000.

The general procedure was used to work-up the NTBAM-co-AM-2 copolymerization. Different procedures were used for the others. The copolymer solutions from NTBAM-co-AM-1a and -1b were separated as a clouded viscous layer and a clear viscous layer. Each layer was freeze-dried for 2 to 3 days without prior dialysis. Gelatinous material was separated from each copolymer solution from NTBAM-co-AM-3 to -6b. The gelatinous material and the copolymer solution were freeze-dried separately for 2 to 3 days without prior dialysis. Control-2 to -4 were freeze-dried for 2 to 3 days without prior dialysis.

2.7. Conversion of Poly(DMAM-co-AM), Poly(MeAM-co-AM), Poly(NTBAM-co-AM), and PAM to Their Cationic Derivatives

The Mannich Reaction followed by quaternization was used to convert the nonionic acrylamide-based homopolymers and copolymers to their cationic derivatives. Copolymers from DMAM-co-AM-7 which included 10 mol % of DMAM in the polymerization feedstock, MeAM-co-AM-2b which included 20 mol % of MeAM in the

Table 9 Copolymerization of N-t-butylacrylamide (NTBAM) with acrylamide (AM) and the control homopolymerizations of AM under equivalent conditions at (50.0 ± 0.2)°C for 16 hours

Experiment	NTBAM mmoles	AM mmoles	Volume 1:1, t-BuOH : H_2O (mL)	Total [monomer(s)] (mmoles / mL)	Mass $K_2S_2O_8$ [a] (g)	Yield [b] (%)
NTBAM-co-AM-1a	52.3	213.4	400	0.66	0.071	ca. 100 (clear layer) ca. 100 (clouded layer)
NTBAM-co-AM-1b	50.1	210.1	500	0.50	0.068	47 (fr.1, clear layer) 48 (fr.1, clouded layer) 55 (fr.2, clear layer) 48 (fr.2, clouded layer)
NTBAM-co-AM-2	100.5	150.3	500	0.50	0.068	ca. 100 [c]
control-2		150.5	300	0.50	0.041	22
NTBAM-co-AM-3	120.0	80.2	400	0.50	0.054	72 (fr.2, gelatinous mat.) 11 (fr.2, solution)
control-3		150.1	300	0.50	0.041	26

Table 9 continued ...

Experiment	NTBAM mmoles	AM mmoles	Volume 1:1, t-BuOH : H_2O (mL)	Total [monomer(s)] (mmoles / mL)	Mass $K_2S_2O_8$ [a] (g)	Yield [b] (%)
NTBAM-co-AM-4	160.47	40.80	400	0.50	0.054	17 (fr.2, gelatinous mat.) 72 (fr.2, solution)
control-4		150.96	300	0.50	0.041	78
NTBAM-co-AM-5a	125.33	0	250	0.50	0.034	16
NTBAM-co-AM-5b	140.42	0	200	0.70	0.038	11
NTBAM-co-AM-6a [d]	160.08	40.66	400	0.50	0.054	13
NTBAM-co-AM-6b [d]	150.17	0	300	0.50	0.041	n/m [e]

a. Added in 2 mL of distilled water. Initiator to monomer ratio 1:1000 throughout.
b. % yields were determined for copolymer fractions which were separated into cloudy and clear layers.
c. % yield was determined for the fraction of copolymer dialyzed against distilled water (3500 MWCO).
d. The polymerization duration was extended from 16 hours to 69.5 hours.
e. n/m denotes not measured.

polymerization feedstock, and NTBAM-co-AM-1b which included 20 mol % of NTBAM in the polymerization feedstock were used for cationic conversion. PAM from control-6 (complementary to MeAM-co-AM-6) was also converted to its cationic derivative.

The Mannich feedstock was prepared by adding 1.5 g of freeze-dried polymer to 300 mL of deoxygenated distilled water in a 500 mL, 2 vertical-necked round bottomed flask (experimental details, Table 10). The contents were sealed under a nitrogen atmosphere and stirred overnight (ca. 16 hours) with mild agitation. Once dissolved, dimethylamine and formaldehyde were added in succession to give a mole ratio of 1.05:1:1 of dimethylamine to formaldehyde to the amido nitrogen content of the polymer while a nitrogen stream purged the reaction flask. The pH of the Mannich feedstock was adjusted to pH 10 with 0.1 N NaOH (when necessary) and the contents were sealed under a nitrogen atmosphere. The Mannich reaction was performed over 18 hours at 25°C.

Following the Mannich reaction, 100 mL of deoxygenated distilled water was added, and then sufficient dimethyl sulfate was added give a 1:1 mole ratio of dimethyl sulfate to amido nitrogen content (experimental details, Table 11). The solution was then adjusted to pH 10 with 0.1 N NaOH, sealed under a nitrogen atmosphere, and allowed to react for 4 hours at 30°C. Upon completion of the quaternization reaction, the pH of the polymer solution was adjusted to approximately pH 6.5.

In one experiment the quaternized polymer solutions were treated with a mixed-bed ion-exchange resin and in another experiment they were not. The mixed-bed ion exchange resin was prepared as a 1:1 mixture of Bio-rad AG1-X8 and AG50W-X8 resins. The AG1-X8 strong anion exchange resin was converted to hydroxide form and the

Table 10 Conversion of poly(DMAM-co-AM), poly(MeAM-co-AM), poly(NTBAM-co-AM), and PAM to weakly cationic derivatives using the Mannich reaction for 18 hours at (25 ± 2)°C

Experiment	Polymer solution (% w/w)	Polymer solution pH	AM nitrogen [a] mmoles	$(CH_3)_2NH$ mmoles	CH_2O mmoles	Reaction starting pH
cationic DMAM-co-AM-7	0.50	5.84	9.62	9.50	9.16	10.53
cationic MeAM-co-AM-2b	0.51	6.14	8.67	8.45	8.05	10.34
cationic NTBAM-co-AM-1b (clouded layer)	0.54	4.18	9.12	8.45	8.05	10.48
cationic control-6	0.50	5.05	10.55	10.56	10.07	10.29

a. mmoles AM nitrogen for the copolymers were calculated from the copolymerization feedstock compositions.

$$mmoles\,AM\,nitrogen = mmoles\,AM(feedstock) \times \frac{1\,mmole\,N}{1\,mmole\,AM}$$

Table 11 Quaternization of the weakly cationic derivatives of poly(DMAM-co-AM), poly(MeAM-co-AM), poly(NTBAM-co-AM), and PAM for 4 hours at (30 ± 2)°C

Experiment	Mannich product [a] %(w/w)	AM nitrogen mmoles	$(CH_3)_2SO_4$ mmoles	Reaction starting pH	Reaction completion pH
cationic DMAM-co-AM-7	0.30	9.62	9.58	9.99	5.11
cationic MeAM-co-AM-2b	0.30	8.67	8.47	10.00	6.66
cationic NTBAM-co-AM-1b (cloudy layer)	0.32	9.12	8.55	9.99	6.20
cationic control-6	0.29	10.55	10.56	10.01	6.99

a. The Mannich Product was diluted with approximately 100 mL of distilled water prior to quaternization.

AG50W-X8 strong cation exchange resin was converted to hydrogen form prior to mixing the resins together. The mixed-bed resin was added to 1.0 g of the unpurified cationic derivative diluted with 400 g of deionized water. The contents were mixed by an overhead stirrer for 3 hours at room temperature and then filtered through sintered glass (ca. 60 μm pore size) and rinsed with several portions of distilled water to remove the mixed-bed resin from the polymer solution.

In preparation for dialysis, the quaternized polymer solutions which were not treated by ion exchange were diluted with 425 g of deionized water. The polymer solutions which were treated by ion exchange were not diluted with additional deionized water. The dialysis tubing (Spectra Por, 3500 MWCO) was soaked in distilled water overnight prior to containing the quaternized polymer solutions. The polymer solutions were dialyzed against 0.1 M NaCl for 8 days and then against distilled water for 21 days.

Following dialysis, the polymer solutions which were ion-exchanged were freeze-dried for 2 to 3 days to yield the purified cationic derivatives. The polymer solutions which were not ion-exchanged were kept as solutions and stored in the dark at approximately 0°C.

2.8. Characterization of the Newly Synthesized, Acrylamide-Based Polymers

2.8.1. Viscometric analysis

All stock solutions were gently stirred magnetically for a minimum of 16 hours (overnight) and then filtered through 0.45 μm disposable syringe filters. Filters containing a nylon hydrophilic membrane were used for solutions prepared in 0.1M NaCl

and filters containing a PTFE hydrophobic membrane were used for the stock solutions prepared in 88% formic acid and 99.8% methanol. The PTFE hydrophobic membranes were converted to a hydrophilic character to be compatible with formic acid solutions by first wetting the membranes with methanol and then passing copious portions of distilled water through the membranes. Both types of filters were connected to 10 mL disposable syringes which were dispensed by syringe pumps at a rate of 0.15 mL/min (nylon) and 0.05 mL/min (PTFE) into 25 mL volumetric flasks which were attached with Parafilm to the exit of the disposable syringe filters.

Ubbelohde dilution viscometers (sizes 1, 1B, 1C, and 2) were used to measure the efflux times of successive 5 mL additions of the stock solutions to 10 mL of the appropriate solvent (0.1M NaCl, 88% formic acid, or 99.8% methanol). As an alternative to using a rubber bulb to draw solution up through the capillary outlet tube of the Ubbelohde viscometer, a 60 mL disposable syringe attached to Tygon tubing was connected to the capillary outlet tube and another segment of tubing was connected to the pressure relief tube. Pinching the tubing connected to the pressure relief tube while applying suction via the 60 mL disposable syringe afforded greater stability to the Ubbelohde viscometer than the method involving the rubber bulb. Measurements were made with the viscometer immersed in a thermostat bath controlled to 25.0 ± 0.1°C with a Haake immersion circulator (model D1). Nitrogen was used to mix the 5 mL additions of the stock solution with the solution in the solution bulb of the Ubbelohde viscometer.

Intrinsic viscosities were determined by extrapolating plots of reduced viscosity versus polymer concentration to zero concentration. Reduced viscosities were calculated

from the following equation.[74]

$$\eta_{red} = \frac{\eta_{sp}}{c} = \frac{(t - t_0)}{t_0} \times \frac{1}{c} \qquad \text{Eq. 17}$$

where n_{red} is the reduced viscosity.

n_{sp} is the specific viscosity.

t is the efflux time of the polymer solution.

t_0 is the efflux time of the particular solvent.

c is the polymer solution concentration.

Viscosity average molecular weights, M_v, for the control homopolymers (PAM) were calculated by the Mark Houwink relationship for polyacrylamide in 0.5 M NaCl at 25°C.[75]

$$[\eta] = (7.19 \times 10^{-3}) M_v^{0.77} \qquad \text{Eq. 18}$$

where $[\eta]$ is the intrinsic viscosity.

M_v's for the control homopolymers (PDMAM) from DMAM-3 and DMAM-co-AM-6 were calculated by the following relationship for poly (N,N-dimethylacrylamide) in water at 25°C.[76]

$$[\eta] = (2.24 \times 10^{-3}) M_V^{0.81} \qquad \text{Eq. 19}$$

(a) Stock solutions of the newly-synthesized homopolymers

Stock solutions of the homopolymers from PAM-1 to -4, PDMAM-3, and the

controls complementary to PDMAM-3, PMeAM-1 to -5, and PNTBAM-1 to -14 were prepared by adding 50-100 mg of the freeze-dried polymer to 25 mL of 0.1 M NaCl. Stock solutions of PMeAM from PMeAM-1 to -5 were prepared by adding 100-150 mg of freeze-dried polymer to 25 mL of 88% formic acid. Stock solutions of PNTBAM from PNTBAM-1, -3, -4, -5, -6, and -7 were prepared from 140-170 mg of the freeze-dried polymer in 25 mL of 99.8% methanol.

(b) Stock solutions of the newly-synthesized copolymers

Stock solutions of the copolymers from DMAM-co-AM-2 to -6, MeAM-co-AM-2b to -5, and NTBAM-co-AM-1b (clouded layer), -1b (clear layer) and -2 were prepared by adding 50-100 mg of the freeze-dried polymer to 25 mL of 0.1 M NaCl. Except for the freeze-dried polymer from NTBAM-co-AM-1b, the freeze-dried polymer from the dialyzed fraction of each polymer solution was used for the stock solutions. Preparation of the stock solutions of the controls complementary to DMAM-co-AM-6, MeAM-co-AM-6, and NTBAM-co-AM-4 included the addition of 80-100 mg of the freeze-dried polymer (dialyzed fraction of control complementary to MeAM-co-AM-6) to 25 mL of 0.1 M NaCl. The stock solution of the homopolymer (PMeAM) for MeAM-co-AM-6 was prepared by adding 116 mg of the freeze-dried polymer to 25 mL of 88% formic acid. Stock solutions of the copolymers and homopolymers (PNTBAM) from NTBAM-co-AM-3, -4, -5a, -5b, -6a, and -6b were prepared by adding 140-160 mg of the freeze-dried polymer to 25 mL of 99.8% methanol. Except for NTBAM-co-AM-4, only the freeze-dried polymer corresponding to the gelatinous material was used for the stock

solutions. For NTBAM-co-AM-4, separate stock solutions were prepared for the freeze-dried polymer from the gelatinous material and the tan coloured solution.

(c) Stock solutions of the cationic derivatives and their nonionic polymer substrates

Stock solutions of the unpurified and purified cationic derivatives originating from DMAM-co-AM-7, MeAM-co-AM-2b, NTBAM-co-AM-1b (clouded layer), and control-6 complementary to MeAM-co-AM-6 were prepared by adding 30-60 g of the cationic derivative solution to 100 g of deionized water. In addition to the unpurified and purified cationic derivatives, stock solutions of the corresponding nonionic copolymers and homopolymer were prepared by adding 70-100 mg of the freeze-dried polymer to 120-150 g of deionized water.

(d) Stock solutions of the commercial polymers

Stock solutions of the commercial polymers; Percol 351 (nonionic PAM), Percol 721 (cationic PAM), and Percol E-24 (anionic PAM), were prepared by adding 80-90 mg of the commercial polymer to 100-150 g of deionized water.

2.8.2. Gel permeation chromatography (GPC) / multi-angle laser light scattering (MALLS) methods and theory

The same stock solutions for viscometry analysis which were prepared for the homopolymers from PAM-1 to -4, PDMAM-3, and the controls complementary to PDMAM-3, PMeAM-1 to -5, and PNTBAM-1 to -14 were analyzed by GPC / MALLS. In addition to the 0.1 M aqueous NaCl used for those solutions, stock solutions of the polymers from PAM-1 to -4 were prepared in pH 5.40 aqueous buffer (sodium acetate /

acetic acid) according to the same methods and concentration ranges.

In addition to the newly synthesized, acrylamide-based polymers, PAM (nonionic, 5,550,000 MW, Polysciences) was used to prepare stock solutions. Each stock solution was prepared by adding approximately 30 mg of PAM to 10 mL of 0.1 M NaCl. From each stock solution duplicate aliquots of ca. 2 mL each were removed and the remaining volume was filtered. The filtered and duplicate unfiltered aliquots for each stock solution were analyzed by GPC / MALLS.

A few mL of each stock solution was added to corresponding septum capped vials which were designed for the Waters 717 Plus Autosampler of the GPC assembly. The autosampler was programmed to delay injection of each polymer sample until 10 mL of the mobile phase (0.1 M NaCl or the pH 5.40 buffer which had been filtered through 0.45 μm and 0.22 μm Millipore filters) had been processed by the Astra software. The mobile phase was directed by the Waters 501 HPLC pump at a flow rate of 0.500 mL/min through the Waters In-Line Degasser and the Waters Pulse Dampener prior to passing the exit of the 100 μL injection loop. From the exit point of the injection loop, the mobile phase was pumped through the Shodex OH pak columns and then through the analyte cell of the Waters Differential Refractometer R401 until passing through the flow cell of the Dawn DSP-F laser photometer and collecting in a waste container. Upon entry of the 100 μL aliquot of the polymer sample into the mobile phase, the solution was directed to the Shodex OH pak columns. The autosampler was programmed to delay injection of the next sample until 20 mL of the polymer-containing, mobile phase had been processed by the Astra software. The Astra software was linked to the autosampler

/ chromatography assembly such that the rate of data aquisition of the software coincided with the flow rates and the delay volumes programmed into the autosampler. In addition, the Astra software was programmed to acquire data at 2 second intervals which yielded "slices" of information. Each 2 second interval represented a fraction of polymer which eluted from the gel permeation chromatography columns and passed through the Waters Differential Refractometer R401 and the flow cell of the Dawn DSP- F laser photometer. The differential refractometer determined the concentration contribution of each "slice" to the total eluted concentration of the polymer and the light scattering data from laser photometer gave the molecular weight contribution of each "slice" to the weight average molecular weight, M_w, of the polymer. By entering the differential refractive index detector calibration constant, AUX1, and the differential refractive index increment, dn/dc, of the solute / solvent solution into the collection program of the Astra software, the eluted concentration of each "slice" was calculated from the injected mass of the polymer (Eq. 20).[77]

$$c_i = \frac{W_{injected}}{\Delta v_i} \times \frac{V_i - V_{i,\,baseline}}{\sum_{peak} (V_i - V_{i,\,baseline})} \qquad \text{Eq. 20}$$

where c_i is the concentration of the solute in the i^{th} "slice".

$W_{injected}$ is the injected mass.

Δv_i is the volume of the i^{th} "slice".

$V_i - V_{i,\,baseline}$ is the difference between the refractive index detector signal voltage and the baseline voltage.

The method of Debye was used for processing the light scattering data.[37,77] For each

"slice" the method of Debye produced a plot of the scattered intensity, R_θ / Kc, versus the angular dependence, $\sin^2(\theta/2)$, for all eighteen detectors of the Dawn DSP-F (Fig. 10). The scattered intensity is defined by the following equation.[77]

$$\frac{R_\theta}{K^* c} = MP(\theta) - 2A_2 M^2 P^2(\theta) \qquad \text{Eq. 21}$$

where R_θ is the excess Rayleigh ratio, $(I_\theta - I_{\theta,solvent})r^2 / (I_0 V)$, where I_θ is the scattered intensity of the solvent, V is the volume of the scattering medium, r is the distance between the scattering volume and the detector, and I_0 is the intensity of the incident radiation.

c is the concentration of solute molecules in the solvent.

M is the molecular weight.

A_2 is the second virial coefficient which is a measure of the interaction between the solute and the solvent.

K is the optical constant, $4\pi^2 n_0^2 (dn/dc)^2 \lambda_0^{-4} N_A^{-1}$, where n_0 is the solvent refractive index, λ_0 is the incident radiation wavelength (632.8 nm), N_A is Avogadro's number (6.022×10^{23}), and dn/dc is the user entered differential refractive index increment of the solute-solvent solution with respect to a change in solute concentration.

$P(\theta)$ is a function which defines a molecules average size, shape, and structure. It is theoretically derived and it is approximately equal to $1 - 2\mu^2 < r^2 > /3! + \cdots$ where $\mu = (4\pi\lambda) sin(\theta/2)$, and $< r^2 >$ is the mean square radius.

A polynomial in $\sin^2(\theta/2)$ was fitted to the Debye plot and extrapolated to zero angle. As

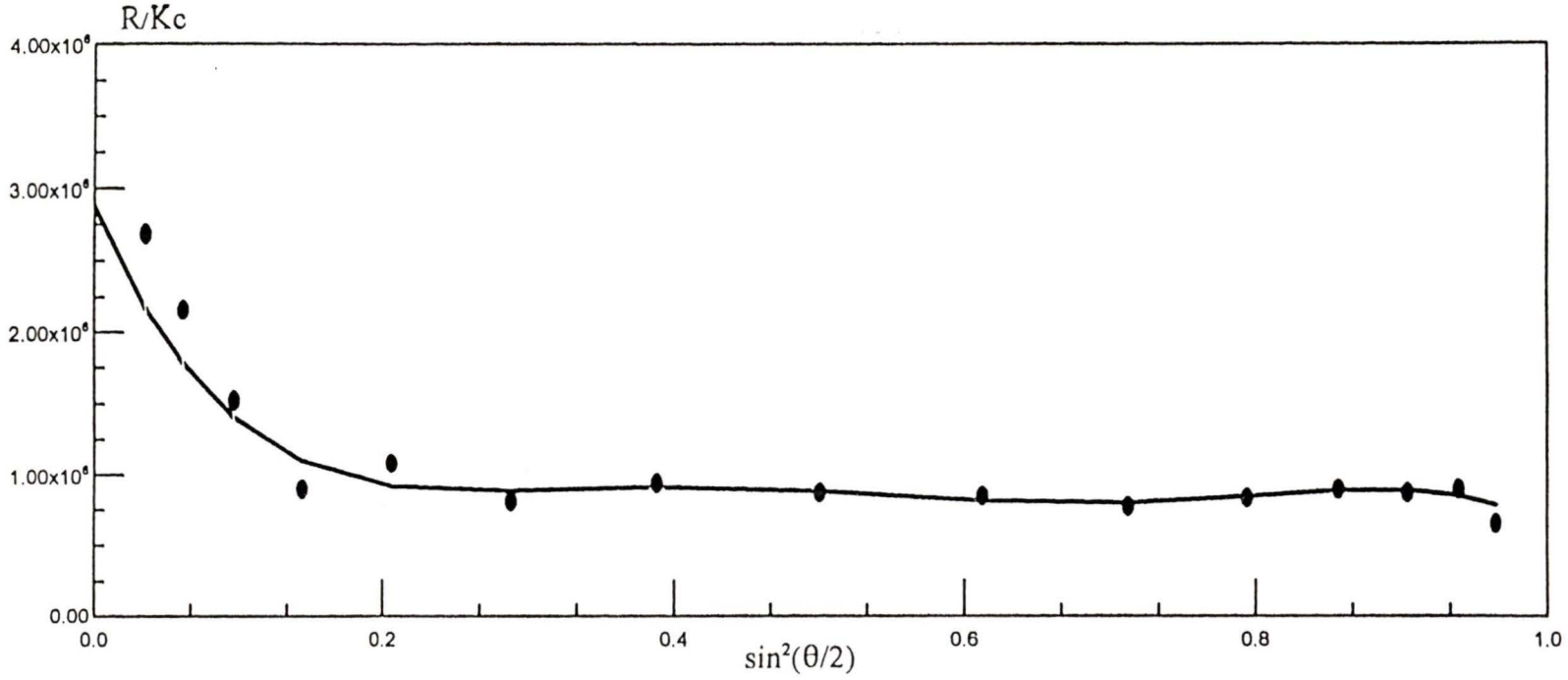

Fig. 10 Debye plot for PAM from PAM-1

θ approached zero, $P(\theta)$ approached unity and Eq. 21 was arranged to solve for the molecular weight of the ith "slice" (Eq. 22).[77]

$$M_i = \frac{2(R_0/Kc)}{1 + \sqrt{1 - 8A_2 c\,(R_0/Kc)}} \qquad \text{Eq. 22}$$

The molecular weight of the polymer may be calculated as a weight-average, number-average, or z-average.[78] Astra computes all three molecular weights but it is common practice to report the weight average molecular weight, M_w.[41,78] M_w was obtained from the molecular weight and concentration contributions of each slice by the following equation.[77]

$$M_w = \frac{\Sigma\,(c_i M_i)}{\Sigma c_i} \qquad \text{Eq. 23}$$

In addition to the calculations of the weight-average, number-average, and z-average molecular weights, Astra computes the weight-average, number-average, and z-average mean square radii of the polymer as well as the polydispersity index. The mean square radius for each slice is determined by the following equation.[77]

$$\langle r^2 \rangle_i = \frac{-3 m_0 \lambda^2}{16\pi^2 M\,(1 - 4A_2 Mc)} \qquad \text{Eq. 24}$$

where $\langle r^2 \rangle_i$ is the mean square radius of the ith slice.

m_0 is the slope at zero angle of the Debye plot,

$m_0 = d[R_\theta/K^*c] / d[sin^2(\theta/2)]_{\theta \to 0}$

It is common practice to report the mean square radius as the z-average mean square radius as shown by the following equation.[77,78]

$$\langle r^2 \rangle_z = \frac{\Sigma(c_i M_i \langle r^2 \rangle_i)}{\Sigma(c_i M_i)} \qquad \text{Eq. 25}$$

The calculation for the polydispersity index is as follows.[41,77]

$$\frac{M_w}{M_n} = \frac{\left(\frac{\Sigma N_x M_x^2}{\Sigma N_x M_x}\right)}{\left(\frac{\Sigma N_x M_x}{\Sigma N_x}\right)} = \frac{\Sigma N_x^2 M_x^2}{(\Sigma N_x M_x)^2} \qquad \text{Eq. 26}$$

where M_w / M_n is the polydispersity index.

N_x is the number of moles of solute from $x = 1$ to $x = \infty$.

M_x is the weight of the number of moles of solute, N_x, from $x = 1$ to $x = \infty$.

2.8.3. Recording photoacoustic FTIR spectra of the newly synthesized, acrylamide-based polymers

The photoacoustic FTIR spectra of the homopolymers and copolymers from DMAM-co-AM-2 to -6, MeAM-co-AM-2b to -6, and NTBAM-co-AM-1a, -1b, -2, -3, -6a, and -6b and the controls complementary to DMAM-co-AM-6, MeAM-co-AM-6, and

NTBAM-co-AM-4 were recorded from the homopolymers and copolymers as solids. For each copolymer sample 100 scan files containing 20 scans per file were averaged and the spectrum for carbon black was subtracted from each copolymer spectrum.

2.8.4. Recording ^{13}C NMR spectra of the newly synthesized, acrylamide-based polymers

^{13}C NMR spectra were obtained for the monomers; AM, DMAM, and MeAM, from solutions of 120-150 mg of monomer in 10 mL of D_2O. The spectrum for NTBAM was taken from a solution of 57.4 mg of monomer in 5 mL of deuterated methanol. ^{13}C NMR spectra for the copolymers from DMAM-co-AM-2 to -5, MeAM-co-AM-2b to -5, and NTBAM-co-AM-1b (clouded layer), -1b (clear layer), and -2, the homopolymer (PDMAM) from DMAM-co-AM-6, and the controls complementary to DMAM-co-AM-6, MeAM-co-AM-6, and NTBAM-co-AM-4 were taken from solutions containing 30-100 mg of the freeze-dried polymer and 60 mg of NaCl in 10 mL of D_2O. All of these samples were from dialyzed polymers except for the copolymer from NTBAM-co-AM-1b (clouded layer).

The homopolymer (PMeAM) from MeAM-co-AM-6 was prepared as a solution in deuterated formic acid by adding 56.9 mg of the freeze-dried polymer to 5 mL of deuterated formic acid. The freeze-dried copolymers from NTBAM-co-AM-3 (gelatinous material), -4 (gelatinous material), and -4 (tan coloured solution) and homopolymers (PNTBAM) from -5a (gelatinous material), and -6a (gelatinous material) were prepared as solutions in deuterated methanol by adding 50-90 mg of the freeze-dried polymer to 5 mL of deuterated methanol. The freeze-dried, tan solution component

of NTBAM-co-AM-3 (29.6 mg) was dissolved in 2.8 mL of 1:1, deuterated methanol / D_2O.

Spectra of the homopolymer and copolymer solutions in D_2O were recorded at CANMET's Western Research Centre with the Bruker MSL 200 MHz NMR Spectrometer using a probe temperature of approximately 298 K. Overnight analysis was required to obtain 15,000 to 20,000 scans. The remaining monomer, homopolymer, and copolymer spectra were obtained at the University of Victoria with the Bruker AMX 360 NMR Spectrometer.

2.8.5. Direct titration to determine the % cationicity of newly synthesized cationic derivatives and Percol 721

The % cationicity of the unpurified and purified cationic derivatives and the commercial polymer, Percol 721 (cationic PAM), were determined by a direct titration which neutralized the cationic polyelectrolyte with an anionic polyelectrolyte. Potassium poly(vinylsulfate) (PVSAK) was used as the titrant and Toluidine Blue O (TBO) was used as the indicator.

A 0.01 N stock solution of PVSAK was prepared by adding 1.6224 g of PVSAK to 1000 mL of distilled water. A 0.002 N standard solution was prepared from this by diluting a 100 mL aliquot of the stock solution to 500 mL with distilled water and then standardized with 0.002 N hexadimethrine bromide (DDPM). This was prepared by dissolving 2.0065 g of DDPM in 1000 mL of distilled water, and then diluting a 100 mL aliquot of the stock solution to 500 mL with distilled water. A 50 mL burette was rinsed and filled with the DDPM standard solution. The analyte solution was prepared by

adding a 25 mL aliquot of 0.002 N PVSAK to 25 mL of distilled water with 3 drops of TBO indicator. The toluidine blue indicator was prepared by dissolving 1 g of TBO to 1000 mL of distilled water. In the presence of TBO, the neutralization point was marked by a color change from blue-purple to light blue. The standardization titrations were done three times and corrected for distilled water by performing blank titrations.

Each purified cationic derivative was added as a 2 mL aliquot to 50 mL of distilled water and 3 drops of TBO indicator. Commercial Percol 721 solution was prepared by dissolving 100.6 mg of polymer to 500 mL of distilled water with gentle stirring overnight. A 2 mL aliquot was then added to 50 mL of distilled water containing 3 drops of TBO indicator, and the titration performed as just described. All analyte solutions were prepared in duplicate. The neutralization point for each analyte solution was determined twice and corrected for distilled water by performing blank titrations.

2.9. Solution Behaviour Measurements of Acrylamide-Based Polymers

2.9.1. Batch multi-angle laser light scattering (MALLS) sample preparation

The solution behaviour of the homopolymers and copolymers from DMAM-co-AM-2 to -7, MeAM-co-AM-2b to -6 (including control-6 complementary to MeAM-co-AM-6), and NTBAM-co-AM-1b (clouded layer) and -2 was studied by MALLS in the batch mode. The homopolymers and copolymers were the freeze-dried solids recovered from the dialyzed fraction of the polymerization solutions except for the copolymer from NTBAM-co-AM-1b (clouded layer) which was not dialyzed. Commercial polymers labelled Percol 351 (nonionic PAM), Percol 721 (cationic PAM), and Percol E-24

(anionic PAM) were also studied by MALLS.

Percol 351, and the newly synthesized, homopolymers and copolymers were prepared as aqueous solutions adjusted to pH 4.00 ± 0.10, pH 6.50 ± 0.20, and pH 10.00 ± 0.10 without added electrolyte and as aqueous solutions adjusted to pH 4.00 ± 0.10 with added electrolyte. Sufficient electrolyte was added to make the solutions 0.001 M, 0.01 M, 0.10 M, and 1.0 M NaCl. Percol 721 and Percol E-24 were studied only as aqueous solutions adjusted to pH 4.00 ± 0.10 with added electrolyte.

Stock solutions of the homopolymers and copolymers from DMAM-co-AM-2 to -7 were prepared by adding between 50 and 100 mg of the freeze-dried polymer to between 100 and 200 g of distilled water (pH study) or the appropriate NaCl solution (study of the effects of added electrolyte). For the study of the effects of added electrolyte, the copolymers from DMAM-co-AM-2 to -7 were added to 0.01 M NaCl and 0.10 M NaCl. In addition, the homopolymer (PDMAM) from DMAM-co-AM-6 was added to 1.0 M NaCl.

Stock solutions of the homopolymers and copolymers from MeAM-co-AM-2b to -6 and NTBAM-co-AM-1b (clouded layer) and -2 were prepared by adding between 80 and 100 mg of the freeze-dried polymer to between 25 and 40 g of distilled water (pH study) or the appropriate NaCl solution (study of the effects of added electrolyte). The stock solutions of the copolymers from MeAM-co-AM-2b to -3 and PAM from control-6 complementary to MeAM-co-AM-6 were prepared by adding between 80 and 100 mg of the freeze-dried polymer to 100 g of 0.01 M or 0.10 M aqueous NaCl solution for study of the effects of added electrolyte. In addition, PAM from control-6 was added to

0.001 M NaCl and 1.0 M NaCl.

Stock solutions of Percol 351 were prepared by adding between 50 and 60 mg of polymer to between 25 and 40 g of distilled water (pH study) and between 80 and 90 mg of polymer to 100 g of 0.001 M, 0.01 M, 0.10 M, and 1.0 M aqueous NaCl (study of the effects of added electrolyte). Stock solutions of Percol 721 and Percol E-24 were prepared by dissolving between 70 and 100 mg of polymer to between 120 and 130 g of the same range of aqueous NaCl concentrations.

The distilled water which was used for preparation of the stock solutions was filtered twice through Millipore 0.45 μm and 0.22 μm hydrophilic membranes. In addition, the various NaCl solutions which were prepared from the filtered distilled water were filtered individually through Millipore 0.45 μm and 0.22 μm hydrophilic membranes.

Each stock solution was stirred gently for approximately 16 hours to completely dissolve the acrylamide-based polymer in the particular solvent. After dissolving the polymer, the stock solutions were added to tared 50 mL beakers and their solution masses were recorded. The solution pH of each stock solution was recorded and then adjusted by the dropwise addition of dilute acid (0.01 M HCl) or dilute base (0.005 M and 0.01 M NaOH). Addition of dilute acid was done through 0.45 μm filters containing nylon hydrophilic membranes and dilute base was done through 0.50 μm filters containing PTFE hydrophobic membranes. The concentrations of the stock solutions were corrected for any added acid or base.

Four polymer solution standards were prepared from each stock solution. The

polymer solution standards included 1, 3, 5, and 7 g of pH adjusted, stock solution. Each standard was diluted to 10 g with the appropriate solvent which was adjusted beforehand to the desired pH except for the pH 10 polymer standards, which were diluted to 12.5 g with distilled water which was adjusted beforehand to pH 10. Each set of four polymer solution standards was stirred gently for 15 minutes and then filtered through disposable syringe filters into 20 mL scintillation vials. A syringe filter with a 0.45 μm nylon hydrophilic membrane was used for all except the pH 10 standards which required a more chemically resistant 0.50 μm PTFE hydrophobic membrane which was converted to hydrophilic character, as before. Syringe pumps were used to filter the standard solutions through the 0.45 μm nylon hydrophilic membrane at a rate of 0.15 mL/min and through the 0.50 μm PTFE membrane at a rate of 0.05 mL/min. Prior to use, the 20 mL scintillation vials were cleaned by rinsing with copious portions of filtered distilled water and then inverting to dry in a fumehood. As a further precaution to avoid particulate contamination, the vials were secured to the disposable syringe filters with Parafilm for the duration of the filtration. After filtration of the polymer standards, the vials were capped and sealed with Parafilm.

2.9.2. Batch multi-angle laser light scattering (MALLS) theory and methods

Calibration and normalization of the Dawn DSP-F laser photometer

Included in the MALLS assembly was a helium/neon laser (vacuum wavelength, 632.8 nm) which was directed at the scintillation vial positioned within the read head assembly of the Dawn DSP-F laser photometer. The read head assembly was modified to

accommodate a 20 mL scintillation vial for macro-batch analysis. Surrounding the read head assembly were 18 photodiode detectors which were positioned at precise angles with respect to the scintillation vial. The light scattered from the scattering medium contained in the 20 mL scintillation vial was recorded by the photodiode detectors as voltages. Rayleigh theory required conversion of the detector voltages to scattered intensities for calculation of the angle dependent light scattering as expressed by the Rayleigh ratio, R_θ.[79]

$$R_\theta = \frac{I_\theta r^2}{I_0 V} \qquad \text{Eq. 27}$$

where R_θ is the Rayleigh ratio at angle, θ.
I_θ is the scattered intensity.
r is the distance between the scattering volume and the detector.
I_0 is the scattered intensity of the incident beam.
V is the volume of the scattering medium.

Prior to measurement of R_θ for the polymer solutions, the laser photometer required calibration of the 90° detector and subsequent normalization of the other 17 detectors to the 90° detector. A calibration procedure within the Dawn 2.06 software was designed to develop a relationship between the 90° detector voltage and R_θ. A known scatterer such as toluene (HPLC grade, filtered through 0.22 μm and 0.10 μm hydrophobic membranes) which has an accepted Rayleigh ratio (1.406×10^{-5} cm^{-1} at a wavelength of 632.8 nm) was used to calibrate the 90° detector according to the following calculation.[79]

$$A_{CSCC} = R_{90} \times \frac{V_{laser} - V_{laser,\,dark}}{V_{90} - V_{90,\,dark}} \qquad \text{Eq. 28}$$

where A_{CSCC} is the Configuration Specific Calibration Constant.

R_{90} is the 90° detector Rayleigh ratio, 1.406×10^{-5} cm^{-1}.

$V_{laser} - V_{laser,\,dark}$ are the laser monitor signal and dark offset.

$V_{90} - V_{90,\,dark}$ are the 90° detector signal voltage and the dark offset voltage.

The Configuration Specific Calibration Constant, A_{CSCC}, which was determined for calibration in toluene could not be entered as a constant into the acquisition programs involving a solvent other than toluene. The A_{CSCC} was dependent on the solvent identity and the cell type for macro-batch analysis. An instrument constant, A_{INST}, which included the properties of another solvent and the geometrical factors of the scattering cell was calculated by the Dawn 2.06 software to permit measurement with a solvent other than toluene. A menu which contained various solvents and cell types was displayed in the calibration program of the Dawn 2.06 software. From the users selection of the appropriate solvent identity and cell type, A_{INST} was calculated. Following calculation of A_{INST}, a new Configuration Specific Calibration Constant, A_{CSCC}, was calculated from A_{INST} and the parameters which apply to the identity of the solvent and the cell type.[79]

$$A_{CSCC} = A_{INST} \times \frac{n_s n_g}{F} \qquad \text{Eq. 29}$$

where A_{INST} is the instrument constant which is independent of the solvent identity and the particular scattering cell.

n_s is the solvent refractive index.

n_g is the cell (scintillation vial) refractive index.

F is a Fresnel factor which describes reflection losses at various interfaces of the cell.

An isotropic scatterer (scatters equally in all directions) was used for normalization of the other 17 detectors to the 90° detector. The isotropic scatterer was polystyrene (30,000 molecular weight, Polysciences) which was prepared as a solution in toluene by adding 130 mg of polystyrene to 10 mL of toluene (HPLC grade) previously filtered through 0.22 μm and 0.10 μm hydrophobic membranes. Following a 16 hour (overnight) dissolution period, the normalization solution was filtered through a 0.50 μm disposable syringe filter containing a PTFE hydrophobic membrane into a 20 mL scintillation vial. A set of normalization coefficients were computed for each detector from the light scattering data acquired from the normalization solution. The normalization coefficients related each detectors particular geometrical factors and sensitivities to those of the 90° detector.[79]

$$N_\theta = \frac{R_\theta}{A_{CSCC}} \times \frac{V_{laser} - V_{laser,\ dark}}{V_\theta - V_{\theta,\ solvent}} \qquad \text{Eq. 30}$$

where N_θ is the normalization coefficient for the detector positioned at angle, θ.

R_θ is the Rayleigh ratio for the detector positioned at angle, θ.

A_{CSCC} is the new Configuration Specific Calibration Constant.

V_{laser} - $V_{laser,\ dark}$ are the laser monitor signal and dark offset.

V_θ - $V_{\theta,\ solvent}$ are the detector voltage and the solvent offset voltage for the detector positioned at angle, θ.

The detector voltages were recorded for the normalization solution and the solvent offset voltages were recorded for toluene. The solvent offset voltages were recorded prior to normalization and then were saved as default parameters.

Acquisition and processing of the light scattering data

The aquisition of light scattering data from each polymer standard solution followed a consistent experimental procedure. Each standard solution was made ready for analysis by inserting the 20 mL scintillation vial into the slot of the read head assembly of the laser photometer. The scintillation vial was rotated until dull illuminations were observed at the glass interface of the vial where the incident laser beam entered and exited. Having achieved proper positioning of the scintillation vial, the concentration of the polymer standard was entered into the collection menu and the acquisition program was activated. At each vial position, the detector voltages were scanned for 7 instrument counts and then averaged for each detector. The Dawn software presented the data as a plot of the normalized voltage versus the detector

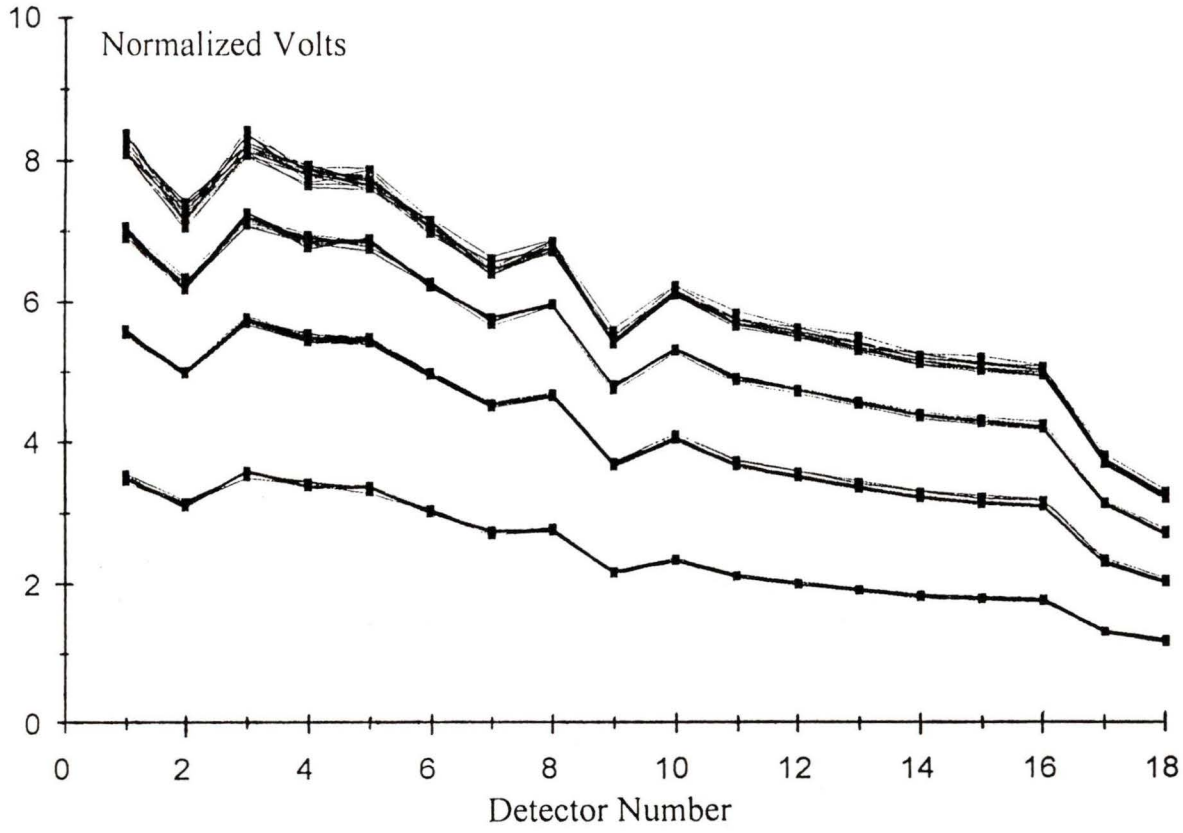

Fig. 11 Plot of normalized voltage versus detector number for PDMAM from DMAM-co-AM-6 at pH 4.0 and containing no added electrolyte

number (Fig. 11). The scan was repeated at least three times at each scintillation vial position to yield a minimum of three plots of the normalized voltage versus the detector number. A minimum of 7 positions were selected for data aquisition to yield a minimum of 21 scans per polymer standard. Upon completion of the data aquisition for each set of four polymer standards, the Aurora Module of the Dawn software was accessed to process the light scattering data by the method of Zimm.[38,77,79] The method of Zimm was used to plot the light scattering intensity versus the angular dependence (Fig. 12) for all 18 detectors and each polymer standard concentration (details, Eq. 15).[79]

$$y = \frac{K \times c}{R_\theta} \quad vs. \quad \sin^2(\theta/2) + kc \qquad \text{Eq. 31}$$

where

$$\frac{K \times c}{R_\theta} = \frac{1}{M_w}\left[1 + \frac{16\pi^2}{3\lambda^2}\langle r_g^2\rangle \sin^2(\theta/2) + \cdots\right] + 2A_2 \qquad \text{Eq. 32}$$

where K is an optical constant, $4\pi^2 n_0^2 (dn/dc)^2 \lambda_0^{-4} N_A^{-1}$, where n_0 is the solvent refractive index, dn/dc is the refractive index increment, λ_0 is the incident wavelength in vacuum (632.8 nm), and N_A is Avogadro's number.

c is the solute concentration in g/mL.

R_θ is the Rayleigh scattering intensity at angle, θ.

$\sin^2(\theta/2)$ is the angular dependence of the scattered light at angle, θ.

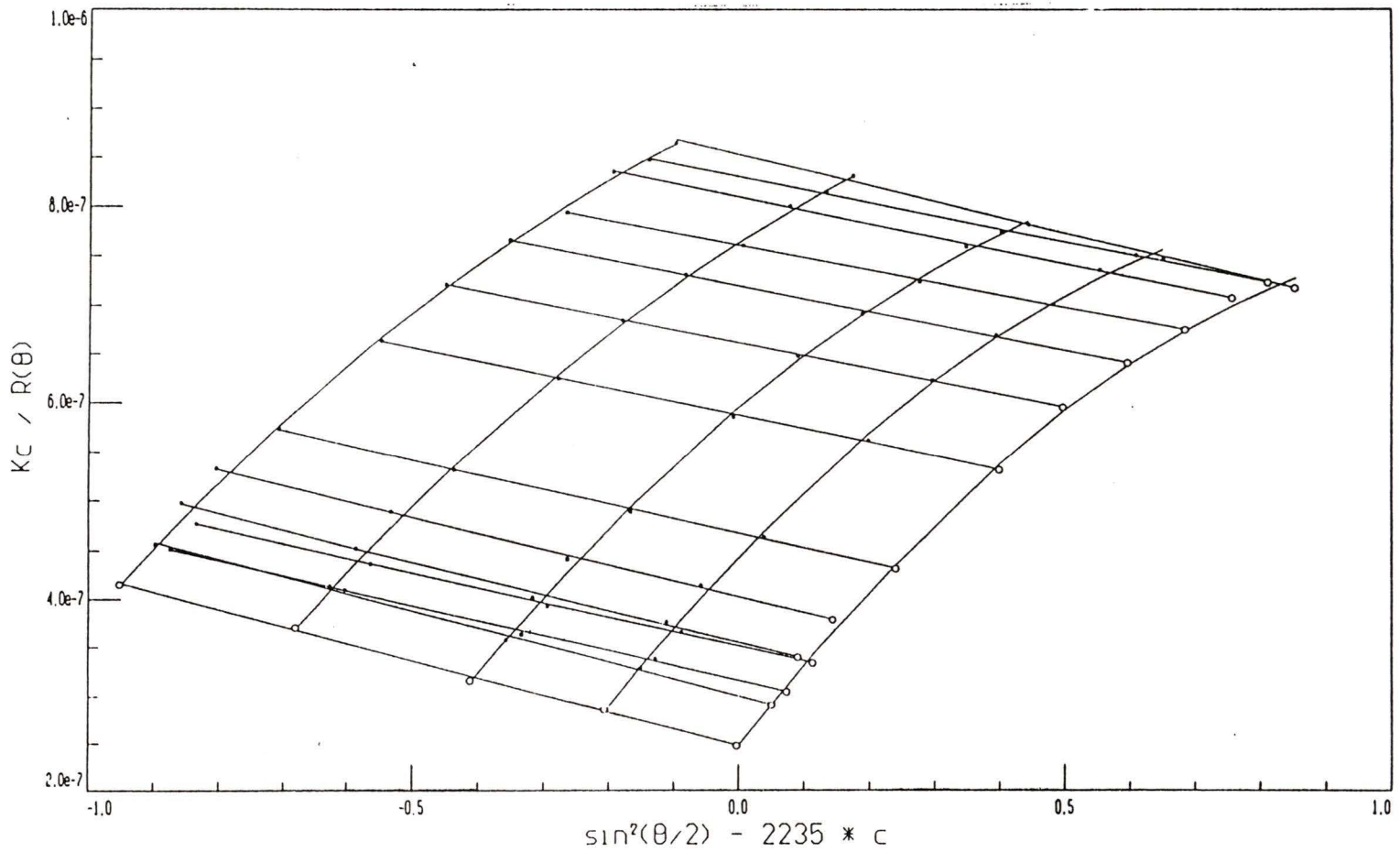

Fig. 12 Zimm plot for PDMAM from DMAM-co-AM-6 at pH 4.0 and containing no added electrolyte

k	is a scaling factor for improving the appearance of the Zimm plot.
M_w	is the weight average molecular weight.
$< r_g^{\,2} >$	is the mean square radius of gyration.
A_2	is the second virial coefficient which accounts for solute / solvent interactions.

From the light scattering data the following variables were known; R_θ, c, K, λ, and θ. By manipulation of the Zimm plot it was possible to obtain the values for the following unknown variables; M_w, $< r_g^{\,2} >$, and A_2. The weight average molecular weight, M_w, was obtained from the Zimm plot by extrapolating the data to zero angle and zero concentration as shown by the following relation.[79]

$$y_{c\theta} = \lim_{c \to 0} \left\{ \lim_{\theta \to 0} \frac{K \times c}{R_\theta} \right\} = \frac{1}{M_w} \qquad \text{Eq. 33}$$

where $y_{c\theta}$ is the y-intercept of the Zimm plot as determined by extrapolating the light scattering data to zero angle and zero concentration.

To determine the second virial coefficient, A_2, the data from the Zimm plot was extrapolated to zero angle. The slope of the projection line to zero angle gave the second virial coefficient as the scaling factor, k, was known (Eq. 34).[79]

$$m_c = \frac{d}{d(kc)} \lim_{\theta \to 0} \frac{K \times c}{R_\theta} = \frac{2A_2}{k} \qquad \text{Eq. 34}$$

where m_c is the slope of the projection line to zero angle which was produced by extrapolating the light scattering data to zero angle.

A value for the mean square radius of gyration, $< r_g^2 >$, was determined by extrapolating the data from the Zimm plot to zero concentration. The slope of the projection line to zero concentration yielded a relationship which involved the mean square radius of gyration, $< r_g^2 >$, and the weight average molecular weight, M_w.[79]

$$m_\theta = \frac{d}{d \sin^2(\theta/2)} \lim_{c \to 0} \frac{K \times c}{R_\theta} = \frac{1}{M_w} \frac{16\pi^2 < r_g^2 >}{3\lambda^2} \qquad \text{Eq. 35}$$

where m_θ is the slope of the projection line to zero concentration as generated by extrapolating the light scattering data to zero concentration.

Since the weight average molecular weight, M_w, was determined by extrapolating the Zimm plot to zero concentration and zero angle, the value for $< r_g^2 >$ was determined by substitution of M_w into Eq. 35. Usually, the z-averaged value was presented for $< r_g^2 >$ which required substitution of M_z into Eq. 35 instead of M_w.[78,79] The z-average molecular weight, M_z, is the ratio of the third moment of the distribution about the molecular weight origin to the second moment about the origin as shown by the following equation.[79]

$$M_z = \frac{\sum_i N_i M_i^3}{\sum_i N_i M_i^2} \qquad \text{Eq. 36}$$

where $N_i M_i$ is the number of molecules, *i*, with a particular molecular weight.

2.10. Measurement of the Refractive Index Increment, dn/dc, for Acrylamide-Based Polymers in Various Aqueous Solvents

2.10.1. Calculation of a calibration constant, dn/dV, to determine dn/dc

NaCl which has an accepted refractive index increment (dn/dc = 0.174) was used to determine dn/dV.[80] NaCl solution standards were prepared from a 2×10^{-3} g/mL NaCl stock solution as 1×10^{-3}, 1.5×10^{-3}, 1.75×10^{-3}, and 2×10^{-3} g/mL solutions. Prior to use, the distilled water which was used to prepare the stock solution and to dilute the standards was filtered through 0.45 μm and 0.22 μm nylon hydrophilic membranes. To calculate the individual refractive indexes, n, of the NaCl solution standards, the refractive index increment for NaCl (dn/dc = 0.174) was multiplied by the individual concentrations. The slope of the best straight line which was fit to a plot of the individual refractive indexes of the NaCl solution standards versus the individual auxiliary detector voltages of the standards gave dn/dV (Fig. 13).

Having determined dn/dV, the refractive index increment, dn/dc, was determined for each set of four polymer solution standards from a plot of the individual refractive indexes of the standards versus the individual concentrations. To determine the individual refractive indexes of the polymer solution standards, the calibration constant,

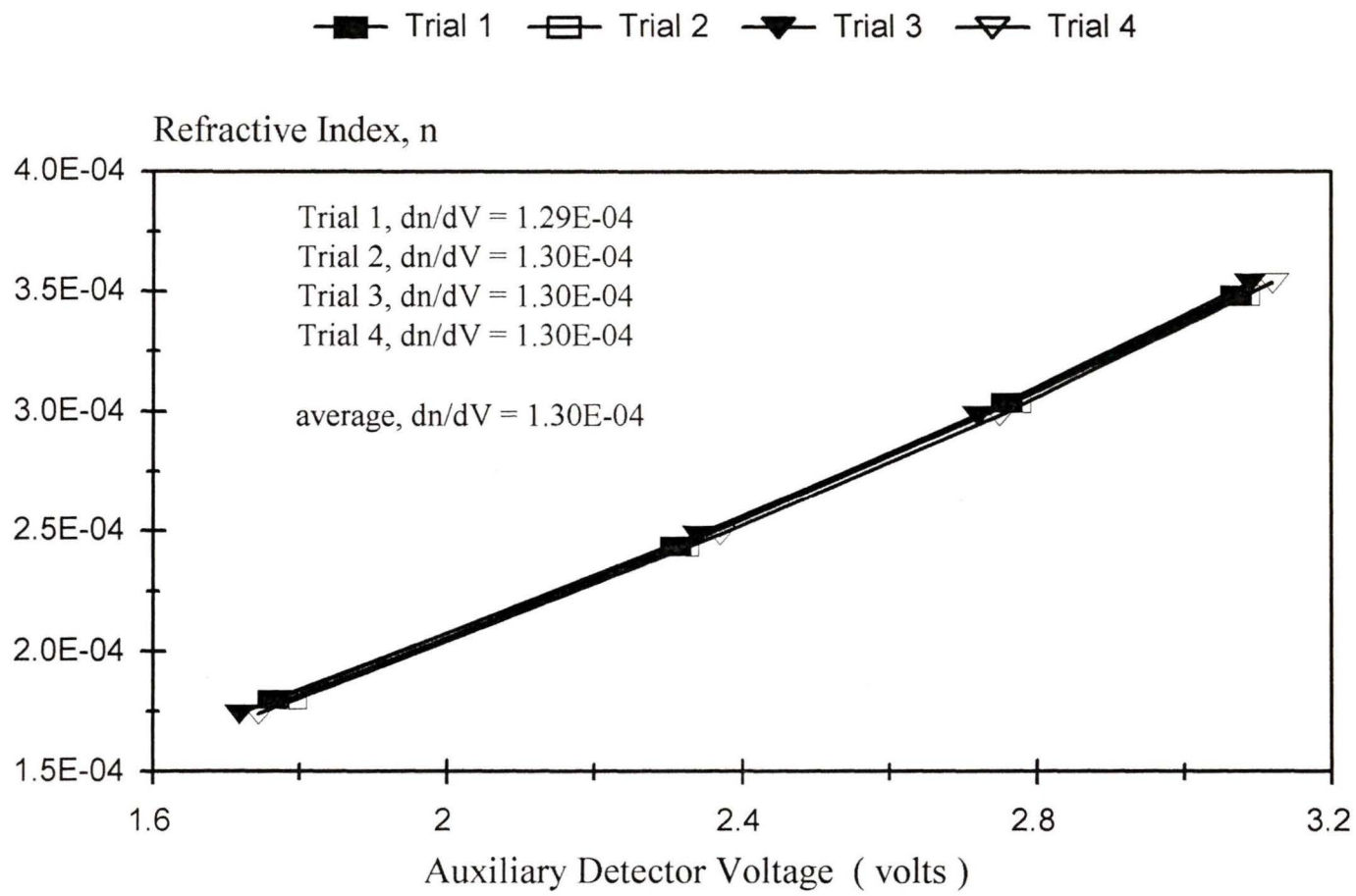

Fig. 13 Refractive indexes, n, versus the auxiliary detector voltages (volts) for NaCl standards. The calibration constant, dn/dV, was the slope of the best straight line calculated by linear regression for each set of data.

dn/dV, was multiplied by the individual auxiliary detector voltages of the standards. Linear regression was used to construct the best straight line from the plot. The slope of the best straight line gave dn/dc.

2.10.2. Experimental procedure

The refractive index increment was measured by an assembly which included the Waters 501 HPLC pump, Waters In-Line Degasser, Waters Pulse Dampener, Rheodyne 2 mL HPLC injection loop, Shodex OH pak columns (KB-805 column with an exclusion limit of 2×10^6 to 4×10^6 molecular weight, and KB-806 column with an exclusion limit of 1×10^7 to 2×10^7 molecular weight), Waters Differential Refractometer R401, and the Dawn DSP-F laser photometer.

The same polymer solution standards which were used to construct Zimm plots from the MALLS data were used to determine the refractive index increment, dn/dc, of the particular acrylamide-based polymer and solvent. Before the polymer standards could be injected into the Rheodyne 2 mL HPLC injection loop, the auxiliary detector voltage of the laser photometer required stabilization against distilled water. The distilled water (filtered beforehand through 0.45 μm and 0.22 μm nylon hydrophilic membranes) was pumped at a rate of 1.0 mL/min from a 4 litre erlenmeyer flask by the Waters 501 HPLC pump. After passing through the Waters In-Line Degasser and Waters Pulse Dampener, the distilled water entered the Rheodyne 2 mL HPLC injection loop. The Shodex OH pak columns were connected in series to the Rheodyne 2 mL HPLC injection loop to provide back pressure to the injection loop. From the HPLC injection

loop, the distilled water passed through the sample cell of the Waters Differential Refractometer R401 and was collected in a waste container. Approximately 3 days (72 hours) were required to stabilize the auxiliary detector of the laser photometer against distilled water.

A syringe pump was used to pass copious portions of distilled water at a rate of 0.50 mL/min through a disposable syringe filter which contained a 0.45 μm nylon hydrophilic membrane and then the reference cell of the Waters Differential Refractometer R401. After 30 to 40 mL of distilled water passed through the reference cell, a 10 mL aliquot of water was used to fill the reference cell. The Waters Differential Refractometer R401 was connected to the auxiliary detector of the Dawn DSP-F laser photometer and the interaction of light with the solution passing through the sample cell was recorded as a voltage.

Having achieved stabilization of the auxiliary detector, the refractive index increment assembly was equipped to analyze the polymer standards. To analyze the polymer standards the reference cell of the Differential Refractometer was filled with the appropriate solvent after copious portions of the solvent were passed through the reference cell. Each set of four polymer standards was analyzed by injection of the standards into the refractive index increment assembly from the lowest standard concentration to the highest. A 5 mL syringe (Hamilton GTS, gastight sampling syringe) was used to inject approximately 3.0 mL of the polymer standard into the 2 mL HPLC injection loop. The greater injected volume ensured that the injection loop held only the current polymer standard. After rotation of the injection lever to introduce the polymer

standard to the distilled water flow, the auxiliary detector voltage was monitored until the voltage signal increased rapidly. The auxiliary detector voltage was recorded 1 minute after the signal increase was observed. Following the analysis of each set of four polymer standards, a 3.0 mL aliquot of filtered distilled water was injected into the 2.0 mL injection loop to clear the loop of any remaining polymer solution.

2.11. Flocculation

2.11.1. Preparation of the flocculation test medium

Heteroionic kaolinite was converted to homoionic Na-kaolinite by a sequence of treatments with deionized water and 2 M NaCl and 1 M NaCl in deionized water. A slurry of kaolinite in deionized water in a weight ratio of 1:2 was mixed via an over-head stirrer for approximately 15 minutes and then was diluted with deionized water to give 1:30 (w/w), kaolinite to water. The diluted slurry was mixed for 15 minutes and then allowed to settle for approximately 24 hours. Following settling, the majority of the supernatant volume of the settled slurry was siphoned away to leave the settled kaolinite at a volume which was equivalent to that of the original 1:2 slurry. The treatment with deionized water was repeated 10 - 12 times. The treatment procedure for 2 M NaCl and 1 M NaCl was identical to that for deionized water except that 2 M or 1 M NaCl was added to the 1:2 kaolinite slurry for the first cycle of the NaCl treatments. The remaining cycles involved treatment with deionized water to remove the excess electrolyte from the clay which continued until the electrolyte concentration in the supernatant of the settled kaolinite slurry approached 1.5×10^{-4} M NaCl and the pH stabilized at 6 - 7. Na-

kaolinite was recovered from the treatment slurry by freeze-drying several 300 mL and 150 mL portions. The entire mass of freeze-dried Na-kaolinite was mixed in a pestle and mortar assembly and then rolled via a drop-sheet.

A 3% (w/w) Na-kaolinite test medium was prepared by adding Na-kaolinite to deionized water on a 10 litre scale. Prior to flocculation testing, the test medium was mixed via an over-head stirrer for approximately 30 minutes each day for 10 days.

A 1% (w/w) kaolinite test medium was also prepared to overcome a lack of response to flocculant concentration shown by the 3% suspension. This was made by the same procedure as used for the 3% test medium, except on a 20 litre scale.

2.11.2. Measurement of the NaCl concentration in the supernatant of the settled slurry

Theory

A strong electrolyte like NaCl yields a linear relationship between the equivalent conductance (S cm^2) and the square root of the concentration $(eq/cm^3)^{0.5}$.[81] Equivalent conductance is calculated from the specific conductance by the following equation.

$$\Lambda = \frac{1000\ k}{C} \qquad \text{Eq. 37}$$

where Λ is the equivalent conductance (S cm^2).

k is the specific conductance (S cm^{-1}).

C is the concentration (eq/cm^3) whereby the equivalent is defined as the gram formula weight of an ionic solute divided by the number of positive or negative charges associated with it.

Experimental

A 1.0×10^{-2} M stock solution was prepared by adding 0.5843 g of NaCl to 1 litre of deionized water in a volumetric flask. From the stock solution, 1.0×10^{-4}, 2.0×10^{-4}, and 5.0×10^{-4} M standard solutions were prepared. The specific conductance (S cm^{-1}) was measured for each of the NaCl standard solutions using the Accumet Model 50 pH / ion / conductivity meter equipped with conductivity and temperature probes. Prior to use, the conductivity meter was standardized by entering 1408.07 µS/cm for a 0.7453 g/L KCl standard.[82] The specific conductance of a 250 mL aliquot of the supernatant of the settled kaolinite slurry was measured. A calibration plot of equivalent conductance (S cm^2) versus the square root of concentration $(eq/cm^3)^{0.5}$ was prepared for the NaCl standards (Fig. 14).

2.11.3. Flocculation test procedure for polymer addition to a 3% Na-kaolinite test medium

The standard mixing tank used for flocculation test work has been described under equipment. For continuous addition of the polymer to the test medium, a 10 mL aliquot of the polymer solution (10^{-4} to 10^{-3} g/mL concentration) was drawn into a 30 mL plastic syringe and then dispensed at a continuous rate by a syringe pump. Polymer solution delivery was through clear plastic tubing secured to the standard mix tank at a location just below the surface of the test medium and between two baffles and the stainless steel shaft of the impeller.

Each flocculation test was designed to add a 10 mL aliquot of polymer standard solution to 290 mL of 3% Na-kaolinite. The concentrations of the stock solution and

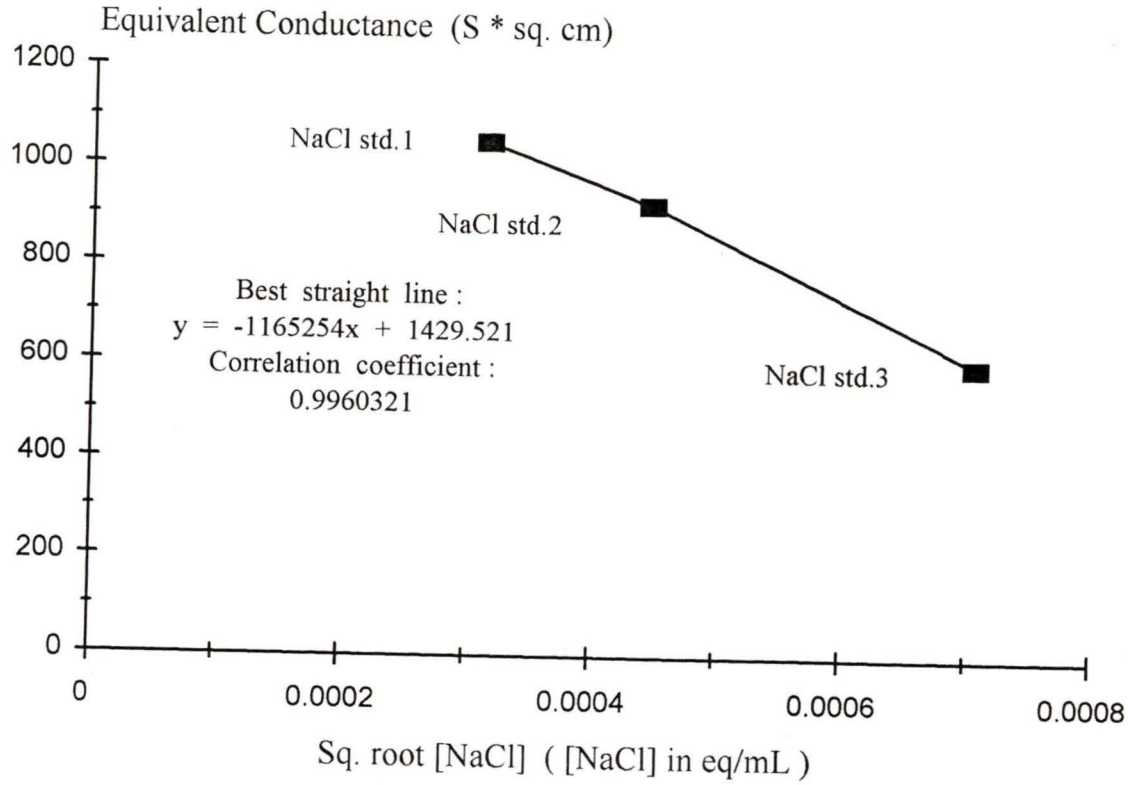

Fig. 14 Calculation of the NaCl concentration in the supernatant of settled Na-kaolinite from the equation for the best straight line calculated for the plot of equivalent conductance (S/cm^2) of NaCl standards versus $([NaCl])^{0.5}$.

standard solutions were based on the ratio of the dry mass of polymer to dry mass of Na-kaolinite for a 10 mL aliquot of polymer solution added to 290 mL of 3% Na-kaolinite. The dry mass content of 290 mL of 3% Na-kaolinite was approximately 9 g. To prepare 0 - 1000 ppm polymer solution standards, a 1000 ppm stock solution was prepared by adding approximately 90 mg of the freeze-dried polymer to 1000 g of deionized water. The stock solution was stirred overnight under mild agitation to completely dissolve the polymer.

Flocculation progress was followed by recording the settling rate, sediment volume, supernatant turbidity, and capillary suction time. To measure settling rates, the flocculant treated slurry was poured through a wide-mouthed funnel into a 250 mL graduated cylinder for which the volume increments were extended to 300 mL to accommodate the entire volume of the flocculated slurry. The graduated cylinder was placed against a black background to assist observation of the interface (mud-line) between the supernatant and the solids phase of the flocculant treated slurry. Timing of the descent of the mud-line was started at the instant the flocculated slurry was poured into the 250 mL graduated cylinder. The first measurement of the elapsed time was recorded following formation of the mud-line and subsequent descent to a marked increment. The remaining measurements of elapsed time for descent of the mud-line were recorded for 10 mL increments from 290 mL to 210 mL and for 20 mL increments from 210 mL to 90 mL.

From the elapsed times for the required volume increments, individual settling rates were calculated. The individual settling rates corresponded to the volume height in

centimetres between successive volume increments (9 cm volume height per 10 mL volume increment) divided by the elapsed time in seconds between the same volume increments. From the individual settling rates, the method of successive averages was used to calculate the initial average settling rate, the average settling rate to compaction, and the average settling rate in units of cm/s.[68] The initial average settling rate corresponded to the average of the maximum individual settling rates. In most cases, the initial average settling rate was calculated for the times elapsed between the volume increments of 290 mL and 250 mL. The average settling rate to compaction and the average settling rate were calculated as the averages of the individual settling rates between the 290 mL and 170 mL levels and the 290 mL and 90 mL levels, respectively.

Following 30 minutes of elapsed time from the instant the flocculated slurry was poured into the graduated cylinder for settling tests, the sediment volume was measured. The sediment volume was defined as the volume increment corresponding to the interface (mud-line) between the less turbid supernatant and the settled material. Immediately after the sediment volume was recorded, the supernatant turbidity was measured to give a 30 minute turbidity measurement for each settling test. To sample the supernatant in the graduated cylinder, a 20 mL glass pipette was fitted with a rubber stopper to ensure that the supernatant was sampled from the 190 mL level for all tests. The 20 mL aliquot was placed into a 30 mL scintillation vial for turbidity analysis. For the turbidity measurements, the 0 to 2000 NTU range of the turbidimeter was selected in order to be able to include measurement of the supernatant of the 3% Na-kaolinite test medium. A 0 to 2000 NTU standard was measured prior to each supernatant sample to

calibrate the instrument.

The 280 mL of settled test solution remaining in the graduated cylinder was redispersed by inversion of the stoppered cylinder several times and then poured into a 400 mL beaker to await measurement of the capillary suction time. The Triton - W.R.C. Multipurpose Filtration Unit included a cylindrical metal reservoir (25 mm height, 18 mm bore) which was placed on a rectangular section of absorbant paper (Whatman No. 17). The absorbant paper was supported by a Plexiglass plate on the underside and covered by a second Plexiglass plate which had an opening for the cylindrical metal reservoir. A timing device was connected to the electrical contacts of the top Plexiglass plate. The electrical contacts touched the surface of the absorbent paper at radii of 3.2 cm and 4.5 cm from the metal reservoir. Capillary suction times were measured by quickly pouring the redispersed slurry through a plastic funnel mounted on the surface of the cylindrical metal reservoir. A volume greater than the capacity of the cylindrical metal reservoir was added. The liquid phase of the flocculated slurry was drawn into the absorbent paper by capillary suction and the timing device was activated once the liquid phase reached the electrical contact positioned at 3.2 cm. When the liquid phase reached the electrical contact positioned at 4.5 cm, the timing device stopped to give the capillary suction time for the flocculated slurry. The capillary suction times were measured in triplicate and averaged to give the reported average capillary suction time.

2.11.4. Investigation of the physical variables associated with the flocculation test procedure

Prior to each flocculation test, the 290 mL aliquot of the Na-kaolinite test medium

was dispersed at 1500 rpm agitation for 5 minutes and then adjusted to the desired rate of agitation for an additional 5 minutes of mixing. PAM from control-6 (complementary to MeAM-co-AM-6) was used to prepare polymer solution standards from 0 to 1000 ppm based on the ratio of the dry mass of polymer to dry mass of 3% Na-kaolinite. Following the addition of the 10 mL aliquot of polymer solution to the Na-kaolinite test medium, agitation was stopped. Only settling rates were used to evaluate the flocculation performance of the individual tests.

To investigate the effect of polymer dosage on flocculation performance, the agitation rate was set to 1000 rpm during polymer addition and the rate of polymer addition was adjusted to add 10 mL of polymer solution over 60 seconds.

Agitation rates of 500, 750, 1000, and 1250 rpm were used to study the effects of agitation on flocculation performance. For each flocculation test the rate of polymer addition was held constant at 10 mL over 60 seconds. In addition, a polymer dosage of 700 ppm was held constant for each flocculation test.

The effects of the rate of polymer addition on flocculation performance were investigated for the addition of 10 mL of polymer solution over 30, 60, and 90 seconds. An agitation rate of 1000 rpm and a polymer dosage of 700 ppm were used for the flocculation tests.

2.11.5. Flocculation of 3% Na-kaolinite using the copolymers from MeAM-co-AM-2b to -4 and control PAM

To measure the sensitivity of the flocculation test procedure to polymer chain extension, average settling rates, supernatant turbidity, sediment volume, and capillary

suction time were measured for the copolymers from MeAM-co-AM-2b to -4 and PAM from control-6 (complementary to MeAM-co-AM-6). The flocculation tests included a polymer dosage of 700 ppm, an agitation rate of 1000 rpm, and the addition of 10 mL of polymer solution (10^{-4} to 10^{-3} g/mL) over 60 seconds.

2.11.6. Flocculation of 1% Na-kaolinite using commercial PAM and control PAM

For a 1% Na-kaolinite test medium, the sensitivity of the flocculation test procedure to polymer chain extension was measured for the PAM from control-6 (5E+06 to 10E+06 MW) and PAM (5E+05 MW, Polysciences). The flocculation tests included polymer dosages from 0 to 1000 ppm, 1000 rpm agitation, and the addition of 10 mL of polymer solution (10^{-4} to 10^{-3} g/mL) over 60 seconds. Settling rates, supernatant turbidity, sediment volume, and capillary suction time were used to evaluate flocculation performance.

2.11.7. Flocculation of 1% Na-kaolinite using 25, 50, and 100 ppm of commercial PAM and control PAM

Flocculation tests were run for PAM from control-6 which was complementary to MeAM-co-AM-6 (5E+06 to 10E+06 MW) and PAM (5E+05 MW, Polysciences) at polymer dosages of 25, 50, and 100 ppm using 1% Na-kaolinite in deionized water. The average settling rates and supernatant turbidities were recorded for agitation rates of 500, 750, 1000, and 1250 rpm, and 10 mL of polymer solution added over 30, 60, and 90 seconds.

2.11.8. Flocculation of 1% Na-kaolinite using the newly synthesized polymers and commercial polymers

The newly synthesized, acrylamide-based polymers and the commercial polymers of the Percol trade-name were examined as flocculants for 1% Na-kaolinite in deionized water. Copolymers from DMAM-co-AM-3 to -6, MeAM-co-AM-2b to -5 (including PAM from control-6), and NTBAM-co-AM-1b (clouded layer), -1b (clear layer), and -2 (dialysis fraction) as well as the purified cationic derivatives originating from DMAM-co-AM-7, MeAM-co-AM-2b, NTBAM-co-AM-1b (clouded layer) and PAM from control-6 (complementary to MeAM-co-AM-6) were introduced individually as 25, 50, and 100 ppm polymer standard solutions to 1% Na-kaolinite in deionized water. Percol 351 (nonionic PAM), Percol 721 (cationic PAM), and Percol E-24 (anionic PAM) were also introduced individually as 25, 50, and 100 ppm polymer standard solutions to 1% Na-kaolinite in deionized water. The flocculation test procedure held constant an agitation rate of 1000 rpm and the addition of 10 mL of polymer solution (10^{-4} to 10^{-3} g/mL) over 60 seconds.

3. Results

3.1. Evaluation of the Sample Preparation Procedure and the Molecular Weight Accuracy of the GPC / MALLS Analysis of Commercial PAM

The GPC / MALLS molecular weight results for commercial PAM were less than one-half of the molecular weight quoted by Polysciences, although there was good internal agreement between the molecular weights of the filtered and unfiltered samples (Table 12).

To process the light scattering data and determine the weight average molecular weight of commercial PAM, the method of Debye required a polynomial fit degree of 5. A polynomial fit degree of 5 is the maximum fit degree made available by the processing function of the Astra software. Earlier experiments which used Polysciences Dextran standards required a polynomial fit degree of 3 to process the light scattering data. The GPC / MALLS technique gave a weight average molecular weight, M_w, of (3.874 ± 0.9)E+04 for Dextran (40,000 mol. wt.) and (1.854 ± 0.4)E+05 for Dextran (170,000 mol. wt.).

The values entered for the AUX1 Calibration Constant and the differential refractive index increment, dn/dc, were used to calculate the eluted mass of the polymer from the GPC columns. The filtered and unfiltered stock solutions of commercial PAM consistently gave eluted masses which were approximately 70 % of that injected. Even the Dextran standards gave eluted masses which were 83 % (Dextran, 40,000 mol. wt.) and 69 % (Dextran, 170,000 mol. wt.) of the injected mass.

Table 12 Molecular weights determined by GPC / MALLS for filtered and unfiltered, duplicate stock solutions of Polysciences PAM

Preparation procedure [a, b]	GPC / MALLS (M_w)
stock soln. 1, unfiltered	(1.969 ± 0.1)E+06
stock soln. 1, unfiltered	(1.833 ± 0.1)E+06
stock soln. 1, filtered	(1.859 ± 0.1)E+06
stock soln. 2, unfiltered	(2.170 ± 0.2)E+06
stock soln. 2, unfiltered	(2.116 ± 0.2)E+06
stock soln. 2, filtered	(1.961 ± 0.2)E+06

a. To evaluate the effect of shear from filtration through 0.45 μm disposable syringe filters, the molecular weights were determined for filtered and unfiltered polymer solutions.
b. Stock solutions were nonionic polyacrylamide of 5,550, 000 molecular weight supplied by Polysciences, dissolved in 0.1 M aqueous NaCl.

3.2. Effect of Polymerization Atmosphere on the Molecular Weight of PAM

PAM from PAM-4 which included nitrogen as the polymerization atmosphere and kept AM separate from the water solvent during the 6 hour nitrogen sparge gave the highest M_w and M_v (Table 13). PAM from PAM-3 which also included nitrogen as the polymerization atmosphere but combined AM and water during the 14 hour nitrogen sparge gave M_w and M_v values which were lower than those for PAM from PAM-4 by approximately a factor of 2. In fact, the experimental uncertainty of M_w for PAM from PAM-3 overlapped the experimental uncertainty of the value for PAM from PAM-1 (filtered air).

3.3. Evaluation of Homopolymerization Experimental Conditions

3.3.1. Homopolymerization of DMAM

Only PDMAM-3 of PDMAM-1 to -3 produced a homopolymer which was water-soluble. The experimental conditions for PDMAM-1 and -2 were identical to those for PDMAM-3 except for the polymerization temperature. PDMAM-1, -2, and -3 were polymerized at 60°C, 30°C, and 50°C, respectively. A polymerization temperature of 60°C over a 3.5 hour duration produced PDMAM as a gelatinous material which would not disperse even with significant dilution and mild heating. However, control-1 (homopolymerization of AM) produced a polymer solution which exhibited a noticeable increase in viscosity without evidence of gelation. Decreasing the polymerization temperature to 30°C showed no evidence of an increase in solution viscosity for either the homopolymer solution from PDMAM-2 or control-2. PDMAM-3 which included a

Table 13 Effect of filtered air, oxygen, and nitrogen atmospheres on the polymerization of acrylamide at 60 °C

Experiment	Polymerization atmosphere	GPC / MALLS [a] (M_w, g/mol)	GPC / MALLS [b] (M_w, g/mol)	Viscometry [c] (M_v, g/mol)
PAM-1	filtered air	(7.567 ± 0.7)E+05	n/m [d]	1.187 E+05
PAM-2	oxygen	(6.588 ± 0.6)E+05	(7.413 ± 2.0)E+05	2.259 E+05
PAM-3	nitrogen	(8.879 ± 0.8)E+05	(7.665 ± 2.0)E+05	4.172 E+05
PAM-4	nitrogen	(1.695 ± 0.1)E+06	(1.710 ± 0.3)E+06	1.107 E+06

a. Stock solutions were prepared in a pH 5.40 buffer solution (sodium acetate / acetic acid). Weight average molecular weights were calculated by the method of Debye.[35,77]
b. The same stock solutions which were used for viscometry analysis were used for analysis by GPC / MALLS. Weight average molecular weights were calculated by the method of Debye.[35,77]
c. Stock solutions were prepared in a 0.1 M NaCl solution. Viscosity average molecular weights were calculated by the Mark Houwink equation for PAM in 0.5 M NaCl at 25.0 °C.[75]
d. n/m denotes not measured.

polymerization temperature of 50°C produced PDMAM from PDMAM-3 and PAM from control-3 as viscous solutions. In fact, the intrinsic viscosities measured for PDMAM-3 and control-3 were nearly identical (Table 14). In addition to the intrinsic viscosities, M_w and M_v values for PDMAM from PDMAM-3 and PAM from control-3 were included in Table 14. For both PDMAM and PAM, M_w which was determined by GPC / MALLS was greater than 1.0 E+06. Similar to the GPC / MALLS results for PAM from PAM-1 to -4, the eluted mass from the GPC columns was calculated as 65 % and 71 % of the injected mass for PDMAM and PAM, respectively. M_v for PAM was also greater than 1.0 E+06 but lower than the corresponding M_w. M_v for PDMAM was lower than the corresponding M_w but greater than M_v for PAM.

3.3.2. Homopolymerization of MeAM

None of PMeAM-1 to -5 produced a homopolymer (PMeAM) which was water-soluble. Of these, PMeAM-4 formed a gelatinous material but none exhibited an increase in solution viscosity. When the freeze-dried homopolymers recovered from PMeAM-1 to -5 were added to distilled water they floated on the surface. Agitation, mild heating, and sonication would not dissolve them. Control-1 to -5 (homopolymerizations of AM) produced solutions which exhibited an increase in viscosity without gel formation.

The only variables for these polymerizations were the mole ratio of the initiator ($K_2S_2O_8$) to MeAM and / or the polymerization duration. The highest intrinsic viscosity was measured for PMeAM from PMeAM-4 which used a mole ratio of $K_2S_2O_8$ to MeAM

Table 14 Molecular weight and intrinsic viscosity for PDMAM and PAM produced under identical experimental conditions

Experiment	GPC / MALLS [a] (M_w , g/mol)	Intrinsic viscosity ([η], cm^3/g)	Viscometry (M_v , g/mol)
PDMAM-3	(3.983 ± 0.3)E+06	354	2.619 E+06 [b]
control-3	(1.824 ± 0.2)E+06	355	1.246 E+06 [c]

a. The weight average molecular weight, M_w , was determined by GPC / MALLS.
b. The viscosity average molecular weight, M_v , was determined using the Mark Houwink Equation for PAM in 0.5 M NaCl at 25°C.[75]
c. The viscosity average molecular weight, M_v, was determined using the relation for PDMAM in water at 25°C.[76]

of 1/1000 and a polymerization duration of 13.25 hours (Table 15). If the polymerization duration was reduced while keeping the mole ratio of $K_2S_2O_8$ to MeAM constant or the mole ratio of $K_2S_2O_8$ to MeAM was increased while keeping the polymerization duration constant lower intrinsic viscosities were obtained. The intrinsic viscosities for control-1 to -5 were not affected by varying the polymerization duration or the mole ratio of $K_2S_2O_8$ to AM, except for control-5 which used a mole ratio of $K_2S_2O_8$ to AM of 1/500. This sample gave the lowest intrinsic viscosity of the controls. Values of M_v for control-1 to -5 approximated 1.0E+06 g/mol for all but control-5. M_w's determined by GPC / MALLS were all greater than 1.0 E+06 g/mol but did not follow the same trends as the intrinsic viscosities or M_v. In addition, the eluted mass from the GPC columns was calculated as 81 - 92 % of the injected mass for the control homopolymers.

3.3.3. Homopolymerization of NTBAM

(a) In methanol and methanol / distilled water mixtures

Solubility tests of NTBAM in MeOH / water mixtures determined that a minimum of 50 % MeOH was required in the polymerization medium to use a 1.0 M NTBAM concentration. Solubility tests of AIBN, and $K_2S_2O_8$ in 99.8 % MeOH, 1:1 MeOH / water, and 1:9 MeOH / water determined that $K_2S_2O_8$ was not soluble in 99.8 % MeOH.

Homopolymerization of NTBAM in 99.8 % MeOH, 1:1 MeOH / water, and 1:9 MeOH / water did not produce homopolymer solutions which exhibited an observable increase in solution viscosity (PNTBAM-1 to -6). However, a tan coloured gel formed for PNTBAM-3. PAM precipitated from the polymerization medium, except for control-

Table 15 The molecular weight and intrinsic viscosity for PMeAM and PAM pairs produced under identical experimental conditions

Experiment	Mole ratio of $K_2S_2O_8$ to monomer	Polym. duration [a] (hours)	GPC / MALLS [b] (M_w, g/mol)	Intrinsic viscosity [c] ([η], cm^3/g)	Viscometry [d] (M_v, g/mol)
PMeAM-1 control-1	1 / 1000	3.58	n/m [e] (1.561 ± 0.1)E+06	83 316	n/m 1.071 E+06
PMeAM-2 control-2	1 / 750	3.5	n/m (1.738 ± 0.2)E+06	56 304	n/m 1.019 E+06
PMeAM-4 control-4	1 / 1000	13.25	n/m	139 302	n/m 1.010 E+06
PMeAM-5 control-5	1 / 500	3.5	(1.750 ± 0.2)E+06	47 186	n/m 5.381 E+05

a. At 60 °C.
b. The weight average molecular weight, M_w, was determined by GPC / MALLS.
c. The intrinsic viscosity for PMeAM was determined in 88% formic acid.
d. The viscosity average molecular weight, M_v, was determined using the Mark Houwink Equation for PAM in 0.5 M NaCl.[75]
e. n/m denotes not measured.

1, -3, and -4. Only control-3 which used a 1:1, MeOH / water medium precipitated PAM with the addition of excess 99.8 % MeOH.

None of PNTBAM from PNTBAM-1 to -6 were soluble in water. From the intrinsic viscosities which were measured in 99.8 % MeOH, PNTBAM from PNTBAM-4 which included 1:9, MeOH / water as the polymerization medium had the highest value (Table 16). From the intrinsic viscosities which were measured in 0.1 M NaCl, PAM from control-3 which used 1:1, MeOH / water as the polymerization medium had the highest value. M_w and M_v values for the controls were all less than 1.0 E+06 g/mol and M_w was greater than M_v by approximately a factor of 2. In addition, the trends in magnitude of M_w were consistent with the trends in magnitude of M_v. The eluted masses from the GPC columns were calculated as 80 - 90 % of the injected masses for the controls, except for the eluted mass calculated for PAM from control-4 which was 43 % of the injected mass.

(b) In t-butanol and t-butanol / distilled water mixtures

Solubility tests of NTBAM in 1:1, t-BuOH / distilled H_2O determined that a minimum solution temperature of 50°C was required for dissolution of a 1.0 M polymerization solution.

Homopolymerization of NTBAM in 98 % t-BuOH, 1:1, t-BuOH / water, and 1:9, t-BuOH / water produced tan coloured solutions which contained tan coloured gel. Homopolymerizations of AM (control-8 to -14) in 1:1, t-BuOH / water and 1:9, t-BuOH / water produced clear solutions which contained clear gel. PAM from control-7

Table 16 Molecular weight and intrinsic viscosity for PNTBAM and PAM pairs produced by homopolymerization under identical experimental conditions

Experiment	Polym. medium (% MeOH)	Polym. temp. (± 0.2°C)	Initiator	GPC / MALLS [a] (M_w, g/mol)	Intrinsic viscosity [b] ([η], cm^3/g)	Viscometry [c] (M_v, g/mol)
PNTBAM-1 [d]	99.8	31.0	$K_2S_2O_8$	n/m [e]	n/m	n/m
control-1						
PNTBAM-2	99.8	55.0	$K_2S_2O_8$	n/m	43	n/m
control-2				(2.088 ± 0.3)E+05	37	6.608 E+04
PNTBAM-3	50	55.0	AIBN	n/m	8	n/m
control-3				(7.383 ± 0.6)E+05	120	3.046 E+05
PNTBAM-4	10	60.0	$K_2S_2O_8$	n/m	88	n/m
control-4				(5.541 ± 0.8)E+05	72	1.569 E+05
PNTBAM-5	99.8	55.0	AIBN	n/m	50	n/m
control-5					n/m	
PNTBAM-6	99.8	60.0	AIBN	n/m	33	n/m
control-6				(1.850 ± 0.3)E+05	17	2.407 E+04

a. The weight average molecular weight, M_w , was determined by GPC / MALLS.
b. The intrinsic viscosities for PNTBAM were determined in 99.8 % methanol.
c. The viscosity avg. molecular weight, M_v , was determined by using the Mark Houwink equation for PAM in 0.5 M NaCl.[75]
d. There was no qualitative evidence of polymer formation for PNTBAM-1 or control-1.
e. n/m denotes not measured. Only PAM samples were soluble in 0.1 M NaCl, used as the mobile phase for GPC / MALLS.

precipitated from the 98% t-BuOH polymerization medium. The quantities of tan coloured gel and clear gel obtained at 70°C diminished as the polymerization temperature was reduced to 45°C.

Only the intrinsic viscosity of the freeze-dried solid recovered from the tan coloured gel component of the NTBAM homopolymerization corresponding to PNTBAM-7 was measured as the tan coloured gel components from PNTBAM-8 to -14 did not freeze-dry to powdered solids but remained gelatinous.

The clear gel component of control-14 gave the highest intrinsic viscosity of those measured in 0.1 M NaCl (Table 17). Whereas M_v was less than 1.0 E+06 g/mol for all polyacrylamides, M_w was greater than 1.0 E+06 g/mol for all controls except control-7, -8, and -10. M_w and M_v values were the highest for PAM from control-14 but they did not follow consistent trends with respect to magnitude. Along with M_w values determined by GPC / MALLS, the eluted masses from the GPC columns were calculated as 70 - 80 % of the injected masses for the controls.

3.4. Evaluation of Copolymerization Experimental Conditions

3.4.1. Copolymerization of DMAM with AM

The initial experimental conditions for copolymerization of DMAM with AM included a 1.0 M total monomer concentration in deoxygenated distilled water, a mole ratio of initiator ($K_2S_2O_8$) to total monomer concentration of 1/1000, a nitrogen atmosphere, a natural pH in the range (5.5 to 7.0), a polymerization temperature of 50.0 ± 0.2°C, and a polymerization duration of 9 hours. Use of these conditions for DMAM-

Table 17 Molecular weights and intrinsic viscosities for PNTBAM and PAM pairs produced by homopolymerization under identical experimental conditions

Experiment	[monomer] (mmoles / mL)	Polym. medium (% t-BuOH)	Polym. temp. (± 0.2°C)	Initiator	GPC / MALLS [a] (M_w , g/mol)	Intrinsic viscosity [b] ([η], cm^3/g)	Viscometry [c] (M_v , g/mol)
PNTBAM-7	0.67	98	70.0	AIBN	n/m [d]	30	n/m
control-7					(4.745 ± 0.5)E+05	52	1.028 E+05
PNTBAM-8	1.00	50	60.0	$K_2S_2O_8$	n/m	n/m	n/m
control-8					(5.662 ± 0.5)E+05	153	4.176 E+05
PNTBAM-9	1.00	50	70.0	AIBN	n/m	n/m	n/m
control-9					(1.533 ± 0.2)E+06	202	5.990 E+05
PNTBAM-10	0.10	10	60.0	$K_2S_2O_8$	n/m	n/m	n/m
control-10					(8.318 ± 1.0)E+05	96	2.280 E+05
PNTBAM-11	1.00	50	60.0	$K_2S_2O_8$	n/m	n/m	n/m
control-11					(1.412 ± 0.1)E+06	136	3.583 E+05
PNTBAM-12	1.00	50	50.0	$K_2S_2O_8$	n/m	n/m	n/m
control-12					(1.582 ± 0.09)E+06	199	5.875 E+05
PNTBAM-13	0.83	50	50.0	$K_2S_2O_8$	n/m	n/m	n/m
control-13					(1.594 ± 0.2)E+06	163	4.533 E+05

Table 17 continued ...

Experiment	[monomer] (mmoles / mL)	Polym. medium (% t-BuOH)	Polym. temp. (± 0.2°C)	Initiator	GPC / MALLS [a] (M_w, g/mol)	Intrinsic viscosity [b] ([η], cm^3/g)	Viscometry [c] (M_v, g/mol)
PNTBAM-14	0.79	50	45.0	$K_2S_2O_8$	n/m	n/m	n/m
PAM					(1.643 ± 0.1)E+06	208	6.22 E+05

a. The weight average molecular weight, M_w, was determined by GPC / MALLS.
b. The intrinsic viscosities for PNTBAM were determined in 99.8 % methanol.
c. The viscosity average molecular weight, M_v, was determined using the Mark Houwink Equation for PAM in 0.5 M NaCl.[75]
d. n/m denotes not measured. Only PAM samples were soluble in the 0.1 M NaCl aqueous solution used as the mobile phase for GPC/ MALLS.

co-AM-1 and control-1 (homopolymerization of AM) resulted in highly viscous polymer solutions which caused the stirrer to stop for both polymerizations well before 9 hours had elapsed. The copolymer solution of DMAM-co-AM-1 was pulled from the polymerization flask as a gel which remained intact regardless of applied stress. The PAM solution was equally difficult to remove because it adhered to the glass walls of the polymerization flask which resulted in its removal in several gelatinous portions.

The total monomer concentration used for DMAM-co-AM-2 to -6 was reduced to 0.5 M which improved the handling of the product copolymer solutions and especially those for DMAM-co-AM-4 and -5. However, the homopolymer solution from DMAM-co-AM-6 containing 100 mol % DMAM in the feedstock still gelled. Therefore, the total monomer concentration was reduced to 0.25 M for DMAM-co-AM-2, -3, -6, and -7 which eliminated handling difficulties for copolymerizations and accompanying control homopolymerizations.

3.4.2. Copolymerization of MeAM with AM

The initial experimental conditions for copolymerization of MeAM with AM included a 0.50 M total monomer concentration in deoxygenated distilled water, a mole ratio of initiator ($K_2S_2O_8$) to total monomer concentration of 1/1000, a nitrogen atmosphere, a natural pH in the range (5.5 to 7.0), a polymerization temperature of 60.0 ± 0.2°C, and a polymerization duration of 16 hours. MeAM-co-AM-1 which included 20 mole % of MeAM in the feedstock generated a copolymer solution which did not exhibit an observable increase in viscosity. AM homopolymerized under the same conditions

did increase in solution viscosity. Based on these results, MeAM-co-AM-2a and -2b were polymerized using total monomer concentrations of 0.75 M and 1.0 M, respectively, and the same proportion of MeAM. Both MeAM-co-AM-2a and -2b polymerizations produced an increase in solution viscosity with the solution from -2b being somewhat greater. MeAM-co-AM-3 to -6 included a 1.0 M total monomer concentration as the only change to the initial experimental conditions. As the content of MeAM in the feedstock increased the copolymer solutions from MeAM-co-AM-3 to -5 appeared to become less viscous. The homopolymer (PMeAM) precipitated from the polymerization medium of MeAM-co-AM-6 as a white gel. PAM's from control-3 to -6 gave increased solution viscosities but without handling difficulties.

3.4.3. Copolymerization of NTBAM with AM

The initial experimental conditions for copolymerization of NTBAM with AM included a 1:1, 98% t-butanol / water polymerization medium, a mole ratio of the initiator ($K_2S_2O_8$) to total monomer concentration of 1/1000, a nitrogen atmosphere, a natural pH in the range (5.5 to 7.0), a polymerization temperature of 50.0 ± 0.2°C, a polymerization duration of 16 hours, and total monomer concentrations of 0.65 M and 0.5 M for NTBAM-co-AM-1a and -1b, respectively. The copolymer solutions generated from these contained a clear viscous layer resting on a clouded viscous layer. The total monomer concentration was set at 0.50 M for NTBAM-co-AM-2 to -4. NTBAM-co-AM-2 produced an increased viscosity without the layered structure of the copolymer solutions from NTBAM-co-AM-1a and -1b. NTBAM-co-AM-3 and -4 produced

copolymer solutions which contained tan coloured, gelatinous material suspended in tan coloured solutions. The tan coloured solutions were not noticeably more viscous than the starting solutions. Similarly, NTBAM-co-AM-6a which used 80 mole % of NTBAM and NTBAM-co-AM-5a, -5b, and -6b which used 100 mole % of NTBAM gave tan coloured polymer solutions without noticeable changes in viscosity and which contained tan coloured gelatinous material. The extended polymerization duration of 69.5 hours used for NTBAM-co-AM-6a and -6b gave increased amounts of gelatinous material. Control-2 to -4 all gave clear solutions which did not exhibit an increase in viscosity, and which contained gelatinous material.

3.5. Characterization of the Copolymers

3.5.1. Viscometric analysis

Intrinsic viscosities were determined for the homopolymers and copolymers from DMAM-co-AM-2 to -6, MeAM-co-AM-2b to -6, and NTBAM-co-AM-1a to -6b and intrinsic viscosities and M_v's were determined for the controls which included equivalent experimental conditions to DMAM-co-AM-6, MeAM-co-AM-6, and NTBAM-co-AM-4.

The intrinsic viscosities of the copolymers from DMAM-co-AM-2 to -5 and the homopolymer (PDMAM) from DMAM-co-AM-6 were all greater than the intrinsic viscosity of the PAM from control-6 (complementary to DMAM-co-AM-6) (Table 18). The intrinsic viscosities increased as the content of DMAM in the copolymer increased except for the copolymer from DMAM-co-AM-5. M_v for PAM from control-6 was calculated as 7.78 E+05 g/mol by the Mark Houwink relationship for PAM in 0.5 M

Table 18 Intrinsic viscosities for the copolymers from DMAM-co-AM-2 to -5, PDMAM from DMAM-co-AM-6, and PAM from control-6

Experiment	Feed mol % DMAM	Intrinsic viscosity, [η] (cm^3 / g)
DMAM-co-AM-2	20	384
DMAM-co-AM-3	40	408
DMAM-co-AM-4	60	424
DMAM-co-AM-5	80	411
DMAM-co-AM-6	100	354 [a]
control-6	0	247 [b]

a. The viscosity average molecular weight, M_v, was calculated from the intrinsic viscosity as 2.62 E+06 g/mol by using a relationship for PDMAM in H_2O at 25°C.[76]
b. The viscosity average molecular weight, M_v, was calculated from the intrinsic viscosity as 7.78 E+05 g/mol by using the Mark Houwink relationship for PAM in 0.5 M NaCl at 25 °C.[75]

NaCl at 25°C,[75] and M_v for PDMAM was calculated as 2.62 E+06 g/mol by a relationship for PDMAM in water at 25°C.[76]

The intrinsic viscosities of the copolymers from MeAM-co-AM-2b to -5 decreased as the content of MeAM in the copolymers increased (Table 19). Also, these intrinsic viscosities were less than that of PAM from control-6 (complementary to MeAM-co-AM-6). M_v for PAM from control-6 was calculated as 1.49 E+06 g/mol by the Mark Houwink equation for PAM in 0.5 M NaCl at 25°C.[75]

The aqueous solution of the copolymer from NTBAM-co-AM-1b (clouded layer) gave the highest intrinsic viscosity (Table 20). The intrinsic viscosity decreased as the NTBAM content in the copolymers increased. Both the cloudy and the clear layers from NTBAM-co-AM-1b gave intrinsic viscosities which were greater than that of PAM from control-4 (complementary to NTBAM-co-AM-4). M_v for PAM from NTBAM-co-AM-4 was calculated as 5.42 E+05 g/mol by the Mark Houwink equation for PAM in 0.5 M NaCl at 25°C.[75] Of the measurements conducted in MeOH, that from NTBAM-co-AM-3 (gelatinous material) gave the highest intrinsic viscosity. Copolymers which contained a higher content of NTBAM than that from NTBAM-co-AM-3 (gelatinous material) gave very low intrinsic viscosities.

3.5.2. Photoacoustic FTIR (PAS-FTIR)

The photoacoustic FTIR spectra of the copolymers and substituted acrylamide homopolymers from DMAM-co-AM-2 to -6 (Fig. 15), MeAM-co-AM-2b to -6 (Fig. 16), and NTBAM-co-AM-1b to -6b (Fig. 17 and 18) were assigned by comparison with the

Table 19 Intrinsic viscosities for the copolymers from MeAM-co-AM-2b to -5, PMeAM from MeAM-co-AM-6, and PAM from control-6

Experiment	Feed mol % MeAM	Intrinsic viscosity, [η] (cm^3/g)
MeAM-co-AM-2b	20	253
MeAM-co-AM-3	40	143
MeAM-co-AM-4	60	65
MeAM-co-AM-5	80	62
MeAM-co-AM-6	100	137 [a]
control-6	0	407 [b]

a. The intrinsic viscosity for PMeAM was determined in 88% formic acid.
b. The viscosity average molecular weight, M_v , was determined as 1.49 E+06 g/mol by using the Mark Houwink relationship for PAM in 0.5 M NaCl at 25°C.[75]

Table 20 Intrinsic viscosities for the copolymers from NTBAM-co-AM-1a, -1b, -2, -3, and -6a, the homopolymer (PNTBAM) from NTBAM-co-AM-6b, and PAM from control-4

Experiment	Feed mol % NTBAM	Intrinsic viscosity, [η] (cm^3/g)
NTBAM-co-AM-1a (clouded layer)	20	240 [a]
NTBAM-co-AM-1b (clear layer)	20	208 [a]
NTBAM-co-AM-2 (dialyzed fraction)	40	127 [a]
NTBAM-co-AM-2 (non-dialyzed fraction)	40	121 [a]
NTBAM-co-AM-3 (gelatinous material)	60	127 [b]
NTBAM-co-AM-3 (tan coloured solution)	60	11 [b]
NTBAM-co-AM-6a (gelatinous material)	80	40 [b]
NTBAM-co-AM-6b	100	31 [b]
control-4	0	187 [a, c]

a. For viscosity measurements in 0.1 M NaCl.
b. For viscosity measurements in 99.8 % methanol.
c. The viscosity average molecular weight, M_v , was determined as by using the Mark Houwink relationship for PAM in 0.5 M NaCl at 25°C.[75]

spectra of PAM and AM from Gupta and Bansil[83] as well as by referral to the spectra of structurally similar compounds.[84-87] Also included were control PAM's complementary to DMAM-co-AM-6 (Fig. 15), MeAM-co-AM-6 (Fig. 16), and NTBAM-co-AM-4 (Fig. 17 and 18).

PAS-FTIR (PAM from control-6 complementary to DMAM-co-AM-6, control-6 complementary to MeAM-co-AM-6 and control-4 complementary to NTBAM-co-AM-4): ν (cm^{-1}) 3323 and 3189 cm^{-1} (asymmetric and symmetric N-H stretching of NH_2), 2960 and 2931 cm^{-1} (C-H asymmetric and symmetric stretching of CH_2), 2867 cm^{-1} (C-H stretching of CH), 1661 cm^{-1} (C=O stretching, amide I band), 1625 cm^{-1} (N-H bending of NH_2, amide II band), 1457 cm^{-1} (C-H bending of CH_2), 1432 cm^{-1} (C-N stretching, amide III band), 1348 and 1328 cm^{-1} (C-H wagging of CH_2 and C-H bending of CH), 1209 cm^{-1} (N-H wagging of NH_2).

PAS-FTIR (PDMAM from DMAM-co-AM-6): ν (cm^{-1}) 2960 and 2931 cm^{-1} (C-H asymmetric and symmetric stretching of CH_2, 2867 cm^{-1} (C-H stretching of CH), 2750 - 3050 cm^{-1} (C–H asymmetric and symmetric stretching of CH_3), 1650 cm^{-1} (C=O stretching, amide I band), 1457 cm^{-1} (C-H bending of CH_2), 1400 and 1325 cm^{-1} (C-H asymmetric and symmetric bending of CH_3)

PAS-FTIR (PMeAM from MeAM-co-AM-6): ν (cm^{-1}) 3323 and 3189 cm^{-1} (N-H asymmetric and symmetric stretching of NH_2), 2990 cm^{-1} (C-H asymmetric stretching of CH_3), 2950 and 2867 cm^{-1} (C–H symmetric stretching of CH_3 and C–H asymmetric and symmetric stretching of CH_2), 1650 cm-1 (C=O stretching, amide I band), 1615 cm^{-1} (N-H bending of NH_2, amide II band), 1480 cm^{-1} and 1380 cm^{-1} (C-H asymmetric and

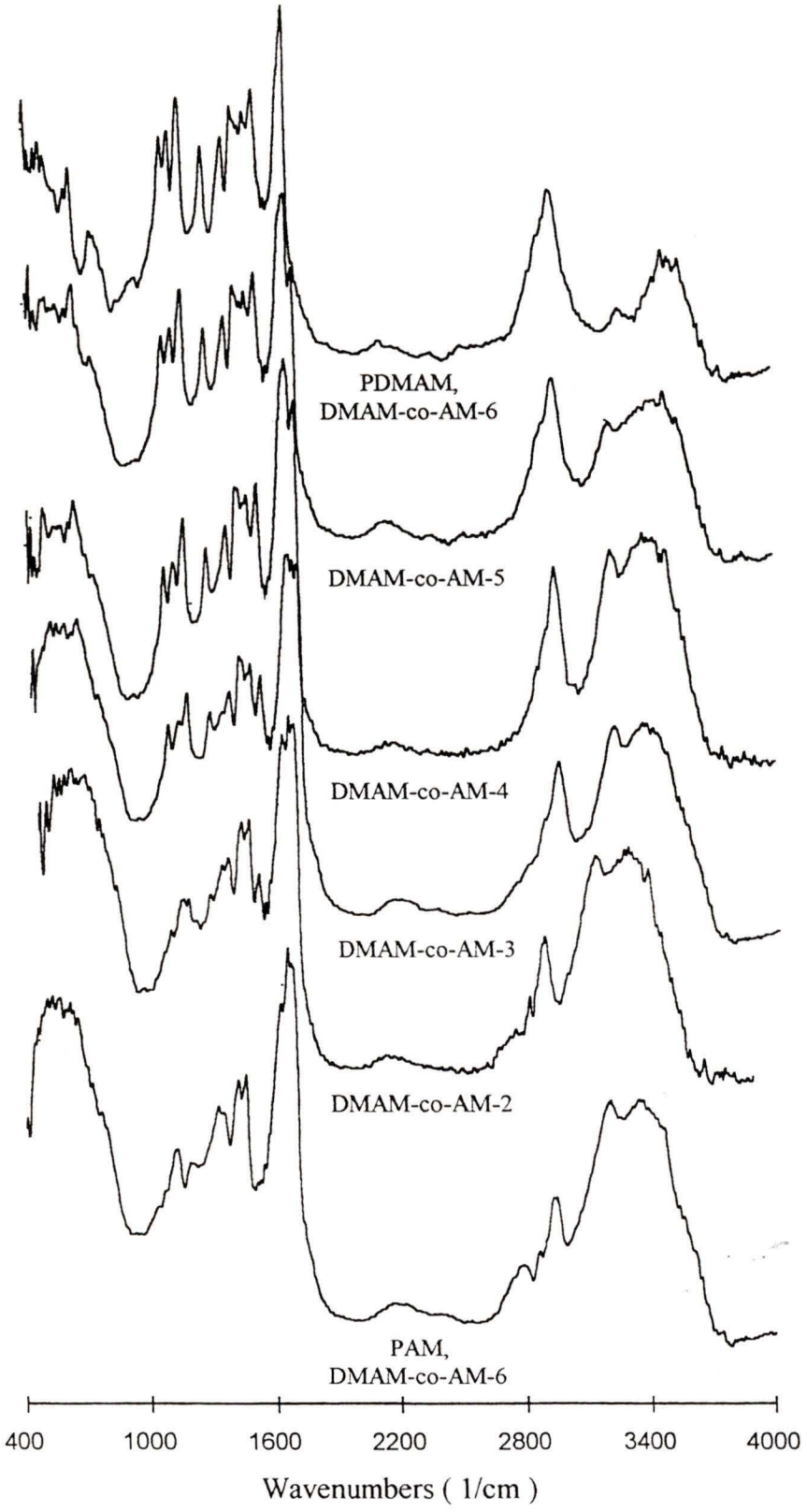

Fig. 15 PAS-FTIR spectra of the copolymers from DMAM-co-AM-2 to -5, PDMAM from DMAM-co-AM-6, and control PAM complementary to DMAM-co-AM-6

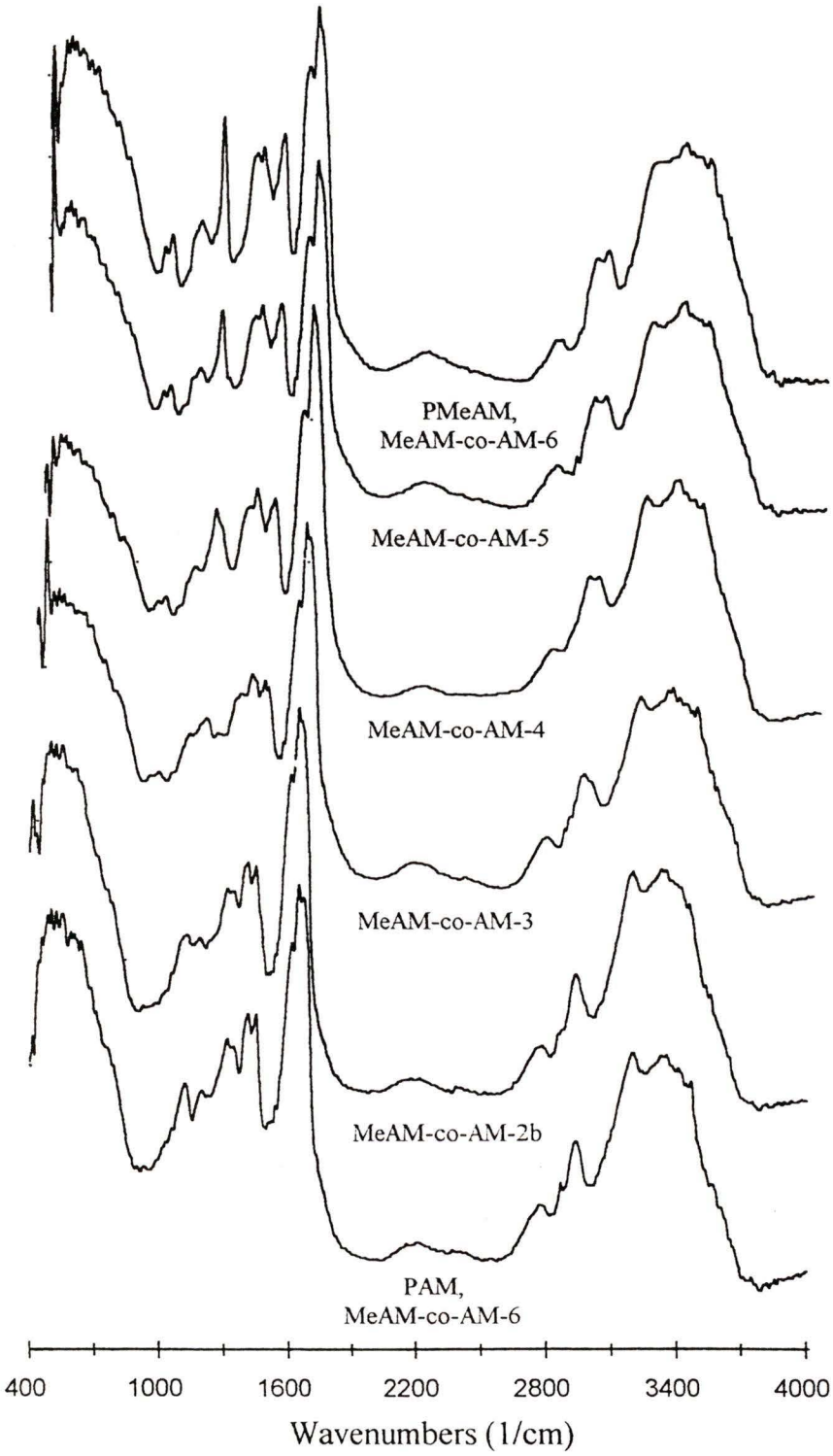

Fig. 16 PAS-FTIR spectra of the copolymers from MeAM-co-AM-2b to -5, PMeAM from MeAM-co-AM-6, and control PAM complementary to MeAM-co-AM-6

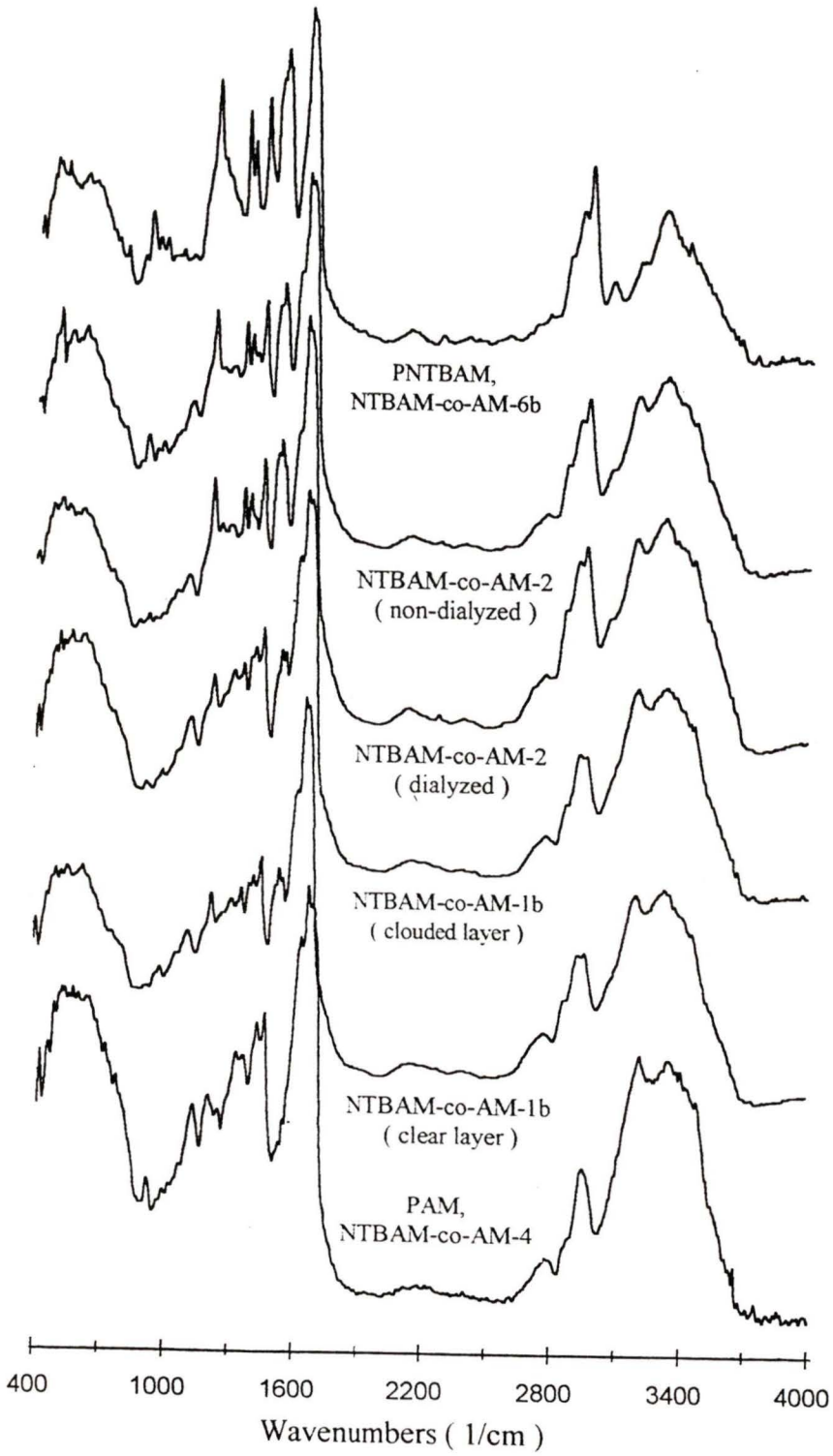

Fig. 17 PAS-FTIR spectra of the copolymers from NTBAM-co-AM-1b and -2, PNTBAM from NTBAM-co-AM-6b, and control PAM complementary to NTBAM-co-AM-4

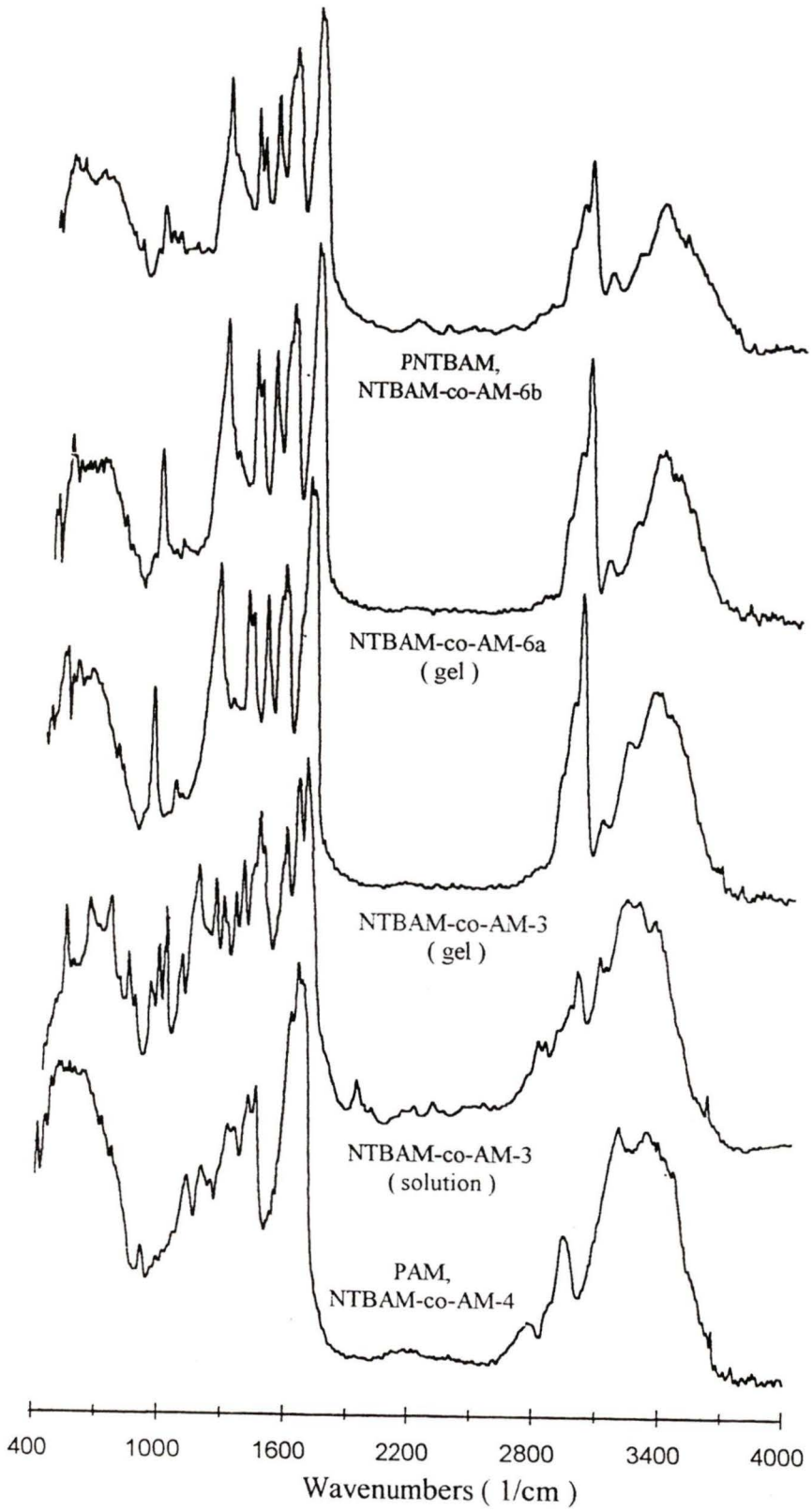

Fig. 18 PAS-FTIR spectra of the copolymers from NTBAM-co-AM-3 and -6a, PNTBAM from NTBAM-co-AM-6b, and control PAM complementary to NTBAM-co-AM-4

symmetric bending of CH_3).

PAS-FTIR (PNTBAM from NTBAM-co-AM-6b): ν (cm^{-1}) 3300 cm^{-1} (N-H stretching of NH), 2980 - 2800 cm^{-1} (C-H asymmetric and symmetric stretching of CH_3 and CH_2 and C–H stretching of CH), 2980 cm^{-1} (C-H asymmetric stretching of CH_3), 1650 cm^{-1} (C=O stretching, amide I band), 1450 cm^{-1} (C-H asymmetric bending of CH_3), 1390 and 1360 cm^{-1} (C-H symmetric bending of CH_3), 1225 cm^{-1} C-N stretching (amide III band).

3.5.3. ^{13}C NMR

The ^{13}C NMR spectra of the homopolymers and copolymers from DMAM-co-AM-2 to -6 (Figs. 24 to 28), MeAM-co-AM-2b to -6 (Figs. 30 to 34), and NTBAM-1b (clouded layer), -1b (clear layer), -2 (dialyzed), -2 (non-dialyzed), -3 (tan coloured solution), -3 (gelatinous material), -6a, and -6b (Figs. 36 to 43) and control-6 (complementary to DMAM-co-AM-6) (Fig. 20), control-6 (complementary to MeAM-co-AM-6) (Fig. 21), and control-4 (complementary to NTBAM-co-AM-4) (Fig. 22) were assigned by comparison to the ^{13}C NMR spectra of AM (Fig. 19), DMAM (Fig. 23), MeAM (Fig. 29), and NTBAM (Fig. 35).

^{13}C NMR data from the spectra of AM and PAM from controls

^{13}C NMR of AM (90.55 MHz, D_2O, ext. ref. $CDCl_3$): δ 170.9 (amide C=O), δ 129.4 (alkene C of CH), δ 128.4 (alkene C of CH_2).

^{13}C NMR of PAM from control-6, complementary to DMAM-co-AM-6 (50.3 MHz, D_2O, 0.1 M NaCl, ext. ref. CD_3OD): δ 179.2 (amide C=O), δ 42.0 (C of CH), δ 34.8 (C

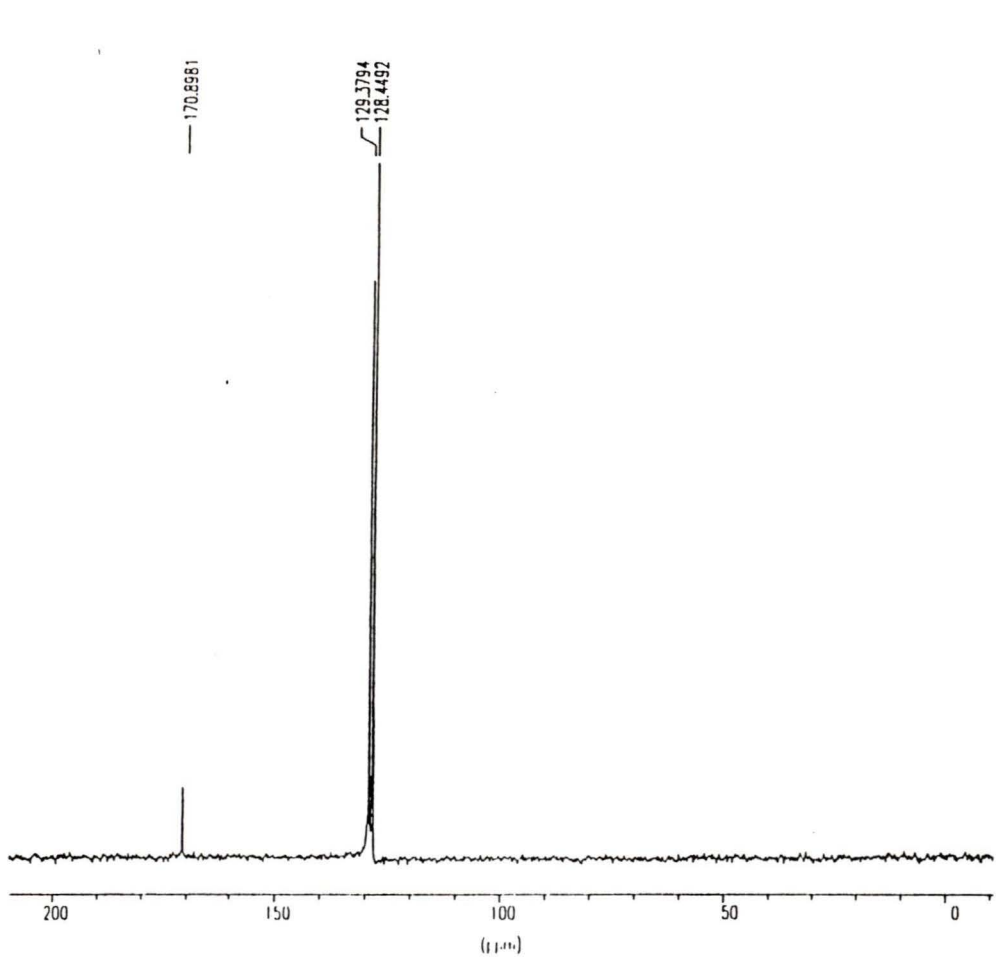

Bruker

••• Current Data Parameters •••

NAME	:	cg1933
EXPNO	:	1
PROCNO	:	1

••• Acquisition Parameters •••

AUNM	:	auzg
FW	:	25000.00 Hz
NS	:	1036
O1	:	15000.00 Hz
O2	:	6600.00 Hz
SFO1	:	90.5650000 MHz
SW	:	220.8359 ppm
TD	:	32768

••• Processing Parameters •••

GB	:	0.0000000
LB	:	10.00 Hz
SF	:	90.5559890 MHz
SI	:	16384
SWp		20000.0000000

••• 1D NMR Plot Parameters •••

SR	:	5989.00 Hz
ppmcm	:	11.50
Hzcm	:	1041.60
AQtime	:	0.8192000 sec

Fig. 19 ^{13}C NMR spectrum of acrylamide (AM)

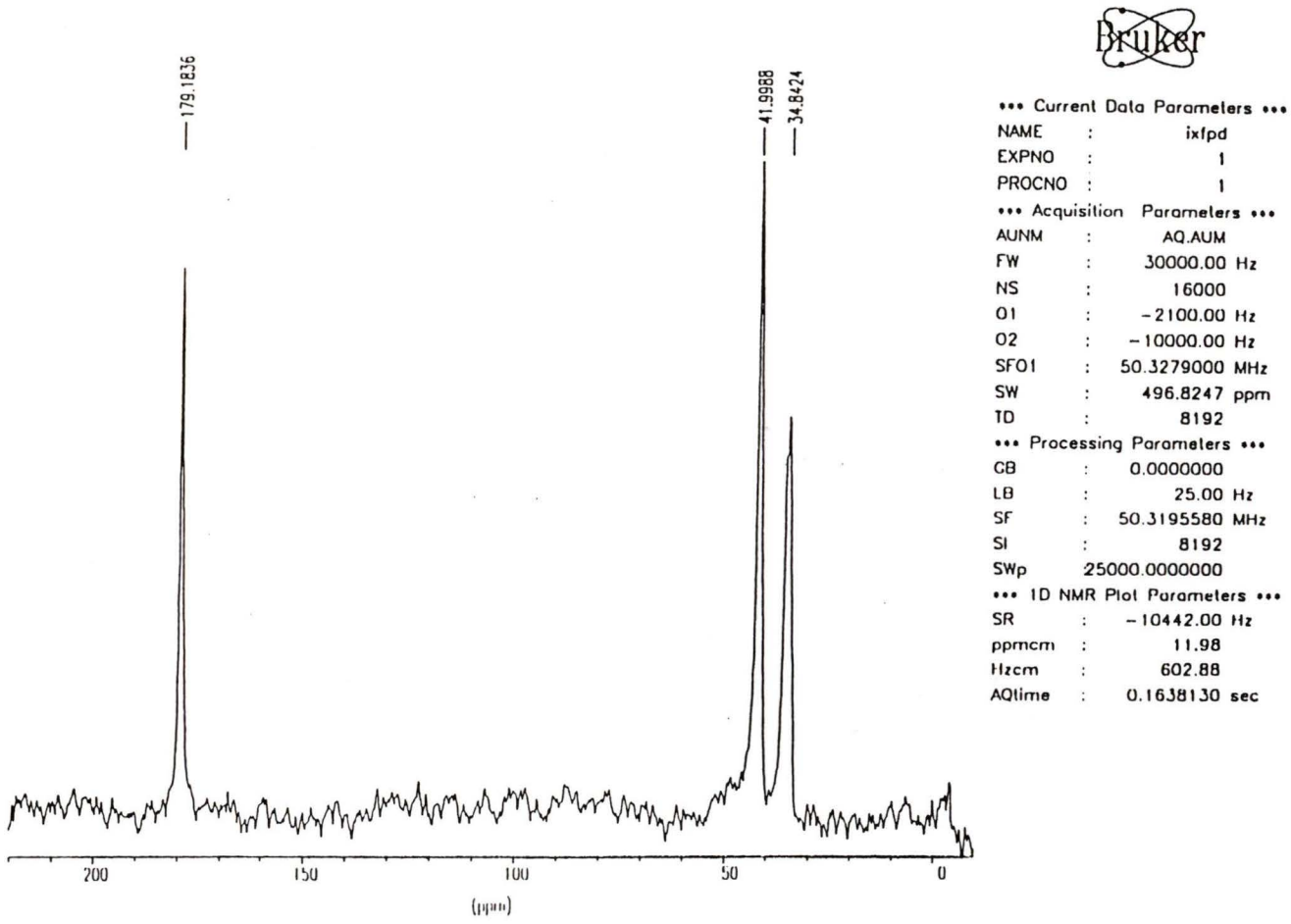

Fig. 20 ^{13}C NMR spectrum of PAM from control-6 complementary to DMAM-co-AM-6

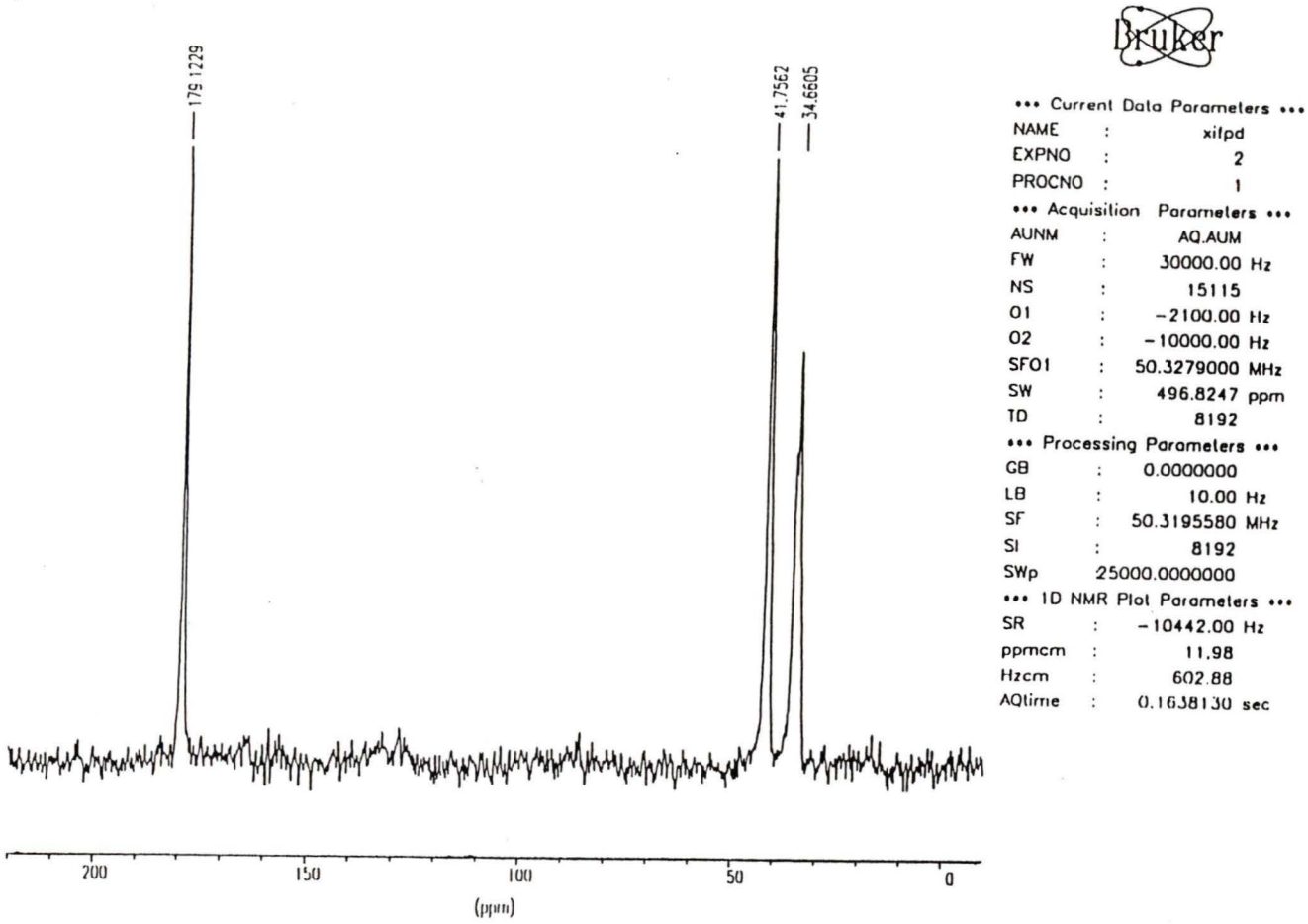

Fig. 21 ^{13}C NMR spectrum of PAM from control-6 complementary to MeAM-co-AM-6

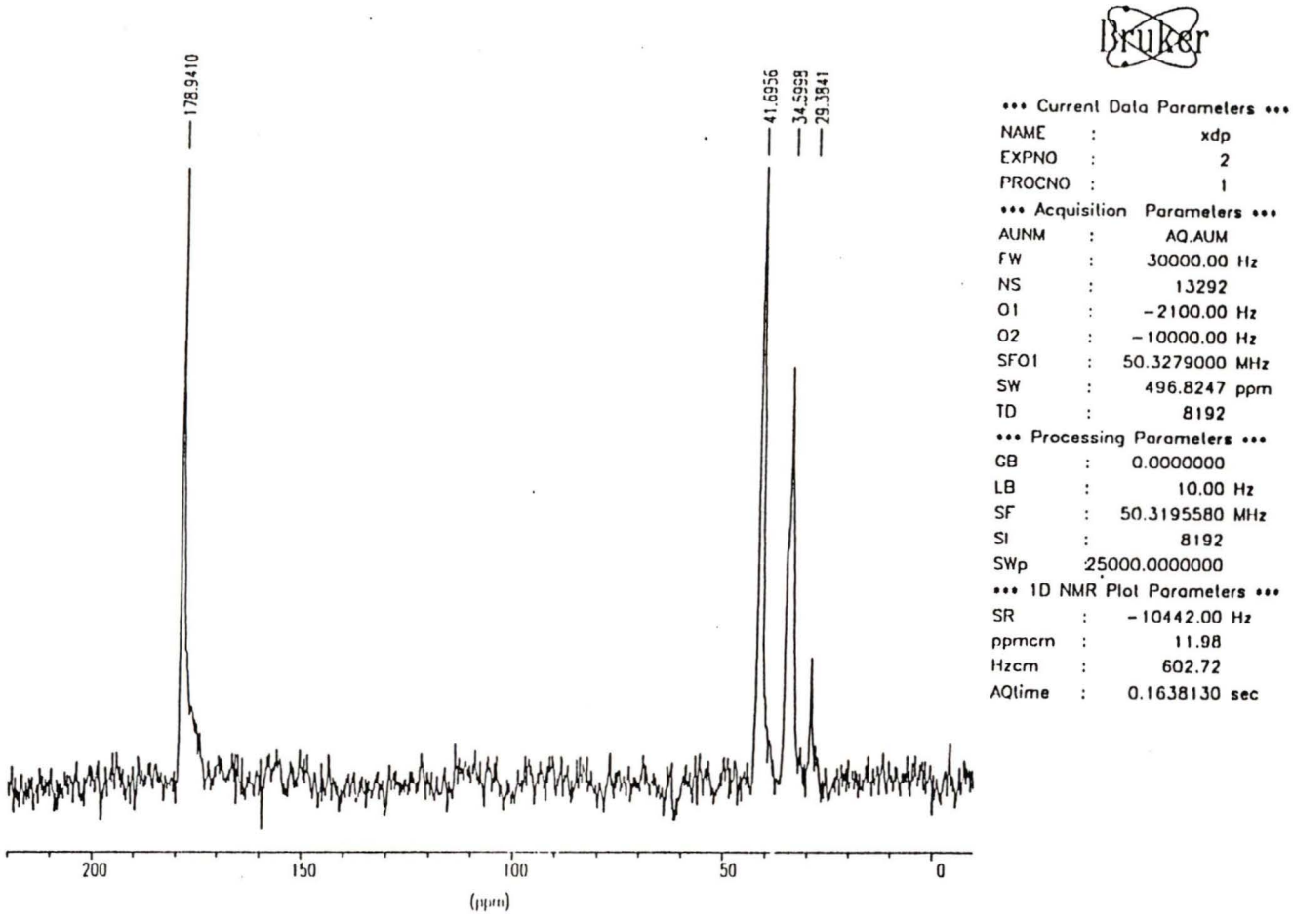

Fig. 22 ^{13}C NMR spectrum of PAM from control-4 complementary to NTBAM-co-AM-4

of CH_2).

^{13}C NMR of PAM from control-6, complementary to MeAM-co-AM-6 (50.3 MHz, D_2O, 0.1 M NaCl, ext. ref. CD_3OD): δ 179.1 (amide C=O), δ 41.8 (C of CH), δ 34.7 (C of CH_2).

^{13}C NMR of PAM from control-4, complementary to NTBAM-co-AM-4 (50.3 MHz, D_2O, 0.1M NaCl, ext. ref. CD_3OD): δ 178.9 (amide C=O), δ 41.7 (C of CH), δ 34.6 (C of CH_2), δ 29.4 (C of CH_3 from 98% t-butanol).

^{13}C NMR data from the spectra of DMAM, PDMAM from DMAM-co-AM-6, and copolymers from DMAM-co-AM-2 to -5

^{13}C NMR of DMAM (90.55 MHz, D_2O, ext. ref. $CDCl_3$): δ 169.0 (amide C=O), δ 127.9 (alkene C of CH_2), δ 127.6 (alkene C of CH), δ 37.5 (alkane C of CH_3), δ 35.6 (alkane C of CH_3).

^{13}C NMR of PDMAM from DMAM-co-AM-6 (50.3 MHz, D_2O, 0.1 M NaCl, ext. ref. CD_3OD): δ 175.5 (amide C=O), δ 35.7 (C of CH, CH_2, and CH_3).

^{13}C NMR spectra of the copolymers from DMAM-co-AM-2 to -5 (50.3 MHz, D_2O, 0.1M NaCl, ext. ref. CD_3OD): δ 179.2 (C=O from AM component), δ 175.8 (C=O from DMAM component), δ 42.2 (C of CH from AM component), δ 35.6 (C of CH_2 from AM component and CH, CH_2, and CH_3 from DMAM component).

^{13}C NMR data from the spectra of MeAM, PMeAM from MeAM-co-AM-6, and copolymers from MeAM-co-AM-2b to -5

^{13}C NMR of MeAM (90.55 MHz, D_2O, ext. ref. $CDCl_3$): δ 174.1 (amide C=O), δ 138.2 (alkene C from tertiary C), δ 122.2 (alkene C from CH_2), δ 17.6 (C from CH_3).

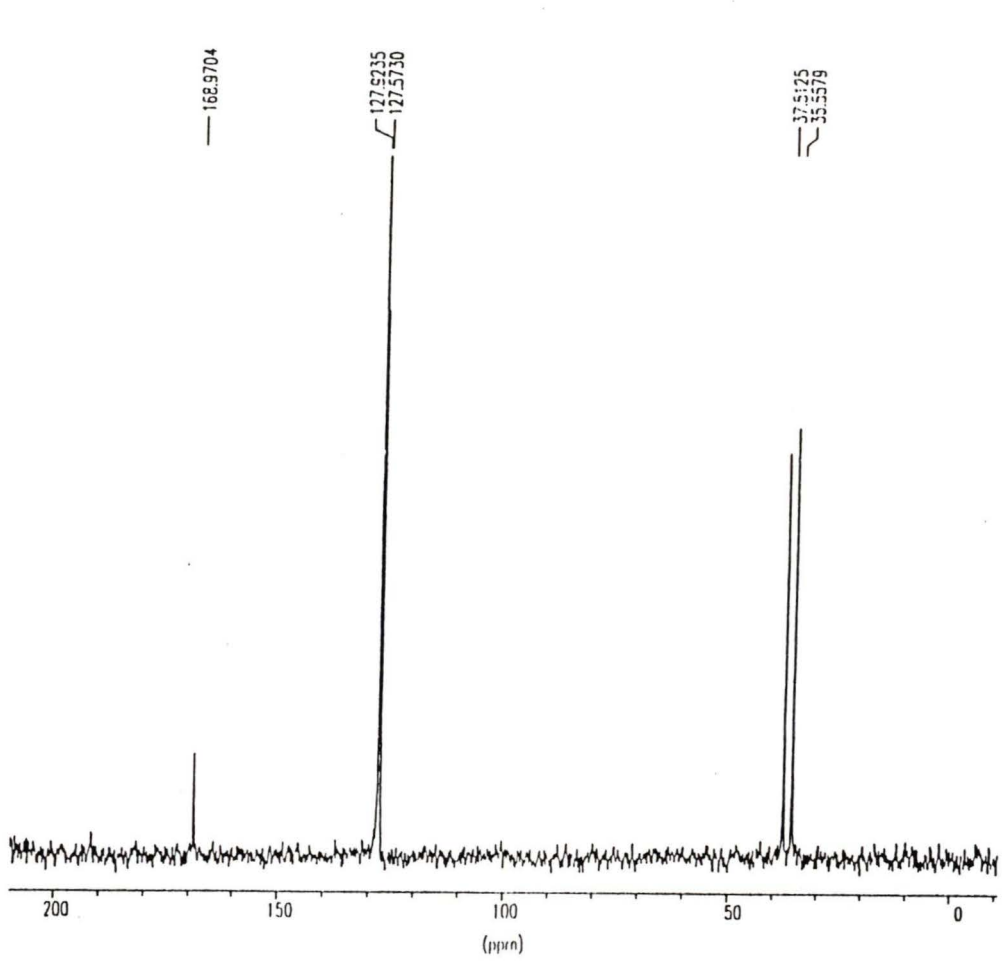

Bruker

*** Current Data Parameters ***

NAME	:	cg1935
EXPNO	:	1
PROCNO	:	1

*** Acquisition Parameters ***

AUNM	:	auzg
FW	:	25000.00 Hz
NS	:	155
O1	:	15000.00 Hz
O2	:	6600.00 Hz
SFO1	:	90.5650000 MHz
SW	:	220.8359 ppm
TD	:	32768

*** Processing Parameters ***

GB	:	0.0000000
LB	:	10.00 Hz
SF	:	90.5559890 MHz
SI	:	16384
SWp		20000.0000000

*** 1D NMR Plot Parameters ***

SR	:	5989.00 Hz
ppmcm	:	11.50
Hzcm	:	1041.60
AQtime	:	0.8192000 sec

Fig. 23 ^{13}C NMR spectrum of N,N-dimethylacrylamide (DMAM)

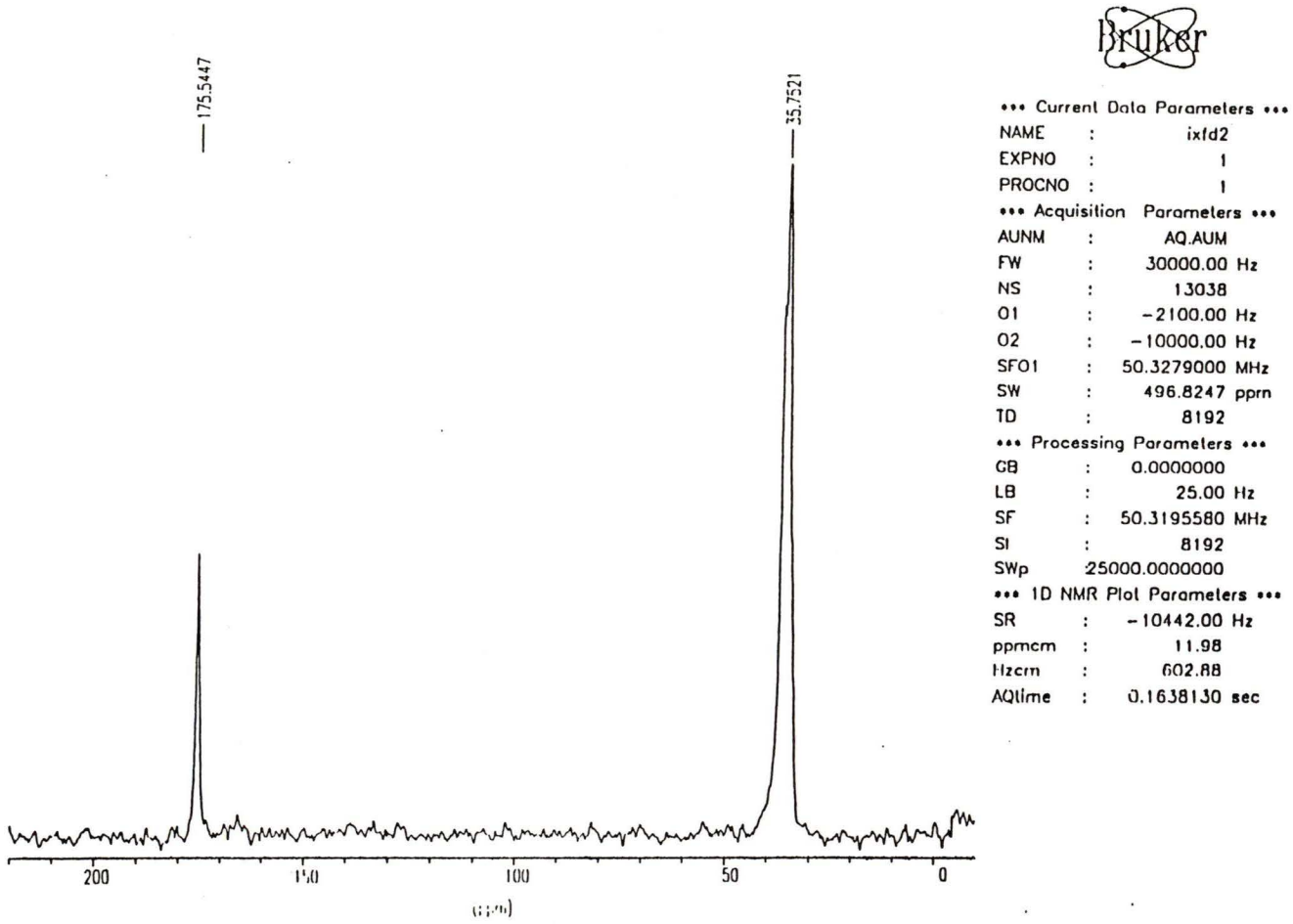

Fig. 24 ^{13}C NMR spectrum of PDMAM from DMAM-co-AM-6

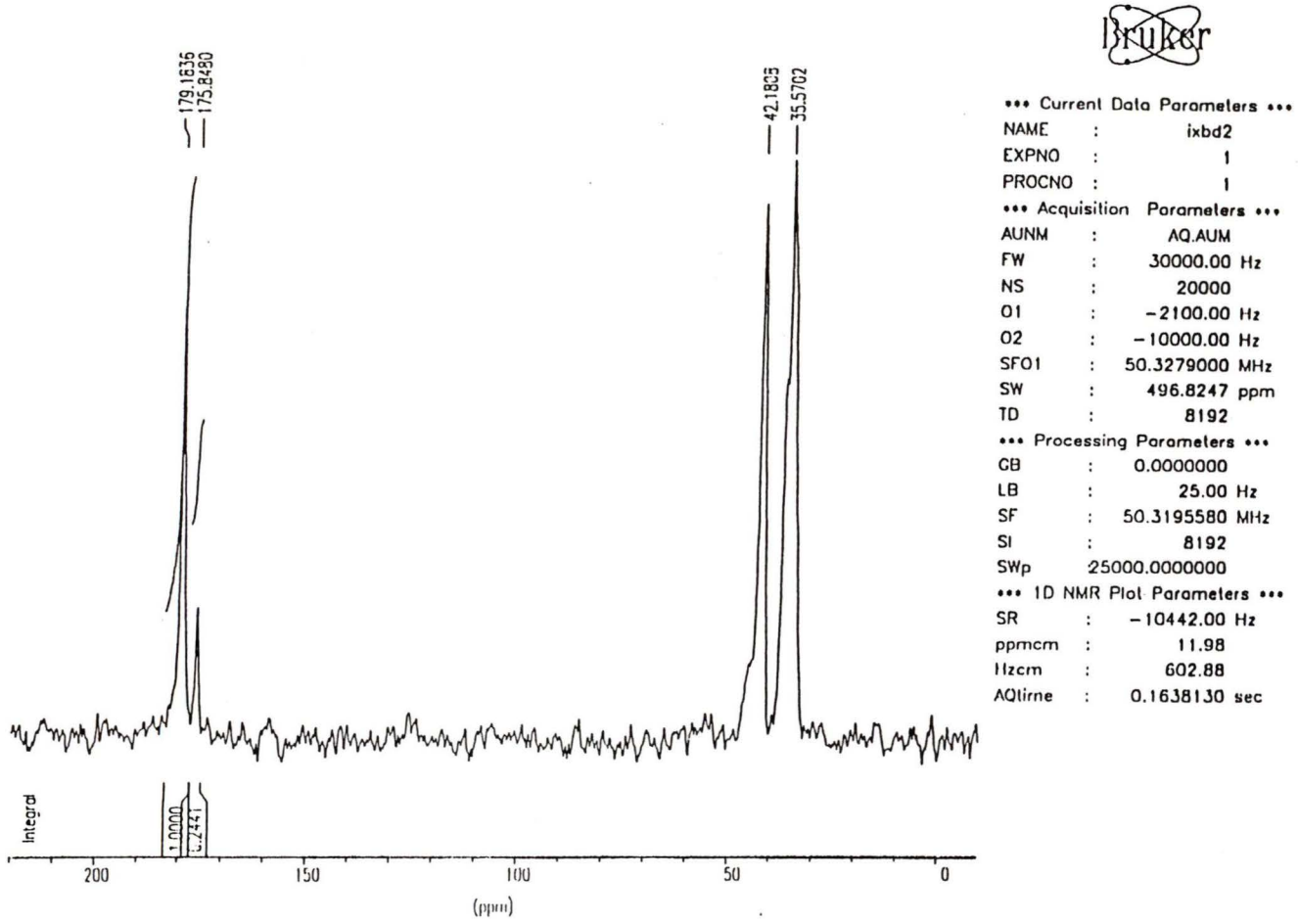

Fig. 25 ^{13}C NMR spectrum of the copolymer from DMAM-co-AM-2

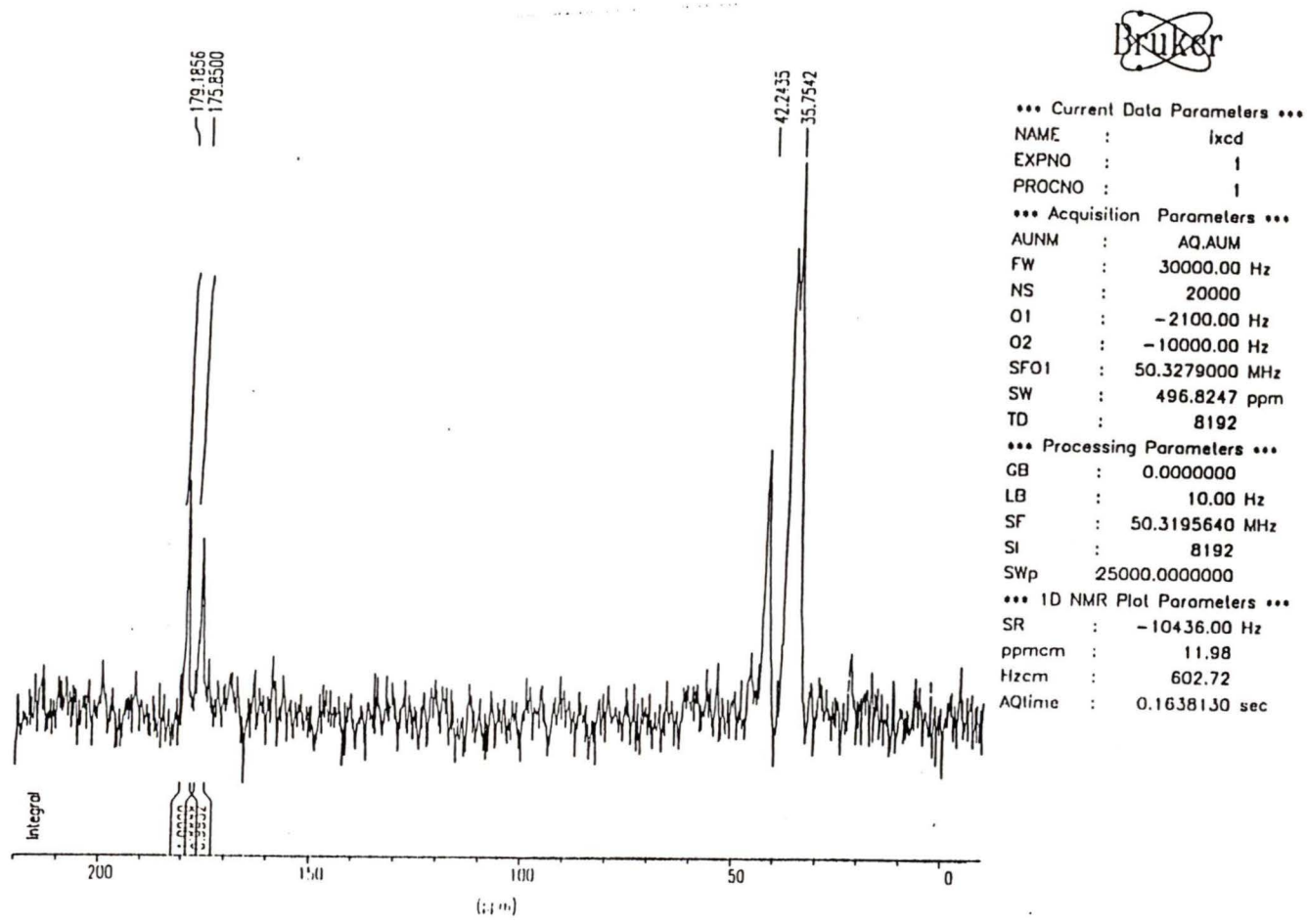

Fig. 26 ^{13}C NMR spectrum of the copolymer from DMAM-co-AM-3

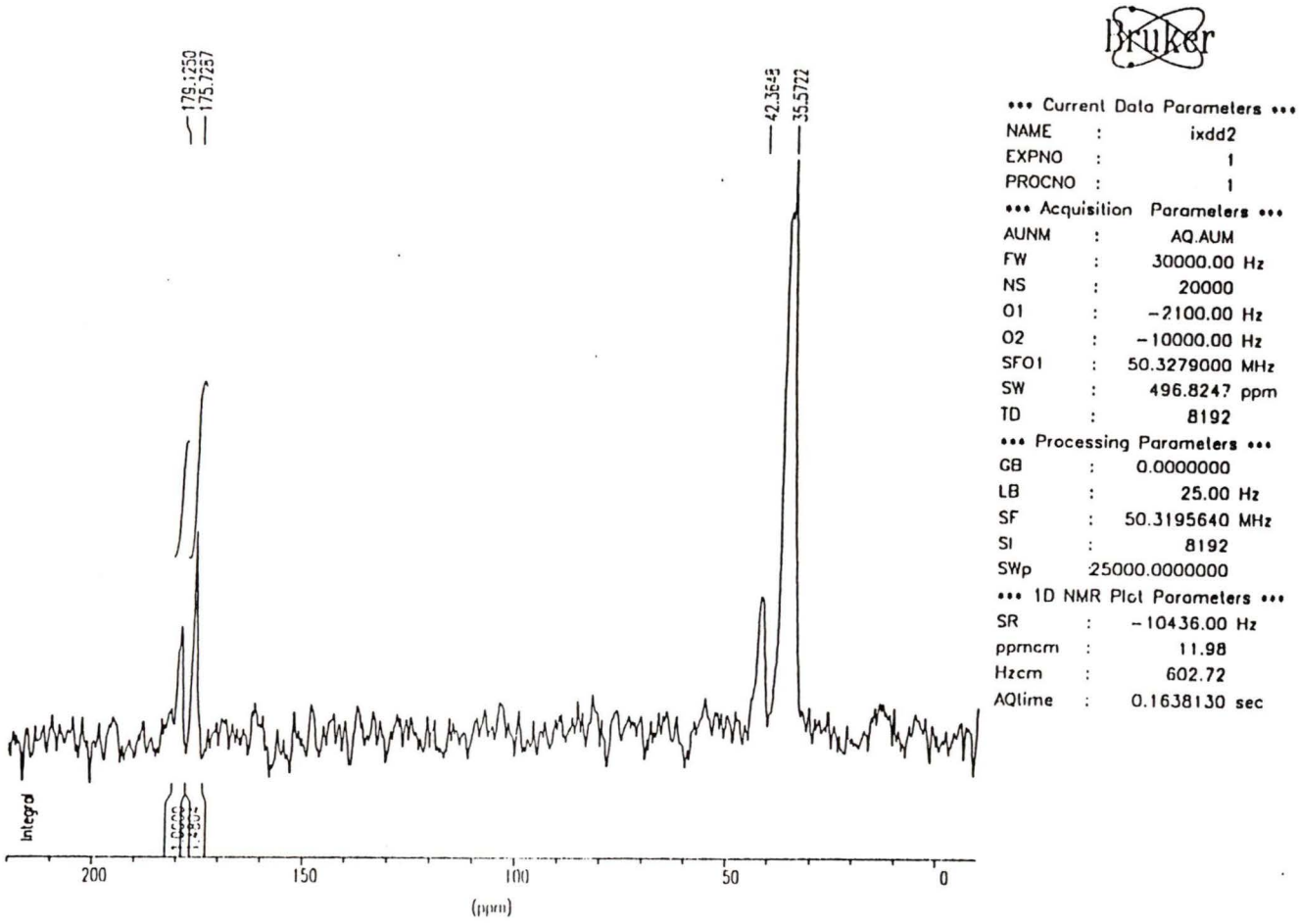

Fig. 27 ^{13}C NMR spectrum of the copolymer from DMAM-co-AM-4

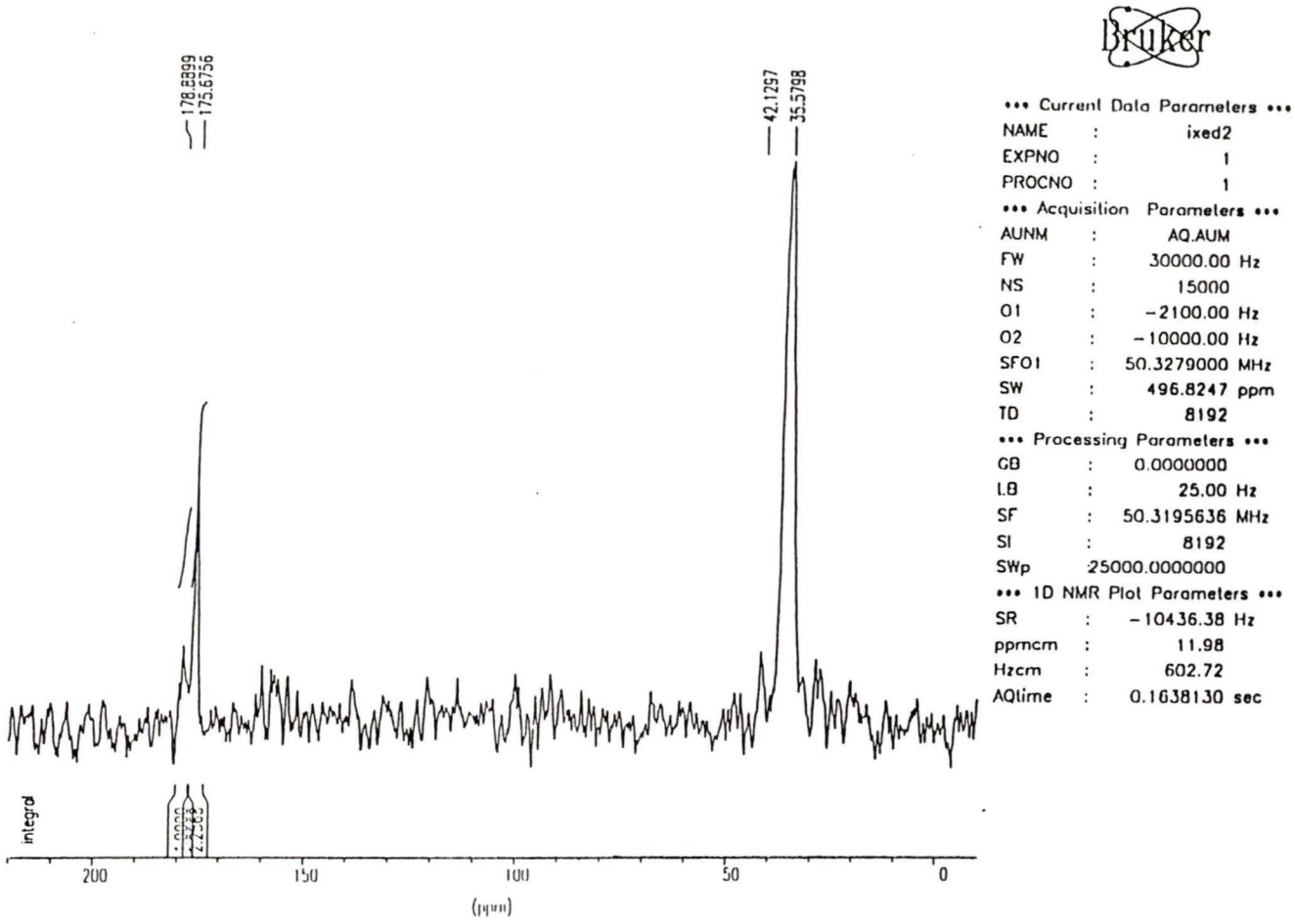

Fig. 28 ^{13}C NMR spectrum of the copolymer from DMAM-co-AM-5

^{13}C NMR of PMeAM from MeAM-co-AM-6 (90.55 MHz, DCO_2D, ext. ref. $CDCl_3$): δ 182.7 and 182.0 (C=O), δ 165.7 to 165.3 (C=O from DCO_2D), δ 52.8 and 51.2 (tertiary C), δ 44.6 (C of CH_2), δ 19.4, 17.9, 16.4, 12.6 (C of CH_3 from MeAM and PMeAM).

^{13}C NMR of the copolymers from MeAM-co-AM-2b to -5 (50.3 MHz, D2O, 0.1 M NaCl, ext. ref. CD_3OD): δ 179.2 (-2b), 180.2 (-3), 181.2 (-4), and 182.5 (-5) (amide C=O), δ 53.6 and 51.4 (-4) and δ 54.1 and 51.9 (-5) (tertiary C from MeAM component), δ 45.3 (-2b), 45.0 (-3), 44.8 (-4), and 44.9 (-5) (C of CH_2 from MeAM component), δ 42.1 (-2b), 41.9 (-3), 41.5 (-4) (C of CH from AM component), δ 35.7 to 34.8 (-2b), 35.6 (-3), 38.7 (-4), 37.9 (-5) (C of CH_2 from AM component), δ 20.5, 18.9, and 17.5 (-2b), 17.1 (-3), 17.4 (-4), 16.3 (-5) (C of CH_3 from MeAM component).

^{13}C NMR data from the spectra of NTBAM, PNTBAM from NTBAM-co-AM-6b, and copolymers from NTBAM-co-AM-1b to -6a

^{13}C NMR of NTBAM (90.55 MHz, CD_3OD, ext. ref. $CDCl_3$): δ 167.4 (amide C=O), δ 133.2 (alkene C of CH), δ 125.6 (alkene C of CH_2), δ 52.0 (tertiary C of t-butyl), δ 49.0 (C of CD_3OD), δ 28.9 (C of CH_3).

^{13}C NMR of PNTBAM (90.55 MHz, CD_3OD, ext. ref. $CDCl_3$): δ 176.8 (amide C=O), δ 167.4 (amide C=O from NTBAM), δ 133.2 (alkene C of CH from NTBAM), δ 125.6 (alkene C of CH_2 from NTBAM), δ 52.2 (tertiary C of t-butyl from NTBAM and PNTBAM), δ 49.2 to 48.8 (C of CD_3OD), δ 43.5 (C of CH from PNTBAM), δ 36.6 (C of CH_2 from PNTBAM), δ 31.1, 29.3, and 28.9 (C of CH_3 from NTBAM and PNTBAM).

^{13}C NMR of the copolymers from NTBAM-co-AM-1b (clouded layer), -1b (clear

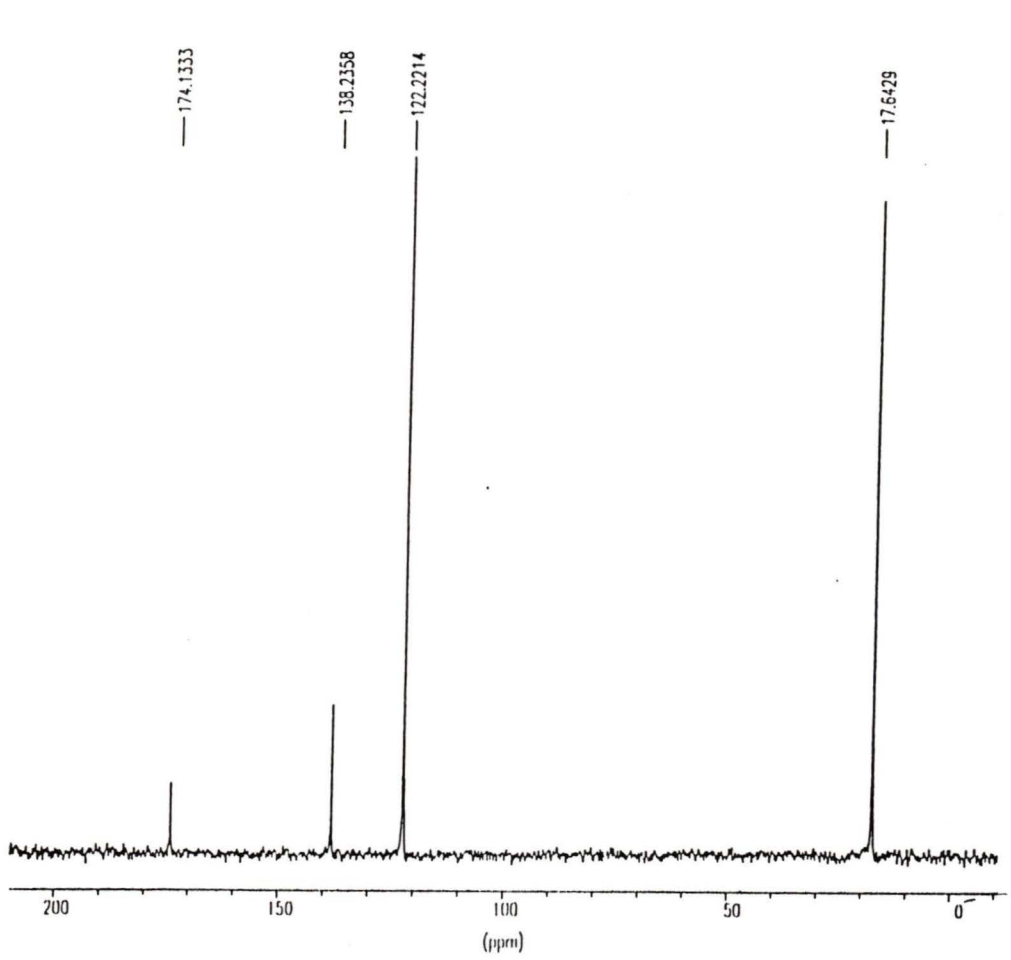

Bruker

*** Current Data Parameters ***
NAME : cg1934
EXPNO : 1
PROCNO : 1
*** Acquisition Parameters ***
AUNM : auzg
FW : 25000.00 Hz
NS : 668
O1 : 15000.00 Hz
O2 : 6600.00 Hz
SFO1 : 90.5650000 MHz
SW : 220.8359 ppm
TD : 32768
*** Processing Parameters ***
GB : 0.0000000
LB : 10.00 Hz
SF : 90.5559890 MHz
SI : 16384
SWp 20000.0000000
*** 1D NMR Plot Parameters ***
SR : 5989.00 Hz
ppmcm : 11.50
Hzcm : 1041.60
AQtime : 0.8192000 sec

Fig. 29 ^{13}C NMR spectrum methacrylamide (MeAM)

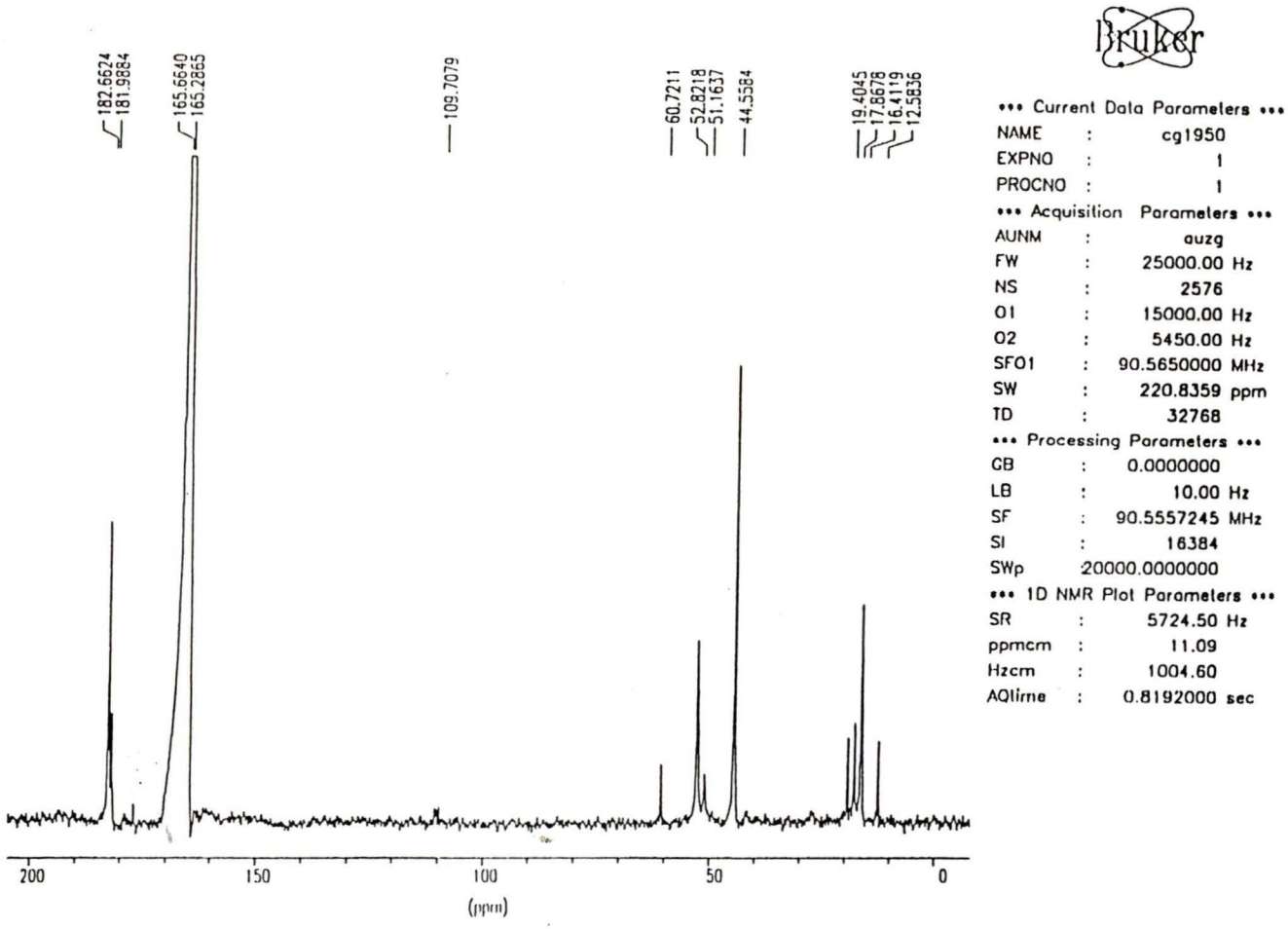

Fig. 30 ^{13}C NMR spectrum PMeAM from MeAM-co-AM-6

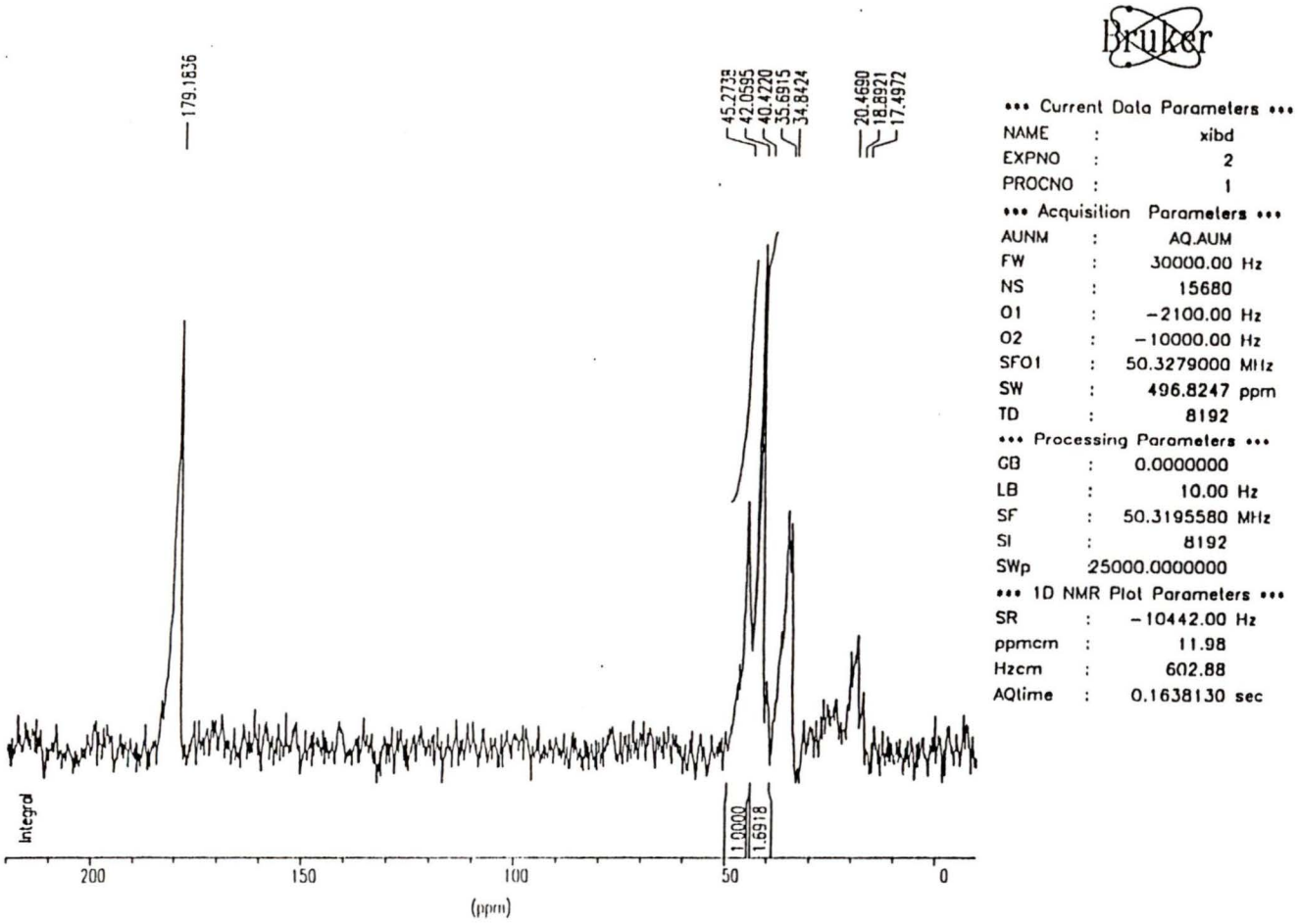

Fig. 31 ^{13}C NMR spectrum of the copolymer from MeAM-co-AM-2b

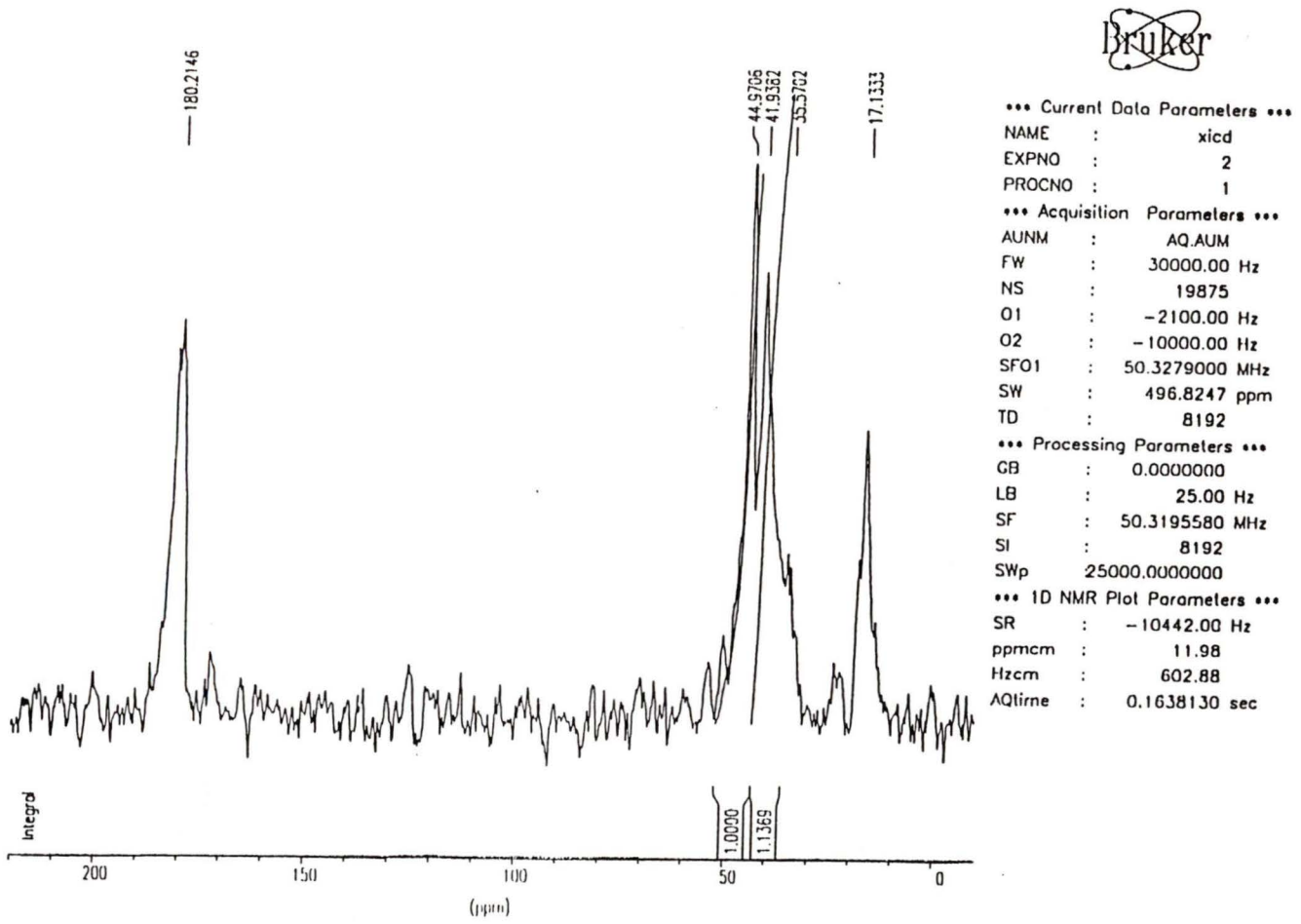

Fig. 32 ^{13}C NMR spectrum of the copolymer from MeAM-co-AM-3

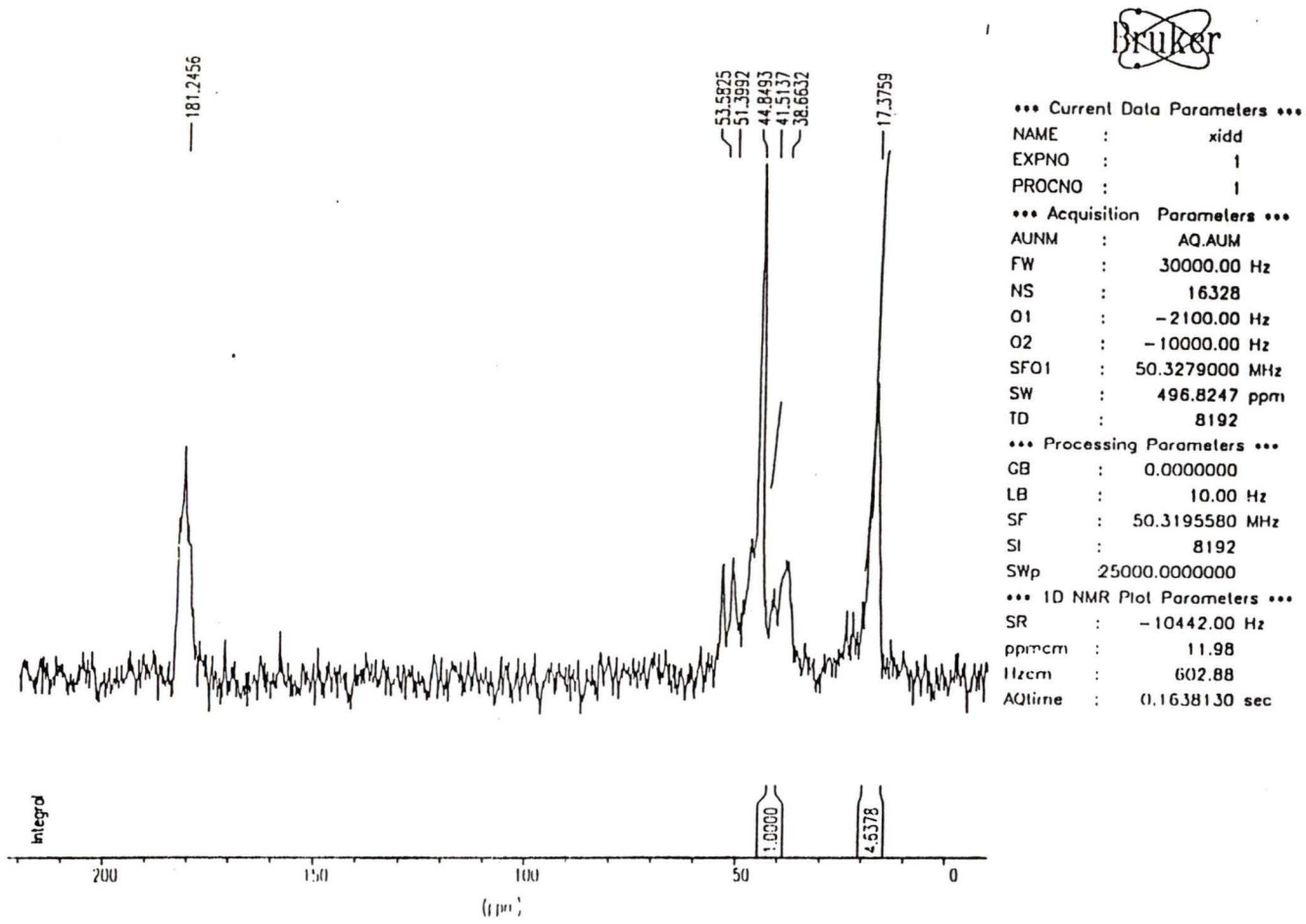

Fig. 33 ^{13}C NMR spectrum of the copolymer from MeAM-co-AM-4

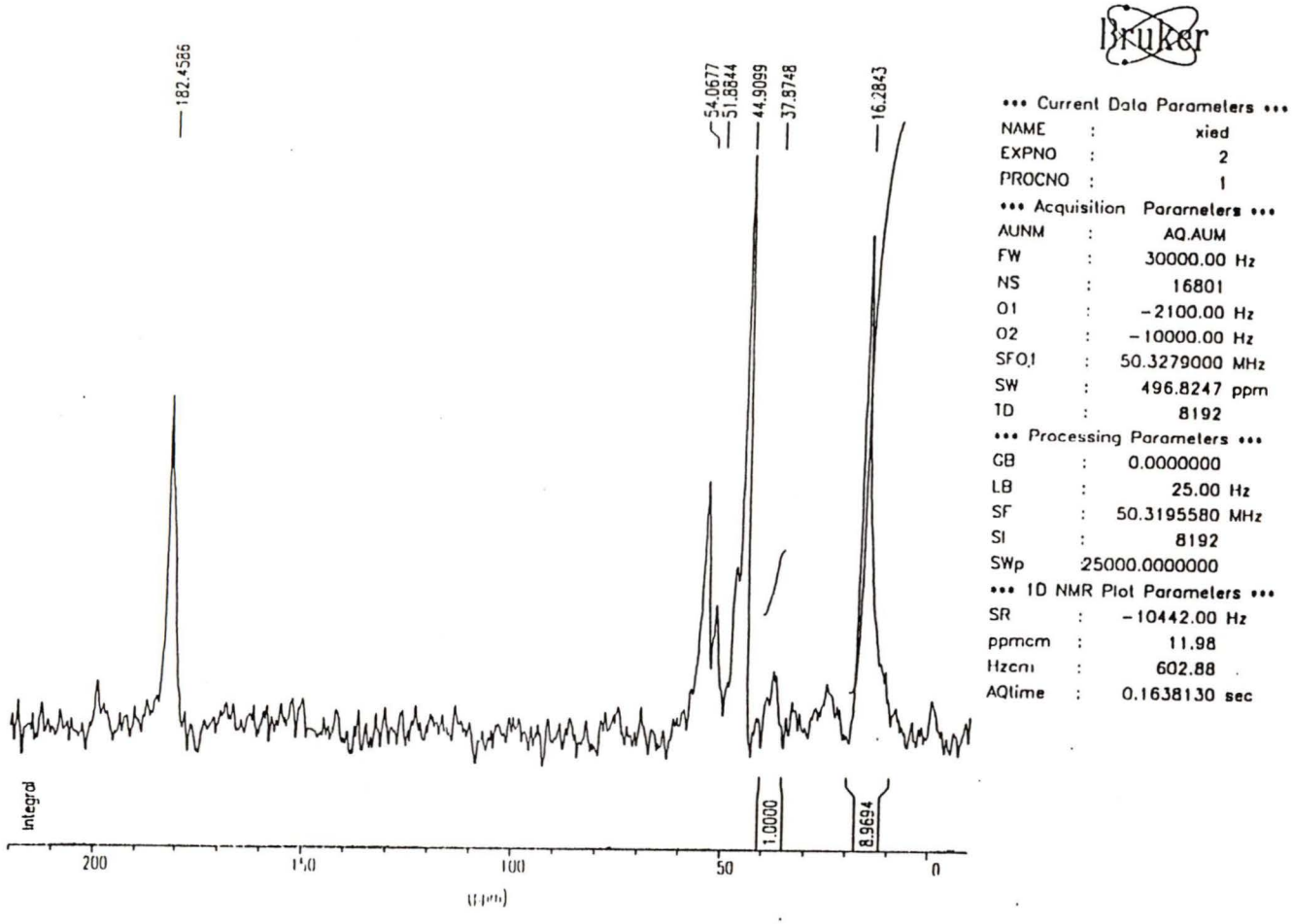

Fig. 34 ^{13}C NMR spectrum of the copolymer from MeAM-co-AM-5

layer), -2 (dialyzed fraction), and -2 (non-dialyzed fraction) (50.3 MHz, D_2O, 0.1M NaCl, ext. ref. CD_3OD): δ 179 (amide C=O from AM component), δ 175 (amide C=O from NTBAM component), δ 127.9 (-1b clouded layer) and 127.8 and 125.7 (-1b clear layer) (alkene C of CH_2 and CH from NTBAM monomer), δ 51 (tertiary C of t-butyl from NTBAM component), δ 42 (C of CH from AM component), δ 35 (C of CH_2 from AM component), δ 28 (C of CH_3 from NTBAM component).

^{13}C NMR of the copolymers from NTBAM-co-AM-3 (gelatinous material) and -6a (gelatinous material) (90.55 MHz, CD_3OD, ext. ref. $CDCl_3$): δ 180 (amide C=O from AM component), δ 176 (amide C=O from NTBAM component), δ167.5 (-6a) (amide C=O from NTBAM monomer), δ 133.2 and 125.6 (alkene C from NTBAM monomer), δ 131.8 and 127.5 (alkene C from AM monomer), δ 69.4 (tertiary C from 98% t-BuOH), δ 52.2 (tertiary C from NTBAM component and NTBAM monomer), δ 49 (C from CD_3OD), δ 44 to 43 (C of CH from AM and NTBAM components), δ 36 (C of CH_2 from AM and NTBAM components), δ 31 to 28 (C of CH_3 from t-butyl of NTBAM monomer, NTBAM component of copolymer, and 98 % t-BuOH).

^{13}C NMR of the copolymer from NTBAM-co-AM-3 (tan coloured solution) (90.55 MHz, 1:1, CD_3OD / D_2O, ext. ref. $CDCl_3$): δ 179.4 (amide C=O from PAM), δ 170.9 (amide C=O from AM), δ 167.7 (amide C=O from PNTBAM), δ 131.1 and 126.2 (alkene C from AM), δ 129.4 and 128.5 (alkene C from PNTBAM), δ 51.2 (tertiary C from PNTBAM and NTBAM monomer), δ 41.7 (C of CH from PAM), δ 27.6 (C of CH_3 from PNTBAM and NTBAM monomer).

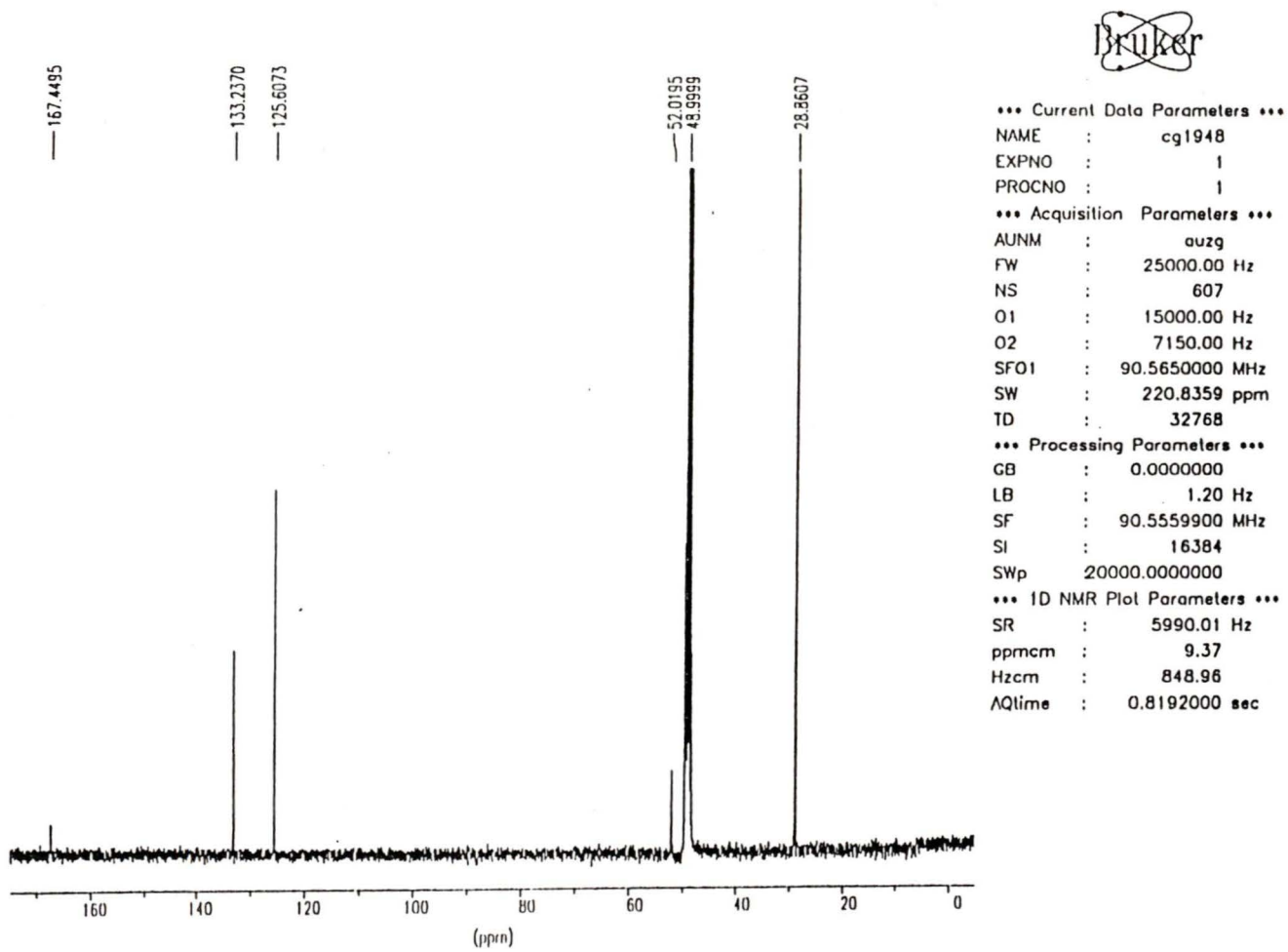

Fig. 35 ^{13}C NMR spectrum of N-t-butylacrylamide (NTBAM)

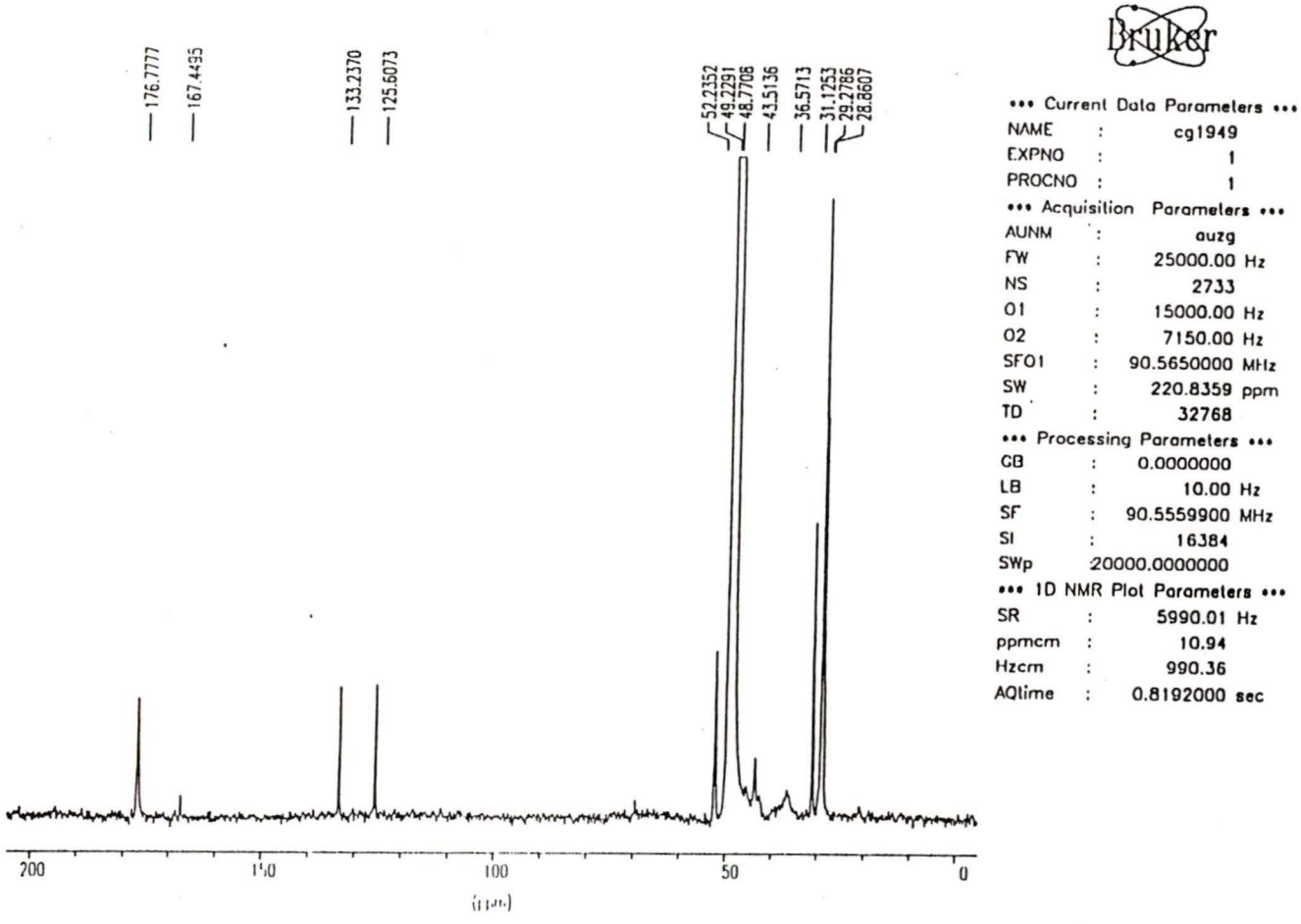

Fig. 36 ^{13}C NMR spectrum of PNTBAM from NTBAM-co-AM-6b

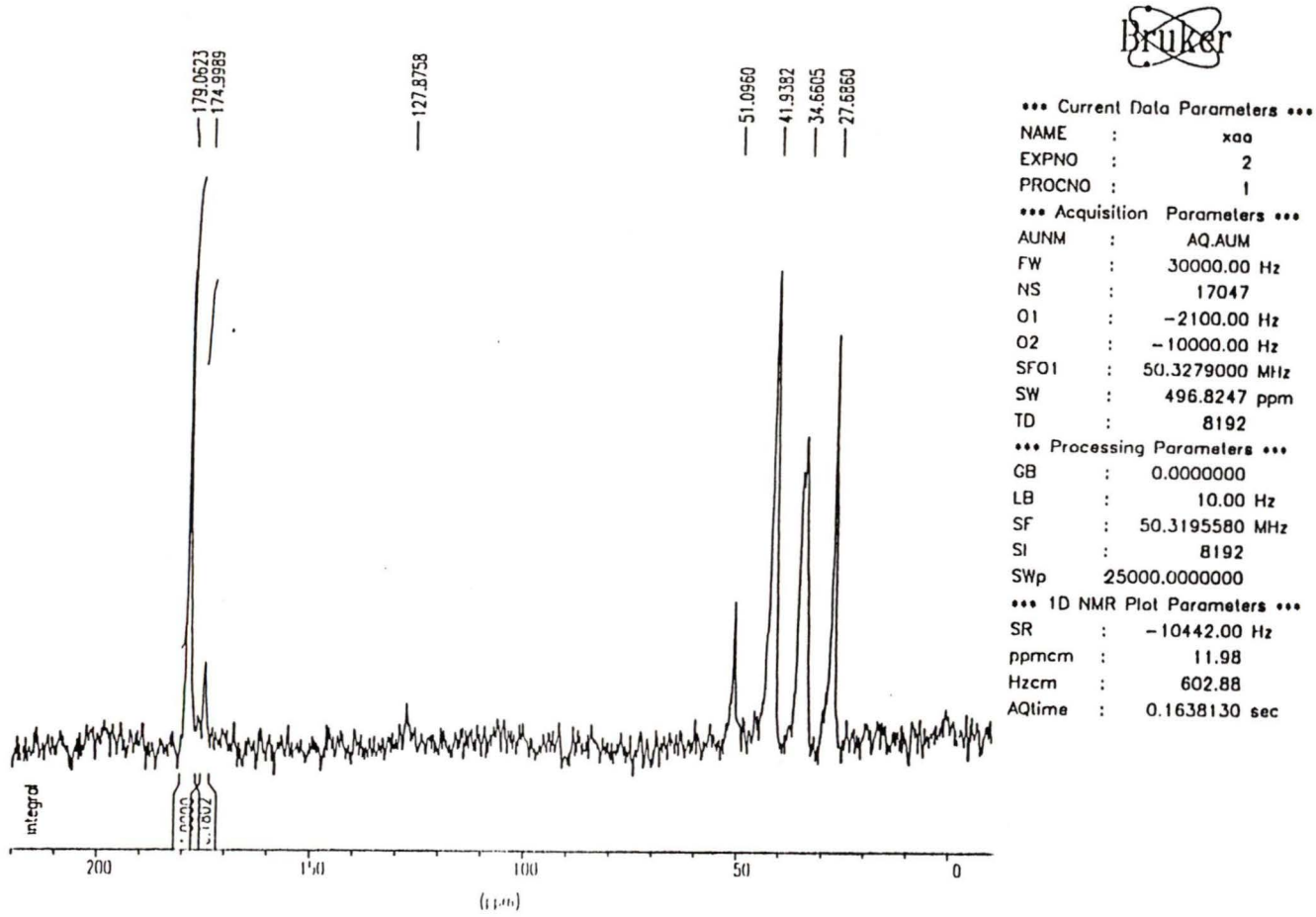

Fig. 37 ^{13}C NMR spectrum of the copolymer from NTBAM-co-AM-1b (clouded layer)

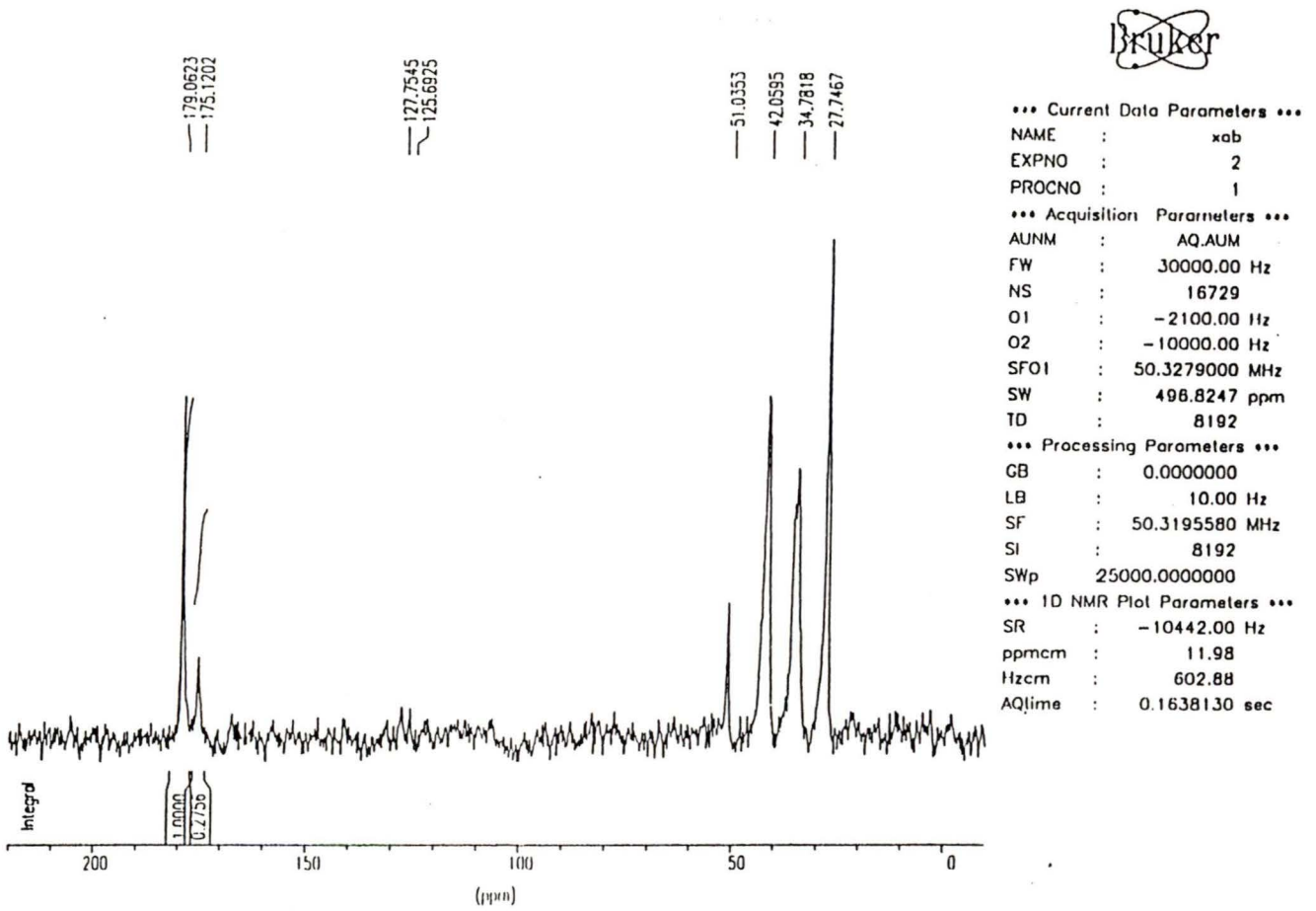

Fig. 38 ^{13}C NMR spectrum of the copolymer from NTBAM-co-AM-1b (clear layer)

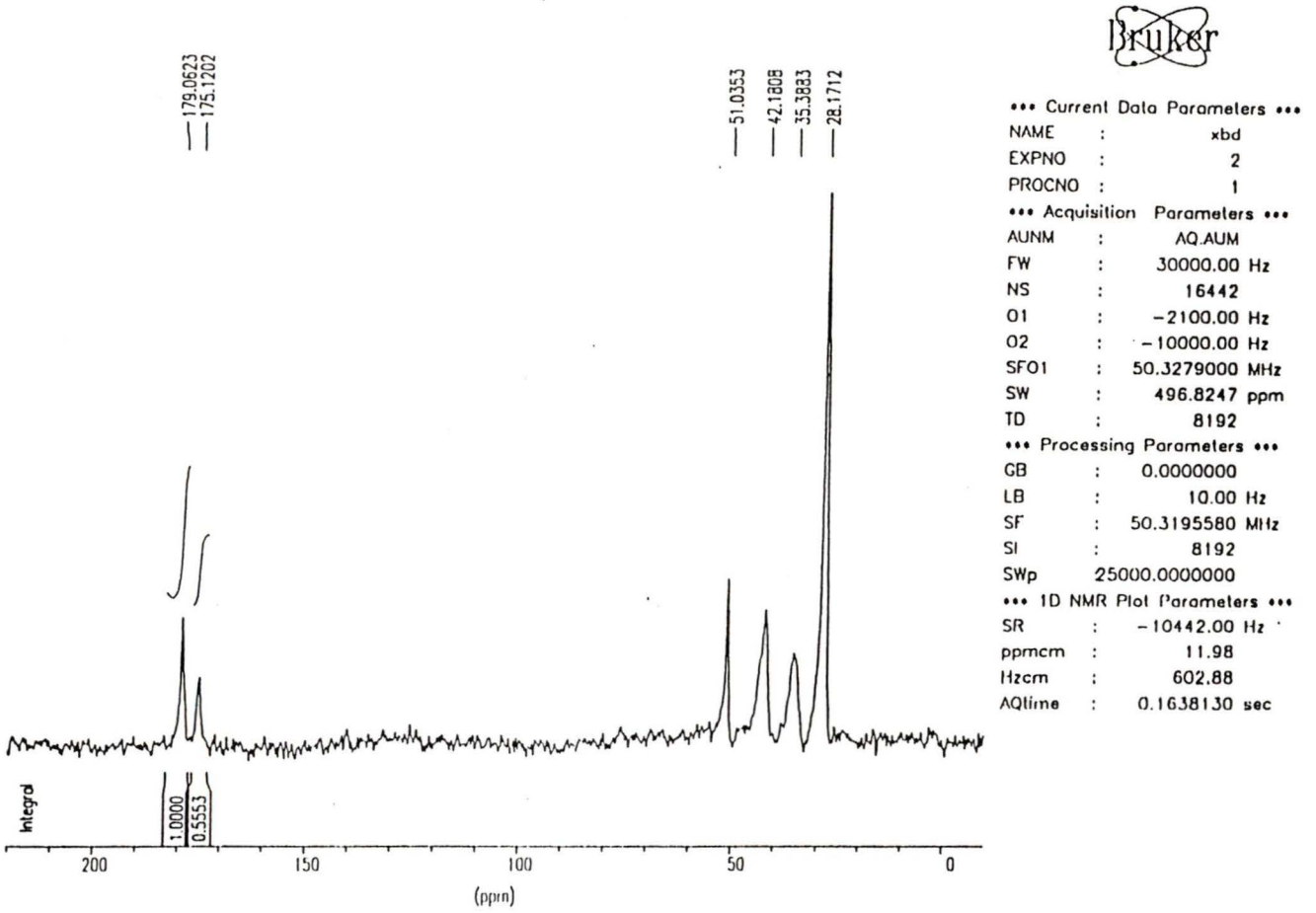

Fig. 39 ^{13}C NMR spectrum of the copolymer from NTBAM-co-AM-2 (dialyzed fraction)

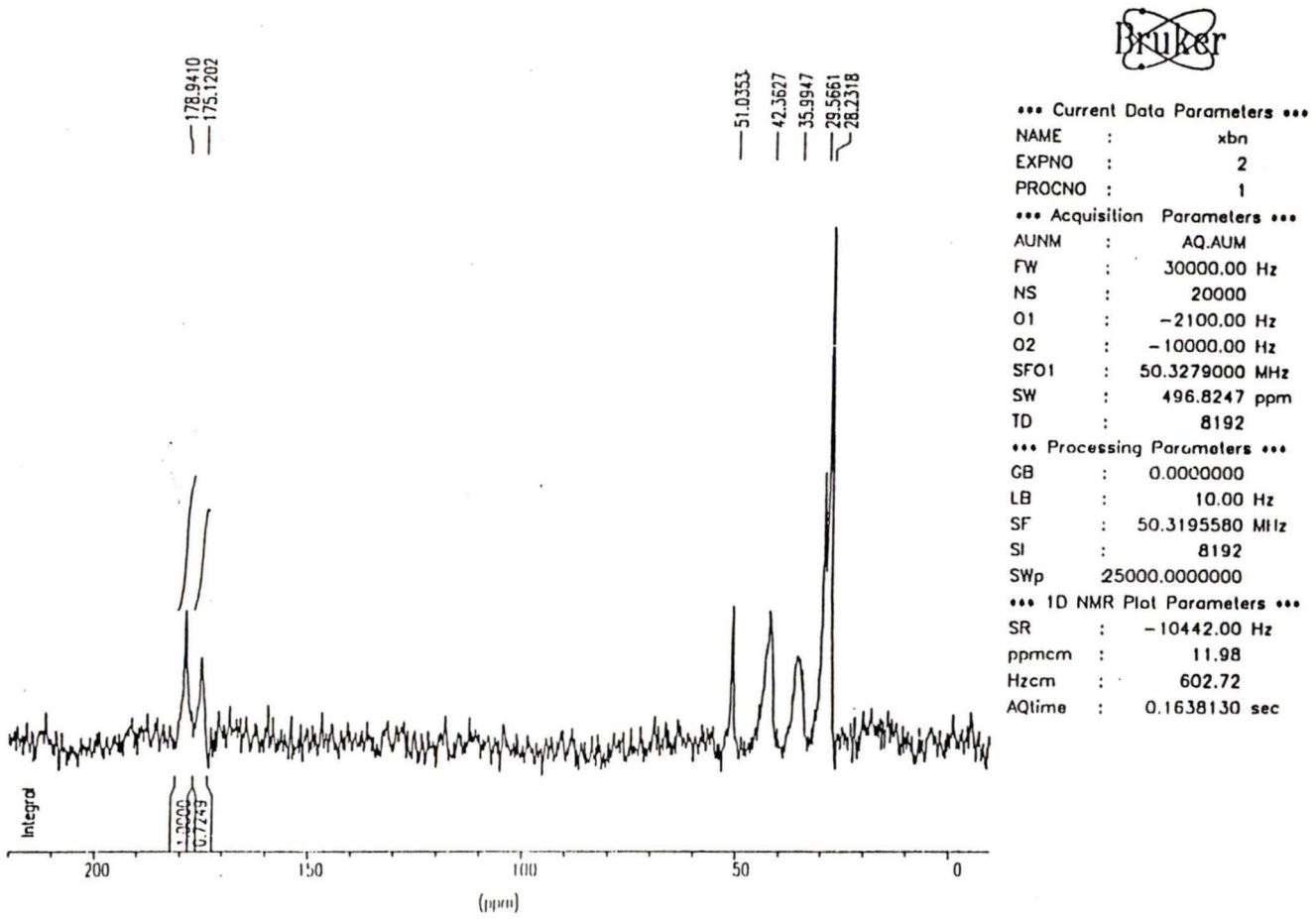

Fig. 40 ^{13}C NMR spectrum of the copolymer from NTBAM-co-AM-2 (non-dialyzed fraction)

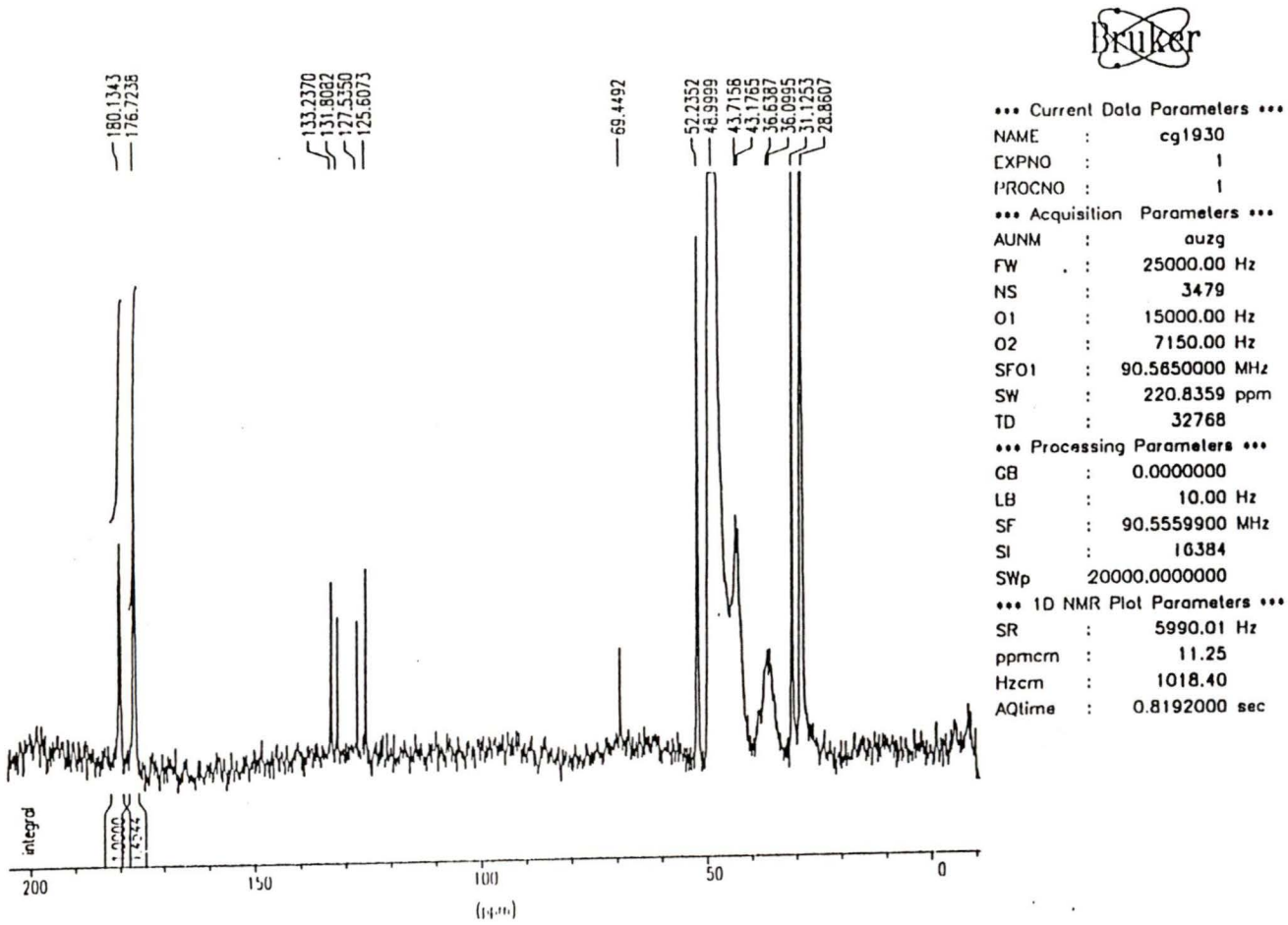

Fig. 41 ^{13}C NMR spectrum of the copolymer from NTBAM-co-AM-3 (gelatinous material)

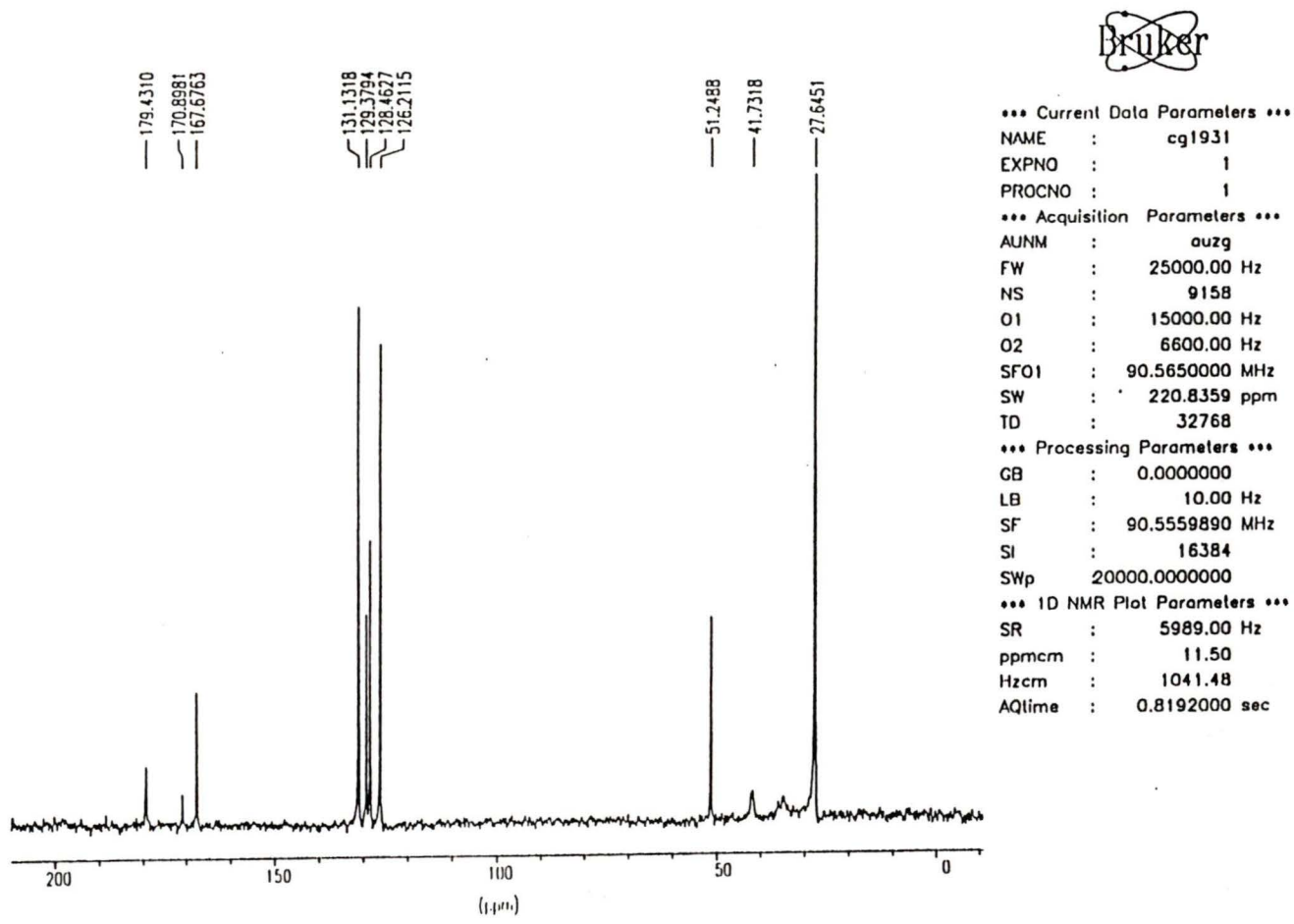

Fig. 42 ^{13}C NMR spectrum of the copolymer from NTBAM-co-AM-3 (tan coloured solution)

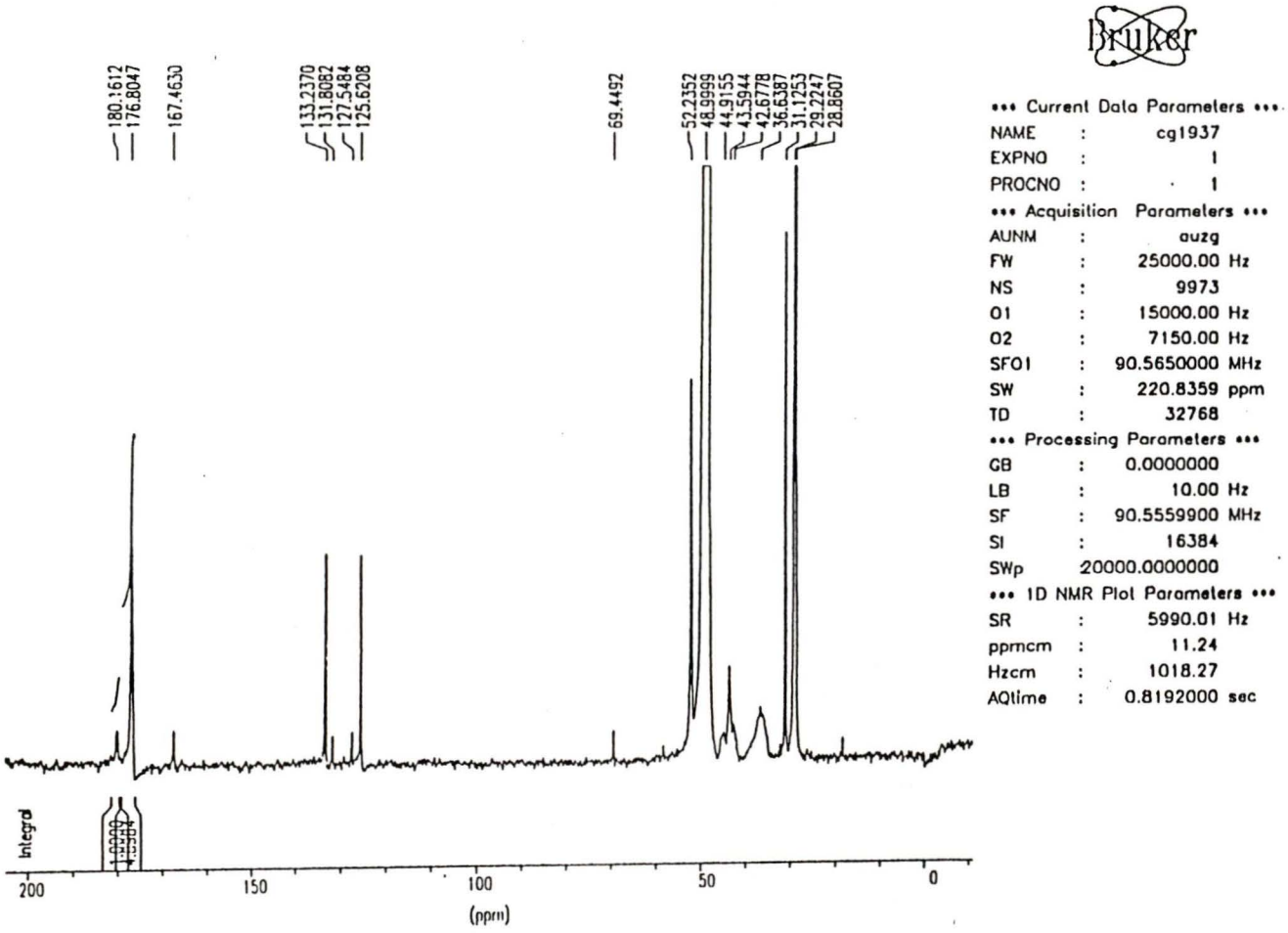

Fig. 43 ^{13}C NMR spectrum of the copolymer from NTBAM-co-AM-6a

3.5.4. Elemental analysis

The results from elemental analysis of the copolymers from DMAM-co-AM-2 to -5 and -7, the copolymers from MeAM-co-AM-2b to -5, homopolymer (PMeAM) from MeAM-co-AM-6, PAM from control-6 (complementary to MeAM-co-AM-6), and commercial PAM are given in Table 21. Weight percentages of carbon, hydrogen, and nitrogen are reported for all the polymers and the weight percentage of oxygen was included for the copolymers from MeAM-co-AM-3 and -4.

There was good agreement between the weight percentages of carbon, hydrogen, and nitrogen obtained by using ordinary combustion techniques and the weight percentages obtained by using V_2O_5 and tin powder as combustion catalysts for the copolymers from MeAM-co-AM-3 and -4. Also, there was good agreement between the weight percentages of carbon, hydrogen, and nitrogen using duplicate samples for the copolymers from MeAM-co-AM-4. In fact, the highest absolute percentage difference between the individual weight percentages and their mean value was calculated as 2.6 % for hydrogen weight percentages obtained for the copolymer from MeAM-co-AM-3. The individual weight percentages obtained for the complete elemental analysis of the copolymers from MeAM-co-AM-3 and -4 summed to give total weight percentages of 95.92 % and 95.33 %, respectively.

3.6. Copolymer Composition

Copolymer compositions for the copolymers from DMAM-co-AM-2 to -5 and -7, and MeAM-co-AM-2b to -5 were calculated using the copolymerization equation

Table 21 Elemental analysis of the copolymers from DMAM-co-AM-2 to -5 and -7, the copolymers from MeAM-co-AM-2b to -5, PMeAM from MeAM-co-AM-6, PAM from control-6, and commercial PAM

Polymer Origin	Elemental analysis			
	Carbon (weight %)	Hydrogen (weight %)	Nitrogen (weight %)	Oxygen (weight %)
DMAM-co-AM-2	46.25	7.27	15.53	n/m [a]
DMAM-co-AM-3	48.28	7.58	14.64	n/m [a]
DMAM-co-AM-4	49.99	8.43	13.69	n/m [a]
DMAM-co-AM-5	51.30	8.21	12.93	n/m [a]
MeAM-co-AM-2b	45.48	7.34	16.45	n/m [a]
MeAM-co-AM-3	48.24	7.38	16.04	24.26
	48.27 [b]	7.69 [b]	16.13 [b]	n/m [a]
	48.26 [b]	7.65 [b]	16.17 [b]	n/m [a]
MeAM-co-AM-4	50.03	7.76	14.87	22.67
	49.98 [d]	7.59 [d]	15.03 [d]	n/m [a]
	49.89 [b]	7.69 [b]	14.84 [b]	n/m [a]
	49.87 [c]	7.84 [c]	14.73 [c]	n/m [a]
MeAM-co-AM-5	47.59	7.99	14.18	n/m [a]
MeAM-co-AM-6	53.23	8.13	15.40	n/m [a]
control-6	49.44	7.29	19.01	n/m [a]
Commercial PAM [e]	46.39	6.82	21.41	n/m [a]

a. n/m denotes not measured.
b. V_2O_5 was used as the combustion catalyst.
c. Tin powder was used as the combustion catalyst.
d. This analysis was done as the duplicate of the first analysis for regular combustion techniques.
e. Aldrich 100% polyacrylamide.

(Eq. 38) and literature values for the monomer reactivity ratios.[32]

$$F_1 = \frac{r_1 f_1^2 + f_1 f_2}{r_1 f_1^2 + 2 f_1 f_2 + r_2 f_2^2} \qquad \text{Eq. 38}$$

where F_1 is the mole fraction of monomer, M_1, in the copolymer.

f_1 is the mole fraction of monomer, M_1, in the feedstock.

f_2 is the mole fraction of monomer, M_2, in the feedstock.

r_1 is the reactivity ratio of monomer, M_1.

r_2 is the reactivity ratio of monomer, M_2.

3.6.1. Copolymers from DMAM-co-AM-2 to -5 and -7

Integration of the resonance peaks at δ 179.2 (C=O from AM component) and δ 175.8 (C=O from DMAM component) of the ^{13}C NMR spectra of the copolymers from DMAM-co-AM-2, -3, -4, -5, and -7 gave the compositions of the copolymers (Table 22). Also, the weight percentages of carbon and nitrogen from elemental analysis of the copolymers were used to determine the copolymer compositions by substitution into Eq. 39.

$$\frac{X}{Y} = \frac{\frac{AW nitrogen}{\%N\ (analysis)} - \frac{AW carbon}{\%C\ (analysis)} \times 3}{\frac{AW carbon}{\%C\ (analysis)} \times 5 - \frac{AW nitrogen}{\%N\ (analysis)}} \qquad \text{Eq. 39}$$

where X is the number of DMAM comonomer units in the copolymer.

Table 22 Comparison of the copolymer compositions obtained for DMAM-co-AM-2, -3, -4, -5, and -7 from the copolymer equation, ^{13}C NMR integration, and elemental analysis

Experiment	Feed Composition	Copolymer Composition by :				
		Copolym. equation [a]	^{13}C NMR integration [b]	Elemental analysis		
	DMAM (mol %)	DMAM (mol %)	DMAM (mol %)	C wt. %	N wt. %	DMAM mol %
DMAM-co-AM-2	20	23.6	19.6	46.25	15.53	23.6
DMAM-co-AM-3	40	44.4	49.8	48.28	14.64	43.3
DMAM-co-AM-4	60	63.5	59.7	49.99	13.69	62.9
DMAM-co-AM-5	80	81.9	69.3	51.3	12.93	81.3
DMAM-co-AM-7	10	12.3	n/m [c]	45.45	16.13	14.3

a. The reactivity ratios for copolymerization of AM (M_1) with DMAM (M_2) as determined by McCormick and Chen using the method of Kelen-Tüdos are $r_1 = 0.78 \pm 0.04$ and $r_2 = 1.10 \pm 0.04$.[18]
b. The ^{13}C NMR integrations included the carbonyl carbon atoms of both the DMAM and AM components of the copolymer.
c. n/m denotes not measured.

Y	is the number of AM comonomer units in the copolymer.
AW nitrogen	is the molecular weight of nitrogen, 14.0067 units.
AW carbon	is the molecular weight of carbon, 12.011 units.
% N (analysis)	is the weight percentage of nitrogen in the copolymer determined by elemental analysis.
% C (analysis)	is the weight percentage of carbon in the copolymer determined by elemental analysis.

3.6.2. Copolymers from MeAM-2b to -5

Integration of the resonance peaks at δ 45.3 (-2b) and δ 45.0 (-3) (C of CH_2 from MeAM component) and δ 35.7 to 34.8 (-2b) and δ 35.6 (-3) (C of CH_2 from AM component) of the ^{13}C NMR spectra of the copolymers from MeAM-co-AM-2b and -3 gave the compositions of the copolymers. Compositions of the copolymers from MeAM-co-AM-4 to -5 were obtained from the integrals of the resonance peaks at δ 38.7 (-4) and δ 37.9 (-5) (C of CH_2 from AM component) and δ 17.4 (-4) and δ 16.3 (-5) (C of CH_3 from MeAM component) of the copolymers from MeAM-co-AM-4 and -5.

Weight percentages of hydrogen from elemental analysis of the copolymers from MeAM-co-AM-2b to -5, the homopolymer (PMeAM) from MeAM-co-AM-6, and PAM from control-6 (complementary to MeAM-co-AM-6) were also used to determine the copolymer compositions. Linear regression was used to calculate an equation for a straight line from the x-coordinate data for the mol % of MeAM in the polymer and the y-coordinate data for the weight percentage of hydrogen in the homopolymer (PMeAM) from MeAM-co-AM-6 and PAM from control-6. The weight percentages of hydrogen in

Table 23 Comparison of the copolymer compositions obtained for MeAM-co-AM-2b to -5 from the copolymer equation, ^{13}C NMR integration, and elemental analyis

Experiment	Feed Composition	Copolymer Composition by :			
		Copolymer. equation [a]	^{13}C NMR integration [b]	Elemental analysis	
	MeAM (mol %)	MeAM (mol %)	MeAM (mol %)	H wt. %	MeAM (mol %)
MeAM-co-AM-2b	20	24.4	37.1	7.67	5.7
MeAM-co-AM-3	40	45.1	46.8	7.91	33.0
MeAM-co-AM-4	60	64.0	82.3	8.07	51.1
MeAM-co-AM-5	80	82.0	90.0	8.35	83.0
MeAM-co-AM-6	100	100	n/a	8.50	100
control-6	0	0	n/a	7.62	0

a. The reactivity ratios used for the copolymerization of AM (M_1) with MeAM (M_2) are $r_1 = 0.74 \pm 0.11$ and $r_2 = 1.10 \pm 0.20$.[1]

b. The ^{13}C NMR integrations for MeAM-co-AM-2b and -3 included the methylene carbon of the MeAM component and the methyne carbon of the AM component of the copolymer. MeAM-co-AM-4 and -5 included the methyl carbon of the MeAM component and the methylene carbon of the AM component of the copolymer.

the copolymers from MeAM-co-AM-2b to -5 were substituted into the equation for the best straight line to determine the mol % of MeAM in the copolymers (Table 23).

3.6.3. Copolymers from NTBAM-co-AM-1b to -3 and -6a

Integration of the resonance peaks at δ 179 (amide C=O from AM component) and δ 175 (amide C=O from NTBAM component) of the ^{13}C NMR spectra of the copolymers from NTBAM-co-AM-1b (clouded layer), -1b (clear layer), -2 (dialyzed fraction), and -2 (non-dialyzed fraction) and -3 gave the compositions of the copolymers. In addition, integration of the resonance peaks at δ 180 (amide C=O from AM component) and δ 176 (amide C=O from NTBAM component) of the ^{13}C NMR spectra of the copolymers from NTBAM-co-AM-3 (gelatinous material) and -6a (gelatinous material) gave the compositions of the copolymers (Table 24).

3.7. Evaluation of the Experiments to Determine the % Cationicity of the Newly Synthesized Cationic Derivatives and the Commercial Polymer, Percol 721

The volumes of titrant required to neutralize the duplicate analyte solutions for the cationic derivatives of the copolymers from DMAM-co-AM-7, MeAM-co-AM-2b, and NTBAM-co-AM-1b (clouded layer) as well as the cationic derivative of PAM from control-6 (complementary to MeAM-co-AM-6) and Percol 721 (cationic PAM) were averaged and then corrected for the average of the blank titrations. The percentage cationicity of the cationic derivatives was calculated using Eq. 40.

$$N_1 V_1 = N_2 V_2 \qquad \text{Eq. 40}$$

Table 24 Copolymer compositions obtained for NTBAM-co-AM copolymers from ^{13}C NMR integration

Experiment	Feed Composition	Copolymer Composition
		^{13}C NMR Integration [a]
	NTBAM (mol %)	NTBAM (mol %)
NTBAM-co-AM-1b (clouded layer)	20	15.3
NTBAM-co-AM-1b (clear layer)	20	21.6
NTBAM-co-AM-2 (dialyzed fraction)	40	35.7
NTBAM-co-AM-2 (non-dialyzed fraction)	40	42.0
NTBAM-co-AM-3 (gelatinous material)	60	59.3
NTBAM-co-AM-6a (gelatinous material)	80	83.0

a. The ^{13}C NMR integrations used the carbonyl functionalities of the NTBAM and AM components of the copolymer. NTBAM-co-AM-1b and -2 were analyzed as solutions in D_2O and NTBAM-co-AM-3 and -6a were analyzed as solutions in CD_3OD.

where N_1 is the normality of the titrant, PVSAK, in equivalents / L.

N_2 is the normality of the analyte solution in equivalents / L.

V_1 is the volume of titrant, PVSAK, in litres.

V_2 is the volume of analyte solution in litres.

From calculation of the normality of the analyte solution, N_2, the normality of the cationic derivative solution was calculated and then converted into molarity. Since the molarity of the cationic derivative solution was based on the number of cationic functionalities, the percentage cationicity was determined from the ratio of the molarity of cationic functionalities in the polymer to the molarity of the nonionic and cationic functionalities in the polymer. The percentage cationicity for the cationic derivatives of the copolymers was 26 % (cationic derivative of DMAM-co-AM-7), 16 % (cationic derivative of MeAM-co-AM-2b), and 18 % cationic derivative of NTBAM-co-AM-1b, clouded layer). The percentage cationicity for the cationic derivative of PAM from control-6 was 14 % and 4.5 % cationicity was determined for Percol 721.

3.8. Comparison of the Intrinsic Viscosities for the Purified andUnpurified Cationic Derivatives of the Nonionic Copolymers and Control PAM with the Intrinsic Viscosities of their Polymer Substrates and Commercial Polymers

The intrinsic viscosities of the purified cationic derivatives were greater than the intrinsic viscosities of the unpurified cationic derivatives, nonionic polymer substrates, and commercial polymers (Table 25). The purified cationic derivative of the copolymer from DMAM-co-AM-7 gave the highest percentage cationicity of the cationic derivatives and also gave the highest intrinsic viscosity. The nonionic copolymer from DMAM-co-

Table 25 Comparison of the intrinsic viscosities of nonionic copolymers, control PAM, and commercial polymers with the intrinsic viscosities of the purified and unpurified cationic derivatives of the nonionic copolymers and PAM

Polymer	Intrinsic viscosity [a] ([η], cm^3/g)
DMAM-co-AM-7	
cationic purified	14700
cationic unpurified	10100
nonionic	765
MeAM-co-AM-2b	
cationic purified	7480
cationic unpurified	4980
nonionic	228
NTBAM-co-AM-1b (clouded layer)	
cationic purified	10100
cationic unpurified	4910
nonionic	309
control-6	
PAM cationic purified	8740
PAM cationic unpurified	5050
PAM nonionic	423
Percol 721 (cationic PAM)	4170
Percol 351 (nonionic PAM)	861
Percol E-24 (anionic PAM)	7260

a. The intrinsic viscosities were determined at 25.0 ± 0.2°C on polymer solutions prepared in deionized water.

AM-7 also gave the highest intrinsic viscosity of the nonionic copolymers including PAM from control-6 (complementary to MeAM-co-AM-6). In fact, the intrinsic viscosity of the copolymer from DMAM-co-AM-7 was only slightly less than the intrinsic viscosity of Percol 351 (nonionic PAM) which was characterized by Allied Colloids as 20 million molecular weight.

3.9. Measurement of the Refractive Index Increment, dn/dc, for Acrylamide-Based Polymers in Var ious Aqueous Solvents

Only the polymer solution standards adjusted to pH 4.00 ± 0.10 and pH 6.50 ± 0.20 without added electrolyte and those adjusted to pH 4.00 ± 0.10 and treated with electrolyte to give 0.01 M NaCl were used to determine the refractive index increments for the copolymers from DMAM-co-AM-2 to -5 and -7 (Table26), MeAM-co-AM-2b to -5 (Table 27), and NTBAM-co-AM-1b (clouded layer), -1b (clear layer), and -2 (dialyzed fraction) (Table 28). In addition to these solvent conditions, polymer solution standards adjusted to pH 4.00 ± 0.10 and treated with electrolyte to give 0.001 M NaCl were used to determine the refractive index increment for PAM from control-6 (complementary to MeAM-co-AM-6). The refractive index increments for PAM from control-6 are included in Table 27. Refractive index increments were also determined for the commercial polymers labelled Percol 351, Percol 721, and Percol E-24 (Table 29). The refractive index increments for Percol 351 were determined by using the solution standards adjusted to pH 4.00 ± 0.10 and pH 6.50 ± 0.20 without added electrolyte and those adjusted to pH 4.00 ± 0.10 and treated with electrolyte to give 0.001 M NaCl and 0.01 M NaCl. Solution standards adjusted to pH 4.00 ± 0.10 and treated with electrolyte to give

Table 26 Refractive index increments, dn/dc, for the copolymers from DMAM-co-AM-2 to -5 and -7 and PDMAM from DMAM-co-AM-6

Experiment	Solvent pH	[NaCl] (moles / litre)	Refractive index increment, dn/dc (cm^3/g)
DMAM-co-AM-2	6.50 ± 0.20	0	0.1987
	4.00 ± 0.10	0	0.2015
	4.00 ± 0.10	0.01	0.1985
DMAM-co-AM-3	6.50 ± 0.20	0	0.1947
	4.00 ± 0.10	0	0.2014
	4.00 ± 0.10	0.01	0.1900
DMAM-co-AM-4	6.50 ± 0.20	0	0.1922
	4.00 ± 0.10	0	0.2053
	4.00 ± 0.10	0.01	0.1666
DMAM-co-AM-5	6.50 ± 0.20	0	0.1495
	4.00 ± 0.10	0	0.1422
	4.00 ± 0.10	0.01	0.1562
DMAM-co-AM-6	6.50 ± 0.20	0	0.1923
	4.00 ± 0.10	0	0.1928
	4.00 ± 0.10	0.01	0.1837
DMAM-co-AM-7	6.50 ± 0.20	0	0.1518
	4.00 ± 0.10	0	0.1861
	4.00 ± 0.10	0.01	0.1455

Table 27 Refractive index increments, dn/dc, for the copolymers from MeAM-co-AM-2b to -5 and PAM from control-6

Experiment	Solvent pH	[NaCl] (moles / litre)	Refractive index increment, dn/dc (cm^3/g)
MeAM-co-AM-2b	6.50 ± 0.20	0	0.1853
	4.00 ± 0.10	0	0.1853
	4.00 ± 0.10	0.01	0.2007
MeAM-co-AM-3	6.50 ± 0.20	0	0.1825
	4.00 ± 0.10	0	n/m [a]
	4.00 ± 0.10	0.01	0.1979
MeAM-co-AM-4	6.50 ± 0.20	0	0.1994
	4.00 ± 0.10	0	0.1532
	4.00 ± 0.10	0.01	0.1581
MeAM-co-AM-5	6.50 ± 0.20	0	0.1367
	4.00 ± 0.10	0	0.2163
	4.00 ± 0.10	0.01	0.1685
control-6	6.50 ± 0.20	0	0.1737
	4.00 ± 0.10	0	0.1786
	4.00 ± 0.10	0.001	0.2133
	4.00 ± 0.10	0.01	0.2046

a. n/m denotes not measured.

Table 28 Refractive index increments, dn/dc, for the copolymers from NTBAM-co-AM-1b (clouded layer), -1b (clear layer), and -2 (dialyzed fraction)

Experiment	Solvent pH	[NaCl] (moles / litre)	Refractive index increment, dn/dc (cm^3/g)
NTBAM-co-AM-1b (clouded layer)	6.50 ± 0.20	0	0.1523
	4.00 ± 0.10	0	0.1636
	4.00 ± 0.10	0.01	0.1563
NTBAM-co-AM-1b (clear layer)	6.50 ± 0.20	0	0.1676
	4.00 ± 0.10	0	0.1780
	4.00 ± 0.10	0.01	0.1538
NTBAM-co-AM-2 (dialyzed fraction)	6.50 ± 0.20	0	0.1594
	4.00 ± 0.10	0	0.1598
	4.00 ± 0.10	0.01	0.1614

Table 29 Refractive index increments, dn/dc, for the commercial polymers Percol 351, Percol 721, and Percol E-24

Commercial polymer	Solvent pH	[NaCl] (moles / litre)	Refractive index increment, dn/dc (cm^3/g)
Percol 351	6.50 ± 0.20	0	0.1845
	4.00 ± 0.10	0	0.1873
	4.00 ± 0.10	0.001	0.2013
	4.00 ± 0.10	0.01	0.1898
Percol 721	6.50 ± 0.20	0	n/m [a]
	4.00 ± 0.10	0	n/m
	4.00 ± 0.10	0.001	0.06783
	4.00 ± 0.10	0.01	0.1412
Percol E-24	6.50 ± 0.20	0	n/m
	4.00 ± 0.10	0	n/m
	4.00 ± 0.10	0.001 M	0.2070
	4.00 ± 0.10	0.01	0.1980

a. n/m denotes not measured.

0.001 M and 0.01 M NaCl were used to determine the refractive index increments for Percol 721 and Percol E-24.

3.10. Solution Behaviour Measurements of Acrylamide-Based Polymers

For the Zimm plots constructed from the light scattering data for the homopolymer and copolymer solution standards from DMAM-co-AM-2 to -7, MeAM-co-AM-2b to -5 (including PAM from control-6), and NTBAM-co-AM-1b (clouded layer), -1b (clear layer), and -2 (dialyzed fraction) polynomial fit degrees of 3 in $\sin^2(\theta)$ and 1 in concentration, c, were selected for the least-squares fit of the light scattering data in extrapolations to zero scattering angle and to zero concentration, respectively. The solution standards used for this were those adjusted to pH 4.00 ± 0.10, pH 6.50 ± 0.20, and pH 10.00 ± 0.10 without added electrolyte and those adjusted to pH 4.00 ± 0.10 and treated with electrolyte to give 0.001 M, 0.01 M, 0.1 M and 1.0 M NaCl. From each Zimm plot the weight average molecular weight, M_w, the root mean squared radius of gyration, $< r_g >$, and the solute / solvent interaction parameter, A_2, were determined. M_w, $< r_g >$, and A_2 were also determined for the Percol 351 under the same solvent conditions as those used for the newly synthesized, acrylamide-based polymers. Only the solvent conditions adjusted to pH 4.00 ± 0.10 and treated with added electrolyte were used for Percol 721 and Percol E-24. Since the refractive index increments, dn/dc, were determined for the solution standards adjusted to pH 4.00 ± 0.10 and pH 6.50 ± 0.20 without added electrolyte and those adjusted to pH 4.00 ± 0.10 and treated with electrolyte to give 0.001 M and 0.01 M NaCl, M_w and A_2 were reported only for these

solvent conditions. The root mean squared radius of gyration, $< r_g >$, was reported for each solvent condition.

3.10.1. Copolymers from DMAM-co-AM-2 to -7 and the homopolymer (PDMAM) from DMAM-co-AM-6

There was reasonable agreement between the M_w's determined from the standard solutions adjusted to pH 4.00 ± 0.10 and pH 6.50 ± 0.20 without added electrolyte and those adjusted to pH 4.00 ± 0.10 and treated with electrolyte to give 0.01 M NaCl (Table 30). The magnitude of the M_w's exceeded 1.0 × E+06 g/mol in every case and approached 20 × E+06 g/mol for the copolymers from DMAM-co-AM-5 and DMAM-co-AM-7. The M_w's of the copolymers increased as the content of DMAM in the copolymers increased except for the copolymer from DMAM-co-AM-7 which gave the highest M_w's.

The trend in M_w as the content of DMAM in the copolymers increased was paralleled by $< r_g >$. The $< r_g >$ values did not vary appreciably for different solvent conditions, except for $< r_g >$ values from standards adjusted to pH 10.00 ± 0.10 which were generally lower than those determined from the other standards. However, $< r_g >$ values determined from standards adjusted to pH 10.00 ± 0.10 for PDMAM from DMAM-co-AM-6 and the copolymer from DMAM-co-AM-3 were consistent with $< r_g >$ values determined from standards having different solvent conditions. The magnitude of $< r_g >$ approached ½ λ_0 (where λ_0 is the wavelength of the incident radiation from the He/Ne laser, 632.8 nm) for the copolymer solution standards from DMAM-co-AM-5 and -7.

Table 30 M_W, $< r_g >$, and A_2 for the copolymers from DMAM-co-AM-2 to -5 and -7 and the homopolymer (PDMAM) from DMAM-co-AM-6

Experiment	Solvent pH	[NaCl] (M)	$M_W \times$ E+06 [a] (g/mol)	$< r_g >$ [b] (nm)	$A_2 \times$ E-04 [c]
DMAM-co-AM-2	4.00 ± 0.10	0	7.48 ± 0.5	198.4 ± 4.9	2.52 ± 0.08
	6.50 ± 0.20	0	8.94 ± 0.4	199.2 ± 4.9	2.32 ± 0.03
	10.00 ± 0.10	0		169.1 ± 4.6	
	4.00 ± 0.10	0.01	6.71 ± 0.3	186.8 ± 5.7	2.08 ± 0.05
	4.00 ± 0.10	0.1		174.9 ± 4.6	
DMAM-co-AM-3	4.00 ± 0.10	0	6.44 ± 0.3	184.9 ± 5.7	2.29 ± 0.04
	6.50 ± 0.20	0	6.98 ± 0.4	170.6 ± 5.7	1.74 ± 0.04
	10.00 ± 0.10	0		171.1 ± 6.1	
	4.00 ± 0.10	0.01	7.03 ± 0.3	178.4 ± 4.5	1.84 ± 0.07
	4.00 ± 0.10	0.1		185.1 ± 4.1	
DMAM-co-AM-4	4.00 ± 0.10	0	10.4 ± 0.09	246.9 ± 10	2.17 ± 0.05
	6.50 ± 0.20	0	12.0 ± 0.09	236.6 ± 6.7	1.94 ± 0.08
	10.00 ± 0.10	0		191.6 ± 6.3	
	4.00 ± 0.10	0.01	13.9 ± 0.1	240.4 ± 12	1.25
	4.00 ± 0.10	0.1		226.4 ± 8.9	
DMAM-co-AM-5	4.00 ± 0.10	0	20.4 ± 0.4	259.8 ± 7.4	1.11
	6.50 ± 0.20	0	20.4 ± 0.1	271.1 ± 8.7	1.24 ± 0.02
	10.00 ± 0.10	0		136.7 ± 4.4	
	4.00 ± 0.10	0.01	15.5 ± 0.2	250.1 ± 10	1.06
	4.00 ± 0.10	0.1		269.8 ± 9.6	
DMAM-co-AM-6	4.00 ± 0.10	0	3.56 ± 0.1	106.0 ± 4.3	2.17 ± 0.04
	6.50 ± 0.20	0	3.99 ± 0.2	118.7 ± 2.7	1.80 ± 0.08
	10.00 ± 0.10	0		113.3 ± 2.3	
	4.00 ± 0.10	0.01	4.04 ± 0.1	122.6 ± 3.3	1.98 ± 0.08
	4.00 ± 0.10	0.1		129.9 ± 3.3	
	4.00 ± 0.10	1.0		111.7 ± 3.2	
DMAM-co-AM-7	4.00 ± 0.10	0	17.3 ± 2.0	285.7 ± 18	1.94 ± 0.07
	6.50 ± 0.20	0	20.8 ± 5.0	227.9 ± 11	1.22
	10.00 ± 0.10	0		221.7 ± 15	
	4.00 ± 0.10	0.01		306.5 ± 22	
	4.00 ± 0.10	0.10		308.5 ± 26	

a. M_W is the weight average molecular weight.
b. $< r_g >$ is the root mean squared radius of gyration.
c. A_2 is the solute / solvent interaction parameter.

Values of the solute / solvent interaction parameter, A_2, are also given in Table 30. The magnitude of A_2 decreased as the content of DMAM in the copolymers increased except for A_2 values of the copolymer from DMAM-co-AM-7 which were lowest. As the solvent conditions were changed from pH 4.00 ± 0.10 without added electrolyte to pH 4.00 ± 0.10 with 0.01 M NaCl A_2 decreased.

3.10.2. Copolymers from MeAM-co-AM-2b to -5 and PAM from control-6

There was reasonable agreement between the M_w's determined from the standard solutions adjusted to pH 4.00 ± 0.10 and pH 6.50 ± 0.20 without added electrolyte and those adjusted to pH 4.00 ± 0.10 and treated with electrolyte to give 0.01 M NaCl (Table 31). M_w values determined for PAM from control-6 (complementary to MeAM-co-AM-6) were greater for the standard solutions adjusted to pH 4.00 ± 0.10 and pH 6.50 ± 0.20 without added electrolyte than those adjusted to pH 4.00 ± 0.10 and treated with electrolyte to give 0.01 M NaCl. The values of M_w decreased as the content of MeAM in the copolymers increased. The copolymer M_w's were approximately 1.0 × E+06 g/mole except for the copolymer from MeAM-co-AM-2b which ranged from 3 × E+06 to 5 × E+06 g/mole.

The values of $< r_g >$ did not vary appreciably for different solvent conditions (Table 31) except for the values of $< r_g >$ for PAM from control-6 which were lower with electrolyte present than without, but increased with increasing electrolyte concentration. Also, PAM solutions adjusted to pH 10.00 ± 0.10 without added electrolyte gave $< r_g >$ values approximately a factor of 2 less than determined for the PAM solutions at pH 4.00

Table 31 M_W, $< r_g >$, and A_2 for the copolymers from MeAM-co-AM-2b to -5 and PAM from control-6

Experiment	Solvent pH	[NaCl] (M)	$M_W \times$ E+06 [a] (g/mol)	$< r_g >$ [b] (nm)	$A_2 \times$ E-04 [c]
MeAM-co-AM-2b	4.00 ± 0.10	0	5.11 ± 0.6	115.1 ± 4.2	1.78 ± 0.07
	6.50 ± 0.20	0	4.57 ± 0.4	105.6 ± 2.1	1.75 ± 0.07
	10.00 ± 0.10	0		116.2 ± 2.2	
	4.00 ± 0.10	0.01	3.21 ± 0.06	101.3 ± 2.5	1.79 ± 0.03
	4.00 ± 0.10	0.1		103.4 ± 3.5	
MeAM-co-AM-3	4.00 ± 0.10	0	1.58 ± 0.06	50.9 ± 3.4	1.38 ± 0.08
	6.50 ± 0.20	0	1.49 ± 0.08	47.5 ± 3.1	1.23 ± 0.1
	10.00 ± 0.10	0		62.5 ± 1.6	
	4.00 ± 0.10	0.01	1.31 ± 0.02	57.8 ± 3.8	1.51 ± 0.02
	4.00 ± 0.10	0.1		65.4 ± 4.2	
MeAM-co-AM-4	4.00 ± 0.10	0	1.55 ± 0.07	31.8 ± 5.4	0.63 ± 0.06
	6.50 ± 0.20	0	1.45 ± 0.08	49.7 ± 7.5	24 ± 1
	10.00 ± 0.10	0		n/m [d]	
	4.00 ± 0.10	0.01	1.75 ± 0.05	49.7 ± 4.6	0.56 ± 0.05
	4.00 ± 0.10	0.1		55.6 ± 3.9	
MeAM-co-AM-5	4.00 ± 0.10	0	0.50 ± 0.06	33.0 ± 3.7	0.28 ± 0.03
	6.50 ± 0.20	0	1.32 ± 0.04	40.5 ± 3.9	0.23 ± 0.04
	10.00 ± 0.10	0		n/m	
	4.00 ± 0.10	0.01	0.87 ± 0.04	38.5 ± 5.8	2.53
	4.00 ± 0.10	0.1		32.6 ± 6.7	
control-6	4.00 ± 0.10	0	16.8 ± 0.8	233.2 ± 7.6	2.06 ± 0.10
	6.50 ± 0.20	0	19.1 ± 0.08	229.4 ± 5.5	2.06 ± 0.07
	10.00 ± 0.10	0		122.0 ± 2.3	
	4.00 ± 0.10	0.001	2.77 ± 0.07	109.8 ± 2.8	2.63 ± 0.08
	4.00 ± 0.10	0.01	6.13 ± 0.3	165.4 ± 4.2	2.12 ± 0.08
	4.00 ± 0.10	0.1		177.3 ± 4.4	
	4.00 ± 0.10	1.0		183.9 ± 4.1	

a. M_W is the weight average molecular weight.
b. $< r_g >$ is the root mean squared radius of gyration.
c. A_2 is the solute / solvent interaction parameter.
d. n/m denotes not measured.

± 0.10 or pH 6.50 ± 0.20 without added electrolyte. Like the trend for M_w values, the values of $< r_g >$ decreased as the content of MeAM in the copolymers increased.

Also included in Table 31 were values for the solute / solvent interaction parameter, A_2. For copolymer solution standards adjusted to pH 4.00 ± 0.10 and pH 6.50 ± 0.20 without added electrolyte the values of A_2 decreased as the content of MeAM in the copolymers increased. The values of A_2 determined for copolymer solution standards with electrolyte decreased as the content of MeAM in the copolymers increased. However, other than the values of A_2 determined for the copolymer from MeAM-co-AM-5, the values of A_2 did not vary appreciably for each copolymer under varied solvent conditions.

3.10.3. Copolymers from NTBAM-co-AM-1b (clouded layer), -1b (clear layer), and -2 (dialyzed fraction)

As shown in Table 32, there was reasonable agreement between the M_w's determined from the standard solutions adjusted to pH 4.00 ± 0.10 and pH 6.50 ± 0.20 without added electrolyte and those adjusted to pH 4.00 ± 0.10 and treated with electrolyte to give 0.01 M NaCl. The M_w's of the copolymer from NTBAM-co-AM-1b (clear layer) were less than those of the copolymer from -1b (clouded layer). As the content of NTBAM in the copolymers increased, the M_w's did not vary appreciably from M_w's of the copolymers having a lower NTBAM content. All M_w's were greater than 1.0 × E+06 g/mol.

The values of $< r_g >$ did not vary appreciably for different solvent conditions, different solvent layers, or different NTBAM content, as found for the M_w's (Table 32).

Table 32 M_W, $< r_g >$, and A_2 for the copolymers from NTBAM-co-AM-1b (clouded layer), -1b (clear layer), and -2 (dialyzed fraction)

Experiment	Solvent pH	[NaCl] (M)	$M_W \times$ E+06 [a] (g/mol)	$< r_g >$ [b] (nm)	$A_2 \times$ E-04 [c]
NTBAM-co-AM-1b	4.00 ± 0.10	0	4.33 ± 0.4	96.4 ± 2.7	1.75 ± 0.06
(clouded layer)	6.50 ± 0.20	0	4.90 ± 0.4	89.4 ± 2.5	1.33 ± 0.04
	10.00 ± 0.10	0		100.7 ± 2.2	
	4.00 ± 0.10	0.01	4.27 ± 0.2	95.6 ± 3.2	1.31 ± 0.05
	4.00 ± 0.10	0.1		102.2 ± 2.6	
NTBAM-co-AM-1b	4.00 ± 0.10	0	2.46 ± 0.2	95.4 ± 2.5	0.76 ± 0.1
(clear layer)	6.50 ± 0.20	0	3.63 ± 0.3	112.8 ± 2.1	0.73 ± 0.06
	10.00 ± 0.10	0		93.7 ± 2.0	
	4.00 ± 0.10	0.01	3.66 ± 0.3	103.1 ± 2.4	0.58 ± 0.09
	4.00 ± 0.10	0.1		107.6 ± 2.6	
NTBAM-co-AM-2	4.00 ± 0.10	0	4.06 ± 0.2	89.6 ± 2.0	0.34 ± 0.03
(dialysis fraction)	6.50 ± 0.20	0	4.39 ± 0.3	96.4 ± 1.5	0.44 ± 0.04
	10.00 ± 0.10	0		8.08 ± 2.6	
	4.00 ± 0.10	0.01	3.79 ± 0.07	96.5 ± 2.5	0.32
	4.00 ± 0.10	0.1		109.0 ± 2.7	

a. M_W is the weight average molecular weight.
b. $< r_g >$ is the root mean squared radius of gyration.
c. A_2 is the solute / solvent interaction parameter.

The values of A_2 determined for NTBAM-co-AM-1b (clear layer) were less than the values of A_2 determined for -1b (clouded layer). As the content of NTBAM in the copolymers increased, the values of A_2 decreased.

3.10.4. Commercial polymers Percol 351, Percol 721, and Percol E-24

There was reasonable agreement between the M_w's determined for Percol 351 under different solvent conditions (Table 33). However, the M_w's determined for Percol 721 were not within the statistical uncertainties of MALLS and the statistical uncertainty corresponding to a particular M_w determined for Percol E-24 was greater than the M_w. There was reasonable agreement between the M_w's determined for Percol 351 and the M_w quoted by Allied Colloids. There was also reasonable agreement between the M_w's determined for Percol 721 and Percol E-24 and the M_w's quoted by Allied Colloids except for the M_w's determined for solutions treated with electrolyte to give 0.001 M NaCl.

The values of $< r_g >$ determined for Percol 351, Percol 721, and Percol E-24 decreased as the electrolyte concentration in the solvent increased (Table 33). All values of $< r_g >$ determined for Percol 721 and the values for $< r_g >$ determined from the solution standards of Percol 351 and Percol E-24 which were adjusted to pH 4.00 ± 0.10 and pH 6.50 ± 0.20 without added electrolyte were near ½ λ_0. The values of $< r_g >$ were greater for cationic PAM (Percol 721) and anionic PAM (Percol E-24) than for nonionic PAM (Percol 351).

The values of A_2 determined for Percol 351 decreased as the electrolyte

Table 33 M_W, $< r_g >$, and A_2 for the commercial polymers Percol 351, Percol 721, and Percol E-24

Experiment	Solvent pH	[NaCl] (M)	$M_W \times$ E+06 [a] (g/mol)	$< r_g >$ [b] (nm)	$A_2 \times$ E-04 [c]
Percol 351	4.00 ± 0.10	0	20.9 ± 4	295.5 ± 12	2.09 ± 0.04
(nonionic PAM)	6.50 ± 0.20	0	19.5 ± 3	278.5 ± 9.7	2.03 ± 0.03
	10.00 ± 0.10	0		291.8 ± 27	
	4.00 ± 0.10	0.001	13.6 ± 2	261.3 ± 11	1.89 ± 0.09
	4.00 ± 0.10	0.01	14.8 ± 3	259.6 ± 9.2	1.69 ± 0.2
	4.00 ± 0.10	0.1		224.2 ± 8.3	
	4.00 ± 0.10	1.0		238.3 ± 8.6	
Percol 721	4.00 ± 0.10	0.001	11.3 ± 6	411.5 ± 30	15.1 ± 0.7
(cationic PAM)	4.00 ± 0.10	0.01	28.1 ± 4	384.9 ± 26	2.45 ± 0.05
	4.00 ± 0.10	0.1		318.4 ± 17	
	4.00 ± 0.10	1.0		333.1 ± 16	
Percol E-24	4.00 ± 0.10	0.001	6.45 ± 10.0	339.6 ± 32	43.3 ± 5
(anionic PAM)	4.00 ± 0.10	0.01	11.4 ± 4	306.4 ± 19	4.82 ± 0.5
	4.00 ± 0.10	0.1		217.3 ± 7.2	
	4.00 ± 0.10	1.0		212.3 ± 6.0	

a. M_W is the weight average molecular weight.
b. $< r_g >$ is the root mean squared radius of gyration.
c. A_2 is the solute / solvent interaction parameter.
d. Molecular weights quoted by Allied Colloids for these materials were Percol 351, 20 million; Percol 721, 20 million; and Percol E-24, 15 million, respectively.

concentration in the solvent was increased (Table 33). Values of A_2 determined for Percol 721 and Percol E-24 were much larger than those for Percol 351. As the concentration of NaCl in the solutions of Percol 721 and Percol E-24 was increased, the values of A_2 decreased.

3.11. Characterization of the Flocculation Test Medium

3.11.1. Measurement of the NaCl concentration in the supernatant of the settled slurry

Using Eq.37 the specific conductance measured for the supernatant of the settled Na-kaolinite was converted to give the following relation for equivalent conductance (Eq. 41).

$$\Lambda = \frac{1000 \times 10.3\ \mu S/cm}{c} = \frac{0.0103\ S/cm}{c} \qquad \text{Eq. 41}$$

where $10.3\ \mu S/cm$ is the specific conductance of the supernatant of the settled Na-kaolinite.

Substituting the above relation for equivalent conductance into the equation for the best straight line calculated from the calibration plot of equivalent conductance versus the square root of concentration for the NaCl standards (see Fig. 14) gave the following cubic equation in concentration, c.

$$c^3 - (1.505 \times 10^{-6})c^2 + (2.106 \times 10^{-11})c - 7.813 \times 10^{-21} = 0 \qquad \text{Eq. 42}$$

Solving the cubic equation for c by using a substitution method outlined in the literature

and then converting equivalents per litre to moles per litre gave the concentration of NaCl in the supernatant of the settled Na-kaolinite as 1.138×10^{-4} M.[88]

3.11.2. Measurement of the surface area of Na-kaolinite

Theory

The surface area of the Na-kaolinite particles was measured from the adsorption isotherm for nitrogen gas on dry Na-kaolinite. The "BET equation" developed by Brunauer, Emmett, and Teller was used to determine the surface area of powdered Na-kaolinite from the adsorption data.[70] The "BET equation" is defined by the following.

$$\frac{x}{n(1-x)} = \frac{1}{cm} + \frac{(c-1)x}{cm} \qquad \text{Eq. 43}$$

where x is the relative vapor pressure p / p_0.

n is the weight of vapor adsorbed at a given vapor pressure.

m is the weight of vapor adsorbed at monolayer coverage.

c is a constant which is related to the energy of adsorption for the first monolayer.

A linear relationship is obtained from a plot of $x / n(1 - x)$ versus x. The weight of vapor at monolayer coverage,m, is determined from the slope of the plot and the constant related to the energy of adsorption for the first monolayer, c, is determined from the intercept by linear regression. Surfaces with known areas were used to calibrate the Digisorb 2600 to yield the surface area covered per molecule of the vapor at monolayer coverage. This calibration factor together with the value for the weight of vapor

adsorbed at monolayer coverage, m, were used to determine the total area per unit weight of Na-kaolinite particles. Since the nitrogen molecules of the nitrogen gas used in the routine BET method do not penetrate between the aluminosilicate layers, the total area per unit weight of clay represents the total external surface area which includes the edge surface area.[70]

Measurement

Linear regression calculated a slope, $m = 0.184548 \pm 0.000965$, an intercept, $c = 0.001543 \pm 0.000141$, and a correlation coefficient, $r = 0.9999$ for the plot of $x / n(1 - x)$ versus x. The BET surface area was calculated as 23.3928 ± 0.1225 m^2/g. The BET surface area of Na-kaolinite for this research was slightly less than 26.8 m^2/g which was reported as the BET surface area of Na-kaolinite of a different origin (Kaolin des Charentes).[89] Both kaolinites were converted from heterionic kaolinite to Na-kaolinite by the same procedure.

3.11.3. Measurement of the isoelectric point of Na-kaolinite

Theory

The isoelectric point in relation to Na-Kaolinite is defined as the pH level at which the mobility of the Na-kaolinite particles in an applied electric field is halted. Alternatively, the isoelectric point may be defined by the zero zeta potential which is related to the mobility of the Na-kaolinite particles by the Helmholtz-Smoluchowski equation.

$$\zeta = \frac{4\pi\mu(V_{particle})}{\varepsilon E_x} \qquad \text{Eq. 44}$$

where ζ is the zeta potential.

μ is the viscosity of the fluid phase.

$V_{particle}$ is the electrophoretic velocity of the colloidal particles.

ε is the permittivity of the fluid phase.

E_x is the intensity of the electric field.

In practice, the electrophoretic mobility of the analyte particles is measured by a microelectrophoresis apparatus in which a voltage is applied across a flat-walled rectangular cell to promote motion of ions to the cathode and anode of the cell. At the stationary plane of the cell whereby the opposing electric and viscous forces acting on the colloid particles are equal, the electrophoretic mobility is measured. The electrophoretic mobility is defined as the electrophoretic velocity at the stationary plane in the cell divided by the electric field gradient at the point of measurement.

With respect to Na-kaolinite, the crystal lattice carries a pH independent, negative charge whereas the particle edges carry a charge which is pH dependent. The electrokinetic properties of Na-kaolinite are determined by the net combination of charges.

Measurements

The isoelectric point of Na-kaolinite was determined by plotting electrophoretic mobility ($cm^2\ s^{-1}\ V^{-1}$) versus solution pH for 50 mg/L, pH adjusted Na-kaolinite

standards. Applied voltages were kept below 60 V to minimize interference due to thermal current induced Brownian motions. In addition, the electric field was kept on for 20 seconds or less and all measurements were performed at 25.0 ± 0.5°C. At zero electrophoretic mobility, the data curve gave a solution pH of 2.7. Typically, the isolectric point of pure Na-kaolinite in deionized water is 3.0.[90-93]

3.12. Flocculation

3.12.1. Effects of polymer dosage, agitation rate, and rate of polymer addition on settling rate using PAM from control-6 (complementary to MeAM-co-AM-6) and 3% Na-kaolinite

The average settling rate (for the individual settling rates between the 290 mL and 90 mL levels) was plotted individually against polymer concentration, agitation rate, and the rate of polymer addition. From the plot of average settling rate versus polymer dosage (Fig. 44), no definitive maximum average settling rate was observed. Instead, the plot showed maxima at polymer dosages of 400, 700, and 1000 ppm (based on the ratio of the dry mass of polymer to dry mass of 3% Na-kaolinite). A maximum average settling rate was determined for a 500 rpm agitation rate from the plot of average settling rate versus impeller speed (Fig. 45). The average settling rate decreased linearly for greater agitation rates. From the plot of average settling rate versus the rate of polymer addition (Fig. 46), a maximum average settling rate was found for the addition of 10 mL of polymer solution (10^{-4} to 10^{-3} g/ml) over 60 seconds.

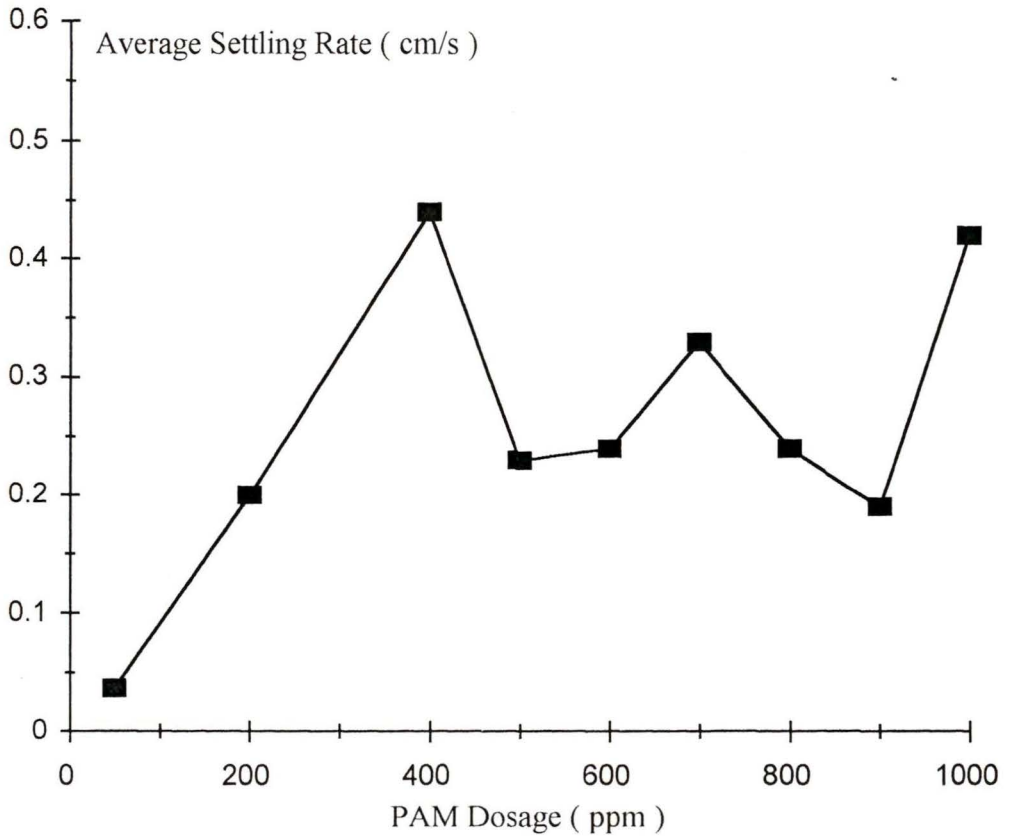

Fig. 44 Average settling rate versus polymer dosage for flocculation of 3% Na-kaolinite using control PAM. Conditions were: 1000 rpm agitation and the addition of 10 mL of control PAM (10^{-4} - 10^{-3} g/mL) over 60 seconds.

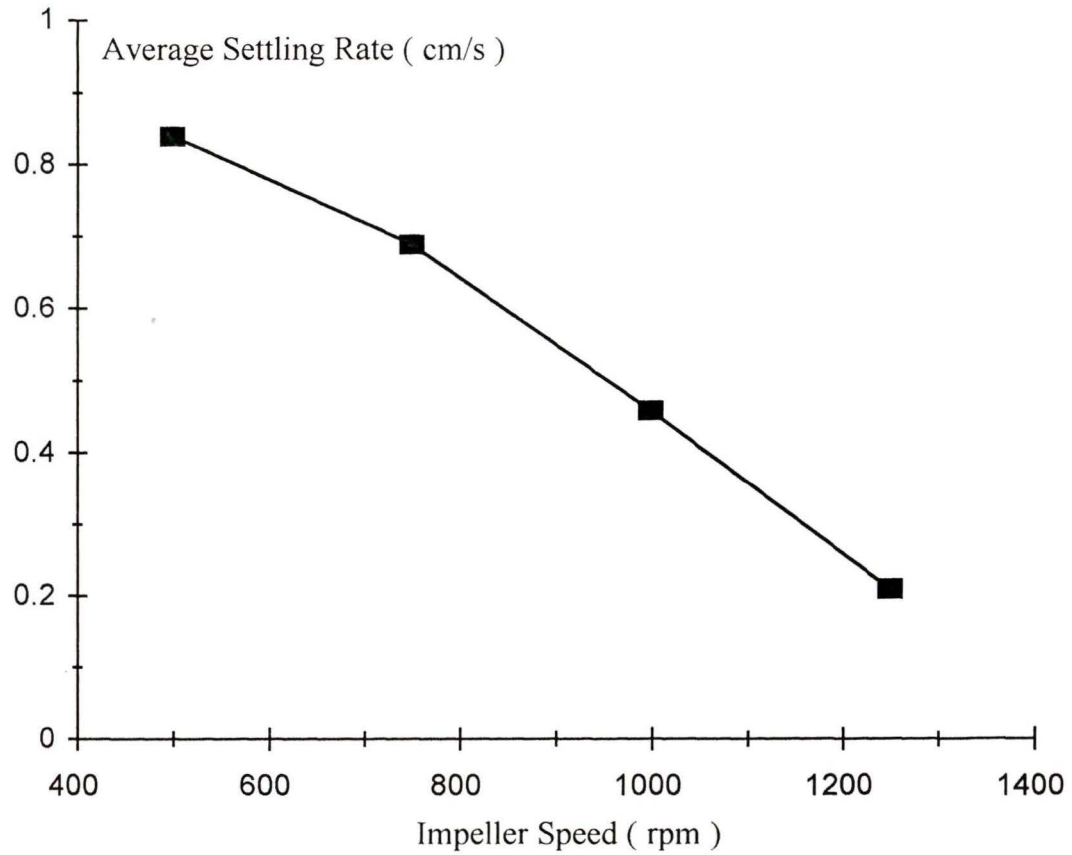

Fig. 45 Average settling rate versus agitation rate for flocculation of 3% Na-kaolinite using control PAM. Conditions were: a polymer concentration of 700 ppm, an agitation duration of 60 seconds, and the addition of 10 mL of polymer solution (10^{-4} - 10^{-3} g/mL) over 60 seconds.

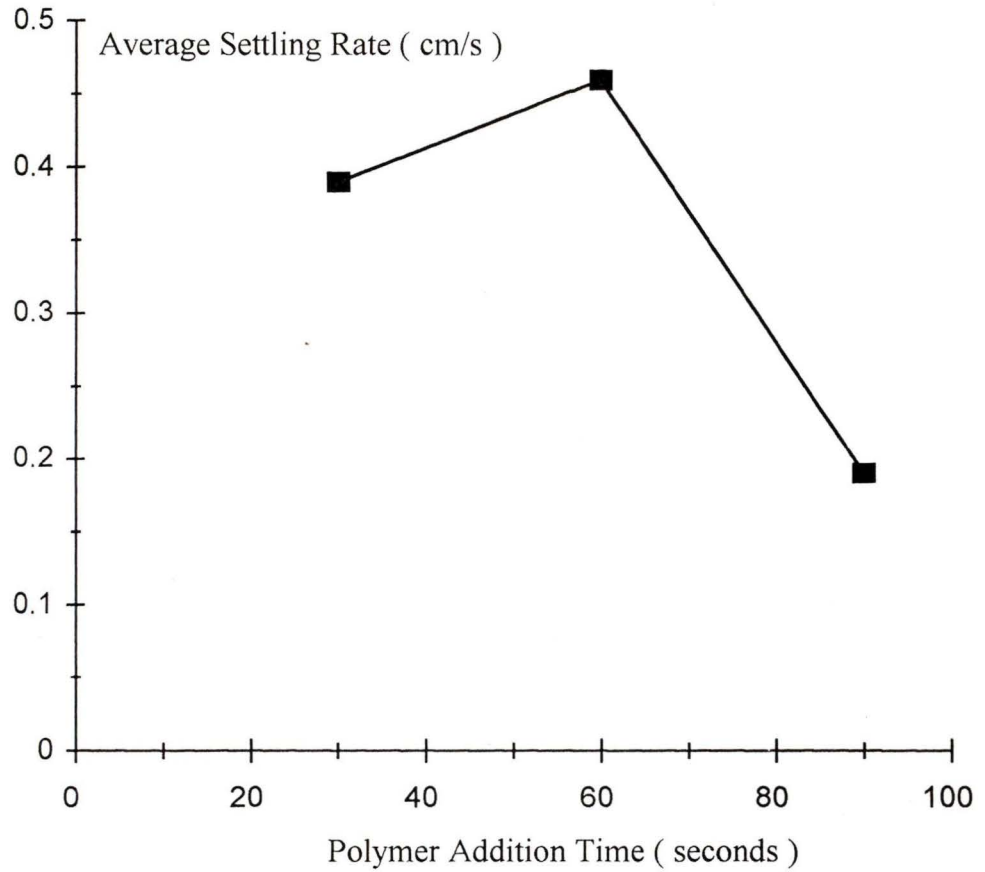

Fig. 46 Average settling rate versus the rate of polymer addition for flocculation of 3% Na-kaolinite using control PAM. Conditions were : 1000 rpm agitation and a polymer concentration of 700ppm.

3.12.2. Comparison of the flocculation performance of copolymers from MeAM-co-AM-2b to -4 and control PAM

The initial average (for individual settling rates between 290 and 250 mL levels), average to compaction (for individual settling rates between 290 and 170 mL levels), and average (for individual settling rates between 290 and 90 mL levels) settling rates for flocculation tests which used the copolymers from MeAM-co-AM-2b to -4 decreased as the content of AM in the copolymer decreased (Table 34). The initial average, average to compaction, and average settling rates determined for the flocculation tests which used PAM from control-6 (complementary to MeAM-co-AM-6) were much greater than those for the copolymers from MeAM-co-AM-2b to -4. In addition, the initial average, average to compaction, and average settling rates for 3% Na-kaolinite without polymer addition were greater than or slightly less than those for flocculation tests which used the copolymers from MeAM-co-AM-3 and -4.

The sediment volume, 30 minute supernatant turbidity, and capillary suction time were also recorded for the flocculation tests. Only the tests which used the copolymer from MeAM-co-AM-2b or PAM gave sediment volumes which were less than that of the flocculation test which used 3% Na-kaolinite without polymer addition. The sediment volume, 30 minute supernatant turbidity, and capillary suction time increased for flocculation tests which used copolymers having a lower content of AM. PAM gave the lowest values for these parameters.

Table 34 Initial average [a], average to compaction [b], and average settling rates [c], as well as sediment volumes, 30 minute supernatant turbidities, and capillary suction times for flocculation of 3% Na-kaolinite using copolymers from MeAM-co-AM-2b to -4 and control PAM. Conditions were : a polymer dosage of 700 ppm, addition of 10 mL of polymer solution over 60 seconds and an agitation rate of 1000 rpm.

Flocculant origin	Feedstock AM content (mole %)	Initial average settling rate (cm/s)	Average to compaction settling rate (cm/s)	Average settling rate (cm/s)	Sediment volume (mL)	Supernatant turbidity 30 minute (NTU)	Capillary suction time (seconds)
3% Na-kaolinite No flocculant	n/a [d]	0.095	0.094	0.086	130	1167	54.7
MeAM-co-AM-2b	80	0.118	0.113	0.102	110	25.5	28.0
MeAM-co-AM-3	60	0.096	0.084	0.079	146	80.3	38.9
MeAM-co-AM-4	40	0.062	0.053	0.053	168	124.2	42.7
control-6	100	0.187	0.174	0.157	102	9.45	27.2

a. Initial average settling rates were measured between 290 mL and 250 mL volume increments.
b. Average to compaction settling rates were measured between 290 mL and 170 mL volume increments.
c. Average settling rates were measured between 290 mL and 90 mL volume increments.
d. n/a denotes not applicable.

3.12.3. Comparison of flocculation of 1% Na-kaolinite by commercial PAM and control PAM

Plots of the initial average (for individual settling rates between 290 and 250 mL levels), average to compaction (for individual settling rates between 290 and 170 mL levels), and average settling rate (for individual settling rates between 290 and 90 mL levels) versus polymer dosage for flocculation tests which used PAM from control-6 (complementary to MeAM-co-AM-6) (5E+06 to 10E+06 MW) and commercial PAM from Polysciences (5E+05 MW) followed similar trends (Fig. 47, 48, and 49). The initial average, average to compaction, and average settling rates showed the greatest increase between 0 and 100 ppm polymer dosages. This increase was much greater for the flocculation tests which used control PAM than those using commercial PAM. For the flocculation tests which used control PAM the intial average, average to compaction, and average settling rates all decreased significantly for polymer dosages between 100 ppm and 200 ppm and did not vary significantly for higher dosages. The settling performance of commercial PAM increased slightly for polymer dosages between 100 ppm and 500 ppm and then levelled off.

There was negligible difference between the polymers in the 30 minute sediment volume versus polymer dosages test (Fig. 50). However, control PAM produced 30 minute supernatant turbidities significantly lower than commercial PAM at lower polymer dosages (Fig. 51) and levelled off to a near constant value at lower polymer dosages than commercial PAM. Commercial PAM gave a slight increase in the average capillary suction time as the polymer dosage increased, whereas control PAM gave a

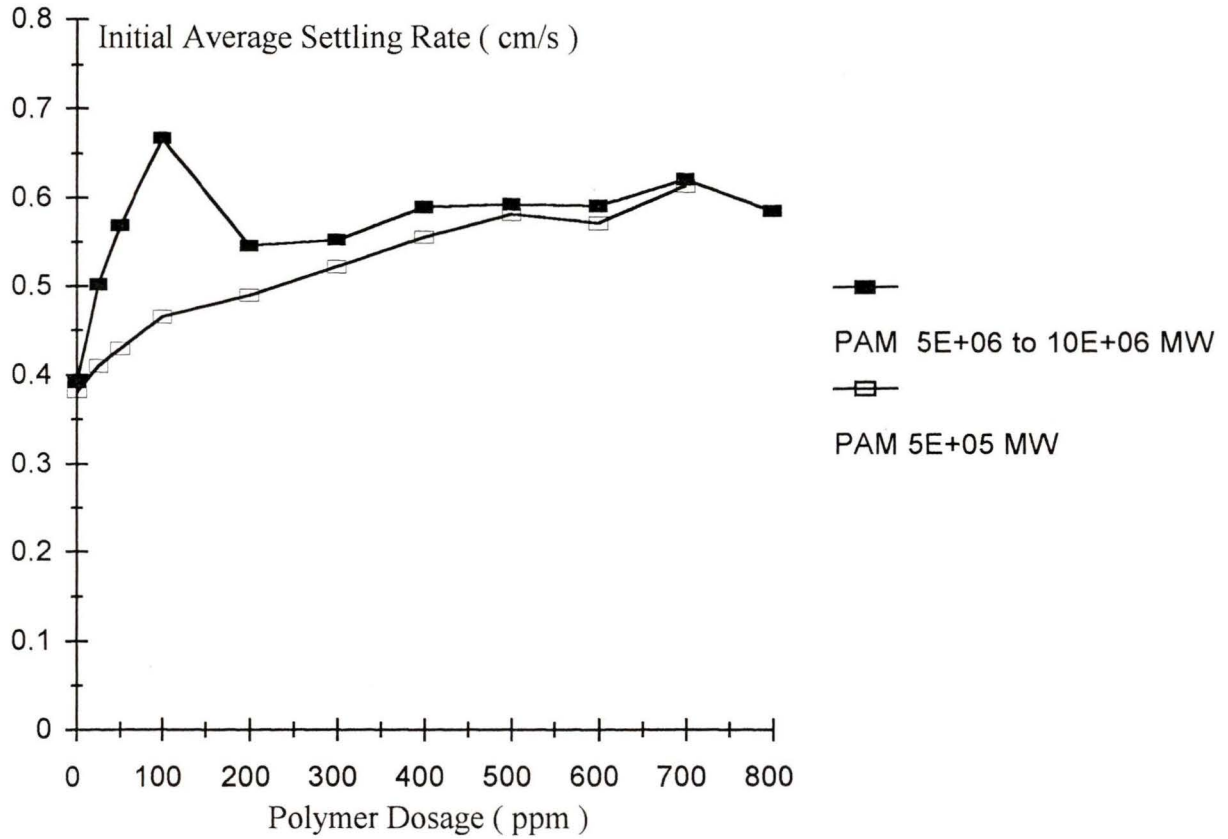

Fig. 47 Initial average settling rate (for individual settling rates between 290 and 250 mL levels) versus polymer dosage for flocculation of 3% Na-kaolinite using PAM (5E+05 MW, Polysciences) and control PAM (5E+06 to 10E+06 MW). Conditions were : 1000 rpm agitation and addition of 10 mL of polymer solution (10^{-4} to 10^{-3} g/mL) over 60 seconds.

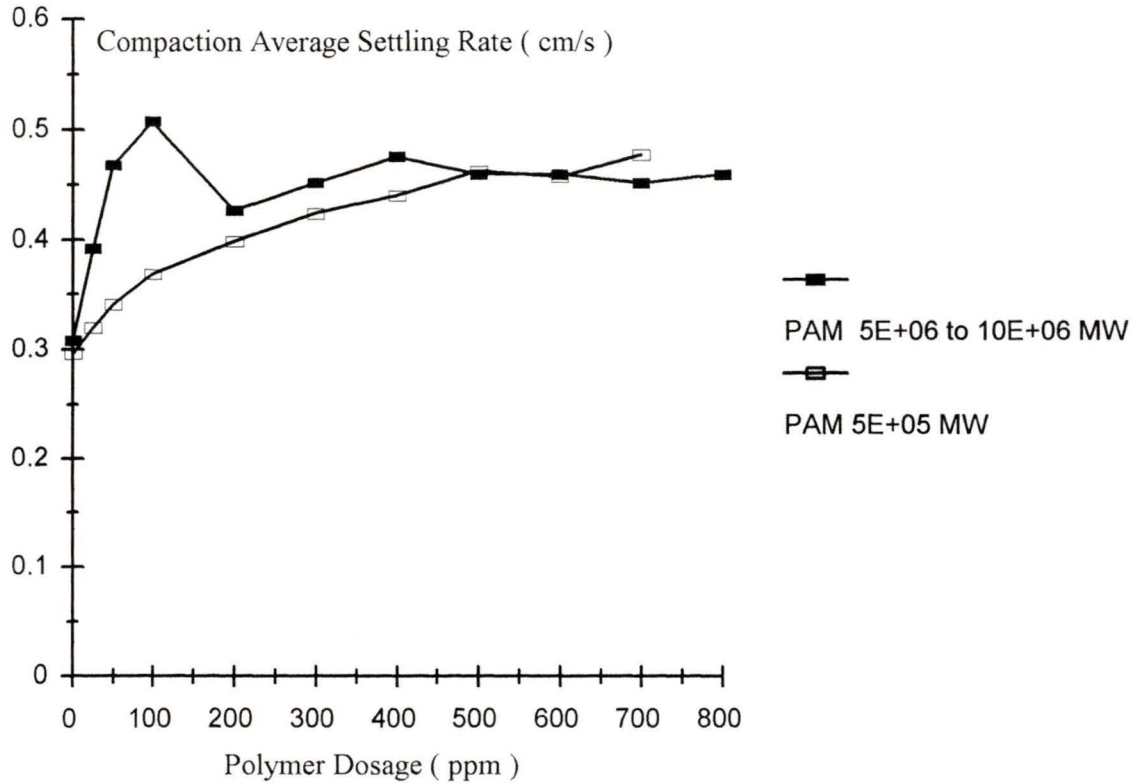

Fig. 48 Average settling rate to compaction (for individual settling rates between 290 and 170 mL levels) versus polymer dosage for flocculation tests which used a 3% Na-kaolinite test medium at neutral pH and individually, PAM (5E+05 MW, Polysciences) and the control homopolymer (PAM, 5E+06 - 10E+06 MW) complementary to MeAM-co-AM-6. Conditions were : 1000 rpm agitation and addition of 10 mLs of polymer solution (10^{-4} to 10^{-3} g/mL) over 60 seconds

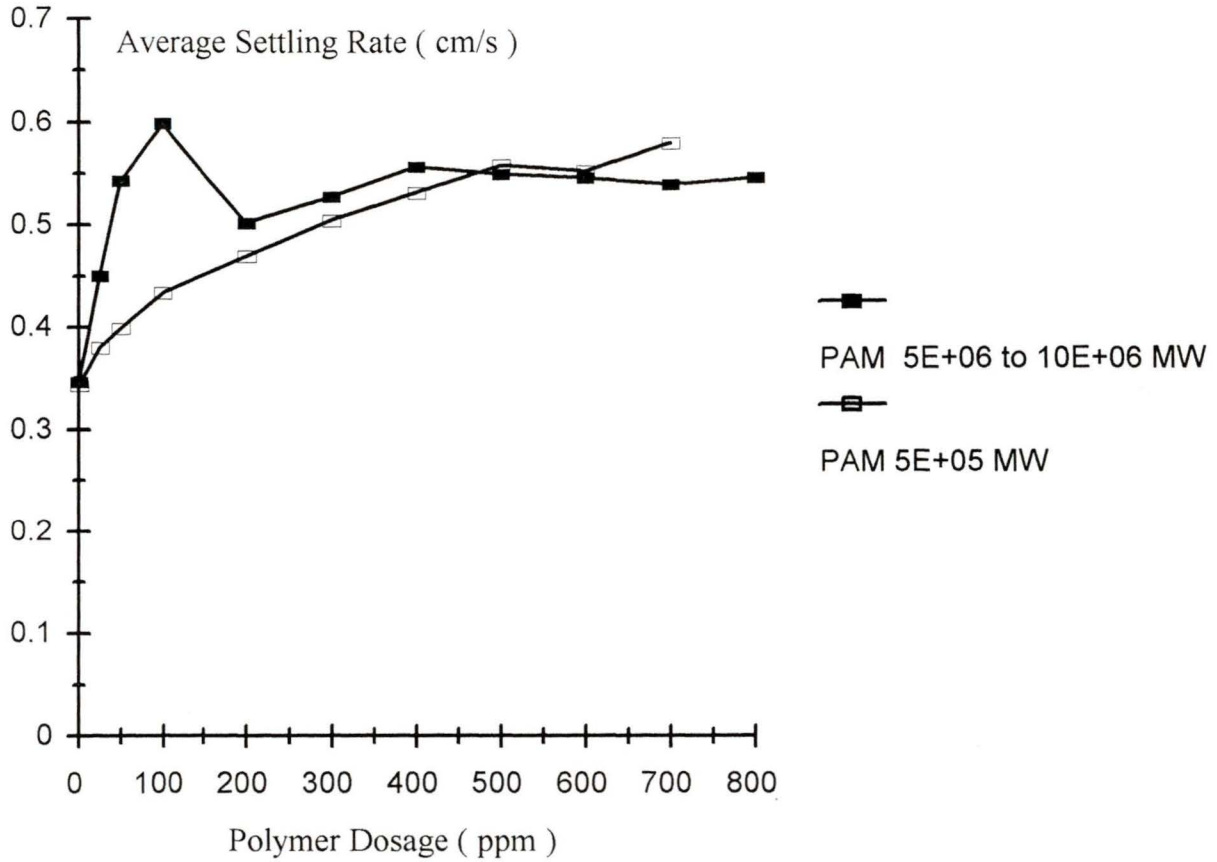

Fig. 49 Average settling rate (for individual settling rates between 290 and 90 mL levels) versus polymer dosage for flocculation of 3% Na-kaolinite using PAM (5E+05 MW, Polysciences) or control PAM (5E+06 - 10E+06 MW). Conditions were : 1000 rpm agitation and addition of 10 mL of polymer solution (10^{-4} to 10^{-3} g/mL) over 60 seconds.

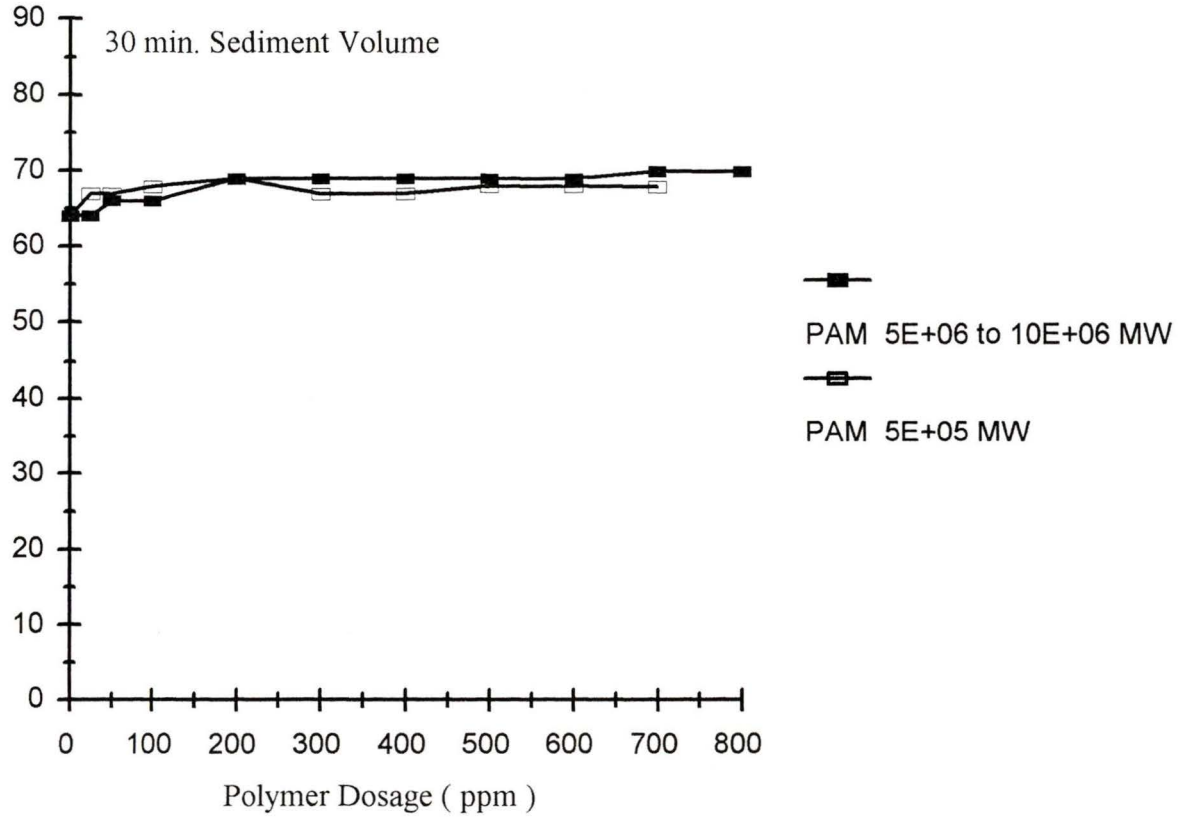

Fig. 50 Sediment volume versus polymer dosage for flocculation of 3% Na-kaolinite using control PAM (5E+06 - 10E+06 MW) or PAM (5E+05 MW, Polysciences). Conditions were : 1000 rpm agitation and addition of 10 mL of polymer solution over 60 seconds.

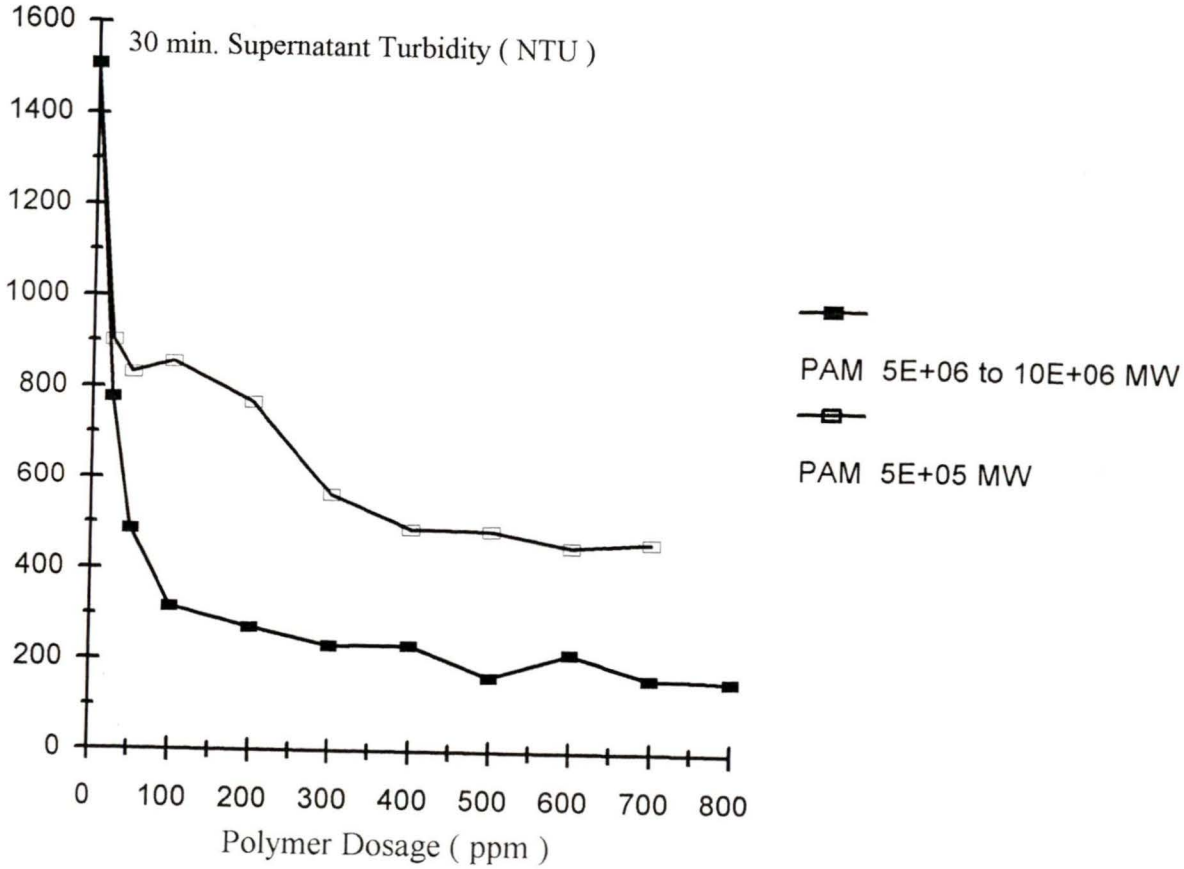

Fig. 51 Supernatant turbidity (30 minute measurements) versus polymer dosage for flocculation of 3%Na-kaolinite using control PAM (5E+06 - 10E+06 MW) or PAM (5E+05 MW, Polysciences). Conditions were : 1000 rpm agitation and addition of 10 mL of polymer solution over 60 seconds.

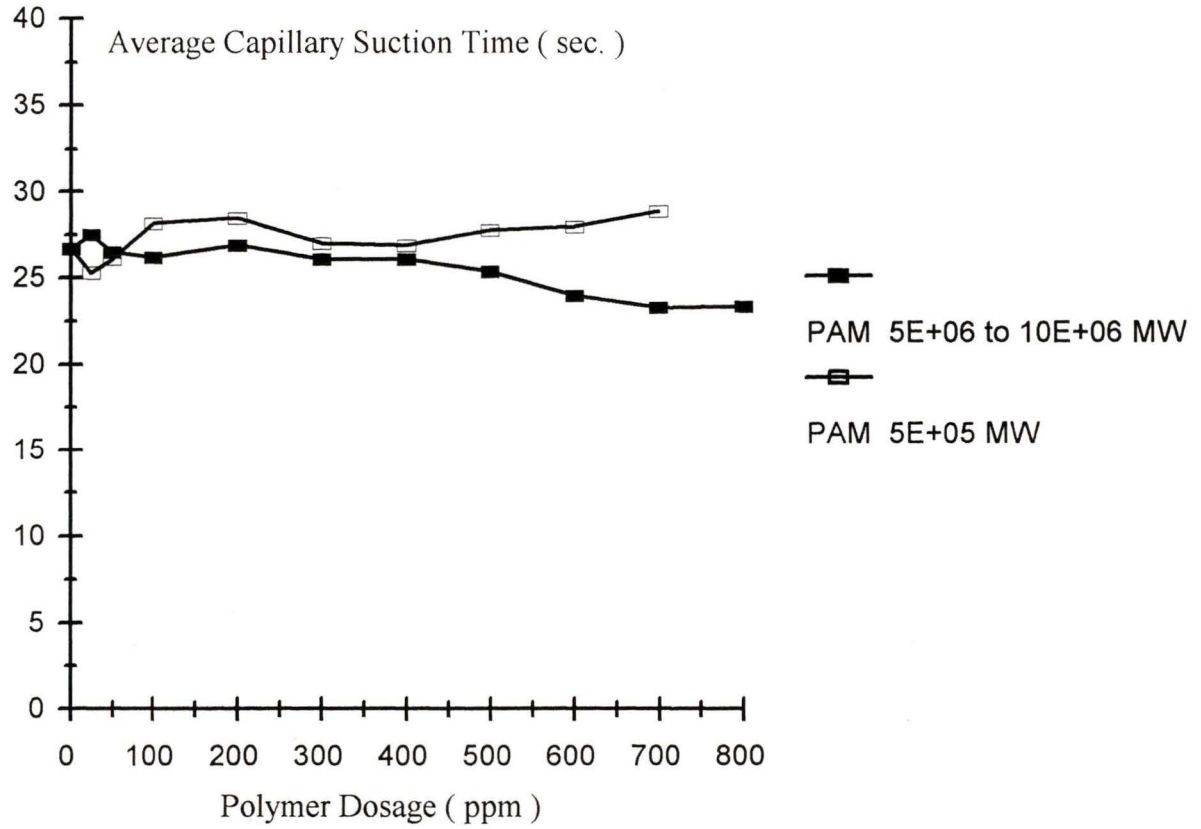

Fig. 52 Average capillary suction time versus polymer dosage for flocculation of 3%Na-kaolinite using control PAM 5E+06 - 10E+06 MW) or PAM (5E+05 MW, Polysciences). Conditions were : 1000 rpm agitation and addition of 10 mL of polymer solution over 60 seconds.

slight decrease in the average capillary suction time as polymer dosage increased (Fig. 52).

3.12.4. Evaluation of flocculation of 1% Na-kaolinite using 25, 50, and 100 ppm of control PAM

Flocculation experiments which used 1000 rpm agitation gave the highest average settling rates when agitation rates of 750, 1000, and 1250 rpm were tested (Fig. 53). The average settling rates increased with polymer dosage for dosages between 0 and 100 ppm for all three agitation rates tested. Agitation at 1000 rpm also gave the lowest 30 minute supernatant turbidities (Fig. 54).

For flocculation tests of polymer addition rates of 10 mL over 30, 60, and 90 seconds, polymer addition at 10 mL over 60 seconds gave the highest average settling rates (Fig. 55) and the lowest supernatant turbidities (Fig. 56). For all three polymer addition rates, the average settling rates increased for polymer dosages between 0 and 100 ppm.

3.12.5. Flocculation of 1% Na-kaolinite using 25, 50, and 100 ppm dosages of newly synthesized, acrylamide-based polymers and commercial polymers

Average settling rates between the 290 mL and 90 mL levels and 30 minute supernatant turbidities were used to evaluate the flocculation performance by the newly synthesized and commercial, acrylamide-based polymers for polymer dosages of 0, 25, 50, and 100 ppm.

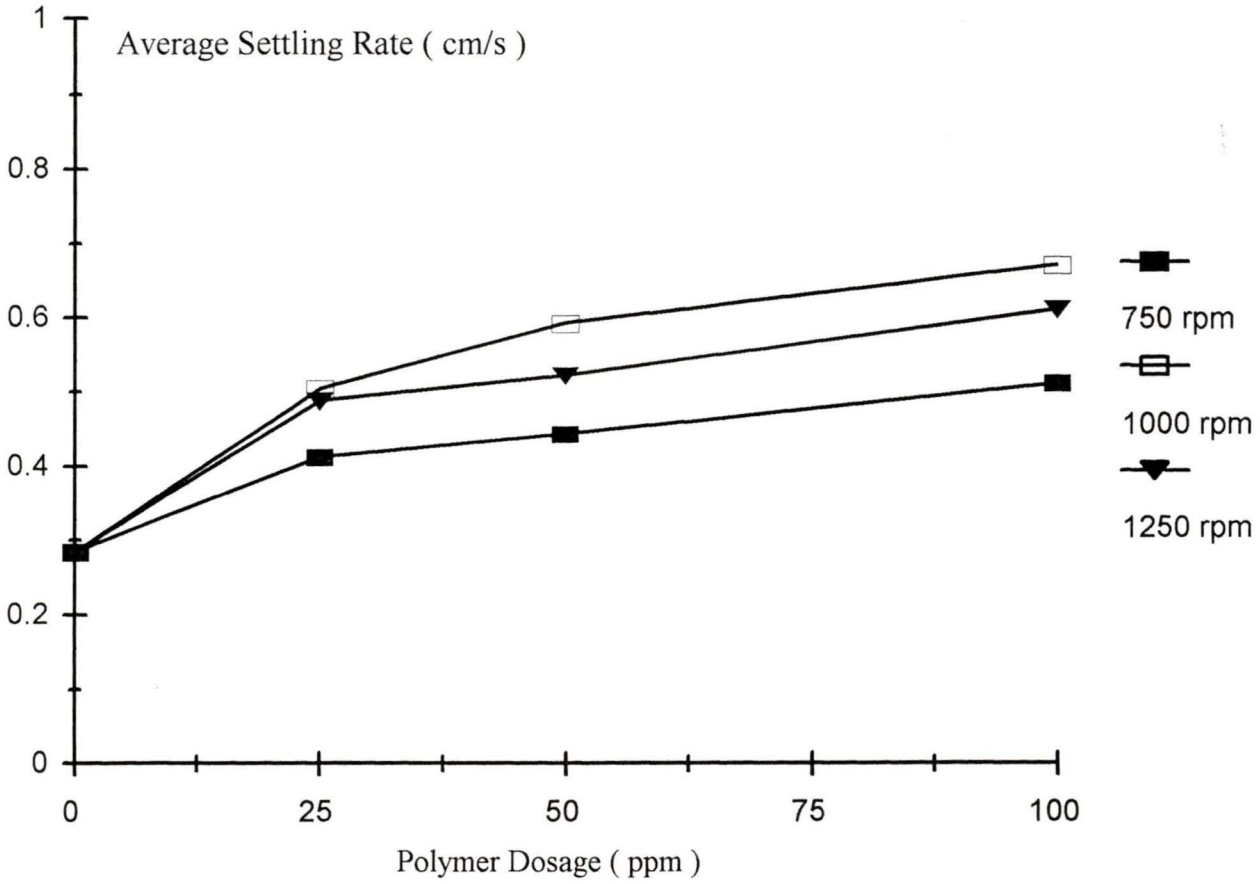

Fig. 53 Average settling rate versus polymer dosage for flocculation of 1% Na-kaolinite using control PAM. Conditions were : polymer dosages of 25, 50, and 100 ppm, agitation rates of 750, 1000, 1250 rpm, and a polymer solution addition rate of 10 mL per 60 seconds.

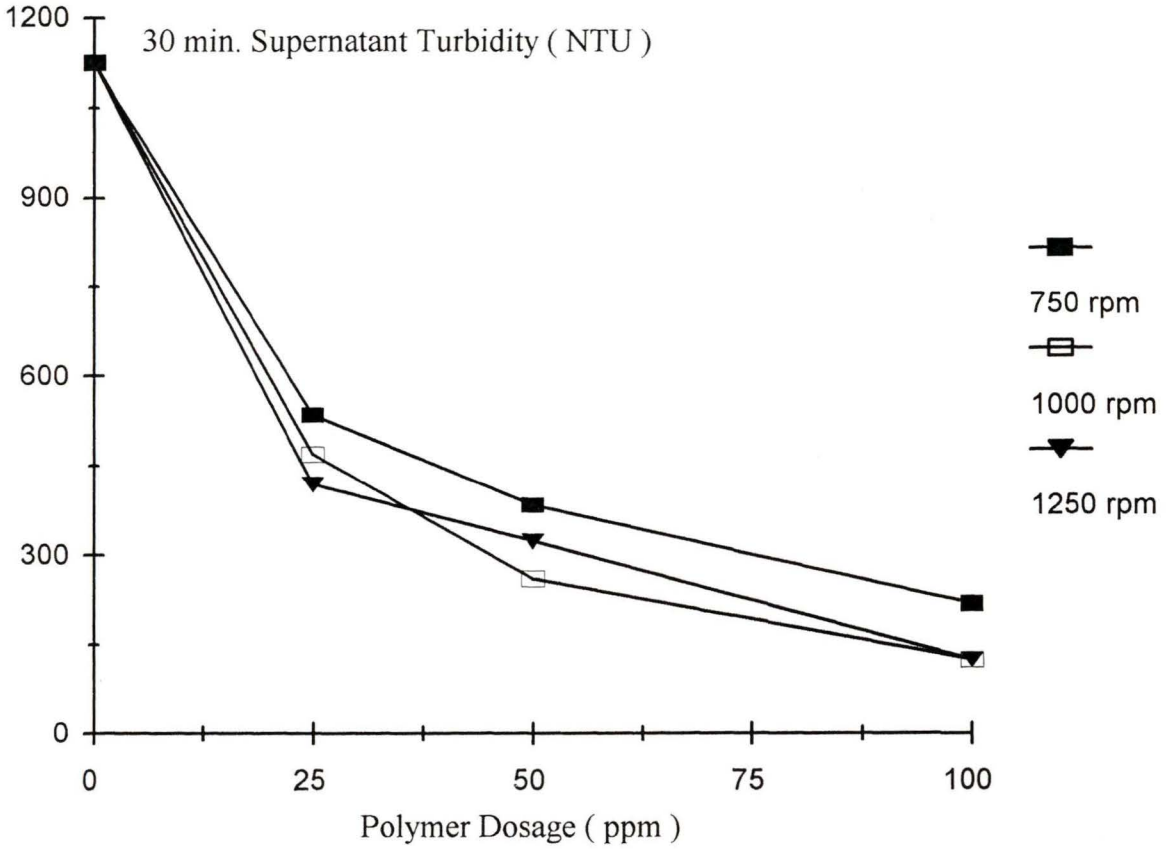

Fig. 54 30 minute supernatant turbidity versus polymer dosage for flocculation of 1% Na-kaolinite using control PAM. Conditions were : polymer dosages of 25, 50, and 100 ppm, agitation rates of 750, 1000, and 1250 rpm, and a polymer solution addition rate of 10 mL per 60 seconds.

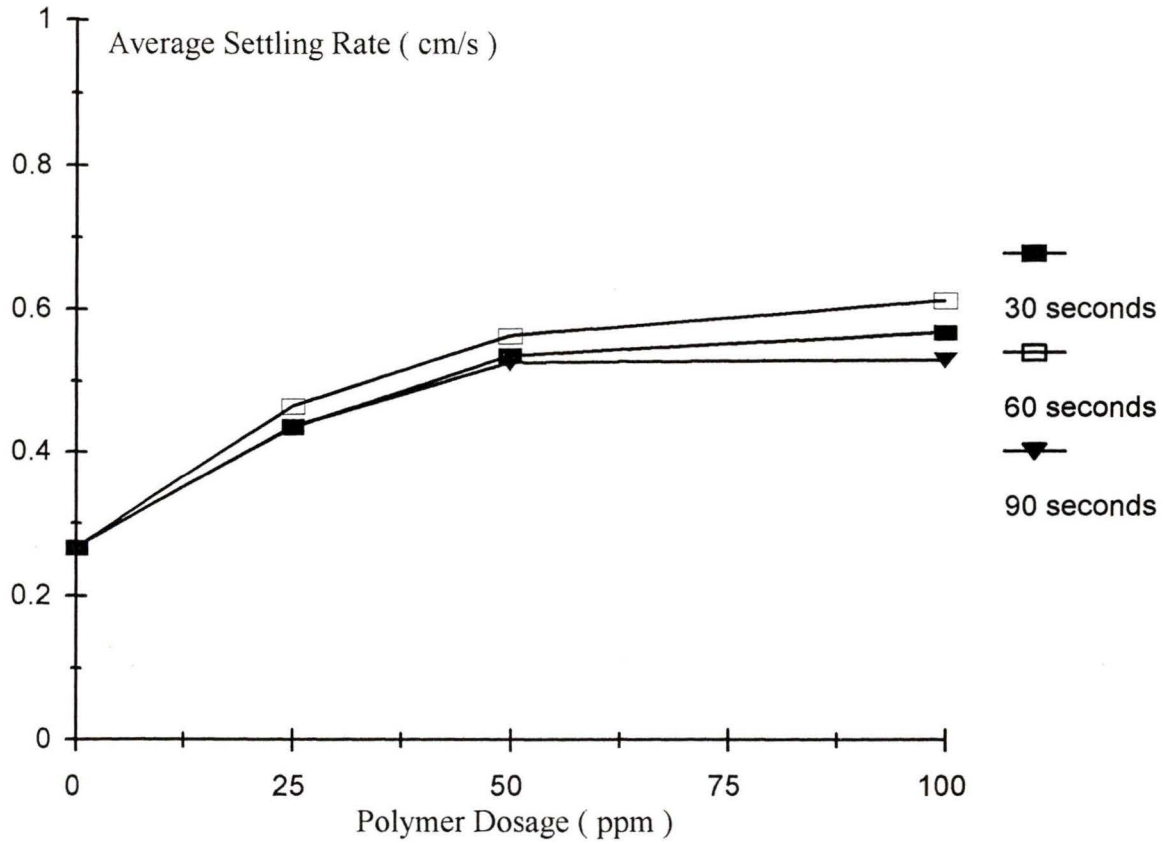

Fig. 55 Average settling rate versus polymer dosage for flocculation of 1% Na-kaolinite using control PAM. Conditions were : polymer dosages of 25, 50, and 100 ppm, an agitation rate of 1000 rpm, and polymer solution addition rates of 10 mL over 30 seconds, 60 seconds, and 90 seconds.

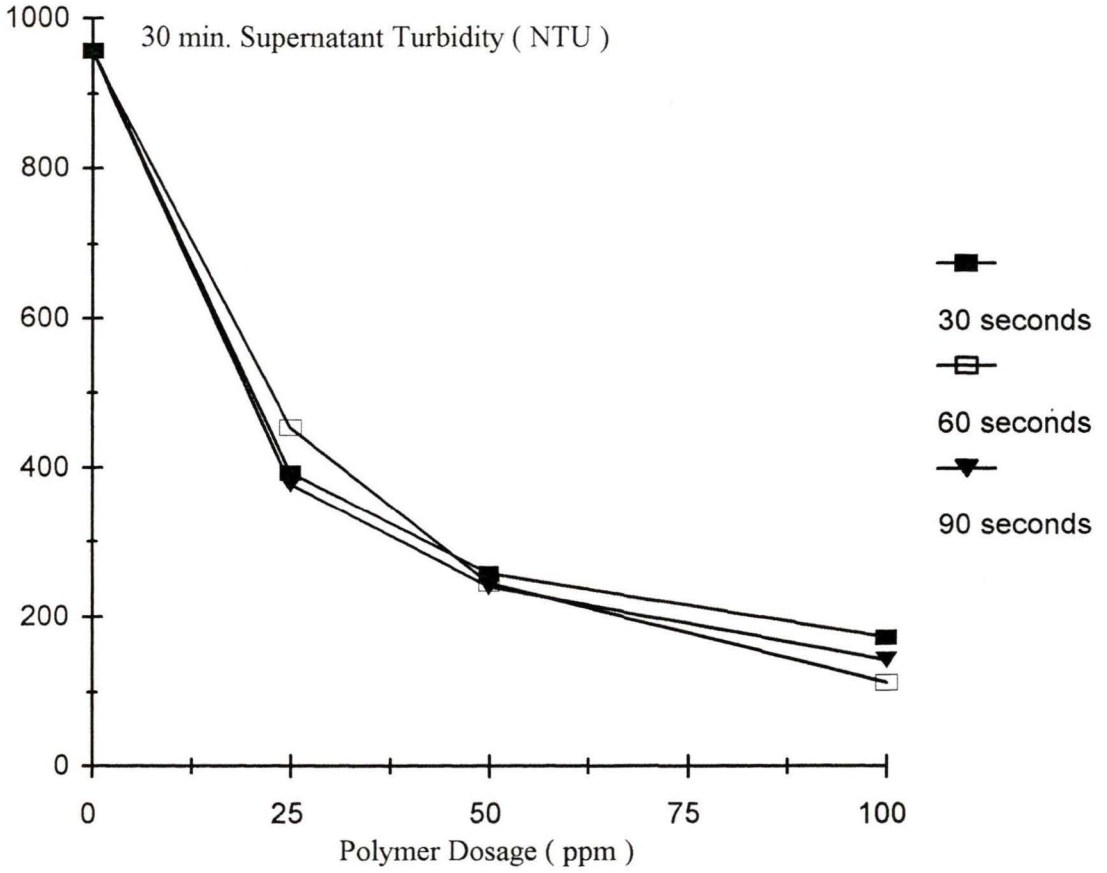

Fig. 56 30 minute supernatant turbidity versus polymer dosage for flocculation of 1% Na-kaolinite using control PAM. Conditions were : polymer dosages of 25, 50, and 100 ppm, an agitation rate of 1000 rpm, and polymer solution addition rates of 10 mL over 30, 60, and 90 seconds.

Copolymers from DMAM-co-AM-3 to -5 and control PAM

Low solubility of the copolymer from DMAM-co-AM-2 and the homopolymer (PDMAM) from DMAM-co-AM-6 limited flocculation test-work to the copolymers from DMAM-co-AM-3 to -5. The copolymer from DMAM-co-AM-7 was not included in the flocculation test-work as its synthesis was done at a later date.

The average settling rates for flocculation tests which used the copolymers from DMAM-co-AM-3 to -5 were greater than those for PAM from control-6 (complementary to DMAM-co-AM-6) (Fig. 57). In addition, the average settling rates decreased as the content of DMAM in the copolymers increased.

Thirty minute supernatant turbidities for flocculation tests which used the copolymers from DMAM-co-AM-3 to -5 were lower than those for PAM (Fig. 58). Also, the supernatant turbidities decreased as the content of DMAM in the copolymer decreased.

Copolymers from MeAM-co-AM-2b to -5 and control PAM

The average settling rates for flocculation tests which used the copolymers from MeAM-co-AM-2b to -5 were less than those of PAM from control-6 (complementary to MeAM-co-AM-6) and decreased as the content of MeAM in the copolymers increased (Fig. 59).

Lower 30 minute supernatant turbidities were obtained for PAM than for tests which used the copolymers from MeAM-co-AM-2b to -5 (Fig. 60). The supernatant turbidities also decreased as the content of MeAM in the copolymers decreased.

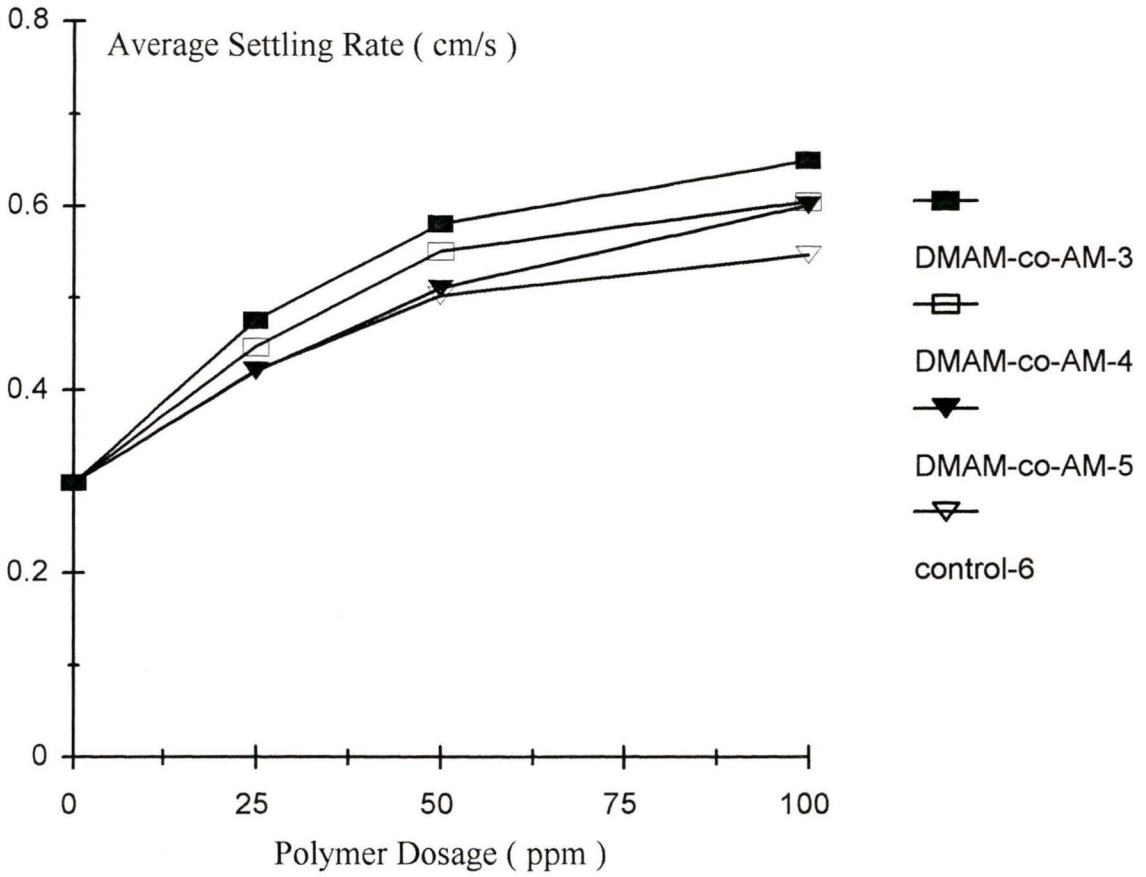

Fig. 57 Average settling rate versus polymer dosage for flocculation of 1% Na-kaolinite using 25, 50, and 100 ppm polymer dosages of the copolymers from DMAM-co-AM-3 to -5 and PAM from control-6. Conditions were : 1000 rpm agitation and addition of 10 mL of polymer solution over 60 seconds.

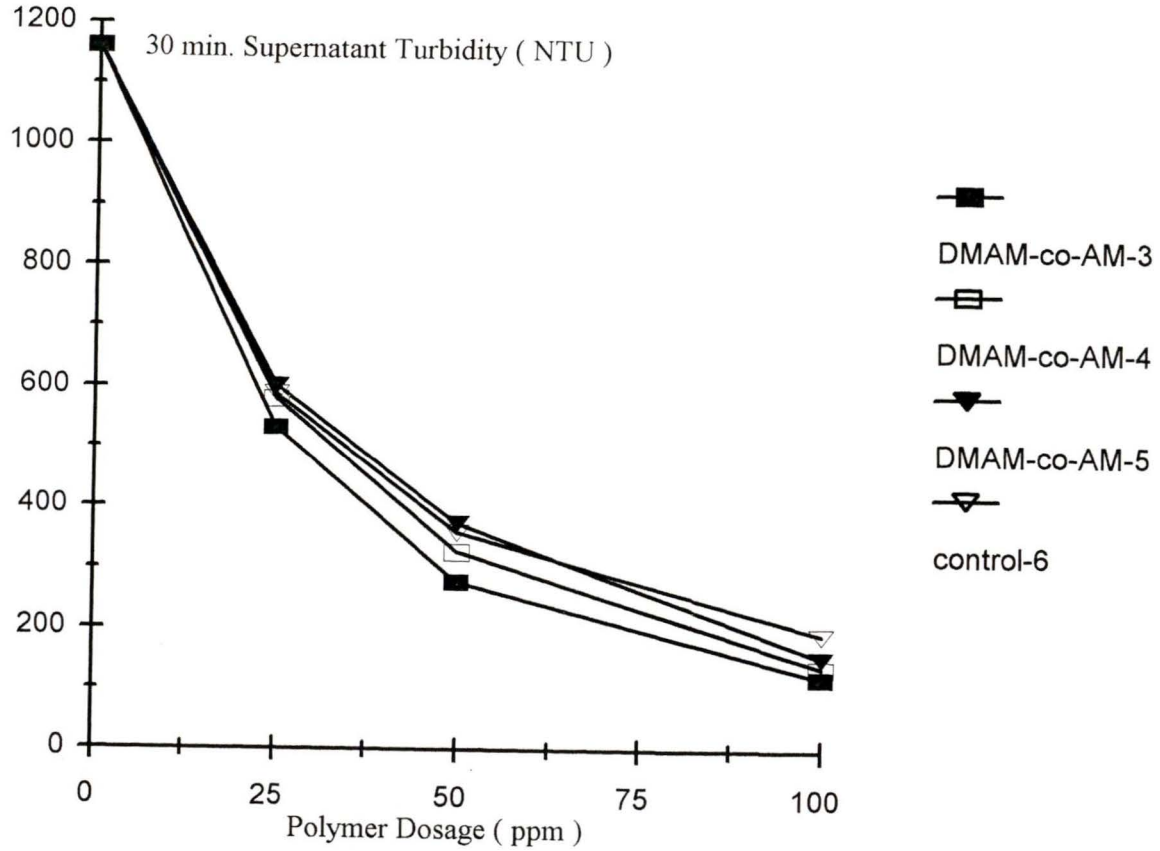

Fig. 58 30 minute supernatant turbidity versus polymer dosage for flocculation of 1% Na-kaolinite using 25, 50, and 100 ppm polymer dosages of the copolymers from DMAM-co-AM-3 to -5 and PAM from control-6. Conditions were : 1000 rpm agitation and addition of 10 mL of polymer solution over 60 seconds.

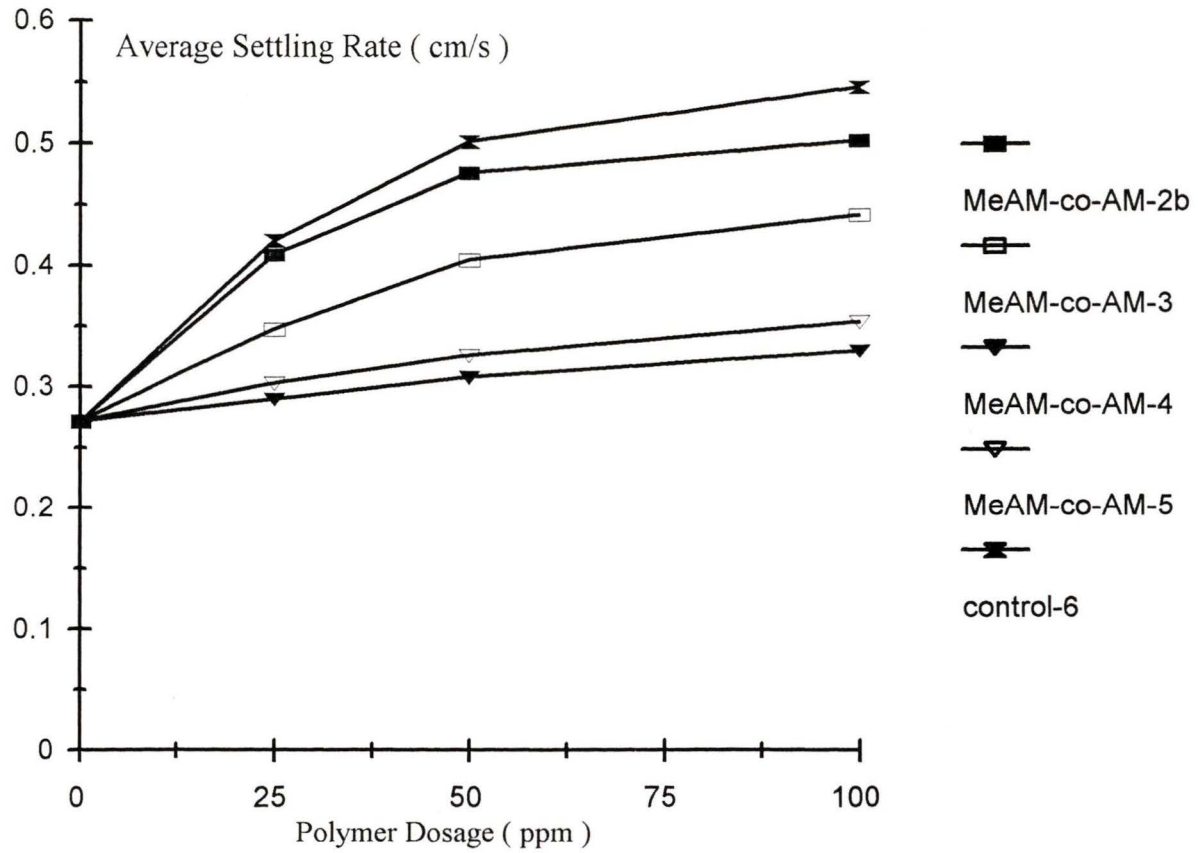

Fig. 59 Average settling rate (for individual settling rates between 290 and 90 mL levels) versus polymer dosage for flocculation of 1% Na-kaolinite using 25, 50, and 100 ppm polymer dosages of the copolymers from MeAM-co-AM-2b to -5 and PAM from control-6.

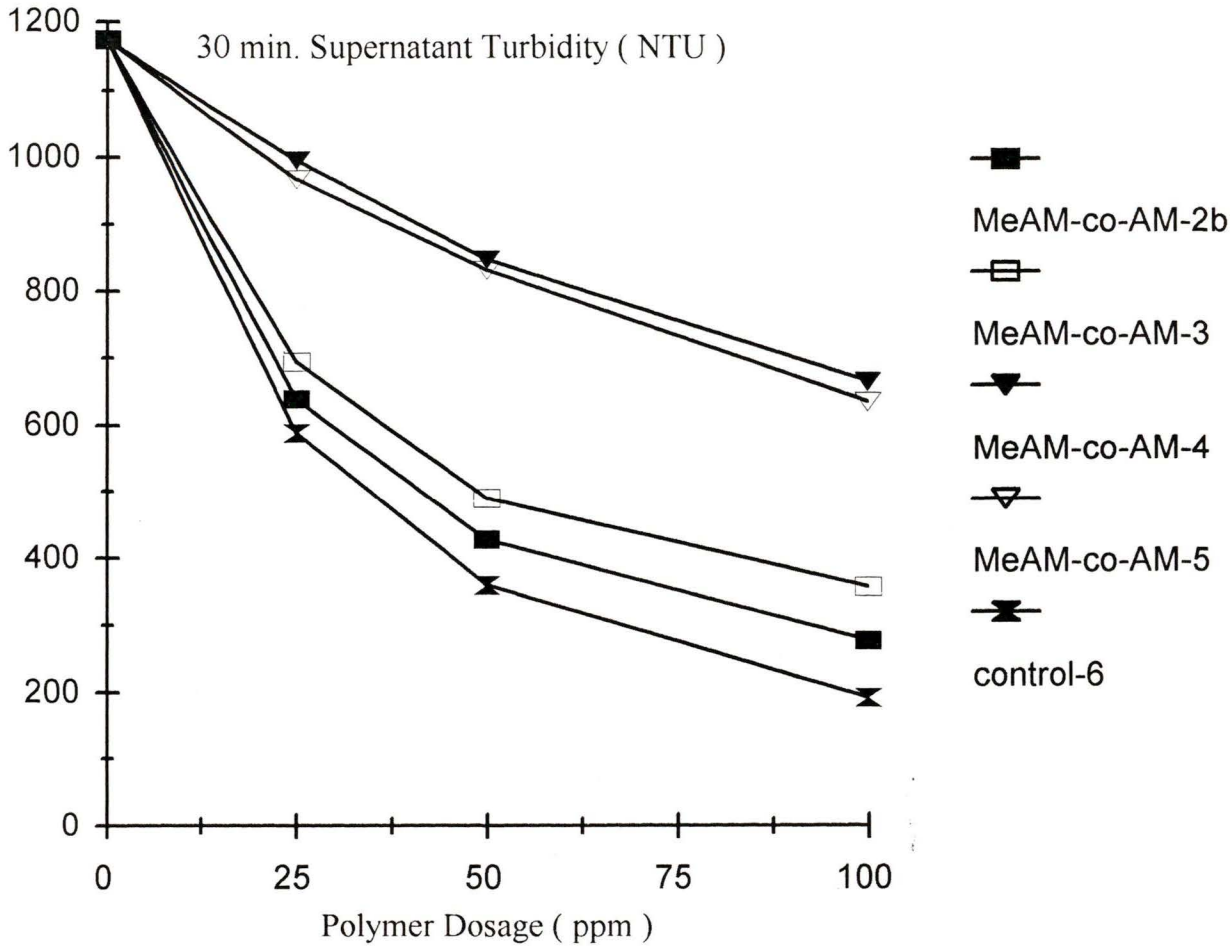

Fig. 60 30 minute supernatant turbidity versus polymer dosage for flocculation of 1% Na-kaolinite using 25, 50, and 100 ppm polymer dosages of the copolymers from MeAM-co-AM-2b to -5 and PAM from control-6.

Copolymers from NTBAM-co-AM-1b (clouded layer), -1b (clear layer), -2 (dialyzed fraction), and control PAM

The copolymers from NTBAM-co-AM-1b (clouded layer), -1b (clear layer), and -2 (dialysis fraction) gave lower average settling rates (Fig. 61) and higher supernatant turbidities (Fig. 62) than PAM from control-6 (complementary to MeAM-co-AM-6). The average settling rates decreased and the supernatant turbidities increased as the content of NTBAM in the copolymers increased.

Purified cationic derivatives of the copolymers from DMAM-co-AM-7, MeAM-co-AM-2b, NTBAM-co-AM-1b (clouded layer), and control PAM

The flocculation tests which used the purified cationic derivative of the copolymer from DMAM-co-AM-7 gave the highest average settling rates of the tests which used the newly synthesized, cationic derivatives (Fig. 63). The average settling rates for a 100 ppm dosage of the nonionic copolymers were greater than the average settling rates for 100 ppm dosages of the cationic derivatives of these polymers, except for the cationic derivative of MeAM-co-AM-2b and its nonionic precursor. Also, the average settling rates for the nonionic PAM from control-6 (complementary to MeAM-co-AM-6) were greater than the average settling rates any of the new cationic derivatives.

For flocculation tests which used individually the newly synthesized, cationic derivatives and their corresponding nonionic polymers, 30 minute supernatant turbidities which exceeded the 2000 NTU limit of the turbidimeter were brought to within the 0 to 2000 NTU range by diluting the 20 mL aliquot of the supernatant taken for measurement, with deionized water. The equivalent turbidities of the undiluted supernatant were

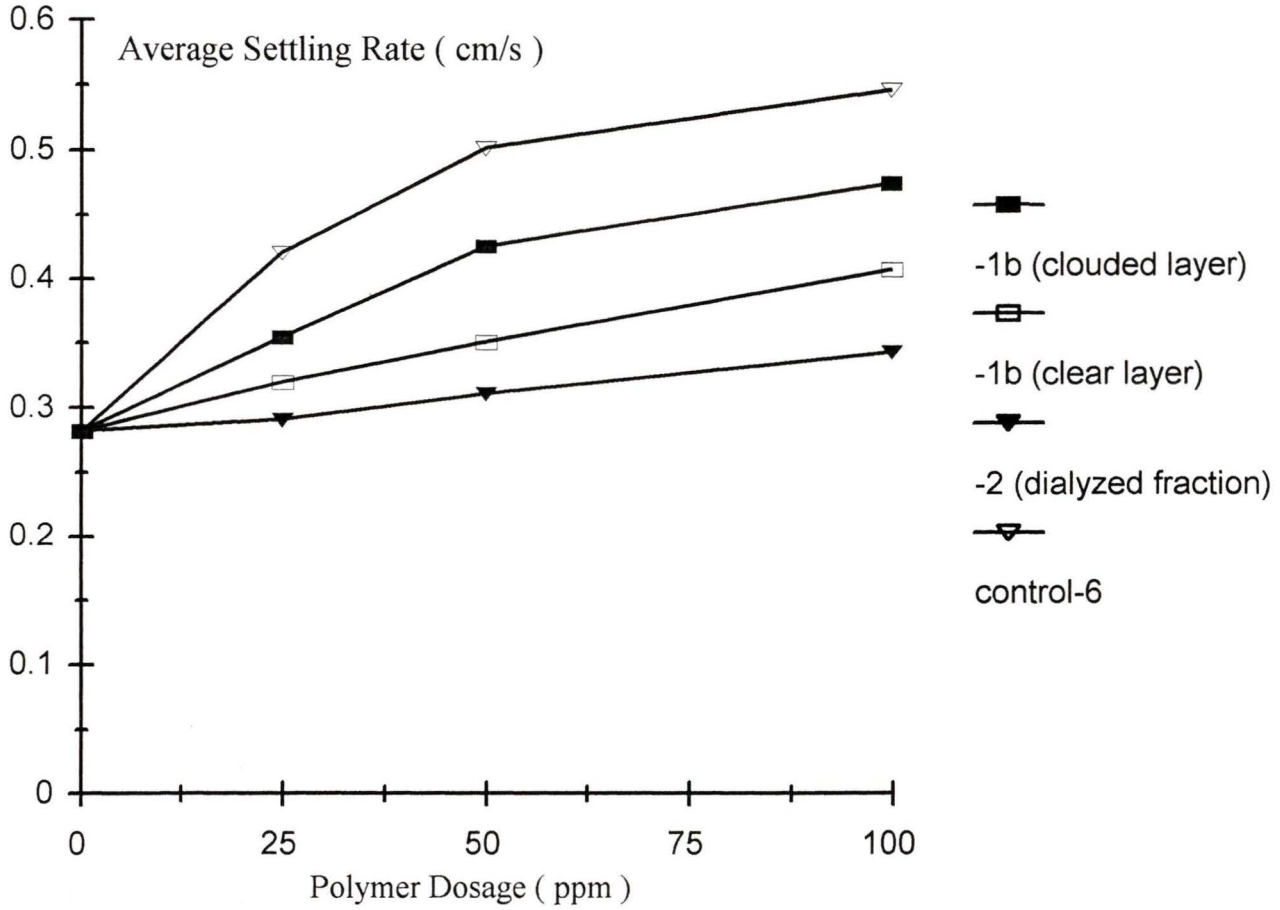

Fig. 61 Average settling rate versus polymer dosage for flocculation of 1% Na-kaolinite using 25, 50, and 100 ppm polymer dosages of the copolymers from NTBAM-co-AM-1b (clouded layer), -1b (clear layer) and -2 (dialyzed fraction) and control PAM. Conditions were : 1000 rpm agitation and addition of 10 mL of polymer solution over 60 seconds.

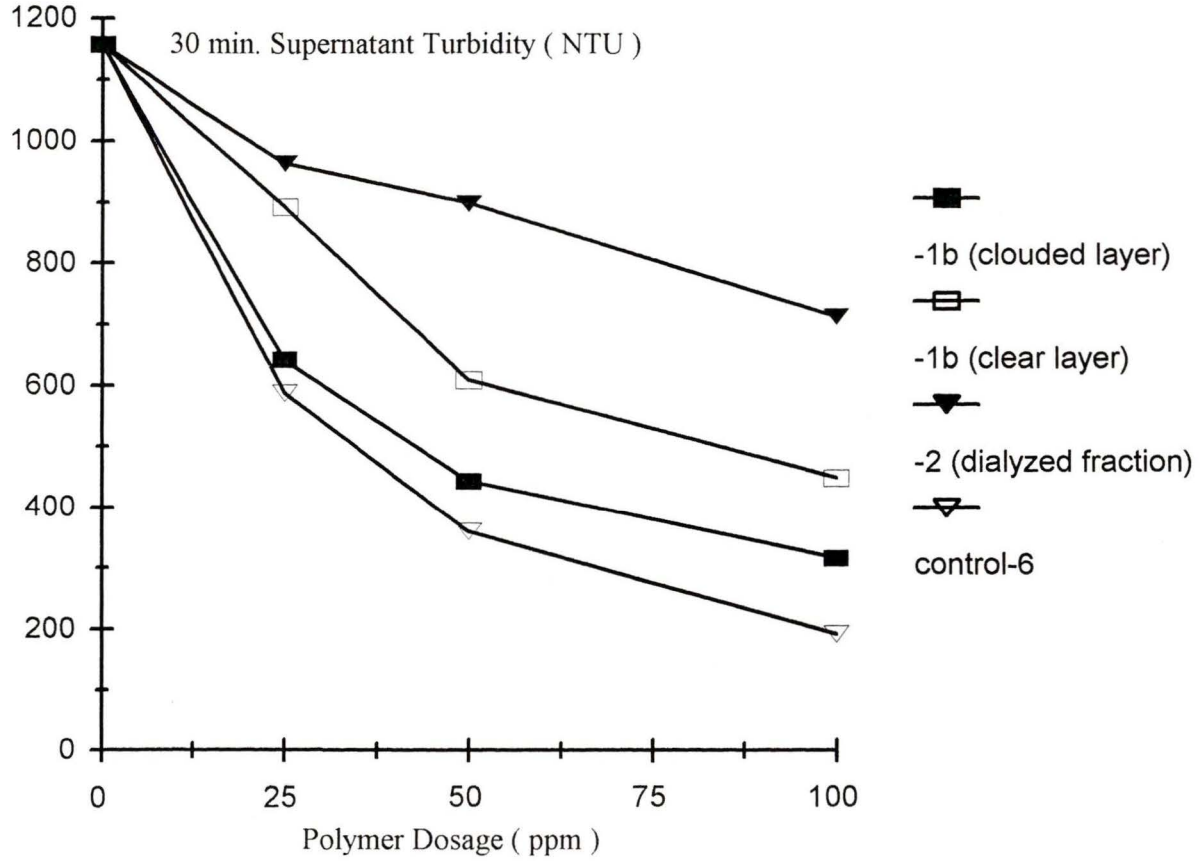

Fig. 62 30 minute supernatant turbidity versus polymer dosage for flocculation of 1% Na-kaolinite using 25, 50, and 100 ppm polymer dosages of the copolymers from NTBAM-co-AM-1b (clouded layer), -1b (clear layer), and -2 (dialyzed fraction) and control PAM. Conditions were : 1000 rpm agitation and addition of 10 mL of polymer solution over 60 seconds.

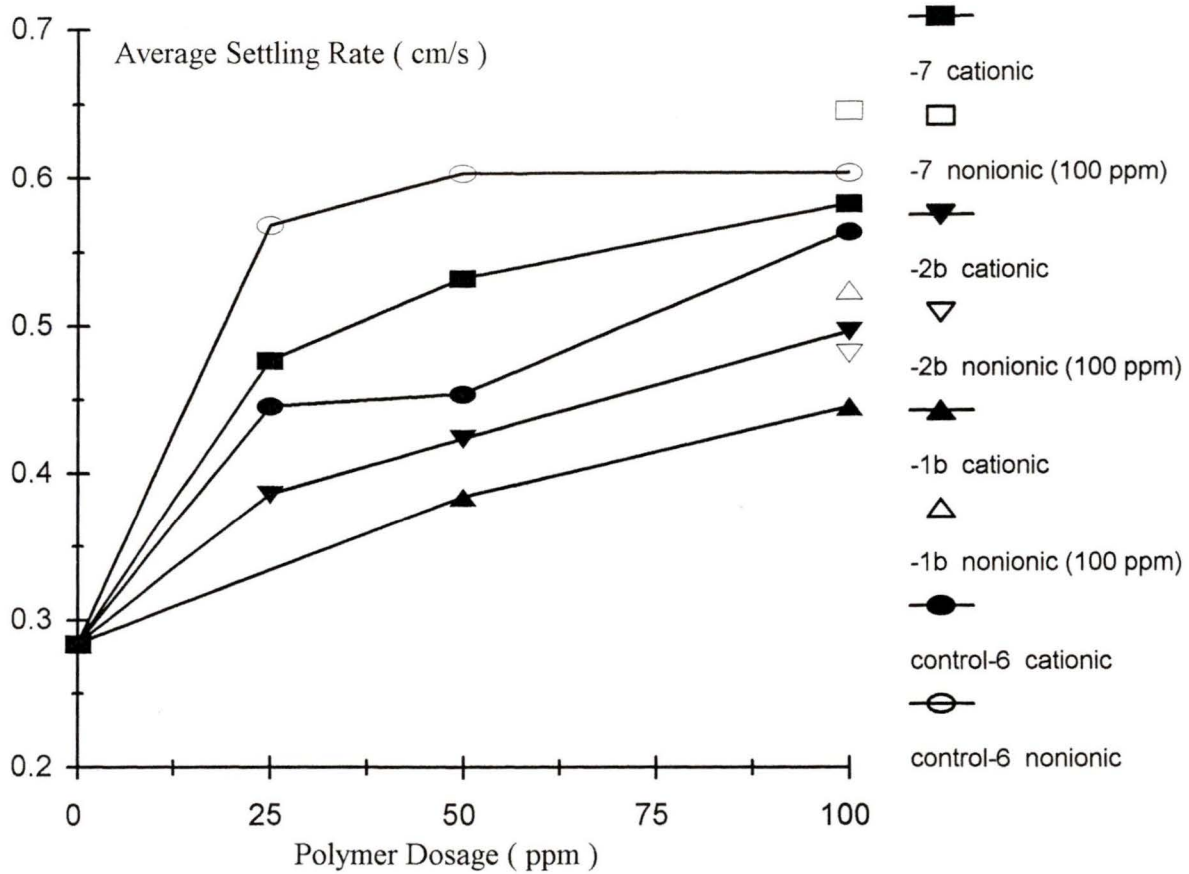

Fig. 63 Average settling rate versus polymer dosage for flocculation of 1% Na-kaolinite using the purified cationic polymers from DMAM-co-AM-7, MeAM-co-AM-2b, NTBAM-co-AM-1b (clouded layer) and control PAM and their nonionic polymer substrates. Conditions were : 1000 rpm agitation and addition of 10 mL of polymer solution over 60 seconds.

calculated by assuming the following relationship.

$$\text{equivalent NTU} = \text{diluted NTU} \times \text{diluted volume} / 20\ \text{mL} \qquad \text{Eq. 45}$$

where	equivalent NTU	is the turbidity approximated outside the 0 to 2000 NTU range.
	diluted NTU	is the turbidity of the diluted supernatant brought within the 0 to 2000 NTU range.
	diluted volume	is the total volume of the 20 mL supernatant aliquot and the volume of deionized water used for dilution.
	20 mL	is the volume of the supernatant aliquot from each flocculation test after 30 minutes of settling time.

The lowest 30 minute supernatant turbidites of the newly synthesized, cationic derivatives were obtained for the cationic derivative of the copolymer from DMAM-co-AM-7 (Table 35). At a polymer dosage of 100 ppm, the 30 minute supernatant turbidity produced by the nonionic copolymer from DMAM-co-AM-7 was about the same as that of its cationic derivative. However, at 100 ppm dosages the nonionic copolymers from MeAM-co-AM-2b and NTBAM-co-AM-1b (clouded layer) and control PAM all gave 30 minute supernatant turbidities which were lower than those produced by their cationic derivatives.

Commercial polymers labelled Percol 351, Percol 721, and Percol E-24 and control PAM

The flocculation tests which used commercial polymers gave higher average

Table 35 30 minute supernatant turbidities for flocculation of 1% Na-kaolinite using the nonionic polymers or their purified cationic derivatives originating from DMAM-co-AM-7, MeAM-co-AM-2b, NTBAM-co-AM-1b (clouded layer), and control-6. Conditions were : 1000 rpm agitation and addition of 10 mL of polymer solution over 60 seconds.

Flocculant	Polymer dosage (ppm)	30 min. supernatant turbidity (NTU) [a]
Blank (1% Na-kaolinite)	0	9792
nonionic DMAM-co-AM (DMAM-co-AM-7)	100	222
cationic DMAM-co-AM (DMAM-co-AM-7)	25	2636
	50	1182
	100	215
nonionic MeAM-co-AM (MeAM-co-AM-2b)	100	1169
cationic MeAM-co-AM (MeAM-co-AM-2b)	25	9696
	50	2862
	100	1305
nonionic NTBAM-co-AM (NTBAM-co-AM-1b, clouded layer)	100	1040
cationic NTBAM-co-AM (NTBAM-co-AM-1b, clouded layer)	25	9360
	50	2738
	100	1370
nonionic PAM (control-6) [b]	25	4335
	50	940
	100	491
cationic PAM (control-6)	25	5448
	50	1820
	100	746

a. Turbidities exceeding 2000 NTU were approximated using Eq. 29.
b. Control-6 used equivalent experimental to MeAM-co-AM-6.

settling rates than the test which used PAM from control-6 (complementary to MeAM-co-AM-6) (Fig. 64). Although Percol 351 (nonionic PAM) and Percol E-24 (anionic PAM) gave higher average settling rates than Percol 721 for dosages of 25 and 50 ppm, Percol 721 (cationic PAM) gave a higher average settling rate at 100 ppm.

All the flocculation tests which used commercial polymers gave lower 30 minute supernatant turbidities than the tests which used control PAM (Fig. 65). At 100 ppm, Percol 721 gave the lowest 30 minute supernatant turbidity although all three commercial polymers gave comparable 30 minute supernatant turbidities.

Overall comparison of the flocculation of 1% Na-kaolinite by the newly synthesized, acrylamide-based polymers and commercial polymers

Of the newly synthesized polymers, the highest average settling rates and lowest supernatant turbidities for each polymer type were recorded for the copolymers from DMAM-co-AM-3, MeAM-co-AM-2b, NTBAM-co-AM-1b (clouded layer), and PAM from control-6 (complementary to MeAM-co-AM-6). These copolymers, control PAM, and commercial polymers were compared by plots of average settling rates and 30 minute supernatant turbidities versus polymer dosage (Fig.66 and 67) for flocculation tests which used 25, 50, and 100 ppm. The commercial polymers gave higher average settling rates and lower supernatant turbidities than the newly synthesized polymers. However, 25 and 50 ppm dosages of the copolymer from DMAM-co-AM-3 gave average settling rates equivalent to those of Percol 721, and at 100 ppm gave a 30 minute supernatant turbidity which was nearly equivalent to that of Percol 721. The largest difference in average settling rates between the commercial polymers and the newly

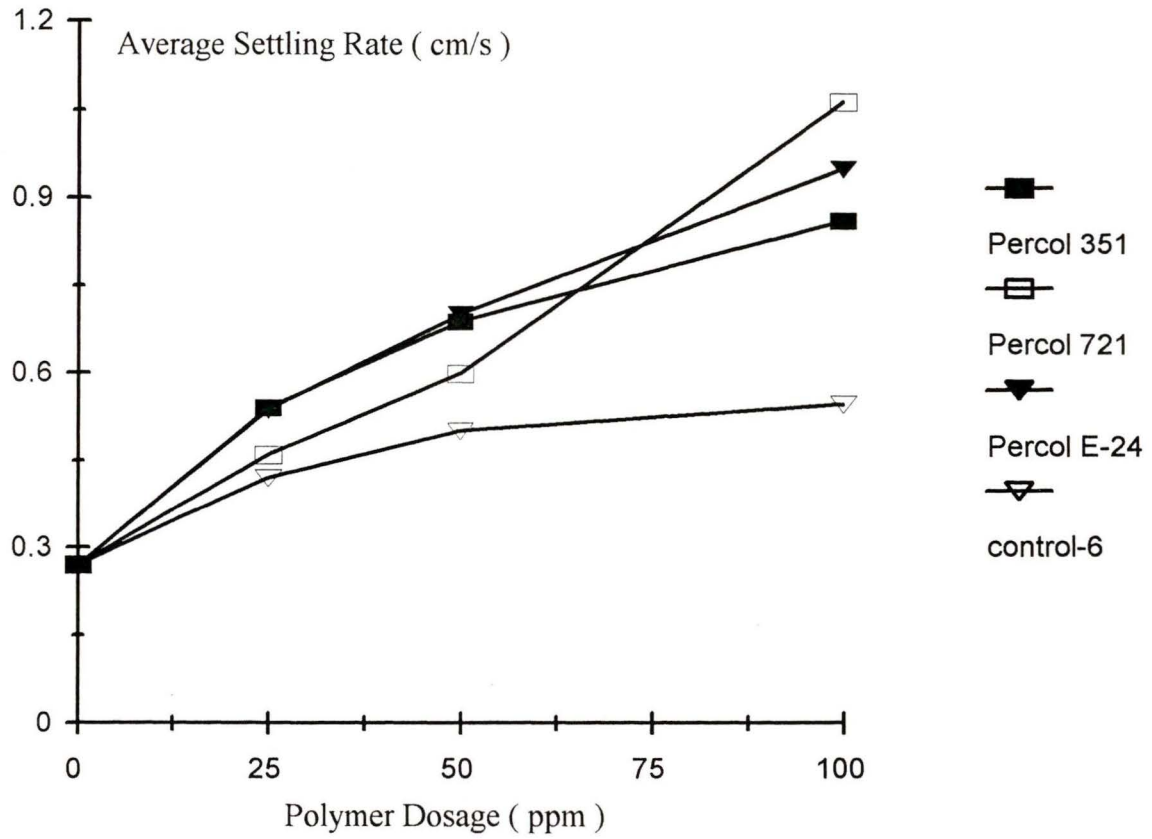

Fig. 64 Average settling rate versus polymer dosage for flocculation of 1% Na-kaolinite using 25, 50, and 100 ppm polymer dosages of control PAM or the commercial polymers labelled Percol 351, Percol 721, and Percol E-24. Conditions were : 1000 rpm agitation and addition of 10 mL of polymer solution over 60 seconds.

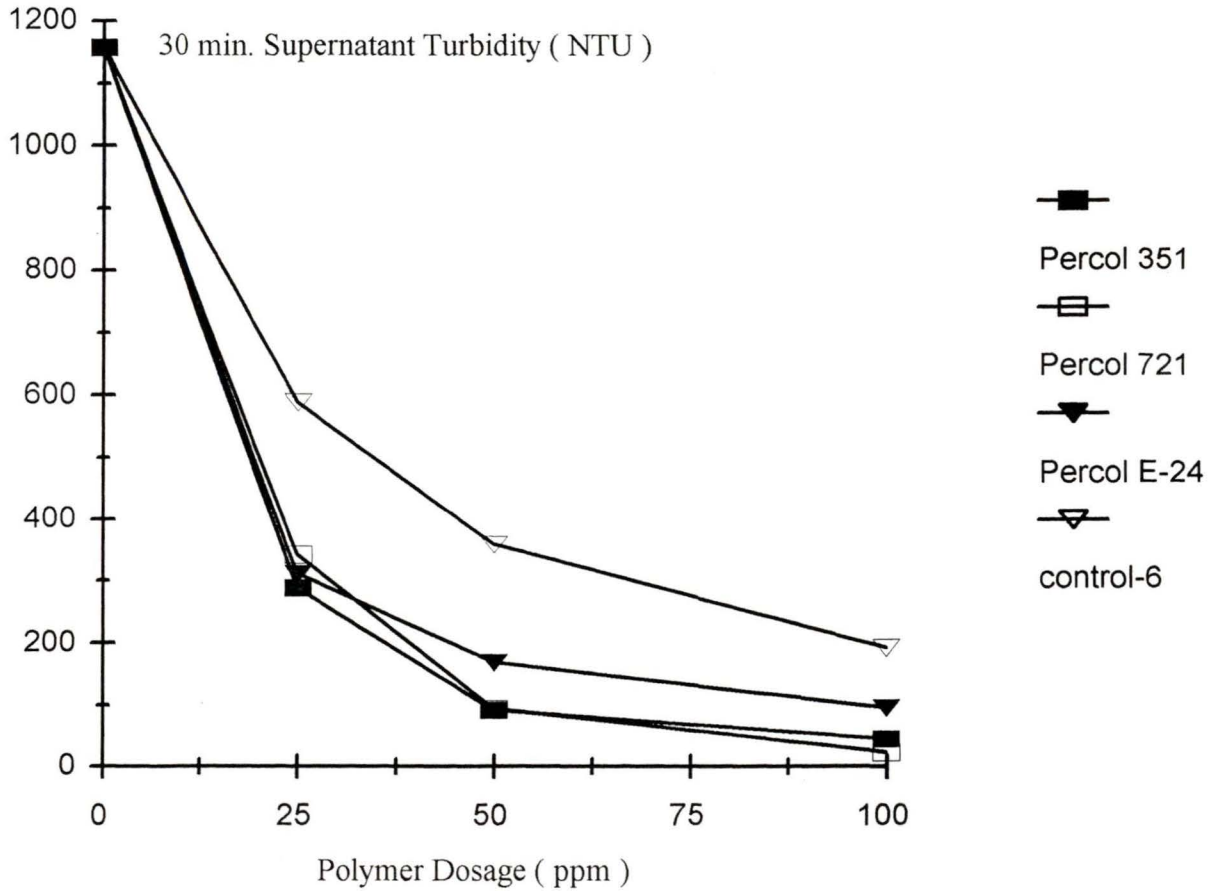

Fig. 65 30 minute supernatant turbiditiy versus polymer dosage for flocculation of 1% Na-kaolinite using 25, 50, and 100 ppm polymer dosages of control PAM or the commercial polymers labelled Percol 351, Percol 721, and Percol E-24. Conditions were : 1000 rpm agitation and addition of 10 mL of polymer solution over 60 seconds.

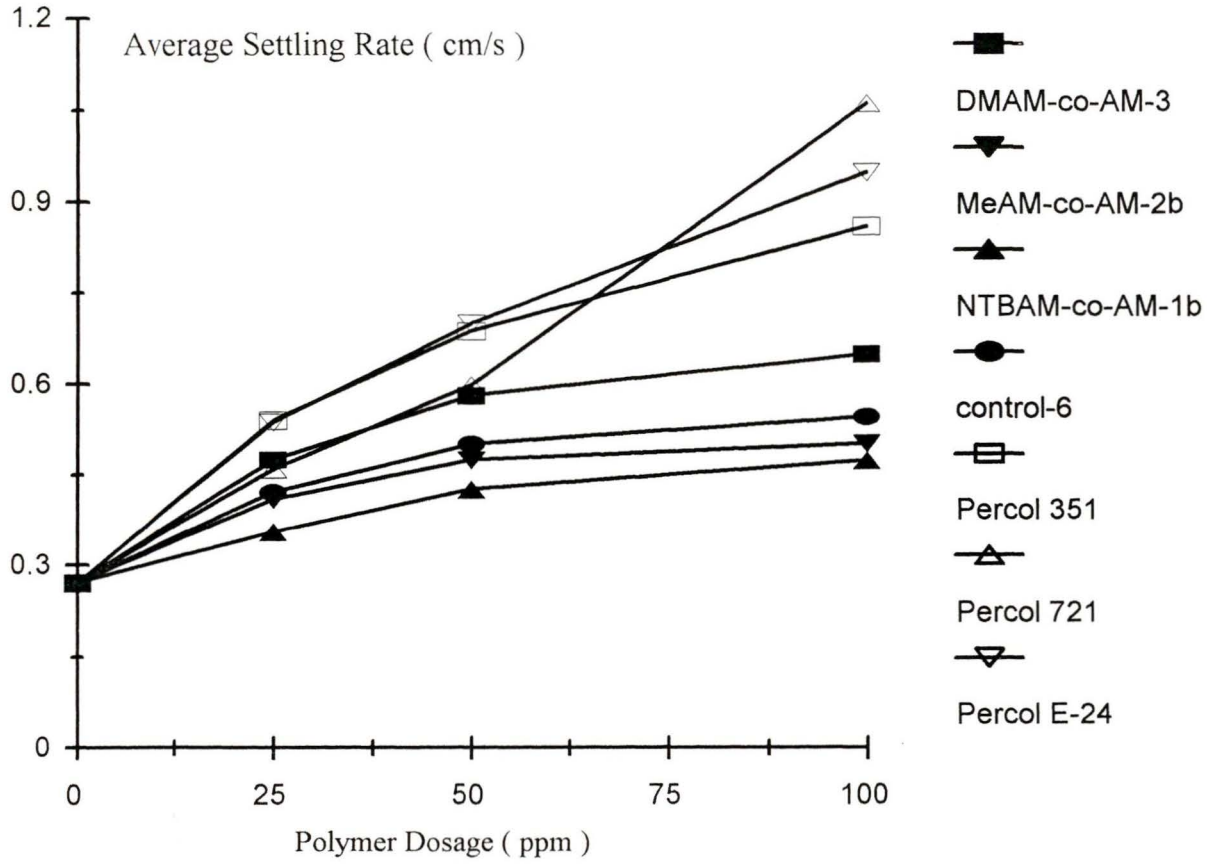

Fig. 66 Average settling rate versus polymer dosage for flocculation of 1% Na-kaolinite using 25, 50, and 100 ppm polymer dosages of the commercial polymers labelled Percol 351, Percol 721, and Percol E-24 and the nonionic copolymers from DMAM-co-AM-3, MeAM-co-AM-2b, and NTBAM-co-AM-1b (clouded layer) and control PAM. Conditions were : 1000 rpm agitation and addition of 10 mL of polymer solution over 60 seconds.

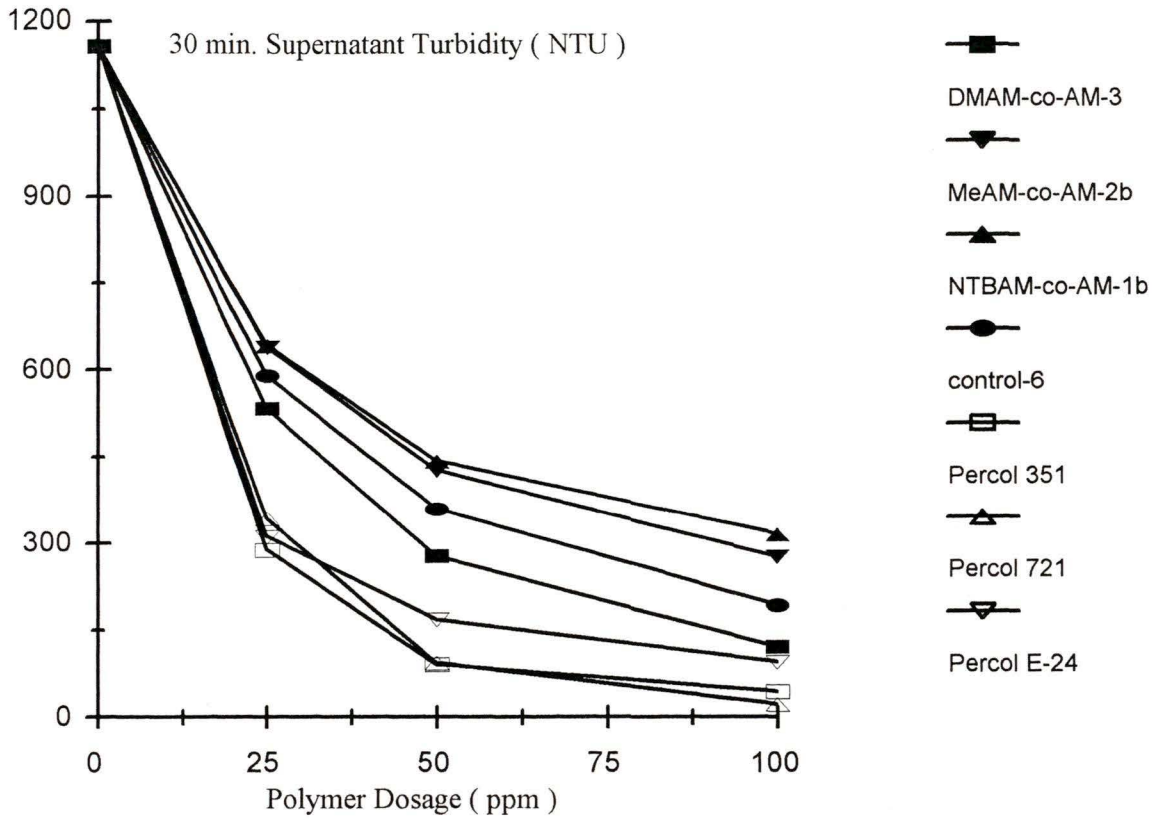

Fig. 67 30 minute supernatant turbidity versus polymer dosage for flocculation of 1% Na-kaolinite using 25, 50, and 100 ppm polymer dosages of the commercial polymers labelled Percol 351, Percol 721, and Percol E-24 and the copolymers from DMAM-co-AM-3, MeAM-co-AM-2b, and NTBAM-co-AM-1b (clouded layer) and control PAM. Conditions were : 1000 rpm agitation and addition of 10 mL of polymer solution over 60 seconds.

synthesized polymers was recorded for a 100 ppm dosage.

4. Discussion

4.1. Evaluation of Sample Preparation Procedure and Accuracy of the Molecular Weights for the GPC / MALLS Analysis of Commercial PAM and Newly Synthesized, Acrylamide-Based Homopolymers

Since the molecular weights of some of the newly synthesized, acrylamide-based polymers were expected to reach 5,000,000 mol. wt. and possibly greater, it was necessary to determine the accuracy of the GPC / MALLS technique for a standard sample of approximately this molecular weight. Polyacrylamide (nonionic, 5,550,000 mol. wt., Polysciences) was selected.

The poor agreement between the M_w's determined by GPC / MALLS and that provided by Polysciences for PAM (Table 12) may be explained by experimental and processing difficulties of the GPC / MALLS technique. Specifically, a maximum polynomial fit degree of 5 which was required by the method of Debye to process the light scattering data was evidence for the tendency of the method of Debye to underestimate high M_w's (ca. 5,000,000 mol. wt. and greater) and a large root mean squared radius (ca. 100 nm and greater).[94] In addition, the low M_w's determined by GPC / MALLS may be attributed to eluted masses from the gel permeation chromatography columns of only 70 % of the injected mass. However, low molecular weight Dextran standards which gave agreement within statistical uncertainty for M_w's determined by GPC / MALLS and supplied by Polysciences also gave eluted masses which were much lower than the injected masses.

The effect of the AUX1 Calibration Constant for the Waters R401 Refractive Index

Detector on calculation of the eluted masses and M_w was investigated. By entering values greater than the default parameter for AUX1 (5.3747 E-05), the eluted masses approached the injected masses. However, as the AUX1 values were increased the values for M_w decreased. Moreover, the adjusted AUX1 value which equalized the eluted mass with the injected mass for a particular experiment was not suitable for other experiments. Along with the AUX1 Calibration Constant, the differential refractive index increment, dn/dc, was required for each polymer for processing. Rather than measuring the value of dn/dc for each PAM standard solution, the literature value for PAM (0.18 mL/g) was entered as the default value.[95] As shown in the literature, temperature and solvent changes only affect dn/dc values for PAM solutions at the third and fourth significant figures. It was found that changes in dn/dc in the third and fourth significant figures and even slight changes in the second gave insignificant changes to calculation of the eluted mass and M_w.

Thus, the AUX1 Calibration Constant and the dn/dc values were eliminated as significant sources of error for processing the light scattering data. It was then reasoned that the gel chromatography columns were a potential source of error. In fact, a technical paper from Wyatt Technology cautioned against the use of GPC / MALLS for high molecular weight polymers due to adhesion of the polymer to the columns.[80] Also, previous users may have affected the performance of the columns for separation of high molecular weight, acrylamide-based polymers.

Even though the M_w's determined for filtered and unfiltered solutions of PAM (nonionic, 5,550,000 mol. wt., Polysciences) agreed within statistical uncertainty (Table

12), the filtration procedure through 0.45 μm disposable syringe filters could not be judged as free from shear. This is because the effect of shear from filtration may have been insignificant to reducing the measured M_w values in comparison to the effect of adhesion of the polymers to the chromatography columns.

4.2. Effect of Polymerization Atmosphere on the Molecular Weight of PAM

Polymerization of AM under a nitrogen atmosphere gives a higher molecular weight polymer than polymerization under a filtered air or oxygen atmosphere, if the monomer is kept separate from the polymerization medium (water) during the lengthy nitrogen sparge. A higher, molecular weight polymer was expected for polymerization under a nitrogen atmosphere, since oxygen is known as a powerful inhibitor. Oxygen reacts with radicals to form a relatively unreactive peroxy radical which reacts with itself or another propagating radical to yield inactive products (Eq. 46).[96]

Peroxy radical

$$Mn\cdot + O_2 \longrightarrow Mn{-}O{-}O\cdot$$

Termination
(coupling with itself)

$$2\ Mn{-}O{-}O\cdot \longrightarrow Mn{-}O{-}O{-}O{-}O{-}Mn$$

Eq. 46

(coupling with polymer radical)

$$Mn{-}O{-}O\cdot + Mn\cdot \longrightarrow Mn{-}O{-}O{-}Mn$$

(disproportionation)

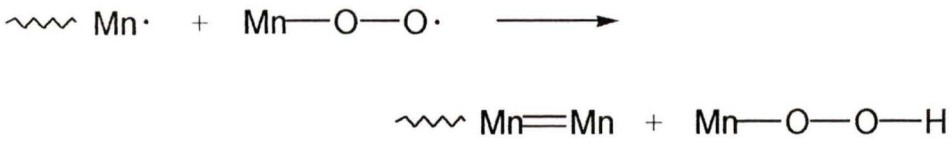

where Mn is polymer.

Unlike oxygen, nitrogen was not expected to interact with the propagating radicals.[1,3,66,97] To explain the low molecular weight for PAM from PAM-3 compared to PAM from PAM-4 (Table 13), the individual polymerization procedures were examined. The only difference between the polymerization procedures was the 14 hour nitrogen sparge of the solution of AM in distilled water for PAM-3 and the 6 hour nitrogen sparge of distilled water while keeping AM separate for PAM-4. Since hydrolysis of amides is usually performed under forcing conditions which include acidic or basic mediums and heating, hydrolysis of AM was not expected for PAM-3 using a natural pH in the range 5.5 to 7.0 and 25°C.[1,15,97] However, by assuming a weakly acidic pH for PAM-3 it is possible that the long duration of the nitrogen sparge was sufficient for hydrolysis of AM to acrylic acid. Even though acrylic acid does not interfere with free radical polymerization, the resultant weight average molecular weight is affected by homopolymerization, or copolymerization with AM. It has been reported that under weakly acidic or near neutral pH conditions the value of the propagation rate constant for the ionized form of acrylic acid is much lower than that of AM.[15] This was attributed to repulsive interactions between the carboxylate groups of the growing polymer chain and monomer. Thus, the

low molecular weight for PAM from PAM-3 could be due to the lower reactivity of the ionized form of acrylic acid.

4.3. Synthesis of Acrylamide-Based Homopolymers

Individual homopolymerizations of DMAM, MeAM, and NTBAM were designed to maximize polymer molecular weight and conversion of monomer to polymer. AM was polymerized alongside each homopolymerization of the substituted acrylamide monomer under the same experimental conditions. Since the long term goal was to establish experimental conditions which would maximize molecular weight and percentage conversion for copolymerization of DMAM with AM, MeAM with AM, and NTBAM with AM, these were varied to determine the best compromise. These initial conditions would serve as the preliminary experimental conditions for copolymerization test-work.

Based on several experimental accounts for solution polymerization of AM[1,3,13,16,66,97] as well as the kinetic theory for free radical polymerization[1,13-15] the preliminary experimental conditions for homopolymerization of the substituted acrylamide monomers and AM, itself, included a 1.0 M monomer concentration in deoxygenated distilled water, a monomer to initiator mole ratio of 1000 :1, a natural pH in the range 5.5 to 7.0, a temperature of 60 °C, and a minimum duration of 3.5 hours.

Modification of the initial conditions was derived from the kinetic theory for free radical polymerization. Since chain transfer to monomer is reported to be the dominant mechanism for reducing the number-average degree of polymerization, X_n, for

polymerization of AM[14,17] and solution polymerization of AM is known to give highly viscous polymer solutions,[2] a low monomer concentration was necessary (i.e. 1.0 M). Even lower monomer concentrations would reduce the rate of polymerization, R_p, which would increase polymerization times and the size of polymerization vessel required for a given quantity of the polymer. Distilled water was selected as the polymerization solvent and it was deoxygenated to minimize the inhibiting effect of oxygen, as described previously. Acrylamide, PAM, and many of the substituted acrylamide monomers and polymers are appreciably soluble in water.[1,15,65] Also, water has a chain transfer constant of nearly zero for polymerization of AM in water.[1]

Since X_n is directly related to the ratio of monomer concentration to the square root of the initiator concentration, $[M] / [I]^{0.5}$, high mole ratios of monomer to initiator will tend to maximize X_n.[13] However, raising the concentration ratio above 1000 risks the possibility of reducing X_n by reducing the rate of polymerization, R_p, and increasing the ratio of termination rate to polymerization rate ($R_t : R_p$). It has been reported that for homopolymerization of AM the ratio $k_p / (k_t)^{0.5}$, which is directly related to X_n, is maximized under acidic conditions and decreased under near neutral and basic conditions.[1,15] However, PAM is susceptible to imidization under acidic and basic conditions and hydrolysis under basic conditions.[1,15,22,97] So the natural pH of the aqueous monomers in the range 5.5 to 7.0 was selected to avoid hydrolysis and minimize imidization.

With respect to polymerization temperature and duration, lowering the temperature and increasing the duration will tend to maximize X_n.[13-15] Intermediate values were

selected for each variable to optimize X_n without requiring unduly long reaction times.

4.3.1. Evaluation of experimental conditions

The success of the experimental conditions for homopolymerization of the acrylamide-based polymers was judged by an increase in the solution viscosity of the polymer solutions from that of the polymerization feedstocks. Quantitative evidence for the success of the experimental conditions was provided by the weight average molecular weight, M_w, from GPC / MALLS analysis and the intrinsic viscosity, [η], and viscosity average molecular weight, M_v, from viscometry analysis.

For reasons given previously, M_w's determined by GPC / MALLS were judged unreliable. Even though the values for [η] and M_v can be considered to be reproducible they cannot be considered accurate because there is no other method which measures [η] and M_v for comparison. Also, intrinsic viscosity measurement of high molecular weight polymers may have 100 % or higher error.[34,98,99] The high error is associated with the approximation of Newtonian behaviour for the polymer solutions. Newtonian flow behaviour requires a linear relationship between the shear force per unit area and the velocity gradient, or simply a single value for viscosity.[34] It applies to solutions of high molecular weight polymers only if a narrow range of the velocity gradient is examined. However, the relationship may not be linear if a wide range of the velocity gradient is examined (pseudoplastic behaviour). With respect to acrylamide-based polymers, the nonlinearity is attributed to the random coil nature of the polymers in solution and the various degrees of solvent interaction about the random coil which alters the relationship

between velocity and frictional resistance. By plotting the reduced viscosity, η_{red}, versus solute concentration, c, and then extrapolating to zero concentration to give the intrinsic viscosity, [η], the complication of non-Newtonian behaviour is avoided but the results may still be misleading. Regardless of these problems, viscosity data for polyacrylamide is still commonly treated this way.[46,100]

Evaluation of the conditions for homopolymerization of DMAM

Due to the poor results from PDMAM-1 and -2 (Table 2), the experimental conditions from PDMAM-3 were determined as the most appropriate to use as the initial conditions for copolymerization of DMAM with AM.

Since [η] is related to the size of a molecule whether it is described as the linear dimensions of the polymer (radius of gyration) or described as the volume occupied by the polymer solution (hydrodynamic volume),[74] the equivalent values of [η] for PDMAM from PDMAM-3 and PAM from control-3 were not expected (Table 14). It was reasoned that PDMAM adopted a more linear conformation in solution than PAM owing to the steric hindrance of the N,N-disubstituted nitrogen atoms of PDMAM. This effect was significant since the ratio $k_p / (k_t)^{0.5}$ which is directly related to X_n is nearly twice as large for polymerization of AM as for polymerization of DMAM.[13,15]

Inappropriate temperatures may explain the poor results (Table 2) for polymerization of DMAM at 30°C (PDMAM-2) and 60°C (PDMAM-1) compared to the good results at 50°C (PDMAM-3). Since neither PDMAM-2 nor control-2 gave an observable increase in solution viscosity, it was reasoned that 30°C did not activate the

initiator, $K_2S_2O_8$. However, it has been reported that both DMAM and AM were successfully polymerized to viscous solutions at 30°C using $K_2S_2O_8$ as the initiator.[18] They conceded that both monomer and solvent required rigorous purification to facilitate polymerization at 30°C.

Since DMAM is hydrophobic and the propagation rate constant for DMAM is nearly as large as that for AM, it is likely that the 60°C polymerization temperature produced high molecular weight polymer rapidly which aggregated into an entangled gel (gel effect)[14]. The "gel effect" is realized for an increase in the rate of polymerization, R_p, with an increase in conversion of monomer to polymer. With respect to the kinetics necessary for the "gel effect", an increasing R_p with increasing conversion results from the rate of termination, R_t, in which the rate constant for translational diffusion (diffusion of two independent propagating radicals to the point of contact) decreases at a faster rate than the increase in the rate constant for segmental diffusion (rearrangement of two independent propagating radicals to the point of contact). Alternatively, it was also possible that by forcing the polymerization to a high conversion, chain transfer to polymer became significant.[14] The outcome from chain transfer to polymer is branching which facilitates chain entanglement and cross-linking. By lowering the polymerization temperature from 60°C to 50°C the gelatinous material was not obtained. It was reasoned that polymerization at 50°C reduced the flexibility of the polymer chains such that the rate of temination, R_t, was not governed by a faster decrease in the rate constant for translation diffusion than the increase in the rate constant for segmental diffusion. Alternatively, it can be rationalized that reducing the flexibility of the polymer chains

decreases the probability for chain transfer to polymer.

Evaluation of the conditions for homopolymerization of MeAM

Even though the homopolymers from PMeAM-1 to -5 were not soluble in distilled water, the experimental conditions from PMeAM-4 and control-4 were selected as the most appropriate initial conditions for copolymerization of MeAM with AM (Table 3). These conditions were selected because PMeAM from MeAM-co-AM-4 gave the highest value of [η] for the PMeAM's and PAM from control-4 gave high values of [η] and M_V (Table 15).

The monomer to initiator mole ratio and the polymerization duration were optimized for PMeAM-4 and control-4. The lower values of [η] obtained for PMeAM from PMeAM-1, -2, -3, and -5 were probably caused by lower monomer to initiator mole ratios and their effect to decrease X_n. Due to a much higher value of $k_p/(k_t)^{0.5}$ for polymerization of AM in comparison to polymerization of MeAM, and the direct relationship between $k_p/(k_t)^{0.5}$ and X_n,[13,15] the lower monomer to initiator mole ratios did not significantly affect [η] for control-1 to -5.

The white gel produced from PMeAM-4 can be explained by three mechanisms. Least likely of the three mechanisms is the "gel effect" as described previously for PDMAM-1. This is not the likely mechanism because the white gel freeze-dried to a white powder which did not swell when added to water, but floated on the surface. Polymer solutions from PMeAM-1, -2, -3, and -5 also freeze-dried to white powders which floated when added to water. Aversion of the white powders for water suggests

cross-linking as a cause of the insolubility for PMeAM-1 to -5. Specifically, intramolecular and intermolecular imidization are possible explanations for insolubility and / or cross-linking of PMeAM (Eq. 47 and Eq. 48).

Intramolecular imidization

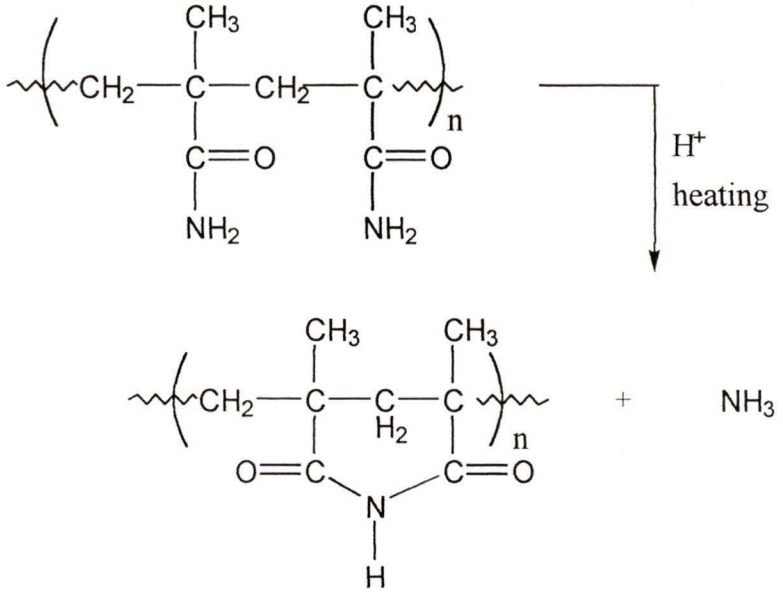

Eq. 47

Intermolecular imidization

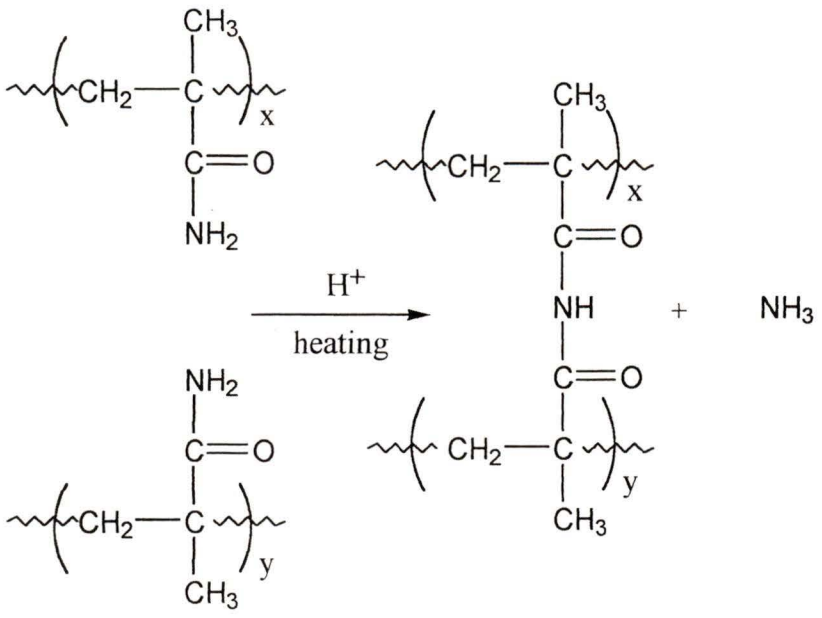

Eq. 48

A thoroughly cross-linked polymer which is completely insoluble in water is represented by the intermolecular imide whereas the intramolecular imide may exhibit only partial insolubility.[1,15,97] Branching from chain transfer to polymer may also explain the insolubility of the polymers from PMeAM-1 to -5, either with or without imidization.

To avoid imidization, one study reported that K_2CO_3 and NaOH were used in separate experiments to adjust the pH of the monomer solution to within pH 6.5 - 8.0.[1] The pH levels for PMeAM-1 to -5 were not adjusted with K_2CO_3 or NaOH to avoid hydrolysis by NaOH and to minimize chain transfer to either K_2CO_3 or NaOH.

To explain imidization for PMeAM from PMeAM-4 and not for PAM from control-4 which was polymerized under identical experimental conditions, it was thought that the reduced flexibility of the polymer back-bone of PMeAM increased the probability for interaction between the adjacent amide functionalities of an isotactic grouping in an

overall atactic structure.[14] Also, the linear conformation of PMeAM in solution owing to the repulsive interactions of the methyl substituent on the α-carbon atoms of the polymer back-bone was thought to contribute to a greater chain transfer to polymer constant for PMeAM than for the coiled, solution conformation of PAM.

The polymer solutions from PMeAM-1, -2, -3, and -5 were soluble upon completion of polymerization but freeze-dried to insoluble white powders. It was thought that these shorter polymerizations (compared to PMeAM-4) caused only partial intermolecular or intramolecular imidization of the polymers. Or possibly, the shorter polymerization times of PMeAM-1, -2, -3, and -5 did not force maximum conversion which limited the significance of chain transfer to polymer. Upon freeze-drying, the water structure surrounding the polar amide functionalities collapsed which caused entanglement of the polymer chains. As a result of partial imidization or branching from chain transfer to polymer and the steric hindrance caused by methyl substitution of the polymer back-bone, it was reasoned that the polymer chains were rendered less flexible such that the water structure necessary for dissolution could not be adopted.

Evaluation of the conditions for homopolymerization of NTBAM

Even though neither PNTBAM nor PAM homopolymerized to highly viscous solutions in the 1:1, t-BuOH / water medium, the homopolymer solutions exhibited similar characteristics as each contained gelatinous material. The highest values of $[\eta]$ and M_v were for PAM from control-14 which was homopolymerized in a 1:1, t-BuOH / water solvent (Table 17). For this reason, the experimental conditions used for control-

14 were selected as the initial conditions for copolymerization of NTBAM with AM (Table 6).

PNTBAM-1 to -6

As a result of the poor solubility of NTBAM in water, organic solvents which gave low chain transfer constants, C_s, were investigated. Methanol and t-butanol were selected to test as polymerization solvents owing to their low chain transfer constants for polymerization of AM,[1,2] miscibility with water[101], and compatability for solubilization of NTBAM and AM[3].

The lack of success for homopolymerizations of NTBAM and AM in methanol and methanol / water mixtures (Table 16) was attributed to initiator difficulty, the poor solubility of NTBAM in water, and precipitation of PAM in methanol. Whereas $K_2S_2O_8$ was insoluble in methanol, AIBN did not initiate polymerization in either methanol or mixtures of methanol / water. In fact, control-5 which used AIBN as the initiator in methanol did not form any PAM precipitate. Since PAM is known to precipitate from polymerization in methanol,[1,2,13] the suitability of AIBN for initiation was questioned. A half life for AIBN in benzene or toluene at 50°C is reported to be 74 hours.[14] Even though data was not available for polymerization in methanol, PNTBAM-6 was planned to use methanol at 60°C, and an initiator concentration (based on the toluene and benzene half life data) to ensure that 7 hours after the addition of the initiator to the polymerization, sufficient initiator would decompose to give a mole ratio of active initiator to the monomer of 1/1000. Even though control-6 did form a precipitate, the

polymerization was not judged successful. Precipitation polymerization (heterogeneous polymerization) in which the monomer is soluble in the polymerization solvent and the polymer is insoluble is known to produce a lower molecular weight polymer than solution polymerization (homogeneous polymerization).[14]

Since the ratio, $k_p/(k_t)^{0.5}$, for polymerization of AM is known to decrease in an organic environment[1,15,97] and previous experimentation showed that AM polymerized to highly viscous solutions in water, homopolymerizations of NTBAM and AM in 1:1 and 1:9, methanol / water mixtures were attempted. Even though PAM did not precipitate from either polymerization solvent which suggests homogeneous polymerization, the polymerizations were not judged successful because the homopolymer solutions did not increase in solution viscosity relative to the starting solutions. An increase in solution viscosity is a strong indication of a successful solution polymerization and possibly the formation of high molecular weight polymer.[1,2] Even the values of $[\eta]$ for control-1 to -6 were much less than values measured for PAM produced in water.

It is suggested that the tan coloured, gelatinous material produced for PNTBAM-3 resulted from agglomeration and subsequent chain entanglement of the hydrophobic PNTBAM in 1:9, methanol / water.

PNTBAM-7 to -14

Results from PNTBAM-1 to -6 demonstrated that both the monomers (NTBAM and AM) and the homopolymers (PNTBAM and PAM) behave in opposition with respect to their interactions with the polymerization solvent. Inverse emulsion polymerization

which has been successful for copolymerization of hydrophilic AM with a hydrophobic comonomer, was considered.[13] However, the draw-backs of the technique were the requirement for a large concentration of surfactant (sodium dodecylsulfate) and consequent difficulties associated with polymer purification. It was hoped that successful homopolymerization of NTBAM and AM in 98 % t-butanol or mixtures of t-butanol / water would eliminate the need for the inverse emulsion technique.

To explain the gelatinous material formed from homopolymerization of NTBAM and AM in 1:1, t-butanol / water, it was reasoned that the "gel-effect" (as described previously for homopolymerization of DMAM) was responsible for agglomeration and subsequent chain entanglement of PAM and PNTBAM. In support of this theory, the amounts of PAM and PNTBAM gelatinous material decreased as the polymerization temperature was reduced from 70°C to 45°C, like the results for homopolymerization of DMAM. However, the gelatinous material may also be explained by branching contributed by chain transfer to polymer which becomes significant under conditions which force maximum conversion. In addition, imidization could be a factor, since it has been reported that polymerization of AM to high conversion in 1:1, acetone / water produced imidization of PAM, which rendered the polymer insoluble. The same report gave results for homopolymerization of AM in 1:1, t-butanol / water but did not give any evidence for product solubility.

4.3.2. Evaluation of Copolymerization Conditions

Copolymerization of DMAM with AM

The M_w's of the copolymers from DMAM-co-AM-2 to -5 and -7 were all greater than 5,000,000 g/mol (Table 30) which is classified as ultra-high molecular weight.[49] In addition, these copolymerizations gave yields greater than 70 % (Table 7) which are reasonable based on published results.[18,19] These high M_w's and reasonable yields for ordinary reagents and routine conditions validate the compatibility of DMAM with AM for copolymerization.

By reducing the total monomer concentration from 1.0 M (DMAM-co-AM-1) to 0.50 M (DMAM-co-AM-4 and -5) and 0.25 M (DMAM-co-AM-2, -3, -6, and -7) for copolymerization of DMAM with AM (Table 7), the rate of polymerization, R_p, was reduced. Since R_p is inversely proportional to the number-average degree of polymerization, X_n, the decrease in total monomer concentration was beneficial to maximizing the molecular weight of the copolymers. To compensate for the effect of the reduced total monomer concentration on R_p, the polymerization time was extended to a minimum of 9 hours in order to maximize the percentage conversion of monomer to polymer.

Copolymerization of MeAM with AM

The M_w of the copolymer from MeAM-co-AM-2b was greater than 1,000,000 g/mol (Table 31) which is classified as high.[49] Copolymers from MeAM-co-AM-3 to -5 gave M_w's all less than 1,000,000 g/mol. They are classified as moderate to low molecular

weights. In addition, these copolymerizations gave yields greater than 60 % (Table 8) which are considered somewhat reasonable based on published results.[18,19] These moderate to low M_w's and somewhat reasonable yields attest to either the incompatibility of MeAM with AM for copolymerization to high M_w's or the need to include specialized reagents and / or less than ordinary conditions.

By increasing the total monomer concentration from 0.50 M (MeAM-co-AM-1) to 1.0 M (MeAM-co-AM-2b to -6) for copolymerization of MeAM with AM (Table 8), R_p was increased. Even though the inverse relationship between R_p and X_n meant that an increase in R_p was not beneficial to maximizing the copolymer molecular weight, the increase in total monomer concentration was justified from the lack of a change in solution viscosity for MeAM-co-AM-1. In addition, an increase in R_p was beneficial to maximizing the percentage conversion of monomer to polymer.

Copolymerization of NTBAM with AM

The M_w's of the copolymers from NTBAM-co-AM-1b and -2 are greater than 1,000,000 g/mol (Table 32) which classifies them as high.[49] NTBAM-co-AM-2 gave a yield of approximately 100% (Table 9) which is considered good based on published results.[18,19] However, NTBAM-co-AM-2 was the only copolymerization which did not exhibit gelatinous material or separate liquid layers. Therefore, copolymerization of NTBAM with AM is not compatible to give high M_w's and good yields unless a certain composition and a less than ordinary reagent (1:1, water / t-butanol) are used.

The formation of clear and clouded layers during the NTBAM-co-AM-1b

copolymerization can be related to the outcome from homopolymerization of AM in 1:1, t-butanol / water. By integration of δ 179 (amide C=O from AM component) and δ 175 (amide C=O from NTBAM component) from the ^{13}C NMR spectra of the copolymers from NTBAM-co-AM-1b (clouded layer) and -1b (clear layer) (Fig. 35 and 36) it was determined that the copolymer from -1b (clouded layer) contained 85 % AM whereas the copolymer from -1b (clear layer) contained 78 % AM. Since the intrinsic viscosities, [η], of the copolymers from -1b (clouded layer) and -1b (clear layer) were nearly equivalent (Table 20), it is suggested that a solute / solvent interaction was more likely than the "gel effect" for the formation of the gelatinous material. Aggregation of the polymer chains due to the incompatability of the hydrophilicity of the polymer with 1:1, t-butanol / water was a more likely explanation for the formation of the gelatinous material (homopolymerization of AM) or a clouded layer (copolymerization of AM with NTBAM). Perhaps the clear layer did not exhibit aggregation of the polymer chains because the copolymer contained a greater proportion of NTBAM which added enough hydrophobic character to the copolymer to facilitate dispersion in 1:1, t-butanol / water. A similar arguement can be made for the copolymerization solution from NTBAM-co-AM-2. However, it is likely that copolymerizations NTBAM-co-AM-3 to -6b introduced sufficient hydrophobic character into the copolymers to force aggregation of the polymer chains and yield gelatinous material. Since attempts to eliminate the formation of gelatinous material by lowering the polymerization temperature (PNTBAM-7 to -14) failed and as attempts to increase the viscosities of the copolymerization solutions by extending the polymerization duration (NTBAM-co-AM-6a and -6b) failed, it was

concluded that only polymerizations which contained less than 60 mole % of NTBAM and more than or equal to 20 mole % of NTBAM were appropriate for copolymerization with AM in 1:1, t-butanol / water.

4.4. Verification of Copolymerizations by PAS-FTIR and ^{13}C NMR

4.4.1. Copolymers of DMAM with AM

Evidence of copolymerization of DMAM with AM rather than a mixture of homopolymers was obtained from the PAS-FTIR spectra of the copolymers from DMAM-2 to -5, homopolymer (PDMAM) from DMAM-co-AM-6, and PAM from control-6 (Fig. 15). At a low proportion of AM in the copolymer (DMAM-co-AM-5), the N-H, asymmetric and symmetric stretching frequencies of NH_2 appeared at frequencies higher than those for the spectrum of PAM (3323 and 3189 cm^{-1}) and then shifted to frequencies which approached 3323 and 3189 cm^{-1} as the proportion of AM in the copolymers increased. A gradual shift in the N-H stretching frequencies suggested some degree of interaction between the DMAM and AM components of a copolymer rather than a homopolymer mixture.

Comparison of the ^{13}C NMR spectra of the copolymers from DMAM-co-AM-2 to -5 (Figs. 25 to 28) and the homopolymer (PDMAM) from DMAM-co-AM-6 (Fig. 24) with the ^{13}C NMR spectra of PAM from control-6 (Fig. 20) and AM (Fig. 19) determined that polymer rather than monomer was present in the copolymers. However, copolymers could not be distinguished from a mixture of homopolymers as the chemical shifts of the carbon atoms in the copolymer were nearly the same as the chemical shifts in the

homopolymers.

4.4.2. Copolymers of MeAM with AM

Evidence for copolymerization of MeAM with AM rather than a mixture of homopolymers was obtained from the PAS-FTIR spectra of the copolymers from MeAM-co-AM-2b to -5, homopolymer (PMeAM) from MeAM-co-AM-6, and PAM from control-6 (Fig. 16). Bands at 3323 and 3189 cm^{-1} (N-H asymmetric and symmetric stretching of NH_2) in the spectrum of PAM from control-6 were present at slightly higher frequencies in the spectrum of PMeAM from MeAM-co-AM-6. As the content of AM in the copolymers increased, the frequencies for N-H asymmetric and symmetric stretching of NH_2 shifted to those of the PAM spectrum. Similarly, the band at 2990 cm^{-1} (C-H asymmetric stretching CH_3) in the spectrum of PMeAM shifted to lower frequency as the content of AM in the copolymers increased and then was obscured by the C-H asymmetric and symmetric stretching of CH_2. Also, the frequency of N-H bending of NH_2 (amide II band) shifted to higher frequency as the AM content of the copolymers increased. Gradual shifts in the N-H stretching frequencies, C-H stretching frequency, and N-H bending frequency suggested some degree of interaction between the MeAM and AM components of a copolymer rather than a homopolymer mixture.

The PAS-FTIR spectra of the copolymers from MeAM-co-AM-2b to -5, PMeAM from MeAM-co-AM-6, and PAM from control-6 (Fig. 16) were used as evidence to connect the insolubility of PMeAM in water to imidization of PMeAM. An imide spectrum is expected to have bands similar to a secondary amide at 3480 - 3270 cm^{-1} (N-

H stretch), 1680 - 1630 cm^{-1} (C=O stretch), 1570 - 1550 cm^{-1} (N-H bending), and 1270 cm^{-1} (C-N stretch).[102] The only band from the spectrum of PMeAM which was not masked by bands from the primary amide of the MeAM component which was not converted to an intramolecular or intermolecular imide was that at 1270 cm^{-1} (C-N stretch). No band at 1270 cm^{-1} was visible in the spectra of the copolymers from MeAM-co-AM-2b and -3, which contained a low proportion of MeAM. However, this band was present in the spectra of the copolymers from MeAM-co-AM-4 and -5 which contained a higher proportion of MeAM as well as in the spectrum of the homopolymer (PMeAM) from MeAM-co-AM-6.

By comparison of the ^{13}C NMR spectra of the copolymers and homopolymers from MeAM-co-AM-2b to -6 (Figs. 30 to 34) with the ^{13}C NMR spectra of AM (Fig. 21) and MeAM (Fig. 29) it was confirmed that polymer had formed. However, copolymers could not be distinguished from a mixture of homopolymers as the chemical shifts of the carbon atoms in the copolymer were nearly the same as the chemical shifts in the homopolymers.

Since the spectrum of PMeAM from MeAM-co-AM-6 (Fig. 30) was obtained for a solution in deuterated formic acid which had a contact time of 7 to 10 days prior to analysis, imidization was expected. In fact, the peaks at δ 182.7 and 182.0, δ 52.8 and 51.2, and δ 19.4, 17.9, 16.4, 12.6 suggested at least two distinct chemical environments for the carbonyl functionality, α-carbon atom, and methyl substituent, respectively. The spectra of the copolymers from MeAM-co-AM-4 and -5 (Figs. 33 and 34) were obtained for solutions prepared in D_2O with added electrolyte which did not present as great a

chance for imidization. Although the spectra of the copolymers from MeAM-co-AM-4 and -5 were less resolved than the spectrum of PMeAM from MeAM-co-AM-6, the spectra displayed peak overlap and chemical shifts consistent with the spectrum of PMeAM. With respect to peak overlap and chemical shifts, the spectra of the copolymers from MeAM-co-AM-2b and -3 (Figs. 31 and 32) which contained a lower proportion of MeAM were not consistent with the spectrum of PMeAM.

4.4.3. Copolymers of NTBAM with AM

The bands at 3300 cm^{-1} (N-H stretching of NH from the NTBAM component) and 3323 cm^{-1} (asymmetric N-H stretching of NH_2 from the AM component) in the PAS-FTIR spectra (Figs. 17 and 18) overlapped, and therefore could not be used diagnostically. However, the bands at 3189 cm^{-1} (symmetric N-H stretching of NH_2 from the AM component) and 1225 cm^{-1} (C-N stretching, amide III band) shifted slightly as the copolymer composition changed. Since shifts in the frequencies of assigned bands would serve as a strong indication of copolymer component interaction, it cannot be concluded from the PAS-FTIR spectra that copolymers rather than a mixture of homopolymers formed.

Since the copolymers and homopolymers from NTBAM-co-AM-1b, -2 (non-dialyzed), -3, -6a, and -6b were not dialyzed, their ^{13}C NMR spectra (Figs. 36-38 and 40-43) displayed evidence of NTBAM and AM. The ^{13}C NMR spectra of the gelatinous material from NTBAM-co-AM-3 (Figs. 41) displayed evidence of copolymer or a mixture of homopolymers, whereas the corresponding tan coloured solutions (Figs. 42)

showed evidence mainly of unreacted monomer (s). The NTBAM-co-AM-2 copolymerization solution, which was dialyzed against distilled water at 3500 MW cut-off, prior to freeze drying, gave a ^{13}C NMR spectrum (Fig. 39) which showed no evidence of residual monomer. Evidence to support the formation of copolymers rather than homopolymer mixtures was not available from the ^{13}C NMR spectra due to the similarity between the chemical shifts of the ^{13}C NMR spectra of the copolymers with those of the homopolymers.

4.5. Evaluation of the Copolymer Compositions

4.5.1. Use of ^{13}C NMR

The accuracy of the integrals for the ^{13}C NMR spectra of the copolymers from DMAM-co-AM-2 to -5 (Figs. 25 to 28), MeAM-co-AM-2b to -5 (Figs. 31 to 34), and NTBAM-co-AM-1b to -2 (Figs. 37 to 40) was hampered by the limitations of broadband decoupling. With the use of broadband decoupling, a pulse of rf radiation is spread across the entire proton chemical shift range by noise modulation. The proton magnetization is saturated and randomized such that the carbon atoms experience both a nuclear Overhauser effect (NOE) and decoupling. Due to the range of relaxation rates of the carbon atoms resulting from various proton distances, a range of NOE's are experienced.[103] In addition to the NOE's, the method of integration, itself, has a lower detection limit of 1 to 10 % for changes in intensity. The range of NOE's and the limitations of integration contributed to the uncertainty of the integrals for the ^{13}C NMR spectra.

In addition to broadband decoupling, inverse gated decoupling was used to produce ^{13}C NMR spectra for the copolymers and homopolymer (PMeAM) from MeAM-co-AM-6 (Fig. 30) and NTBAM-co-AM-3 to -6b (Figs. 36, 41-43). With this decoupling method, the decoupler is on only during the pulse and acquisition, but is off during the relaxation delay.[103] The effect of inverse gated decoupling is to equalize all the NOE's by making them all equal to zero. Consequently, the integrals from spectra obtained using inverse gated decoupling are more reliable than those from spectra obtained using broadband decoupling.

By integration of the peaks assigned to the carbonyl carbon atoms of each monomer component of the copolymers from DMAM-co-AM-2 to -5 and NTBAM-co-AM-1b to -2, it was assumed that the NOE enhancement of the carbonyl carbon atoms of each monomer component was similar. This assumption was based on the similar chemical environments with respect to proton interaction of the carbonyl carbon atoms of each monomer component of the copolymer and carbonyl chemical shifts which differed by less than a few ppm. Except for the copolymer composition determined for the copolymer from DMAM-co-AM-5, the copolymer compositions determined by integration of the resonance peaks at δ 179.2 (C=O from AM component) and δ 175.8 (C=O from DMAM component) agreed with the compositions calculated using the copolymerization equation (Table 22). Even though literature values were not available for the reactivity ratios corresponding to copolymerization of AM with NTBAM, the copolymer compositions determined by integration of the resonance peaks corresponding to the carbonyl carbon atoms of each monomer component appeared reasonable based on

the composition of the feedstocks (Table 24).

The copolymer compositions determined by integration of the ^{13}C NMR spectra of the copolymers from MeAM-co-AM-2b to -5 did not approximate the copolymer compositions calculated by the copolymerization equation, except for the composition determined for the copolymer from MeAM-co-AM-3 (Table 23). Since the chemical shifts of the carbon atoms used for integration differed by several ppm and the chemical environments of the carbon atoms included adjacent protons and protons one carbon atom away, it was reasoned that a broad range of NOE's contributed significant error to the integrals of the ^{13}C NMR spectra. Also, reactivity ratios used in the copolymerization equation were obtained for copolymerizations taken to low conversion whereas this research forced maximum conversion.[104-106]

4.5.2. Use of elemental analysis

For the copolymers from DMAM-co-AM-2 to -5 and -7 there was good agreement between the copolymer compositions determined by elemental analysis using the weight percentages of carbon and nitrogen in the copolymers and the copolymer compositions calculated from the copolymerization equation (Table 22). Even though the weight percentages of carbon, hydrogen, and nitrogen were determined, only the copolymer compositions determined from the weight percentages of carbon and nitrogen agreed with the results from the copolymerization equation. It was reasoned that the weight percentages of hydrogen were more susceptible to error due to the potential for contamination from moisture in the air and the impact of this contamination on the low

weight percentages of hydrogen in the copolymers.

For the copolymers from MeAM-co-AM-2b to -5 there was poor agreement between the copolymer compositions determined by elemental analysis using the weight percentages of hydrogen in the copolymers and the copolymer compositions calculated from the copolymerization equation (Table 23). However, the copolymer compositions determined from the weight percentages of hydrogen gave better agreement than copolymer compositions determined from any combination of the weight percentages of carbon, hydrogen, or nitrogen or the weight percentages of carbon, itself, or nitrogen, itself. Even though the weight percentages of carbon, hydrogen, and nitrogen were shown to be reproducible as duplicate samples and as samples with or without added catalyst, incomplete combustion of the samples was thought to be the cause of total weight percentages less than 100 % for complete elemental analysis of the copolymers from MeAM-co-AM-3 and -4. Adjusting the weight percentages of carbon, hydrogen, and nitrogen for the copolymers from MeAM-co-AM-2b to -5 to a total weight percentage of 95.7 % (average of 96.2 % and 95.2 %) instead of 100 % did not significantly improve the agreement between the copolymer compositions calculated from the copolymerization equation and those determined directly from the analytical results. It was expected that the weight percentages of carbon, hydrogen, and nitrogen in the copolymers would fall in the range of the weight percentages in the comonomers, yet the carbon content differed by as much as 4 % from this range. Low weight percentages of carbon were also obtained for elemental analysis of commercial PAM. Due to the apparent limitation of elemental analysis for high molecular weight polymers, it could

not be determined whether branching from chain transfer to polymer, or imidization (intramolecular or intermolecular) or other factors were responsible for the poor agreement between the copolymer compositions determined from elemental analysis and those calculated using the copolymerization equation.

4.6. Homopolymer and Copolymer Conversion to Cationic Derivatives

4.6.1. Experimental conditions

Published sources give the details for experimental procedures for conversion of PAM to its cationic derivative via the Mannich reaction and subequent quaternization of the Mannich product.[1,21,28-31] This supported formation of the cationic derivative without chain shortening. A typical route to the cationic derivative of PAM involving the Mannich reaction with formaldehyde and dimethylamine and subsequent quaternization with dimethylsulfate is shown by the reaction scheme in Fig. 2.[31]

Alternatively, the cationic derivative of PAM may be prepared by the Hofmann degradation reaction with alkaline hypochlorite or hypobromite which is then followed by methylation to give the tertiary amine and quaternization to give the cationic derivative (Fig. 1).[1,21,26,27] However, low yields of amine functionalities and significant hydrolysis of the amide functionalities to carboxyl groups reported for the Hofmann degradation reaction,[1,21,26] prompted selection of the Mannich reaction followed by quaternization to prepare the cationic derivatives of poly(DMAM-co-AM), poly(MeAM-co-AM), poly(NTBAM-co-AM), and PAM.

Both PAM and copolymers of AM with MeAM which contained less than 20 mole

% of MeAM in the copolymer have been previously converted to cationic derivatives using the Mannich reaction followed by quaternization.[28,29] In addition, the same literature source cautioned against using copolymers with more than 20 mole % of a comonomer in order to obtain good yields. For these reasons only the copolymers from DMAM-co-AM-7, MeAM-co-AM-2b, and NTBAM-co-AM-1b (clouded layer) were used for cationic conversion. Also, PAM from control-6 (complementary to MeAM-co-AM-6) was converted to its cationic derivative.

The Mannich reagents were added to deliver a mole ratio of 1.05:1:1 of dimethylamine to formaldehyde to the amido nitrogen content of the particular polymer (Table 10) in order to minimize the reaction of formaldehyde with PAM. Formaldehyde reacts with the amide groups of PAM to form methylol amide groups which may react with an amide functionality of another PAM chain to give methylene crosslinking.[29] Significant crosslinking can give an insoluble Mannich product. Reports cautioned against the use of more than a slight excess of dimethylamine due to the formation of amino byproducts which would reduce the yield of the Mannich product.[28] Mannich reagents were added under a nitrogen atmosphere to avoid the oxygen initiated free radical polymerization of formaldehyde.[107] Also, basic conditions involving NaOH were used because the hydroxide anion was known to be too weak to initiate polymerization of formaldehyde[107] and basic conditions avoid imine formation.[108]

Dimethyl sulfate was used as the quaternization reagent based on the high methylation yields reported in the literature.[28] Even though a 1:1 mole ratio of dimethyl sulfate to amido nitrogen content was used (Table 11), it was unlikely that 100 % of the

amide functionalities were converted to the tertiary amines by the Mannich reaction. However, reports indicated that the addition of a gross excess of dimethyl sulfate to the Mannich product had neither an effect on the yield of the cationic derivative nor an effect on the % cationicity introduced to the polymer.[28]

Dialysis of the quaternized polymer solutions against 0.1 M NaCl was necessary to establish the chloride ion as the sole counterion. This was followed by dialysis against distilled water for 21 days, which was necessary to force the equilibrium of the Mannich reaction to the reactant side to eliminate unquaternized tertiary amines from the polymer. A literature source which described the use of conductometric titrations to follow the dialysis of quaternized polymer solutions against distilled water reported that dialysis for 14 days was sufficient to remove the unquaternized tertiary amines from the cationic derivative.[31] Since the 14 day period was subject to the sensitivity of the conductometric titration technique, a 21 day period was used for dialysis to maximize the removal of the unquaternized tertiary amines from the cationic derivative.

4.6.2. Evaluation of experimental conditions for cationic derivatization

The freeze-dried, purified cationic derivatives which included mixed-bed ion exchange as a purification technique swelled upon addition to water. Since the positively charged groups on neighboring polymer chains tend to repel each other, it was thought that methylene crosslinks were responsible for the polymer "gel". Although steps were taken experimentally to minimize crosslinking, the Mannich reaction is an equilibrium reaction which is believed to cycle between decomposition of the Mannich base and

recombination of the starting reagents.[29] The 18 hour duration which was used to maximize the yield of the Mannich product may have allowed for methylene crosslinking as recombination of formaldehyde with dimethylamine became less likely than combination of formaldehyde with PAM. Since the Mannich product and subsequent quaternized polymer were not rendered insoluble, it was rationalized that freeze-drying caused polymer chain entanglement and the methylene crosslinks inhibited the formation of a water structure required to redissolve the polymer. Alternatively, it has been reported that methylene crosslinking can result from the freeze-drying process.[30] During freeze-drying the concentration of the quaternized polymer gradually increases as water is removed from the polymer as a gas. As the concentration of the quaternized polymer increases to greater than 10 %, the quaternized polymer may react with water to form methylene crosslinks (Fig. 68).

The percentage cationicities of the cationic derivatives as determined by the direct titration technique (refer to section 3.7.) are judged reasonable based on published results for conversion of PAM to its cationic derivative.[28-31] Although PAM from control-6 and the copolymer from MeAM-co-AM-2b provided the greatest proportions of sterically unhindered amide functionalities for combination with the Mannich base, the purified cationic derivative of the copolymer from DMAM-co-AM-7 analyzed to give the highest percentage cationicity and the largest intrinsic viscosity, [η] (Table 25). Due to the large [η] and high M_w of the copolymer from DMAM-co-AM-7, it is thought that the solution conformation of the copolymer was chain extended with a greater number of accessible amide functionalities than the nonionic polymers from MeAM-co-AM-2b, NTBAM-co-

Methylene crosslinking

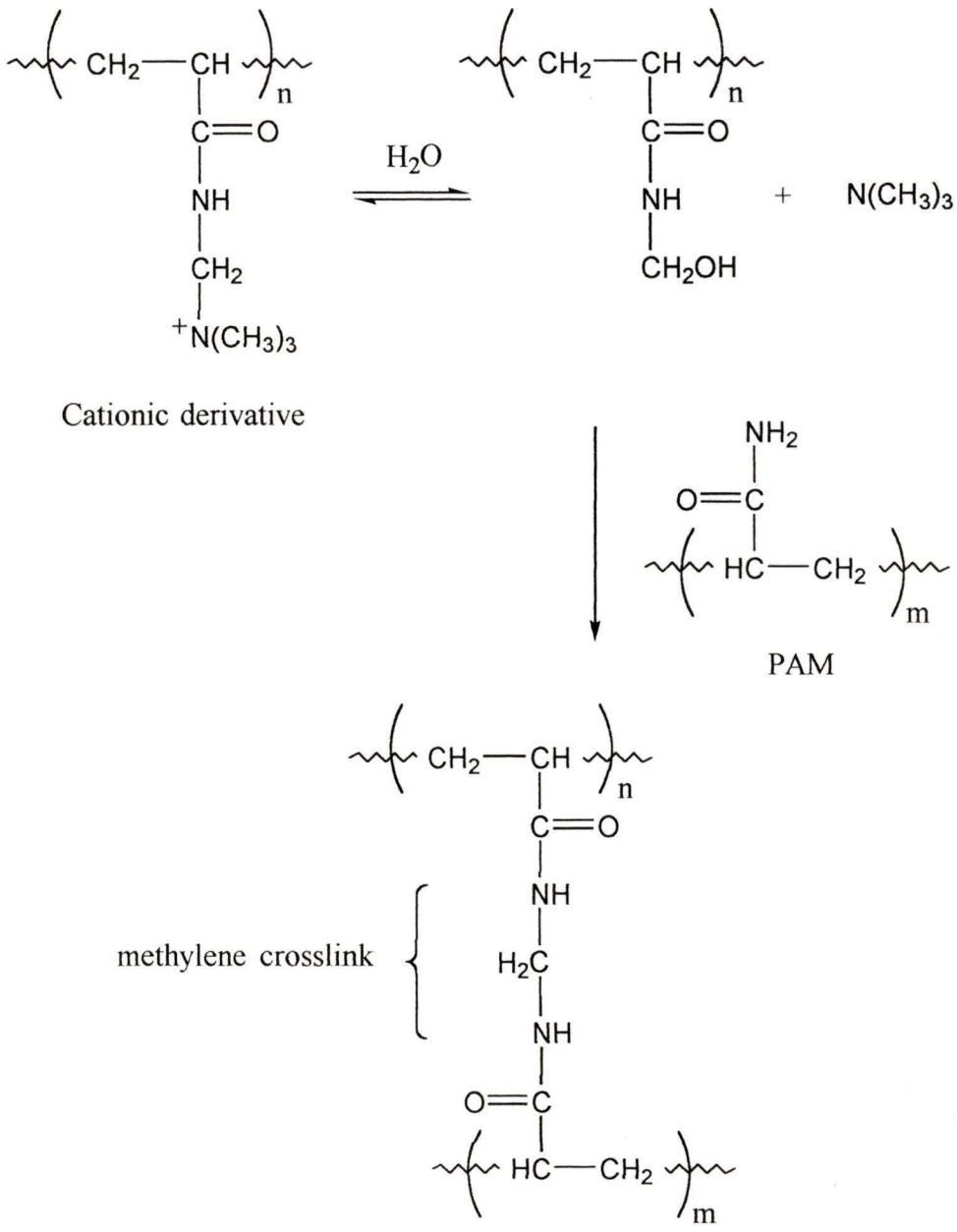

Fig. 68 Reaction scheme for methylene crosslinking of the cationic derivatives of nonionic polyacrylamides

AM-1b (clouded layer), and PAM. Easier access to the amide functionalities of the copolymer from DMAM-co-AM-7 and prior knowledge of the random coil conformation of PAM in solution are used to explain the high percentage cationicity and large [η] of the purified cationic derivative of the copolymer from DMAM-co-AM-7. Due to the much larger values of [η] for the solutions containing the purified cationic derivatives than for the solutions containing the nonionic polymers it was concluded that polymer chain extension was influenced more strongly by the incorporation of charge rather than steric bulk. In addition, the large increase in [η] for the purified cationic derivatives in comparison to the nonionic polymer precursors made apparent the limited chain extension caused by the steric bulk of the substituted acrylamide comonomers.

Higher charge densities and, therefore, greater polymer chain extensions were used to explain the larger values of [η] for the purified cationic derivatives of the copolymers from DMAM-co-AM-7, MeAM-co-AM-2b, and NTBAM-co-AM-1b (clouded layer) and PAM from control-6 than for Percol 721 (4.5 % cationicity by analysis) and Percol E-24 (10 % anionicity as given by Allied Colloids).

4.7. Evaluation of the Measurements of the Refractive Index Increments, dn/dc

Among other things, the accuracy of the M_w values depended on the accuracy of the dn/dc values which required knowledge of the copolymer microstructure. For copolymers having a heterogeneous microstructure the presence of differing scattering elements leads to an apparent molecular weight which is greater than the true M_w.[45,109] Also, the M_w values for heterogeneous polymers are not within the experimental

uncertainty of the light scattering technique for different solvent conditions. Bushuk and Benoit derived a relation to obtain the true M_w for a heterogeneous copolymer and the molecular weights of component segments from separate measurements of specific refractive index increments in three different solvents and then solving three simultaneous equations.[109] The free radical mechanism and published reactivity ratios for copolymerization of DMAM, MeAM, or NTBAM with AM suggest random microstructures and, therefore, homogeneous polymers. However, the same success for determining M_w by the method of Bushuk and Benoit for homogeneous polymers could not be assured.

Technical information provided by Wyatt Technology describes a graphical procedure for determining dn/dc from a calibration constant, dn/dV, which is obtained from a compound having an accepted dn/dc (usually NaCl). This procedure assumes a homogeneous polymer microstructure.[80,109] Since in most cases the M_w's agreed within the statistical uncertainties of MALLS for solutions of copolymers adjusted to different pH levels and electrolyte concentrations (Tables 30 to 33), calculation of dn/dc from dn/dV was justified and the copolymer microstructures were assumed to be homogeneous.

Values for dn/dc were necessary to determine M_w from the Zimm plots but were not required for $< r_g >$.[77,79] Thus, only the polymer solution standards adjusted to pH 4.00 ± 0.10 and pH 6.50 ± 0.20 without added electrolyte and those adjusted to pH 4.00 ± 0.10 with added electrolyte to give 0.001 M and 0.01 M NaCl were used to measure values for dn/dc and calculate M_w (Tables 26 to 29). Values for M_w determined from 3 sets of

polymer solution standards were judged sufficient to determine an average value of M_w for the particular polymer, within the statistical uncertainty of the MALLS technique.

In order to determine whether the polymers remained soluble in the higher electrolyte concentrations, an attempt was made to determine dn/dc and then calculate M_w for the polymer solution standards adjusted to pH 4.00 ± 0.10 with added electrolyte to give 0.1 M and 1.0 M NaCl. However, the voltages of the individual standards did not vary as the large voltages resulting from 0.1 M or 1.0 M NaCl masked any voltage contributions made by the polymer component of the solutions. Even replacing water with 0.1 M NaCl as the mobile phase did not improve the results for dn/dc as slight variations in NaCl concentration between the individual standards and the mobile phase gave greater voltage contributions than the polymer component of the solutions.

Irregularities in the plots of the individual refractive indexes of the standards versus the individual concentrations of the polymer solution standards adjusted to pH 10.00 ± 0.10 without added electrolyte were attributed to the standard pre-cleaning procedure and, in particular, filtration difficulties through the 0.45 μm hydrophobic membranes. Even though the hydrophobic membranes were converted to a hydrophilic character and the polymer solution standards were filtered at a rate was which was slower than that suggested by the manufacturer of the hydrophobic membranes, the membranes were prone to clogging. As a result of the filtration difficulties uncertainty was attached to the concentrations of the polymer solution standards adjusted to pH 10.00 ± 0.10. The corresponding M_w values were not recorded. Due to the scatter of dn/dc values for PAM determined by various authors,[95] no attempt was made to establish trends for the values

of dn/dc as a function of solvent condition. Possible explanations for the scatter of dn/dc values determined for PAM under equivalent conditions are the water content of the polymer solids used for preparation of the solution standards and aging effects.[45,75]

4.8. Solution Behaviour of Acrylamide-Based Polymers

4.8.1. Evaluation of MALLS for the study of the solution behaviour of acrylamide-based polymers

The accuracy of M_w, $< r_g >$, and A_2 depended on the method used to process the light scattering data. Of the available Debye, Berry, and Zimm methods, the method of Zimm was selected to process the light scattering data. For very high molecular weight polymers (M_w= 5,000,000 g/mol) with a radius approaching 100 nm or greater, the Zimm and Debye methods were compared in a technical publication from Wyatt Technology.[94] Whereas the Debye method required a high-order, polynomial fit degree, the Zimm method was very sensitive to the fit order and the detectors used in the fit. The fit order applies to Rayleigh theory whereby a true random coil gives light scattering data which gives a first order fit but deviation from the theoretical random coil model requires a - higher order fit degree. Whereas Debye plots did not produce good fits for any order fit degree to the light scattering data generated for the study of the solution behaviour of the acrylamide-based polymers, Zimm plots gave good fits using a polynomial fit degree of 3 (maximum fit order = 5) and ommiting detectors 2, 7, 9, 17, and 18. As further support to the use of the Zimm method, M_w's obtained for Percol 351 as solutions adjusted to pH 4.00 ± 0.10 and pH 6.50 ± 0.20 agreed within the statistical uncertainty of MALLS with M_w quoted by Allied Colloids (Table 33). This also justified the adequacy of MALLS for

the study of the solution behaviour of acrylamide-based polymers.

4.8.2. Evaluation of the solution behaviour of the acrylamide-based polymers as given by values for M_w, $< r_g >$, and A_2.

Since an objective of the acrylamide-based homopolymer and copolymer synthesis was for their function as flocculants, it is necessary to link their solution behaviour to their performance as flocculants. The solution behaviour of the polymers was interpreted by the average polymer chain extension as measured by the root mean squared radius of gyration, $< r_g >$. Complementary to the trends in $< r_g >$ were the values for the second virial coefficient, A_2. The weight average molecular weight, M_w, added further evidence to the characterization of the polymers and served as a basis on which to judge the reliability of $< r_g >$ and A_2 values which were obtained from various solvent conditions. Polymer solution concentrations in the range of 10^{-4} to 10^{-3} g/mL were used to minimize polymer chain entanglements which are known to contribute to misleading results for $< r_g >$.[1,110,111]

The individual effects of solution pH and electrolyte concentration on the average polymer chain extension were investigated for a broad range of conditions to provide relevant background information for prospective industrial uses. Since extreme pH's are unlikely for waste-water streams, test solution pH levels were limited to pH 4.00 ± 0.10, pH 6.50 ± 0.20, and pH 10.00 ± 0.10.[1,2,9,10,11] To determine the sensitivity of polymer conformation to electrolyte concentration and to mimic the high electrolyte concentrations often encountered in industry, 0.001 M, 0.01 M, 0.10 M, and 1.0 M NaCl adjusted to pH 4.00 ± 0.10 were selected for tests.[4,5,6]

4.8.3. Effect of solution pH on polymer chain extension

It has been reported that the solution conformation of PAM is insensitive to solution pH.[1,2,46] Agreement within the statistical uncertainty of MALLS for $< r_g >$ values for Percol 351 (nonionic PAM) under acidic, near neutral, and alkaline conditions confirms this claim (Table 33). Due to the filtration difficulties described previously for solution standards adjusted to pH 10.00 ± 0.10, only the $< r_g >$ values determined at acidic and near neutral pH levels for PAM from control-6 (complementary to MeAM-co-AM-6) were found to agree within the statistical uncertainty of MALLS (Table 31). It was thought that preparation and measurement of the solution standards at room temperature and the quantities of reagents used to adjust the solution standards to acidic, near neutral, and alkaline pH levels were unlikely to cause hydrolysis of PAM or interfere with the competitive hydrogen bonding by water molecules with amide groups. This was supported by nearly constant values for the solute / solvent interaction parameter, A_2, for both Percol 351 and PAM from control-6 in acidic and near neutral pH solutions.

The stability of the solution conformations of copolymers from DMAM-co-AM-2 to -7 (Table 30), MeAM-co-AM-2b to -5 (Table 31), and NTBAM-co-AM-1b (clouded layer), -1b (clear layer), and -2 (dialyzed fraction) (Table 32) to acidic, near neutral, and alkaline pH levels was credited to the substituted acrylamide component of the copolymers. Like the apolar, polymer backbone of PAM and the copolymers, it was reasoned that the water molecules became more ordered around the hydrocarbon component of the substituted acrylamide component of the copolymers. The steric bulk

of water molecule layers surrounding each hydrophobic substituent of the substituted acrylamide component of the copolymers and the hydrophobic substituents, themselves, forced a more linear rather than random coil conformation of the copolymers. In fact, the $< r_g >$ values for the copolymers from DMAM-co-AM-5 and -7 were greater than the $< r_g >$ values for PAM from control-6 (complementary to MeAM-co-AM-6) for comparable M_w's. Since comparable M_w's constitute a smaller kinetic chain length for the copolymers from DMAM-co-AM-5 and -7, the effect of steric bulk on the average polymer chain extension was significant. In relation to PAM, the steric hindrance exhibited by the substituted acrylamide component of the copolymers was reasoned as additional resistance to hydrolysis under acidic or alkaline conditions. Unlike PAM, it was rationalized that the steric hindrance of the copolymers minimized any influence to solution conformation from competitive hydrogen bonding of water molecules with the amide functionalities of the acrylamide component of the copolymers.

4.8.4. Effect of electrolyte concentration on polymer chain extension

Conflicting results have been reported for the effect of added electrolyte. As examples, Klein and Conrad[48] determined that the intrinsic viscosity of PAM decreased with increasing NaCl concentration, Eliassaf and Silberberg[112] reported that the specific viscosity of PAM was not altered by the addition of up to 3.66 N NaCl and Muller, Laine, and Fenyo[46] found that the reduced viscosity of PAM increased with increasing NaCl concentration. Here, the polymer chain extension as given by $< r_g >$ for aqueous electrolyte solutions of Percol 351 was found to decrease with increasing NaCl

concentration and then level off at high electrolyte concentrations. However, the $< r_g >$ values for aqueous electrolyte solutions of PAM from control-6 (complementary to MeAM-co-AM-6) increased with increasing NaCl concentration. Agreement within the statistical uncertainty of MALLS was obtained for M_w's for solutions of Percol 351 (nonionic PAM) with and without added electrolyte and poor agreement for M_w's for solutions of PAM from control-6 with and without added electrolyte. These results favour a decrease in $< r_g >$ values with increasing NaCl concentration. The poor agreement of M_w's for solutions of PAM from control-6 with or without added electrolyte may be due to polymer chain entanglements, which can persist in aqueous solvent for weeks but usually disappear in aqueous electrolyte solutions.[111] A decrease in [η] and $< r_g >$ values with increasing NaCl concentration is explained by dehydration of the amide dipole of PAM to release sufficient water molecules for solvation of added NaCl.[42] A more coiled conformation results from removal of water molecules from the amide dipole.[40]

Unlike the variation in $< r_g >$ values with increasing NaCl concentration for Percol 351 and PAM from control-6, $< r_g >$ values for the newly synthesized acrylamide-based polymers were less sensitive to NaCl concentration and in most cases insensitive, within the statistical uncertainty of MALLS. This is attributed to the dependence of the solution conformation on the steric constraints of the substituted acrylamide comonomers and the insensitivity of the steric bulk to electrolyte concentration. Like the polymer backbone, the steric bulk of the substituted acrylamide comonomers is hydrophobic which causes greater ordering of water molecules around the hydrophobic substituents. This ordering

around the hydrophobic substituents causes depletion of electrolyte from their vicinity and is probably responsible for the insensitivity of the acrylamide-based polymers to electrolyte concentration. Unlike the more coiled conformation of PAM at higher NaCl concentrations, dehydration of the amide dipole of the acrylamide component of the copolymers at higher NaCl concentrations apparently has an insignificant effect on the copolymer conformation.

4.8.5. Trends in M_w, $< r_g >$, and A_2 from MALLS and in [η] from viscometry

As a result of the kinetic differences between each of the comonomers and AM such as the ratio, $k_p/(k_t)^{0.5}$, and differences in reactivity as exhibited by the reactivity ratios, the number average degree of polymerization, X_n, was expected to vary for each set of copolymers. Therefore, the trends in M_w, $< r_g >$, and A_2 values from MALLS and in [η] from viscometry would be related to the copolymer composition as well as X_n. However, the significance of X_n was expected to be minimal in comparison to copolymer composition due to high M_w's and their effect to minimize the significance of changes in X_n. Assuming a narrow molecular weight distribution which does not vary appreciably for a particular set of copolymers, an estimate of X_n was obtained by substituting M_w for M_n in the following equation.

$$X_n = \frac{\left(\frac{\%\ M_1}{100}\right)}{AW\ (M_1)} M_n + \frac{\left(\frac{\%\ M_2}{100}\right)}{AW\ (M_2)} M_n \qquad \text{Eq. 49}$$

where M_n is the number average molecular weight.

$\% M_1$ is the mole % of component 1 of the copolymer.

$\% M_2$ is the mole % of component 2 of the copolymer.

$AW(M_1)$ is the atomic weight of component 1.

$AW(M_2)$ is the atomic weight of component 2.

The estimated values of X_n for the copolymers from DMAM-co-AM-2 to -5 and -7 (Table 36), MeAM-co-AM-2b to -5 (Table 37), NTBAM-co-AM-1b (clouded layer), -1b (clear layer), and -2 (dialyzed fraction) (Table 38) showed significant differences within a copolymer series and even more significant differences between copolymer types. Therefore, the trends in M_w, $< r_g >$, and A_2 values from MALLS and in [η] from viscometry were dependent on copolymer composition as well as X_n.

Commercial polymers

The inadequacy of MALLS for the study of the solution behaviour of polyelectrolytes in electrolyte-free solvents was attributed to the small contribution of the polyelectrolyte to detector voltages at acceptable concentrations (10^{-4} to 10^{-3} g/mL). At higher polyelectrolyte concentrations which gave adequate detector voltages, the polyelectrolyte standard solutions were too viscous to permit acceptable pre-cleaning. It was thought that higher polyelectrolyte concentrations were necessary to overcome low local concentration levels resulting from the repulsive interactions between individual polyelectrolyte chains. As shown by the individual statistical uncertainties of M_w for Percol 721 (cationic PAM) and Percol E-24 (anionic PAM) in 0.001 M NaCl (Table 33), higher electrolyte concentrations such as 0.01 M NaCl were necessary to obtain M_w

Table 36 Estimated X_n values for the copolymers from DMAM-co-AM-2 to -5 and -7

Experiment	Copolymer composition [a] (mol % DMAM)	$M_w \times E+06$ [b] (g/mol)	$X_n \times E+05$
DMAM-co-AM-2	23.6	7.71 ± 0.4	1.01 ± .10
DMAM-co-AM-3	43.3	6.71 ± 0.3	0.83 ± .07
DMAM-co-AM-4	62.9	12.1 ± 0.9	1.40 ± .21
DMAM-co-AM-5	81.3	18.8 ± 0.2	2.04 ± .04
DMAM-co-AM-7	14.3	19.1 ± 3.5	2.58 ± .95

a. As determined by elemental analysis (Table 22).
b. Each M_w value was the average of those determined by MALLS for various solvent conditions (Table 30).

Table 37 Estimated X_n values for the copolymers from MeAM-co-AM-2b to -5 and PAM from control-6

Experiment	Copolymer composition [a] (mol % MeAM)	$M_w \times E+06$ [b] (g/mol)	$X_n \times E+04$
MeAM-co-AM-2b	5.7	4.30 ± 0.40	5.99 ± 1.10
MeAM-co-AM-3	33.0	1.46 ± 0.05	1.94 ± 0.13
MeAM-co-AM-4	51.1	1.58 ± 0.07	2.03 ± 0.18
MeAM-co-AM-5	83.0	0.90 ± 0.05	1.09 ± 0.12
control-6	0	11.2 ± 0.31	15.76 ± 0.87

a. As determined by elemental analysis (Table 23).
b. Each M_w value was the average of those determined by MALLS for various solvent conditions (Table 31).

Table 38 Estimated X_n values for the copolymers from NTBAM-co-AM-1b (clouded layer), -1b (clear layer), and -2 (dialyzed fraction)

Experiment	Copolymer composition [a] (mol % NTBAM)	$M_w \times$ E+06 [b] (g/mol)	$X_n \times$ E+04
NTBAM-co-AM-1b (clouded layer)	15.3	4.50 ± 0.33	5.90 ± 0.87
NTBAM-co-AM-1b (clear layer)	21.6	3.25 ± 0.27	4.14 ± 0.69
NTBAM-co-AM-2 (dialyzed fraction)	35.7	4.08 ± 0.19	4.84 ± 0.45

a. As determined by ^{13}C NMR integration (Table 24).
b. Each M_w value was the average of those determined by MALLS for various solvent conditions (Table 32).

Table 39 Estimated X_n values for the commercial polymers, Percol 351, Percol 721, and Percol E-24

Experiment	Polymer Composition (mol % charged groups)	$M_w \times$ E+06 [c] (g/mol)	$X_n \times$ E+05
Percol 351 (nonionic PAM)	0	17.2 ± 3.0	2.42 ± 0.56
Percol 721 (cationic PAM)	4.5 [a]	19.7 ± 5.0	2.70 ± 1.37
Percol E-24 (anionic PAM)	10 [b]	11.4 ± 4.0 [d]	1.60 ± 1.12

a. As determined by colloid titration.
b. As quoted by Allied Colloids.
c. Each M_w value was the average of those determined by MALLS for various solvent conditions (Table 33).
d. The M_w value determined for solution standards in 0.01 M NaCl was used.

values with reasonable statistical uncertainties.

The higher values of $< r_g >$ for cationic PAM and anionic PAM than for nonionic PAM in 0.001 M and higher values of [η] for cationic PAM and anionic PAM than for nonionic PAM in deionized water emphasized the effect of charged groups on the average polymer chain extension. In fact, near equivalent values of X_n for Percol 351 and Percol 721 and a slightly lower value of X_n for Percol E-24 (Table 39) added further support to the impact of charged groups on the average polymer chain extension. The sensitivity of polyelectrolytes to NaCl concentration was displayed by the larger decrease in $< r_g >$ values for Percol 721 and Percol E-24, than for Percol 351.

Due to the dependence of A_2 values on M_w and the poor agreement between the M_w's for Percol 721 and Percol E-24 in 0.001 M NaCl and M_w quoted by Allied Colloids, only the A_2 values determined for Percol 721 and Percol E-24 in 0.01 M NaCl were compared with the A_2 values for Percol 351. The larger A_2 values for Percol 721 and Percol E-24 than for Percol 351 are attributed to the greater interaction of the solvent ions with the charged groups of polyelectrolytes than amide dipoles of nonionic macromolecules as evidenced by the large decrease in $< r_g >$ values of both Percol 721 and Percol E-24 with increasing salt concentration.

Copolymers of DMAM with AM

The increased M_w's for increasing proportions of DMAM in the copolymers from DMAM-co-AM-2 to -5 were attributed to the greater contribution to M_w by increasing proportions of DMAM in the copolymers and to increased values of X_n (Table 36).

Increased values of X_n were not expected for increasing proportions of DMAM in the copolymers, as $k_p/(k_t)^{0.5}$ and, therefore, X_n for homopolymerization of AM was reported to be at least twice that for homopolymerization of DMAM.[13,15] In addition, the reactivity ratios ($r_1 = 0.78 \pm 0.03$ and $r_2 = 1.10 \pm 0.04$ for AM as M_1 with DMAM as M_2) favoured incorporation of DMAM into the copolymers.[18] Since chain transfer to monomer was the dominant mechanism for limiting M_w for polyacrylamide,[113] it was reasoned that the steric hindrance imparted by DMAM and / or polymer chains ending with the DMAM radical impeded chain transfer to monomer. This was more significant to a greater X_n for the copolymers than the slightly lowerer reactivity of polymer chains ending with the DMAM radical was to limiting X_n for the copolymers, as the proportion of DMAM increased in the copolymerization feedstock. However, the high value of M_w for the copolymer from DMAM-co-AM-7 which had the lowest proportion of DMAM in the copolymerization feedstock suggested that only when there were higher proportions of DMAM in the feedstock did this offset the greater radical reactivity of polymer chains ending with the AM radical.

Since the copolymer composition and, therefore, X_n varied for each copolymer of a particular set, it was difficult to determine which variable had the greatest impact on $< r_g >$ and [η]. However, the slight difference in $< r_g >$ values for the copolymers from DMAM-co-AM-5 and -7 (Table 30) for X_n values which overlapped by their uncertainties and for a large difference in copolymer composition suggested that increasing amounts of steric bulk rendered less effect on the magnitude of $< r_g >$ and [η]. Whereas the trend in $< r_g >$ values paralleled the trend in X_n, non-Newtonian effects for high molecular

weight polymers could possibly explain the low value of [η] relative to the trend in X_n observed for the copolymer from DMAM-co-AM-5. Unless the random coil conformation of PAM in 0.1 M NaCl was considered,[40] it was difficult to understand the lower value of [η] for PAM from control-6 (complementary to MeAM-co-AM-6) than for the copolymers.

Decreasing values of A_2 for increased proportions of DMAM in the copolymers from DMAM-co-AM-2 to -5 (Table 30) were attributed to the hydrophobic nature of the DMAM component of the copolymers. Polymer chain entanglement was considered a possible explanation for the low value of A_2 for the copolymer from DMAM-co-AM-7 which contained the lowest proportion of DMAM. Although not proven, polymer chain entanglement may also explain the high value of $< r_g >$ and [η] for the copolymer from DMAM-co-AM-7.

Copolymers of MeAM with AM

The contribution to M_w for each MeAM component of the copolymers was greater than that of each AM component. Therefore, decreased M_w's for an increasing proportion of MeAM in the copolymers from MeAM-co-AM-2b to -5 are attributed to decreased values of X_n (Table 37). The decreased values of X_n could have resulted from the much lower value of $k_p/(k_t)^{0.5}$ and, therefore, X_n for homopolymerization of MeAM than for homopolymerization of AM, as described previously. In addition, the copolymerization reactivity ratios ($r_1 = 0.74 \pm 0.11$ and $r_2 = 1.1 \pm 0.20$ for AM as M_1 with MeAM as M_2) favoured incorporation of MeAM into the copolymers.[1,114] Further

evidence of decreased values of X_n for a greater proportion of MeAM in the copolymerization feedstocks was obtained from the greater value of the constant for chain transfer to monomer of MeAM than the constant for chain transfer to monomer of AM.[13,15] The resonance stabilized structure for chain transfer to monomer of MeAM[66] and the greater reactivity of polymer chains ending with the AM radical than chains ending with the MeAM radical were recognized by the large difference in magnitude between M_w's for the copolymers from MeAM-co-AM-2b to -5 and the PAM from control-6 (complementary to MeAM-co-AM-6) (Table 31).

Since the steric interactions of the methyl-substituted, α-carbon atoms of MeAM were expected to increase the average polymer chain extension of the copolymers with respect to the average polymer chain extension of PAM, the decreased values of $< r_g >$ (Table 31) and [η] (Table 19) as the proportion of MeAM in the copolymers increased are attributed to decreased values of X_n (Table 37).

Since methyl substitution of the α-carbon atoms in MeAM does not suggest any significant change to solute / solvent interaction with respect to AM, branching or imidization could explain the decrease in A_2 values as the proportion of MeAM in the copolymers increased (Table 31). Equivalent values of A_2 for both electrolyte-free and electrolyte-containing solutions for the copolymers from MeAM-co-AM-2b to -5 suggests a structural modification like imidization or branching rather than polymer chain entanglement which disappears in electrolyte-containing solutions.[111]

Copolymers of NTBAM with AM

Since $k_p/(k_t)^{0.5}$ and, therefore, X_n were reported to be 7 times greater for homopolymerization of AM than for homopolymerization of NTBAM, the lower value of M_w for the copolymer from NTBAM-co-AM-1b (clear layer) than that for the copolymer from -1b (clouded layer) was attributed to a lower value of X_n for the copolymer from -1b (clear layer) (Table 38). It was reasoned that the lower value of X_n for the copolymer from -1b (clear layer) resulted from the higher proportion of NTBAM in -1b (clear layer) than in -1b (clouded layer) and the associated lower reactivity of polymer chains ending with the NTBAM radical than polymer chains ending with the AM radical. In addition, it was thought that the steric hindrance imparted by NTBAM impeded chain transfer to monomer. This was insignificant to increasing X_n for the copolymers relative to the much lower reactivity of polymer chains ending with the NTBAM radical than AM was to limiting X_n for the copolymers, as the proportion of NTBAM increased in the copolymerization feedstock. Comparable values of X_n and M_w for the copolymer from NTBAM-co-AM-2 (dialyzed fraction) which had a higher proportion of NTBAM in the copolymer to those for the copolymers from -1b (clear layer) and -1b (clouded layer) is rationalized by noting that dialysis of the copolymer from -2 removed low molecular weight material.

The similarity between $< r_g >$ values (Table 32) and the similarity between [η] values (Table 20) for the copolymers from NTBAM-co-AM-1b (clear layer), -1b (clouded layer), and -2 (dialyzed fraction) is attributed to similar values of X_n and the diminishing effect of steric bulk on polymer chain extension.

The lower values of A_2 (Table 32) for increasing proportions of NTBAM in the copolymers from NTBAM-co-AM-1b (clear layer), -1b (clouded layer), and -2 (dialyzed fraction) is credited to the hydrophobicity of the t-butyl substituent. Also, the steric bulk of the t-butyl substituent could interfere with hydrogen bonding by water molecules with the amide dipole of the AM component of the copolymers.

4.9. Flocculation

4.9.1. Development of a flocculation test procedure

To evaluate the performance of the acrylamide-based polymers as flocculants and link this performance to their solution behaviour, a reproducible test procedure was required which was sensitive to polymer structure and the average polymer chain extension. This required careful consideration of the chemical and physical variables associated with flocculation and their relation to flocculation performance.

Selection and modification of the flocculation test medium

Many authors prefer kaolinite as a flocculation test medium.[115-121] Thus, kaolinite has been studied extensively so that its chemistry with respect to solution behaviour is well understood.[57,70,122,123] Kaolinite is the most common clay mineral of the kaolin group of minerals. By classification as a "clay", kaolinite belongs to the fraction of soil with particles less than 2 μm in diameter. It has the 1:1 layered structure common to the kaolin group, and comprises a layer of silicon oxygen tetrahedra joined by one of the four oxygen atoms of each tetrahedron or a hydroxyl group to a layer of aluminum oxygen-hydroxyl octahedra (Fig. 69). Van der Waals attractive forces, electrostatic interactions,

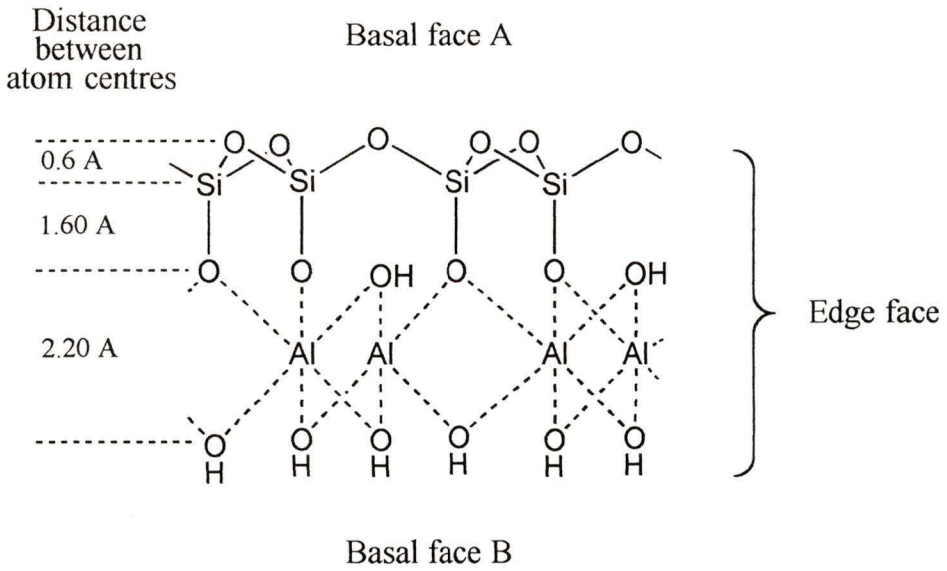

Fig. 69 Atom arrangement in the unit cell of a 1:1 layer mineral

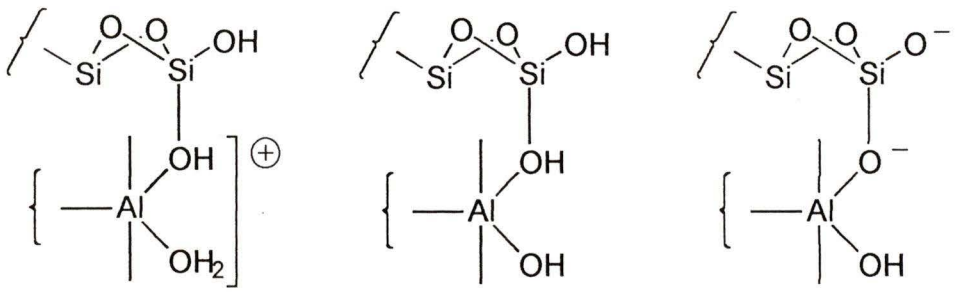

Fig. 70 Variations in edge face charge characteristics with solution pH for the edge face of kaolinite

and hydrogen bonding are responsible for binding together several 1:1 aluminosilicate layers. Cleavage parallel to the 1:1 aluminosilicate layers gives hexagonal platelets (fine material) or vermicular stacks (coarse material) as the characteristic kaolinite particles.

In aqueous solution the net charge on the kaolinite particles is negative due to isomorphic substitution within the lattice and broken bonds on the edge of the crystal. Possible substitution of Si^{4+} by Al^{3+} and limited substitution of Al^{3+} by Fe^{2+} or Mg^{2+} gives only a slight negative charge to the silicon oxygen tetrahedra surface (basal face A) of the kaolinite layer (see Fig. 69). Studies have confirmed that the basal face A of the kaolinite layer is not hydrated in an aqueous medium.[120] Conversely, the aluminum oxygen-hydroxyl octahedra surface (basal face B) of the kaolinite layer is hydrated in an aqueous medium. Silica and alumina are exposed at the broken edges of the kaolinite particles. Under acidic conditions ($pH < 5$) the edges of the kaolinite particles are positively charged owing to protonation of the aluminol units. Above pH 8 the aluminol and silanol units are deprotonated which yields a net negative charge to the edges of the kaolinite particles. Between pH 5 and pH 8 the edges of the kaolinite particles are considered neutral in charge. Variations in charge characteristics of the edge face of kaolinite under acidic, neutral, and alkaline conditions are shown in Fig. 70.

To evaluate the performance of the acrylamide-based polymers as flocculants, it was necessary to ensure that the flocculation test medium was consistent for every test. In addition, it was necessary to ensure that the polymers were unhindered for function as flocculants within the test medium. Crude kaolinite is known to contain counterions such as Al^{3+}, Fe^{2+}, or Mg^{2+}.[120,123] A study confirmed that the presence of counterions

(Al^{3+}, Fe^{3+}, or H^+) at the basal face A of kaolinite caused ion exchange with hydrogen atoms involved in intramolecular hydrogen bonding.[120] The same study reported that the presence of Na^+ as the counterion at the basal face A of kaolinite did not cause ion exchange with bound hydrogen atoms. Since the acrylamide-based polymers were susceptible to protonation by hydrogen atoms which could be made available by ion exchange, the heteroionic kaolinite was converted to Na-kaolinite by the method of van Olphen, as described previously. As a final requirement of the procedure for conversion of heterionic kaolinite to Na-kaolinite, the NaCl concentration in the supernatant of the Na-kaolinite slurry was reduced to 1.138×10^{-4} M to minimize adsorption of Na^+ on the basal face A while preventing hydrolysis in an aqueous medium.[120] By minimizing the possibility for polymer-clay and solvent-clay interactions at the basal face A of Na-kaolinite, the edges of the Na-kaolinite particles were isolated as the site for polymer-clay interactions. The basal face B of the clay was not expected to interact with the acrylamide-based polymers since efficient hydrogen bonding of the hexagonal array of aluminol groups with water precluded any further interaction.[120]

Suitability of the test medium for bridging flocculation

Based on several studies which involved kaolinite as the flocculation test medium, preliminary flocculation test-work included a 3% (w/w) Na-kaolinite test medium.[115] Having measured the pH of the 3% Na-kaolinite test medium as 7.0 ± 0.2 in deionized water, it was recognized from other studies that at neutral pH the edges of the clay particles were prone to intramolecular hydrogen bonding.[120] For adsorption of the

acrylamide-based polymers to the edges of the clay particles, the intramolecular hydrogen bonding of the clay provided competition for the hydrogen bonding ability of the acrylamide-based polymers. It was reasoned that competitive hydrogen bonding would hinder bridging flocculation but enhance the sensitivity of the evaluation techniques to polymer structure and the average polymer chain extension. In addition, an isoelectronic point at pH 2.7 for the Na-kaolinite used in this research as well as the low electrolyte concentration (1.138×10^{-4} M NaCl) suggested only minimal contribution to flocculation from face-face and edge-face agglomeration.[70,120]

The average plate diameter was not measured for the Na-kaolinite used for this research. However, it was assumed from reasonable agreement between the BET surface area of this Na-kaolinite and that of the Na-kaolinite which originated from Kaolin des Charentes that the average plate diameters were similar.[89] Having an estimate of the average plate diameter (0.21 μm) and edge thickness (0.04 μm) and knowing the approximate thickness of the electric double layer accompanying each Na-kaolinite particle, it was possible to estimate the length of polymer which was necessary for bridging flocculation. It was reported that the thickness of the electric double layer varied from 1 to 100 nm in an aqueous medium, depending on the electrolyte concentration.[50,51] Assuming that adsorption of nonionic, acrylamide-based polymers increased the double layer thickness by displacing the counterions of the Stern layer into the diffuse layer,[51] the high limit of double layer thickness (100 nm) required polymer loops or trains to extend 200 nm for bridging flocculation. Due to little shielding of the electrostatic repulsive forces between Na-kaolinite particles in an aqueous solution

containing a low electrolyte concentration, it was reasoned that Brownian motion could bring Na-kaolinite particles to the point of contact of the electric double layers. Even though this approximation represents the high limit for polymer chain extension, many of the nonionic, acrylamide-based polymers exhibited sufficient average polymer chain extensions to permit bridging. Although bridging flocculation may not have been the dominant flocculation mechanism for acrylamide-based polyelectrolytes, the average polymer chain extensions of the tested polyelectrolytes were sufficient to extend beyond 200 nm.

By assuming a perfect hexagon for the Na-kaolinite platelets and using the platelet dimensions of the Na-kaolinite from Kaolin des Charentes, the number of Na-kaolinite particles and volume per particle in the 3% Na-kaolinite test medium were calculated. Calculation of the number of water molecules and volume per molecule in the 3 % Na-kaolinite test medium indicated a volume of water molecules per Na-kaolinite particle nearly 100 times greater than that of a single Na-kaolinite particle. Thus, the dilute conditions of the 3 % Na-kaolinite test medium were sufficient to accommodate even the theoretical high limit of double layer thickness without any problem of double layer overlap.

Equipment for flocculation tests

The ASTM standard flocculation test (D2035-80) describes instantaneous addition of the flocculant to a stirred test medium and the ISO/CD standard test (10086-1) uses instantaneous addition of the flocculant to a still test medium and then mixing of the

flocculant and test medium. Although both standard tests were easy to use, Hogg showed that good mixing and the addition of the flocculant over a prescribed duration increased the probability for uniform contact of the flocculant with the test medium and decreased the probability for surface saturation of colloidal particles.[115] In addition, Hogg's procedure focussed on the chemical and physical variables associated with flocculation such as flocculant dosage, flocculant addition rate, agitation rate during flocculant addition, and agitation rate and extent following flocculant addition.

In accordance with Hogg's procedure a standard mixing tank described by Holland and Chapman was constructed for the flocculation test-work based on the engineering requirements for mixing and scale-up.[71] The tank was fitted with baffles to suppress vortexing, maintain a constant liquid level, and ensure uniform turbulence throughout the test medium. By using a low percent solids test medium which was added to give a solution volume equivalent in height to the tank diameter and careful alignment of the six-bladed turbine impeller to rest above the tank bottom a height equivalent to the impeller diameter, the fluid dynamic behaviour of the stirred test medium matched that described by Holland and Chapman. The injection point of the polymer solution into the test medium (Fig. 8) was a region of high turbulence in which mixing of the polymer solution with the test medium would be rapid.[71,125]

Although Hogg's test procedure appeared to be very scientific with respect to the chemical and physical variables associated with flocculation, the injected volume of polymer solution and the associated concentration changes were not defined. Industrial scale-up favours a low injection volume,[125] whereas polymer chain entanglement effects

favours dilute concentrations.[1,111] Since the purpose of the flocculation test-work was to evaluate flocculant performance as attributable to polymer chain extension, polymer solutions were prepared as 10^{-4} to 10^{-3} g/mL concentrations and added as 10 mL volumes to minimize polymer chain entanglement.

Evaluation of the chemical and physical variables associated with the flocculation test procedure using a 3% Na-kaolinite test medium

By preparation of the 3% Na-kaolinite test medium on a 10 litre scale, and resuspension and then settling of the test medium every 24 hours for 10 days, a sufficient volume of homogeneous and completely hydrated test medium was made available for the preliminary test-work.[115,126]

To determine the physical and chemical parameters most suitable for evaluating the flocculation performance of the newly synthesized, acrylamide-based polymers and commercial polymers, tests were run to investigate the effects of polymer dosage, agitation rate, and addition rate on flocculation efficiency (Figs. 44 to 46). Since the results of polymer synthesis and polymer solution behaviour were gauged against PAM, PAM from control-6 (complementary to MeAM-co-AM-6) was used as the control test reagent for the flocculation study. As reported by Hogg for flocculation tests involving acrylamide-based polymers and 3% Na-kaolinite, 1000 rpm agitation and flocculant addition over 60 seconds were considered suitable initial conditions for tests.[115]

Effect of polymer concentration on flocculation efficiency

Although flocculant addition improved the flocculation efficiency of 3% Na-

kaolinite, the effect of polymer dosage on the average settling rates did not follow the expected pattern (Fig. 44). The average settling rate was expected to increase with increasing polymer dosage to a maximum value and then decrease with further increases in polymer dosage. At high polymer dosages the clay particles were expected to be covered by polymer sheaths which usually favoured repulsion at close proximities (steric stabilization).[50,51,59,60] Even though the range of polymer dosages approximated the flocculant dosages recommended by Allied Colloids for Percol 351 (nonionic PAM), it was possible that this range was too narrow to observe a decrease in average settling rate at higher polymer dosages. However, it was reported that the thickness of the polymer sheath influenced the nature of van der Waals and electrostatic forces between particles, and the goodness of the solvent for the polymers affected the osmotic pressure within the overlap region of contact polymer sheaths.[51,60] Therefore, it is possible that a combination of factors were responsible for the observed trend in the average settling rates.

Effect of agitation rate on flocculation efficiency

The effects of agitation rate on flocculation efficiency were investigated for tests which used the desired agitation rate only for the time during which flocculant was being added to the test medium (Fig. 45). It is accepted that agitation following flocculant addition causes mainly degradation of the floc.[115,125]

Based on the classification of tip speeds for a low solids content medium (i.e. 3% Na-kaolinite), the agitation rates of 500, 750, 1000, and 1250 rpm were classified as very

low, low, medium, and high agitation, respectively.[71] Even though medium to high agitation rates were necessary for uniform distribution of the polymer within the test medium, it was reasoned that the lower shearing forces at 500 rpm agitation were responsible for the larger flocs. Therefore, higher average settling rates were observed for flocculation tests which used 500 rpm agitation.

Effect of addition rate on flocculation efficiency

Lower average settling rates were observed for flocculant addition over 30 seconds and 90 seconds than for flocculant addition over 60 seconds (Fig. 46). This is attributed to a more variable distribution of the polymer within the test medium for flocculant addition over 30 seconds and the higher probability for floc degradation for flocculant addition over 90 seconds. For the short additions it was thought that some clay particles would receive greater polymer coverage than others and, therefore, steric stabilization. Flocculant addition over 90 seconds would increase the duration of exposure of the growing flocs to shearing forces.

Sensitivity of the flocculation test procedure to polymer chain extension

For copolymers from MeAM-co-AM-2b to -4 and control PAM

The chemical and physical parameters used for the flocculation tests using the copolymers from MeAM-co-AM-2b to -4 and PAM from control-6 (complementary to MeAM-co-AM-6) did not include the optimum values determined previously, because it was thought that a set of parameters which simply obtained flocculation, rather than optimized flocculation, were better suited to the test procedure being sensitive to

polymer chain extension. This reasoning complements the use of the Na-kaolinite test medium at neutral pH to hinder bridging flocculation by allowing competitive hydrogen bonding between the hydroxyl functionalities of the clay for themselves and polymer for hydroxyl functionalities at the edge face, as described previously.

The average settling rates, supernatant turbidities, and capillary suction times showed trends which were representative of the sensitivity of bridging flocculation to polymer chain extension (Table 34). The lower average settling rates for the copolymers from MeAM-co-AM-3 and -4 than for untreated 3% Na-kaolinite were attributed to the insufficient average polymer chain extension of these for bridging flocculation. Imidization or branching of these copolymers, as suggested previously, could also reduce hydrogen bonding of the copolymers to the clay particles.

For commercial PAM from Polysciences and control PAM

It was realized that the varied composition and, therefore, the structure of the copolymers from MeAM-co-AM-2b to -4 may have affected the flocculation performance. Therefore, PAM (5E+05 MW, Polysciences) and PAM from control-6 (complementary to MeAM-co-AM-6, 5E+06 to 10E+06 MW) were used to test the sensitivity of the flocculation test procedure to only the average polymer chain extension. A 1% Na-kaolinite suspension was used in place of 3 % to hinder bridging flocculation to obtain greater sensitivity of the test to the average polymer chain extension. Polymer concentration was also varied from 0 to 1000 ppm to determine the effect of polymer dosage on the average settling rates of 1% Na-kaolinite.

Since dilution of the 3% Na-kaolinite test medium to 1% did not produce flocculated slurries which showed lower average settling rates for higher polymer concentrations beyond the maximum average settling rate (Figs. 47 to 49), the same explanations apply which were given for the tests which used 3% Na-kaolinite. Further to this explanation, the isoelectronic point of the edges of the Na-kaolinite particles has been reported to be equivalent to the natural pH of the Na-kaolinite test medium (pH 7.0).[70,120] Therefore, it is possible that edge to edge agglomeration contributed to the flocculation efficiency. However, this would depend on the affinity of a particle edge for another particle edge, in competition with hydrogen bonding to added polymer. Even though the increases in average settling rate at low polymer dosages indicate a preference of the particle edge for polymer, it was thought that at high polymer dosages the probability for edge-edge agglomeration may be increased by polymer-polymer association (so called incipient flocculation).[49-51,60] Support for this reasoning came from the persistence of polymer to polymer association reported for an electrolyte free solution.[1,111] However, the likelihood of edge to edge agglomeration occurring in the presence of double layer repulsion between basal surfaces was questioned with respect to the small specific surface area of the edge in relation to the surface area of the basal face of the Na-kaolinite particles.[120]

Even though dilution of the 3% Na-kaolinite test medium to a 1% Na-kaolinite test medium did not give the expected trend for the average settling rates at very high polymer dosages, the large differences in average settling rates and supernatant turbidities recorded for polymer dosages between 0 and 100 ppm for each PAM and

between the PAM's is consistent with a sensitivity of the flocculation test procedure to the average polymer chain extension and to at least initial increases in polymer dosage (Figs. 47 to 52).

Suitability of the evaluation techniques for the flocculation test procedure

Settling rate, sediment volume, and supernatant turbidity are used to evaluate the performance of polymeric flocculants by the ASTM standard test (D2035-80),[67] the ISO/CD standard test (10086-1),[68] and in many literature studies.[115-121] This research used the same evaluation techniques to make comparisons possible. A capillary suction time instrument was also available, so this additional information was also collected to evaluate flocculant performance.

Settling rate

The settling of a flocculated system is classified as zone or line sedimentation based on settling rates which are independent of particle size.[127] As the particles of the dispersion medium become compacted by the weight of the particles lying above them, the classification as zone or line sedimentation is replaced by compression. The interface height was recorded as a function of time for the flocculated slurry in the settling tank, a 250 mL graduated cylinder. There was an initial induction period of increasing settling rate which was followed by a constant rate period and then by the compression point as defined by decreasing settling rates.

The average settling rates for this research were calculated as the initial average, average to compaction, and average settling rate to include the various stages of settling.

The volume height limits for calculation of the initial average settling rate varied due to the induction period for interface formation between the settling slurry and the less turbid supernatant. In many cases the interface formed quite rapidly and usually as an uneven surface. Even though the average to compaction settling rate and the average settling rate were calculated for constant volume heights for successive tests, the average settling rate, which included the induction period, constant rate period, and compression point was considered more representative of each flocculating system. Therefore, the average settling rate was the only record of settling rate for future flocculation tests. It was reasoned that no information would be lost by reporting only the average settling rate since trends in the initial, average to compaction, and average settling rate as functions of polymer concentration were equivalent.

Even though much consideration was given to the sensitivity of the flocculation test procedure to the average polymer chain extension, reproducibility of the average settling rate was necessary to link the flocculation performance to the average polymer chain extension with certainty. The average settling rates for the treated (control PAM) and untreated 1% Na-kaolinite were considered reproducible, since the percentage difference of the average settling rates from their respective mean values was $\leq$ 5 % for flocculation tests performed within a few to several days of each other. However, the comparison between average settling rates was restricted to tests performed within a few days of each other because the percentage difference from the respective mean values was nearly 15 % for flocculation tests performed within a few months of each other.

Supernatant turbidity

The supernatant turbidities were relative measurements rather than absolute, since supernatant turbidities for this research were not measured against a standard with a known concentration. Whereas higher average settling rates are generally attributed to floc size, lower supernatant turbidities are generally attributed to the floc density.[125,128] Since floc size and floc density are inversely related with respect to the average settling rate or supernatant turbidity, any attempt to maximize the average settling rate would sacrifice the clearity of the supernatant and vice versa.

Similar to the average settling rates, the supernatant turbidities for the treated (control PAM) and untreated Na-kaolinite were considered reproducible when measured within a few days of each other, but not when measured a few months apart. Aging effects of the 1% Na-kaolinite test medium involving hydrolysis of the clay probably explain the differences in supernatant turbidities and settling rates over a period of a few months.[126]

Sediment volume

It was thought that additional information concerning floc density and floc size could be obtained from sediment volume. Whereas increased floc density is expected to favour a lower sediment volume, increased floc size is expected to favour a higher sediment volume. In either case, the sediment volume of a flocculated suspension was greater than the sediment volume of the untreated test medium. The sensitivity of sediment volume to floc size and floc density was examined to see if it could provide

information concerning the average polymer chain extension and the flexibility of polymer chains. Whereas increased average polymer chain extension should favour floc size and, therefore, a higher sediment volume, greater flexibility of the polymer chains should favour floc density and, therefore, a lower sediment volume.

The low percentage of solids in the flocculation test medium combined with the concave bottom of the settling tank (a 250 mL graduated cylinder) made it difficult to measure 30 minute sediment volumes. Therefore, it was not possible to establish trends with respect to the average polymer chain extension and the flexibility of polymer chains. Sediment volume was not recorded in further flocculation tests.

Capillary suction time

Capillary suction time is representative of the filterability of a slurry. For a flocculated slurry, the filterability can be related to the floc size and floc density. Whereas increased floc size is expected to favour a lower capillary suction time, increased floc density is expected to favour a higher capillary suction time. Capillary suction time (CST) can also be related to floc strength with respect to the shear and / or compressive stresses of filtration.[72,127]

Since the flocculated slurry contained a low percentage of solids, a funnel was attached to the central metal reservoir of the CST apparatus and a larger volume of flocculated slurry was added than held by the central metal reservoir. An exact volume of flocculated slurry was not required to measure the capillary suction times because the hydrostatic pressure exerted on the volume of flocculated slurry added to the central

metal reservoir was quoted as 40 times less than the capillary suction pressure of Whatman No.17 absorbant paper.[72]

Trends in capillary suction time and average settling rate are usually complementary. The erratic results obtained for capillary suction times are attributed to a thin filter cake as a result of the low percentage of solids in the flocculated slurry. For a thin filter cake it is reported that CST measurements were a better indication of blocking filtration rather than filter cake permeability.[127,129] Both particle size and the rate of deposition of the particles on the absorbant paper surface influenced blocking filtration. Variations in particle size and, therefore, the rate of particle deposition probably also contributed to the erratic results for the CST measurements.

It was thought that by removing more than the 20 mL aliquot of clear supernatant from the settled slurry for turbidity analysis that the percentage solids content could be increased to give sufficient thickness to the filter cake. However, it was realized that resuspension of a more concentrated slurry could promote particle-particle agglomeration in addition to the bridging flocculation.[50,51,59] Therefore, it was decided not to include the CST measurements in further flocculation tests.

Evaluation of the physical variables associated with the flocculation test procedure using 1% Na-kaolinite

An optimum set of physical parameters was not necessary for these measurements. However, changes in agitation rate and polymer addition rate were necessary to observe the effect of these physical parameters. These experiments served as trial runs for further flocculation tests which used a 1% Na-kaolinite test medium and polymer dosages

between 0 and 100 ppm. They also helped to determine the adequacy of settling rate and supernatant turbidity as the only evaluation techniques to be used for further test-work.

Since average settling rates and supernatant turbidities were sensitive to polymer dosage and the difference in the average polymer chain extension between PAM (5E+05 MW) and PAM (5E+06 to 10E+06 MW) for any combination of agitation rates and polymer addition rates, it was reasoned that any combination of these physical parameters would be suitable for further flocculation tests (Figs. 53 to 56). Moreover, small differences in the average settling rates and supernatant turbidities observed for any combination of agitation rate and polymer addition rate and large differences in the average settling rates and supernatant turbidities for changes in polymer dosage for each PAM and between the PAM's suggested a greater sensitivity of the flocculation test procedure to the average polymer chain extension than physical parameters. For these reasons, 1000 rpm agitation and the addition of polymer over 60 seconds were arbitrarity selected from other tested parameters for use in the flocculation test procedure for further tests.

4.9.2. Evaluation of the flocculation performance of newly synthesized, acrylamide-based polymers

Flocculation of the 1% Na-kaolinite test medium by nonionic, acrylamide-based polymers could be related to a bridging mechanism and, therefore, the average polymer chain extension, and to adsorption which would be affected by the copolymer structure. The average settling rate can be correlated to the proportion of the substituted acrylamide component in the copolymers which affects the average polymer chain extension and the

hydrogen bonding ability of the copolymers. The supernatant turbidity can be correlated to the proportion of the substituted acrylamide component in the copolymers which affects the flexibility of the polymer chains.

Average settling rate of nonionic, newly synthesized polymers

Even though the average polymer chain extension increased for a greater proportion of DMAM in the copolymers from DMAM-co-AM-3 to -5 (Table 30), it was reasoned that the decline in average settling rate observed for greater average polymer chain extensions was due to hindered hydrogen bonding (Fig. 57). Whereas the bridging ability should be enhanced by a greater proportion of DMAM in the copolymers, adsorption should be hindered by the steric bulk of DMAM and the reduced proportion of AM in the copolymers. However, the effect of hindered hydrogen bonding was not as significant as the effect of bridging on flocculation performance as the higher average polymer chain extensions of the copolymers from DMAM-co-AM-3 to -5 gave greater average settling rates than those of control PAM.

In contrast to the copolymers from DMAM-co-AM-3 to -5, the decline in average settling rates (Fig. 59) for a greater proportion of MeAM in the copolymers from MeAM-co-AM-2b to -5 is attributed to decreased average polymer chain extensions (Table 31) and, therefore, decreased bridging capability. However, it was conceded that intramolecular imidization of the copolymers containing a high proportion of MeAM would hinder hydrogen bonding and, therefore, hinder adsorption. The greater average settling rates obtained by using PAM than obtained by using the copolymers from

MeAM-co-AM-2b to -5 can be explained by both the higher average polymer chain extension and, therefore, superior bridging ability and unhindered hydrogen bonding and, therefore, unhindered adsorption of PAM.

Similar to the copolymers from DMAM-co-AM-3 to -5, the decline in the average settling rate (Fig. 61) for a greater proportion of NTBAM in the copolymers from NTBAM-co-AM-1b (clouded layer), -1b (clear layer), and -2 (dialyzed fraction) was attributed to hindered hydrogen bonding and, therefore, hindered adsorption. Since the average polymer chain extensions were nearly equivalent for the copolymers from -1b (clouded layer), -1b (clear layer), and -2 (dialyzed fraction) (Table 32) it was reasoned that the bridging ability of the copolymers was not a factor in the observed trend of the average settling rate. Like the copolymers from MeAM-co-AM-2b to -5, the higher average settling rates obtained by using PAM than those obtained by using the copolymers from -1b (clouded layer), -1b (clear layer), and -2 (dialysis fraction) are attributed to the higher average polymer chain extension and unhindered hydrogen bonding of PAM.

Supernatant turbidity of nonionic, acrylamide-based polymers

Since supernatant turbidity is related to floc density, it was thought that more flexible polymer chains could permit closer approach of bridged particles and, therefore, increased floc density. This reasoning is supported by the lower supernatant turbidities and, therefore, higher floc densities observed for flocculation tests which used copolymers with a decreasing proportion of the substituted acrylamide component.

However, it was realized that the proportion of the substituted acrylamide component in the copolymers not only affected polymer chain flexibility but also affected adsorption and, therefore, the degree of flocculation.

Lower supernatant turbidities for flocculation tests which used the copolymers from DMAM-co-AM-3 to -5 than for those using PAM from control-6 (complementary to MeAM-co-AM-6)) (Fig. 58) suggests that flocculation efficiency and, therefore, lower supernatant turbidity are promoted by the greater average polymer chain extension of the copolymers from DMAM-co-AM-3 to -5 rather than the greater polymer chain flexibility of PAM. In contrast to the copolymers from DMAM-co-AM-3 to -5, the lower supernatant turbidities for flocculation tests which used PAM than for those which used the copolymers from MeAM-co-AM-2b to -5 (Fig. 60) and NTBAM-co-AM-1b (clouded layer), -1b (clear layer), and -2 (dialyzed fraction) (Fig. 62) are attributed to the greater average polymer chain extension and the unhindered hydrogen bonding of PAM. As before, the greater average polymer chain extension provided superior bridging and the unhindered hydrogen bonding provided unhindered adsorption.

4.9.3. Comparison of the flocculation performance of the newly synthesized, acrylamide-based polymers and their cationic derivatives

Typically, flocculation of a charged test medium by an oppositely charged polyelectrolyte proceeds by a bridging mechanism for polymers having a high average polymer chain extension and a low charge density or by a charge neutralization mechanism for polymers having a low average polymer chain extension and a high charge density.[49,54,60-62] Since the cationic derivative having the greatest average polymer

chain extension and the highest percentage cationicity gave the highest average settling rate, it could not be confirmed whether flocculation developed from the bridging mechanism, charge neutralization mechanism, or both. However, the charge neutralization mechanism has been reported to involve reversible adsorption of the polyelectrolyte to the charged particle, whereas adsorption is irreversible for the bridging mechanism.[49,60] To test this, the flocculated slurry was exposed to high shear agitation for several minutes and then allowed to stand, when the flocculated slurry reformed. This result supports qualitatively the charge neutralization mechanism. In charge neutralization the polyelectrolyte adopts a flat configuration on the oppositely charged particle surface which diminishes the possibility of bridging.[49,54,60]

To explain the lower average settling rates (Fig. 63) and higher supernatant turbidities (Table 35) recorded for flocculation tests which used the cationic derivatives than for tests which used the nonionic polymer substrates, it was reasoned that the high average polymer chain extensions of the cationic derivatives covered a significant proportion of the particle surface and, therefore, hindered interaction with the surfaces of similarly treated particles. In addition, it was thought that the moderate charge densities of the cationic derivatives may have somewhat overcompensated for the slight negative charge on the particle surfaces and, therefore, hindered the approach of similarly treated particles.

4.9.4. Comparison of the Flocculation Performance of the Newly Synthesized Acrylamide-Based Polymers and Commercial Polymers

The higher average settling rates (Fig. 66) and lower supernatant turbidities (Fig.

67) observed for flocculation tests which used the commercial polymers than observed for tests which used the newly synthesized polymers are attributed to the greater average polymer chain extensions, and therefore, greater bridging abilities of the commercial polymers. Unlike the cationic derivatives of the nonionic, acrylamide-based polymers, it was reasoned that the low charge density of Percol 721 (cationic PAM) favoured the bridging mechanism over charge neutralization. Like the nonionic, acrylamide-based polymers, Percol E-24 (anionic PAM) and Percol 351 (nonionic PAM) would adsorb at the Na-kaolinite edges by hydrogen bonding.

The highest average settling rates (Fig. 64) and lowest supernatant turbidities (Fig. 65) of flocculation tests which used Percol 721 were attributed to unhindered adsorption to the oppositely charged surface of Na-kaolinite particles and superior polymer chain extension. Even though adsorption of Percol E-24, Percol 351, and the newly synthesized polymers to the edges of the Na-kaolinite particles competed with intramolecular hydrogen bonding, flocculation performances comparable to that from using Percol 721 indicated that polymer-clay hydrogen bonding prevailed over intramolecular hydrogen bonding of the clay particles.

The lack of sensitivity of the solution conformation of the copolymer from DMAM-co-AM-3 to solution pH and electrolyte concentration as well as a flocculation performance comparable to that of the commercial polymers and, especially, the polyelectrolytes suggests a potential application of this type of copolymer to media exhibiting extremes in solution pH, electrolyte concentration, or both.

5. Conclusions

5.1. Synthesis

Copolymerizations of DMAM with AM to give copolymers having 14.3, 22.6, 43.3, 62.9, and 81.3 mol % DMAM (as per elemental analysis), yields greater than 70 % (conversion of monomer to polymer), and M_w's greater than 5,000,000 g/mol were achieved by using a polymerization temperature of 50 °C and total monomer concentrations of 0.50 M and 0.25 M in deoxygenated, distilled water. These ultra-high M_w's and reasonable yields for ordinary reagents and routine conditions justify the compatibility of DMAM with AM for copolymerization. Also, the copolymers from DMAM-co-AM-2 to -7 gave greater M_w's and, more importantly, greater kinetic chain lengths than PAM, for equivalent experimental conditions.

Even though copolymerizations of MeAM with AM were designed to give copolymers having 24.4, 45.1, 64.0, and 82.0 mol % MeAM (as per the copolymerization equation) possible imidization or branching of the copolymers prevented accurate analysis of the copolymer compositions. For equivalent experimental conditions which included a 1.0 M total monomer concentration in deoxygenated distilled water, a natural pH in the range 5.5 to 7.0, and a polymerization temperature of 60 °C, the copolymers from MeAM-co-AM-2b to -5 gave yields greater than 60 % and lower M_w's and shorter kinetic chain lengths than PAM. In fact, only the copolymerization containing 80 mol % AM in the feedstock produced a copolymer with a M_w greater than 1,000,000 g/mol. These moderate to low M_w's and somewhat reasonable yields attest to either the

incompatibility of MeAM with AM for copolymerization to high M_w's or the need to include specialized reagents and / or less than ordinary conditions.

Copolymerizations of NTBAM with AM to give copolymers containing 15.3, 21.6, 35.7, 42.0, 59.3, and 83.0 mol % NTBAM (from ^{13}C NMR integration) and yields greater than 40 % were achieved by using 1.0 M and 0.50 M total monomer concentrations in deoxygenated 1:1, water / t-BuOH and a temperature of 50°C. Although copolymerization of NTBAM with AM is not compatible to give high M_w's and good yields unless a certain composition and a less than ordinary reagent (1:1, water / t-butanol) are used, success may be claimed from the ability to copolymerize hydrophilic AM with hydrophobic NTBAM using mainly ordinary reagents and routine conditions. Only the copolymers containing 21.6, 35.7, and 42.0 mol % NTBAM were compatible with the polymerization solvent. Copolymers having lower or higher proportions of NTBAM than these formed gelatinous products. The M_w's and kinetic chain lengths of the copolymers from NTBAM-co-AM-1 to -6 were less than that of PAM, for equivalent experimental conditions.

The higher M_w's for increasing proportions of DMAM in the copolymerization feedstock were related to the steric hindrance imparted by DMAM and / or polymer chains ending with the DMAM radical to chain transfer to monomer. This effect was more significant to producing a greater kinetic chain length for the copolymers than the slightly lower reactivity of polymer chains ending with the DMAM radical than AM radical was to limiting the kinetic chain length of the copolymers. Conversely, the lower M_w's for increasing proportions of NTBAM in the copolymerization feedstock were

related to the steric hindrance imparted by NTBAM and / or polymer chains ending with the NTBAM radical to chain transfer to monomer. This effect was less significant to producing a greater kinetic chain length for the copolymers than the much lower reactivity of polymer chains ending with the NTBAM radical than AM radical was to limiting the kinetic chain length of the copolymers. Unlike the copolymerizations of DMAM with AM or NTBAM with AM, lower M_w's for increasing proportions of MeAM in the copolymerization feedstock were attributed to the larger chain transfer to monomer constant for MeAM than AM and, also, the much lower reactivity of polymer chains ending with the MeAM radical than polymer chains ending with the AM radical.

The nonionic polymer substrates from DMAM-co-AM-7, MeAM-co-AM-2b, NTBAM-co-AM-1b (clouded layer) and control-6 (complementary to MeAM-co-AM-6) were converted to their cationic derivatives having cationicities of 26, 16, 18 and 14 mol %, respectively. These cationicities were considered reasonable for the given experimental conditions. Derivatization was achieved by using a mole ratio of 1.05:1:1 of dimethylamine, to formaldehyde, to amido nitrogen content of the polymer substrates for the Mannich reaction, and a mole ratio of 1:1 of dimethylsulfate to amido nitrogen content for quaternization. To avoid insolubility of the cationic derivatives in water due to methylene crosslinks which resulted during freeze-drying or became evident after freeze-drying, the cationic derivatives were left as solutions. The higher percentage cationicity of the cationic derivative of the copolymer from DMAM-co-AM-7 was attributed to its greater kinetic chain length and, more importantly, its chain extended solution conformation which enhanced the accessibility of the Mannich reagents to the

amide functionalities.

5.2. Solution Behaviour

The solution conformation of PAM (Percol 351) was insensitive to the small quantities of reagents required to adjust the solvent pH at room temperature. The copolymers of AM with DMAM, MeAM, and NTBAM were also insensitive to solvent pH for pH 4.00 ± 0.10 and pH 6.50 ± 0.20 and, in cases where solution standard pre-cleaning did not exhibit filter clogging, pH 10.00 ± 0.10. It is likely that the copolymer solution conformations would also be resistant to the acidic or alkaline conditions necessary for hydrolysis of PAM. This was attributed to the steric bulk of the substituted acrylamide component of the copolymers and its effect to maintain the average polymer chain extensions as well as hinder nucleophilic attack.

Unlike their resistance to solvent pH, the decrease in $< r_g >$ and [η] for PAM (Percol 351) as the concentration of NaCl in the solvent increased was attributed to coiling of the polymer chains. It is thought that this is due to the release of water molecules surrounding the polar amide functionalities to solvate additional NaCl ions, upon increasing the NaCl concentration. In contrast to the solution conformation of PAM, $< r_g >$ and [η] for the copolymers only showed slight variation and in most cases no variation with increasing NaCl concentration. This was probably due to the steric bulk of the substituted acrylamide component of the copolymers and its effect to maintain the average polymer chain extension in spite of the release of water molecules surrounding polar amide functionalities to solvate additional NaCl ions. For increasing

concentrations of NaCl, $< r_g >$ and [η] for polyelectrolytes such as Percol 721 (cationic PAM) and Percol E-24 (anionic PAM) decreased probably due to suppressed diffusion of the counterions from within the polyelectrolyte and, therefore, shielding of repulsive interactions between charged groups.

Since X_n varied significantly within a copolymer series and between copolymer types, no general trends could be established between values of $< r_g >$ or [η] and the copolymer compositions. However, it was found that for a particular example having comparable values of X_n, steric bulk increased the value of $< r_g >$ and [η] for the copolymer relative to $< r_g >$ and [η] for PAM. It was also found that as the proportion of the substituted acrylamide component in the copolymers increased, the effect of steric bulk on $< r_g >$ and [η] became less significant. The large values of $< r_g >$ and [η] for Percol 721 (cationic PAM) and very large values of [η] for the cationic derivatives relative to [η] for their nonionic precursors demonstrated the greater effect of charged groups to increasing $< r_g >$ and [η] than steric bulk.

5.3. Flocculation Test-Work

A flocculation test procedure was developed which was sensitive to the average polymer chain extension, $< r_g >$, and the structure of acrylamide-based polymers by careful selection and modification of the chemical and physical variables associated with flocculation. A standard mixing tank as described by Holland and Chapman was constructed for the flocculation test procedure to promote uniform mixing of the polymer with the test medium and thereby improve the reproducibility of flocculation tests. The

flocculation test medium was prepared as 1% Na-kaolinite at its natural pH with the supernatant electrolyte concentration reduced to 1.138×10^{-4} M NaCl. These parameters were used to isolate the edges of the Na-kaolinite particles and, therefore, restrict flocculation to bridging by acrylamide-based polymers. The effects of polymer dosage, agitation rate, and polymer addition rate on flocculation performance were measured by recording the settling rates and supernatant turbidities for PAM's of high and low molecular weight. From these results it was determined that polymer dosages of 25, 50, and 100 ppm, agitation at 1000 rpm for the duration of polymer addition, and polymer addition over 60 seconds (as a 10 mL aliquot of 10^{-4} to 10^{-3} g/mL solutions) were suitable conditions to show sensitivity of the flocculation test to polymer structure and chain extension. Also, average settling rates and supernatant turbidities of equivalent tests having percentage differences of $\leq$ 5 % from mean values indicates the reproducibility of the flocculation test procedure.

Although the bridging ability of the nonionic, acrylamide-based polymers is directly related to $< r_g >$, the hydrogen bonding ability of the polymers is related to polymer structure and, therefore, copolymer composition. The decrease in average settling rates for increasing proportions of DMAM and increasing values of $< r_g >$ in the copolymers from DMAM-co-AM-3 to -5 is attributed to hindered hydrogen bonding. This could be due to the increasing amounts of steric bulk and the lower proportion of unsubstituted amide groups capable of hydrogen bonding. In contrast to the copolymers from DMAM-co-AM-3 to -5 the decrease in average settling rates for increasing proportions of MeAM in the copolymers from MeAM-co-AM-2b to -5 and decreasing values of $< r_g >$ is

attributed to the diminished bridging ability of the copolymers. Unlike the copolymers from DMAM-co-AM-3 to -5 and the copolymers from MeAM-co-AM-2b to -5, the decrease in average settling rates for an increasing proportion of NTBAM in the copolymers from NTBAM-co-AM-1b to -2 was credited to both hindered hydrogen bonding and the diminished bridging ability of the copolymers.

Even though it was thought that floc density and, therefore, supernatant turbidity were related to polymer chain flexibility and, therefore, lower proportions of the substituted acrylamide component in the copolymers, it was determined that supernatant turbidity was influenced mainly by the bridging ability of the copolymers and, therefore, floc size. The lowest values for supernatant turbidity paralleled the highest average settling rates and no clear distinction could be made between floc size and floc density in the low percent solids test medium.

The greater chain extensions of the cationic derivatives of the nonionic copolymer precursors suggests greater bridging ability and, therefore, improved flocculation efficiency. However, flocculation tests using the cationic derivatives gave lower average settling rates and higher supernatant turbidities. This was probably due to the higher charge densities of the cationic derivatives in relation to commercial polyelectrolytes and, therefore, repulsive interactions hindering the approach of colloid particles having adsorbed polymer. The higher average settling rates and lower supernatant turbidities for flocculation tests using Percol 721 (cationic PAM) than for tests using the newly synthesized cationic derivatives or their nonionic precursors were attributed to the low charge density, greater $< r_g >$, and, therefore greater bridging ability of Percol 721.

The greater M_w and $< r_g >$ values measured for the commercial polymers than measured for the newly synthesized copolymers explains the higher average settling rates and lower supernatant turbidities observed for flocculation tests which used the commercial polymers. However, for a comparable M_w value and a slightly lower $< r_g >$ value, the copolymer from DMAM-co-AM-3 gave settling rates and supernatant turbidities comparable to those of the commercial polymers. If this performance is considered alongside the resistance of the newly synthesized copolymers to pH changes and to the presence of an electrolyte, it is likely that these acrylamide-based polymers containing steric bulk could have a broader industrial application than the current commercial polyelectrolytes, or PAM. Procedures developed here, have also shown that copolymerization of AM with substituted acrylamides using ordinary reagents can produce values of M_w and $< r_g >$ which are adequate for function as flocculants and, therefore, economical for industrial use.

6. References

1. W. M. Thomas and D.W. Wang, "Acrylamide Polymers," in Encyclopedia of Polymer Science and Engineering, 2nd ed., Vol. 1, H.F. Mark, N.M. Bikales, C.G. Overberger, G. Menges (eds.), Wiley: New York, 169-211 (1986).

2. J. Bock, D.N. Schulz, and C.L. McCormick, "Water-Soluble Polymers," in Encyclopedia of Polymer Science and Engineering, 2nd ed., Vol. 17, H.F. Mark, N.M. Bikales, C.G. Overberger, G. Menges (eds.), Wiley: New York, 730-784 (1986).

3. E.L. Carpenter and H.S. Davis, J. Appl. Chem., 7, 671-676 (1957).

4. D.E. Graham, "Polymers in Oil Recovery and Production." in Chemistry and Technology of Water-Soluble Polymers, C.A. Finch (ed.), Plenum Press: New York, 321-340 (1983).

5. J.K. Borchardt, "Chemicals Used in Oil-Field Operations," in Oil-Field Chemistry: Enhanced Recovery and Production Stimulation", J.K. Borchardt and T.F. Yen (eds.), ACS: Washington, 27-39 (1989).

6. J.K. Borchardt, "Viscosity Behaviour and Oil Recovery Properties of Interacting Polymers," in Oil-Field Chemistry: Enhanced Recovery and Production Stimulation, J.K. Borchardt and T.F. Yen (eds.), ACS: Washington, 446-465 (1989).

7. G.J. Howard, F.L. Hudson, and J. West, J. Appl. Polym. Sci., 21, 1-16, (1977).

8. *Ibid.* Ref. 7 (pages 29-43).

9. L.H. Allen and R.H. Pelton, Colloid & Polymer Science, 261, 485-492 (1983).

10. M.F. McCarty and R.S. Olson, Mining Engineering, 11, 61-65 (1959).

11. G. Moody, Minerals Engineering, 5, 479-492 (1992).

12. M. Smollen, Water SA, 12, No. 3, 127-132 (1986).

13. D.N. Schulz, "Water-Soluble Polymer Synthesis," in Water-Soluble Polymers: ACS Symp. Ser. 467, G.B. Butler, C.L. McCormick and W. Shalaby (eds.), ACS: Washington, 57-73 (1991).

14. G. Odian, Principles of Polymerization 3rd ed., Wiley, New York, 198-331 (1991).

15. R.A.M. Thomson, "Methods of Polymerization for Preparation of Water-Soluble Polymers" in Chemistry and Technology of Water-Soluble Polymers, C.A. Finch (ed.), Plenum Press: New York, 321-340 (1983).

16. T.W. Campbell and W.R. Sorenson, Preparative Methods of Polymer Chemistry 2nd ed., Interscience: New York, 248 (1968).

17. T. Ishige and A.E. Hamielec, J. Appl. Polym. Sci., 17, 1479 (1973).

18. G.S. Chen and C.L. McCormick, J Polym. Sci. Polym. Chem. Ed., 22, 3633-3647 (1984).

19. J.K. Baird, I.W. Cottrell, and J.L. Shim, U.S. Patent 4,254,249, Mar. 3, 1981.

20. F.S. Dainton and W.D. Sisley, Trans. Faraday Soc., 53, 1385-1389 (1962).

21. A.M. Schiller and T.J. Suen, Ind. & Eng. Chem., 48, 2132-2137 (1956).

22. J. Moens and G. Smets, J. Polym. Sci., 23, 931-946 (1957).

23. N. Vorchheimer, "Synthetic Polyelectrolytes," in Polyelectrolytes for Water and Wastewater Treatment, W.L.K. Schwoyer (ed.), CRC Press: Boca Raton, Florida, 1-45 (1981).

24. R.M. Goodman, "Dispersants," in Kirk-Othmer: Encyclopedia of Chemical Technology, Vol. 7, 3rd ed., Wiley: Toronto (1978).

25. F.W. Burtch, Polym. Prep., 22, 14-17 (1981).

26. M. Mullier and G. Smets, J. Polym. Sci., 23, 915-930 (1957).

27. J.F. Lane and E.S. Wallis, Organic Reactions, 3, 267-306 (1946).

28. E.G. Ballweber, J.R. Hurlock, K.G. Phillips, U.S. Patent 4,179,424, Dec. 18, 1979.

29. R. Rabinowitz and C.R. Witschonke, U.S. Patent 3,988,277, Oct. 26, 1976.

30. K. Fujimura and K. Tanaka, U.S. Patent 3,790,529, Feb. 5, 1974.

31. R.H. Pelton, J. Polym. Sci. Polym. Chem. Ed., 22, 3955-3966 (1984).

32. *Ibid.* Ref. 14 (pages 452-529).

33. M.B. Hocking and K.A. Klimchuk, J. Polym. Sci. Part A: Polym. Chem., 34, 2481-2497 (1996).

34. P.C. Hiemenz, Polymer Chemistry: The Basic Concepts, Dekker: New York, 659-722 (1984).

35. D.W. Shortt and P.J. Wyatt, Instruction Manual for the Dawn DSP Model F, Wyatt Technology Corporation: Santa Barbara, A-1 - A-9, (1993).

36. P.W. Atkins, Physical Chemistry 4th ed., Freeman: New York, 693-698 (1990).

37. P. Debye, J. Phys. Coll. Chem., 51, 18-32 (1947).

38. B.H. Zimm, J. Chem. Phys., 16, 1093-1099 (1948).

39. W. Heller, Rec. Chem. Prog., 20, No.4, 209-233 (1959).

40. M. Kerker, The Scattering of Light, Academic Press: New York (1969).

41. *Ibid.* Ref.14 (pages 19-24).

42. I.M. Koltz, Fed. Proc., 24, S-24 - S-33, (1965).

43. J. Israelachvili and H. Wennerström, Nature, 379, 219-225 (1996).

44. V.F. Sergeeva, Russ. Chem. Rev., 34, 309-318 (1965).

45. M.J. Garvey, J. Chem. Soc. Faraday Trans. 1, 75, No.5, 993-1000 (1979).

46. J.C. Fenyo, G. Muller, and J.P. Laine, J. Polym. Sci. Polym. Chem. Ed., 17, 659-672 (1979).

47. T.M. Aminabhavi, M. Chmelir, D.E. Hoffman, P. Munk, and P. Williams, Macromolecules, 13, 871-875 (1980).

48. K.D. Conrad and J. Klein, Makromol. Chem., 179, 1635 (1978).

49. J.K. Dixon, "Flocculation," in Encyclopedia of Polymer Science and Engineering, 2nd ed., Vol. 7, H.F. Mark, N.M. Bikales, C.G. Overberger, G. Menges (eds.), Wiley: New York, 211-233 (1986).

50. J.C. Berg, Surface and Colloid Science: Part I - Text, Department of Chemical Engineering, University of Washington: Washington, IV-1 - IV-57 (1993).

51. J. Lyklema, "The Colloidal Background of Agglomeration," in The Scientific Basis of Flocculation, K.J. Ives (ed.), Sijtjoff & Noordhoff International Publishers: Alpen aan den Rifh, The Netherlands, 3-36 (1978).

52. T.M. Riddick, Control of Colloid Stability through Zeta Potential, Livingston Publishing Company: Wynnewood, Pennsylvania, 208-239 ( ).

53. H. van Olphen (ed.), An Introduction to Clay Colloid Chemistry, Wiley: New York, 12-17 (1977).

54. J Gregory, "Polymeric Flocculants," in Chemistry and Technology of Water-Soluble Polymers, C.A. Finch (ed.), Plenum Press: New York, 307-320 (1983).

55. *Ibid.* Ref. 50, (pages V-1 - V-52).

56. J.G. Penniman, "Electrokinetics," in Polyelectrolytes for Water and Wastewater Treatment, W.L.K. Schwoyer (ed.), CRC Press: Boca Raton, Florida, 61-89 (1981).

57. *Ibid.* Ref. 53, (pages 57-82).

58. E.J.W. Verwey and J.Th.G. Overbeek, Theory of the Stability of Lyophobic Colloids, Elsevier: Amsterdam, New York, 1948.

59. D.H. Napper, "The Role of Polymers in the Stabilization of Disperse Systems," in Chemistry and Technology of Water-Soluble Polymers, C.A. Finch (ed.), Plenum Press: New York, 233-248 (1983).

60. J. Gregory, "Effects of Polymers on Colloid Stability," in Chemistry and Technology of Water-Soluble Polymers, C.A. Finch (ed.), Plenum Press: New York, 101-130 (1983).

61. B. Vincent, Adv. Coll. Inter. Sci., 4, 193-277 (1974).

62. J. E. Edzwald, "Cationic Polyelectrolytes in Water Treatment," in Flocculation, Sedimentation and Consolidation, B.M. Moudgil and P. Somasundaran (eds.), Proceedings of the Engineering Foundation Conference: Georgia, 171-180 (1985).

63. R.H. Smellie and V.K. La Mer, J. Coll. Sci., 13, 589-599 (1958).

64. R. Hogg, "Evaluation of a Macroscopic Model for Polymer Adsorption," in Polymer Adsorption and Dispersion Stability: ACS Sym. Ser. 240, E.D. Goddard and B. Vincent (eds.), ACS: Washington, 23-37 (1984).

65. C.L. McCormick, "Structural Design of Water-Soluble Copolymers," in Water-Soluble Polymers: ACS Symp. Ser. 467, G.B. Butler, C.L. McCormick and W. Shalaby (eds.), ACS: Washington, 2-24 (1991).

66. A.E. Hamielec and D. Hunkeler, "Mechanism and Kinetics of the Persulfate-Initiated Polymerization of Acrylamide," in Water-Soluble Polymers: ACS Symp. Ser. 467, G.B. Butler, C.L. McCormick and W. Shalaby (eds.), ACS: Washington, 82-118 (1991).

67. ASTM Committee on Standards, "Standard Practice for Coagulation-Flocculation Jar Test of Water," in Annual Book of ASTM Standards, Vol. 11.01, D 2035 - 80 (Reapproved 1990), ASTM: Philadelphia, 750-753 (1990).

68. ISO/TC 27/ SC 1, "Methods for the Comparison of the Performance of Flocculants for Use in Coal Preparation Plants: Part 1- Flocculants for Clarification and Thickening Applications (Sedimentation Test)," in ISO/CD 10086-1, ISO: Australia, 1-10 (1992).

69. *Ibid.* Ref. 53 (pages 248-252).

70. *Ibid.* Ref. 53 (pages 83-110).

71. F.A. Holland and F.S. Chapman, Liquid Mixing and Processing in Stirred Tanks, Reinhold Publishing: New York (1966).

72. R.C. Baskerville and R.S. Gale, Wat. Pollut. Cont., 67, 233 (1968).

73. M.V. Norris in Encyclopedia of Industrial Chemical Analysis, Wiley: New York, Vol. 4, 160-168 (1967).

74. *Ibid.* Ref. 34 (pages 583-658).

75. K.D. Conrad and J. Klein, Makromol. Chem., 179, 1635-1638 (1978).

76. M. Meirone and L. Trossarelli, J. Polym. Sci., 57, 445-452 (1962).

77. D.W. Shortt and P.J. Wyatt, Astra for Windows: Version 4, Wyatt Technology Corporation: Santa Barbara, 1-57, (1995).

78. D.W. Shortt, Wyatt Technical Notes, Wyatt Technology Corporation: Santa Barbara, 35-36 (1993).

79. D.W. Shortt and P.J. Wyatt, Dawn: Software Manual, Wyatt Technology Corporation: Santa Barbara, A-1 - A-9, (1993).

80. D.W. Shortt and J. Howie, Wyatt Technical Notes, Wyatt Technology Corporation: Santa Barbara, 10-15 (1993).

81. D.A. Skoog, Principles of Instrumental Analysis 3rd ed., Saunders College Publishing: New York, 704-712 (1985).

82. R.C. Weast, Handbook of Chemistry and Physics 67th ed., CRC Press: Boca Raton, Florida, D-164, (1986-1987).

83. R. Bansil and M.K. Gupta, J. Polym. Sci.: Polym. Phys. Ed., 19, 353-360 (1981).

84. J. Jonathan, J. Mol. Spectrosc., 6, 205-214 (1961).

85. T. Miyazawa, S. Mizushima, and T. Shimanouchi, J. Chem. Phys., 24, 408-418 (1956).

86. M. Beer, H.B. Kessler, and G.B.B. Sutherland, J. Chem. Phys., 29, 1097-1104 (1958).

87. L.S. Bellamy, The Infrared Spectra of Complex Molecules, Methuen and Company: London, England, (1954).

88. D.W. Green, J.O. Maloney, and R.H. Perry, Perry's Chemical Engineers' Handbook 50th Ed., McGraw-Hill Book Company: New York, 2-15 (1984).

89. O. Lietard, thèse, Institut National Polytechnique de Lorraine, Nancy (1977).

90. D.J.A. Williams and K.P. Williams, J. Coll. Inter. Sci., 65, 79-87 (1978).

91. B. Dobiáš, K.A. Wierer, J. Coll. Inter. Sci., 122, 171-177 (1988).

92. A.S. Buchanan and N. Street, Aust. J. Chem., 23, 450-466 (1956).

93. G.A. Parks, "Aqueous Surface Chemistry of Oxides and Complex Oxide Minerals, Isoelectronic Point, and Zero Point of Charge," in Equilibrium Concepts in Natural Water Systems, R.F. Gould (ed.), ACS: Washington, Adv. Chem. Ser. 67, 121-160, (1967).

94. D.W. Shortt, "Wyatt Technical Notes," Wyatt Technology Corporation: Santa Barbara, 28-32 (1993).

95. J. Brandrup and E.H. Immergut (eds.), Polymer Handbook 3rd Ed., Interscience: New York, VII / 419 (1989).

96. *Ibid.* Ref. 14 (page 265).

97. D.C. McWilliams, "Polyacrylamide and Related Amides," in Functional Polymers, E.B. Nyquist and R.H. Yocum (eds.), Marcel Dekker: New York (1973).

98 H. Morawetz, Macromolecules in Solution 2nd Ed., Interscience: New York, 324-335 (1975).

99 J. Bares, F.W. Billmeyer, and E.A. Collins, Experiments in Polymer Science, Wiley-Interscience: New York, 146-153 (1972).

100. "Polyacrylamide Method No. 6," The Dow Chemical Company: Midland, Michigan, 1-6 (1971).

101. M. Windholz, The Merck Index 10th Ed., Merck & Company: Rahway, N.J., pages 1521 and 5816 (1983).

102. G.S. Kriz, G.M. Lampman, and D.L. Pavia, Introduction to Spectroscopy: A Guide for Students of Organic Chemistry, Saunders College: Philadelphia (1979).

103. B.K. Hunter and J.K.M. Sanders, Modern NMR Spectroscopy: A Guide for Chemists, Oxford University Press: New York (1987).

104. T. Kelen and F. Tudos, J. Macromol. Sci.-Chem., A9, 1-27 (1975).

105. M. Fineman and S. S. Ross, J. Polym. Sci., 5, 259-262 (1950).

106. F.R. Mayo and F.M. Lewis, J Am. Chem. Soc., 66, 1594-1601 (1944).

107. *Ibid.* Ref. 14 (pages 356-451).

108. T.W. Graham Solomons, Organic Chemistry 3rd Ed., Wiley: New York, 727-728 (1984).

109. H. Benoit and W. Bushuk, Can. J. Chem., 36, 1616-1626 (1958).

110. *Ibid.* Ref. 34 (pages 124-127).

111. J. Francois, D. Sarazin, T. Schwartz, and G. Weil, Polymer, 20, 969-975 (1979).

112. J. Eliassaf and A. Silberberg, J. Polym. Sci., 41, 33 (1959).

113. A.E. Hamielec and S.M. Shawki, J. Appl. Polym. Sci., 23, 3323-3339 (1979).

114. J. Brandrup and E.H. Immergut (eds.), Polymer Handbook 2nd Ed., Wiley: New York, page II-111 (1975).

115. P. Bunnaul, R. Hogg, and H. Suharyono, Miner. Metall. Process., 10, No.2, 81-85 (1993).

116. P.J. Dodson and P. Somasundaran, J. Coll. Inter. Sci., 97, 481-487 (1984).

117. S. Friberg, K. Roberts, and J. Kowalewska, J. Coll. Inter. Sci., 48, 361-367 (1974).

118. D. Dollimore and T.A. Harridge, J. Coll. Inter. Sci., 42, 581-588 (1973).

119. Y. Bocquenet and B. Siffert, Coll. Surf., 9, 147-161 (1984).

120. L. Nabzar and E. Pefferkorn, J. Coll. Inter. Sci., 108, 243-248 (1985).

121. C.C. Gryte, A.F. Hollander, and P. Somasundaran, "Adsorption of Polyacrylamide and Sulfonated Polyacrylamide on Na-Kaolinite," in Fine Particle Processing, P. Somasundaran (ed.), AIME: New York (1980).

122. A. Carroy, L. Nabzar, and E. Pefferkorn, J. Coll. Inter. Sci., 106, 94-103 (1985).

123. H.H. Murray, Appl. Clay Sci., 5, 379-395 (1991).

124. J.A. Kitchener, "Flocculation in Mineral Processing," in The Scientific Basis of Flocculation, K.J. Ives (ed.), Sijtjoff & Noordhoff International Publishers: Alpen aan den Rifh, The Netherlands, 283-328 (1978).

125. R. Hogg and R.O. Keys, "Mixing Porblems in Polymer Flocculation," in AIChE Symposium Series, Vol. 75, No.190, 63-72 (1978).

126. *Ibid.* Ref. 53 (pages 16-28).

127. Billmeyer, F.W. (ed.), Textbook of Polymer Science, Wiley-Interscience: New York, 142-161 (1984).

128. *Ibid.* Ref. 62 (pages 39-56).

129. P.R. Karr and T.M. Keinath, Filtration and Separation, November / December, 543-544 (1978).

VITA

Surname: Klimchuk Given Names: Keith Adrian

Place of Birth: Castlegar, British Columbia, Canada

Educational Institutions Attended:

University of Victoria	1994 to 1997
Selkirk College	1991 to 1992
University of Victoria	1988 to 1991
Selkirk College	1986 to 1988

Degrees Awarded:

B.Sc.	University of Victoria	1992

Honours and Awards:

University of Victoria Fellowship	1996
University of Victoria Fellowship	1993-1994
Selkirk College President's Excellence Award	1987
Selkirk College Marty Martin Memorial Scholarship	1987
Selkirk College Biology Award	1987

Publications:

M.B. Hocking and K.A. Klimchuk, J. Polym. Sci. Part A: Polym. Chem., 34, 2481-2497 (1996).

PARTIAL COPYRIGHT LICENSE

I hereby grant the right to lend my thesis (the title of which is shown below) to users of the University of Victoria Library, and to make single copies only for such users or in response to a request from the Library of any other university, or similar institution, on its behalf or for one of its users. I further agree that permission for extensive copying of this thesis for scholarly purposes may be granted by me or a member of the University designated by me. It is understood that copying or publication of this thesis for financial gain shall not be allowed without my written permission.

Title of Thesis / Dissertation:

Synthesis, Characterization, and Testing of Acrylamide-Based Polymers

Author 

Keith Klimchuk

September 10, 1997